



University  
of Glasgow

<https://theses.gla.ac.uk/>

Theses Digitisation:

<https://www.gla.ac.uk/myglasgow/research/enlighten/theses/digitisation/>

This is a digitised version of the original print thesis.

Copyright and moral rights for this work are retained by the author

A copy can be downloaded for personal non-commercial research or study, without prior permission or charge

This work cannot be reproduced or quoted extensively from without first obtaining permission in writing from the author

The content must not be changed in any way or sold commercially in any format or medium without the formal permission of the author

When referring to this work, full bibliographic details including the author, title, awarding institution and date of the thesis must be given

Enlighten: Theses

<https://theses.gla.ac.uk/>  
[research-enlighten@glasgow.ac.uk](mailto:research-enlighten@glasgow.ac.uk)

A Study of Nucleoprotein Interactions in Mammalian Systems

ALAN B. BARCLAY, B.Sc.

Submitted in partial fulfilment of the requirement of the degree  
of Doctor of Philosophy, University of Glasgow.

ProQuest Number: 10662342

All rights reserved

INFORMATION TO ALL USERS

The quality of this reproduction is dependent upon the quality of the copy submitted.

In the unlikely event that the author did not send a complete manuscript and there are missing pages, these will be noted. Also, if material had to be removed, a note will indicate the deletion.



ProQuest 10662342

Published by ProQuest LLC (2017). Copyright of the Dissertation is held by the Author.

All rights reserved.

This work is protected against unauthorized copying under Title 17, United States Code  
Microform Edition © ProQuest LLC.

ProQuest LLC.  
789 East Eisenhower Parkway  
P.O. Box 1346  
Ann Arbor, MI 48106 – 1346

## ACKNOWLEDGEMENTS

I should like to thank Professor J. N. Davidson, F.R.S. and Professor R. M. S. Smellie for providing the facilities for undertaking this work, and Dr. R. Eason for his constant encouragement and advice.

I should also like to thank Dr. J. D. Pitts for his guidance and advice in the second year of my work. I am much indebted to Miss J. A. Cowan for her patience in typing this thesis. I am grateful to Mr. D. S. Lohead for assistance and advice on the ORD experiments.



## ABBREVIATIONS

The abbreviations used in this thesis are those approved by the editorial board of the Biochemical Journal (Biochem. J., 116, (1970), 1). The following abbreviations are also used:-

AL	-	Arginine-lysine rich histone
C. D.	-	Circular dichroism
cRNA	-	Chromosomal ribonucleic acid
C. T. DNA	-	Calf thymus deoxyribonucleic acid
GAR	-	Glycine-arginine rich histone
mRNA	-	Messenger ribonucleic acid
ORD	-	Optical rotatory dispersion
SV40	-	Simian virus 40
tRNA	-	Transfer ribonucleic acid

# CONTENTS

	<u>Page</u>
<u>INTRODUCTION</u>	1
1. General Introduction	1
2. Structure organisation of chromatin	3
2.1 Components of chromatin	3
2.1.1 DNA	4
2.1.2 Histones	5
2.1.3 Non.Histone Proteins	11
2.1.4 Chromosomal RNA (cRNA)	12
2.2 Nucleoprotein Structure	13
3. Biological function of chromatin	18
3.1 Nature of gene expression	18
4. Association of proteins	22
4.1 Light scattering	23
4.2 Osmotic pressure	23
4.3 Molecular sieve chromatography	24
4.4 Analytical ultracentrifugation	26
4.4.1 Ultracentrifugal analysis of polydispersity	30
4.4.2 Ultracentrifugal analyses of associating protein systems	32
5. Hydrodynamic characterization of DNA	37
6. Aim of experimental studies	40
<u>MATERIALS AND METHODS</u>	
1. Materials	41
1.1 Biochemicals	41
1.2 Chemicals	41
1.3 Organic Chemicals	41

1.3.1	Stains	41
1.3.2	Polyacrylamide gel reagents	41
1.3.3	Intercalating dyes	42
1.4	Dialysis tubing	42
1.5	Ultrafiltration	42
1.6	Buffers	42
1.7	Materials for column chromatography	43
1.8	Biological material	43
2.	Methods	44
2.1	Purification of the Glycine-Arginine Rich Histone	44
2.2	Polyacrylamide gel electrophoresis of purified histone species	46
2.3	Amino acid analysis of purified histone species	47
2.4	Isolation of intra-cellular SV40-DNA	47
2.5	Preparation of GAR-DNA complexes	49
2.6	Estimation of concentration of GAR histone solutions	50
2.7	Estimation of partial specific volume of GAR	51
2.8	Analytical gel filtration chromatography	51
2.9	Thermal denaturation studies	53
2.10	Analytical ultracentrifugation	53
2.10.1	Two component equilibrium ultracentrifugation of GAR	53
2.10.2	Analytical band sedimentation	54
2.10.3	Boundary sedimentation experiments	55
2.11	Optical rotatory dispersion	55
2.11.1	Determination of $\alpha$ Helix content of GAR histone	55
2.12	Data processing	58

	<u>Page</u>
<u>RESULTS</u>	59
1. Purification and initial characterization of GAR histone in calf thymus tissue	59
2. Analytical gel filtration of GAR histone	69
3. Ultracentrifugal analyses of GAR histone in salt conditions	78
4. Gel filtration analyses of association of GAR	118
5. Effect of pH on association of GAR histone	130
6. ORD analysis of GAR histone	146
7. Characterization of C. T. DNA	155
8. Analysis of GAR histone C. T. DNA complexes	159
8.1 Thermal denaturation studies	159
8.2 Sedimentation analysis of GAR histone C. T. DNA complexes	166
9. Preparation and Characterization of SV40 DNA	181
10. Analysis of GAR histone-SV40 DNA complexes	186
11. Model structures of SV40 DNA-GAR histone complexes	206
<u>DISCUSSION</u>	213
1. Association of GAR histone	213
2. Analysis of C. T. DNA-GAR histone complexes	225
3. Analysis of SV40 DNA-GAR histone complexes	235
4. Conclusions	245
<u>SUMMARY</u>	246
<u>APPENDIX 1</u>	
Adams Theory for analysis of association systems	249
<u>APPENDIX 2</u>	256
Molecular sieve chromatography	256

	<u>Page</u>
(a) Calibration of column	256
(b) Analysis of association systems using the method of Chun et al. (1969) and Chun and Kim (1969)	257
<u>REFERENCES</u>	261.

## INTRODUCTION

## INTRODUCTION

One of the major problems of modern biochemistry is the elucidation of precise molecular mechanisms whereby the genetic content of cells of higher organisms is selectively expressed according to the particular functions of individual cells. An understanding of such mechanisms would provide a clearer insight into the processes of differentiation in developing organisms. In multi-cellular organisms, each cell-type is characterized by a unique morphology and carries out a unique function. Such phenotypic variation is remarkable when it is considered that all somatic cells of a single higher organism contain the same overall genetic complement, or genotype. (Davidson and Leslie, 1950 a, b; Mirsky and Ris, 1951). Since DNA is the repository of genetic information in the cell, phenotypic differences in cells of the same genotype probably occur as a result of selective masking, or repression, of portions of the genome. That is, certain segments of the DNA molecule are not available to those cellular processes which express the information contained in the sequence of bases of the DNA. DNA in mammalian cells is very large and exists in vivo as a complex nucleoprotein structure, called chromatin. Characterization of the mechanism of selective repression of DNA in such complex systems is difficult and simpler biological systems have therefore been used to investigate such processes.

The bacterial genome is very small compared to that of mammalian cells and is not extensively complexed with protein. The relatively simple nature of the bacterial genome compared with the mammalian genome has thus enabled extensive investigation of the processes of selective repression of DNA (Jacob and Monod, 1961). A model of the molecular mechanisms involved in the selective expression of bacterial DNA has been

constructed on the basis of these studies. In bacterial cells, the synthesis of certain enzymes can be greatly increased by exposure of the cells to some regulatory molecule, or inducer. Such a phenomenon is termed induction. The molecular mechanisms of repression and induction in bacterial systems have been explained by Jacob and Monod (1961) by assuming the existence of two distinct types of genes, structural genes and regulator genes. Structural genes contain the genetic information which by the intracellular processes of protein biosynthesis, direct the combination of specific amino acids to form functional enzyme molecules. Regulator genes, on the other hand, produce a molecular species called the repressor, capable of associating reversibly with a small segment of DNA, the operator, adjacent to the structural genes. The operator and structural genes are collectively termed an operon. Association of the repressor with the operator blocks the formation of mRNA by the adjacent structural genes to prevent protein synthesis. Interaction of the inducer with the repressor causes a change in conformation of the repressor, affecting its ability to bind to the operator. The structural genes can thus be fully expressed, permitting the synthesis of enzyme molecules.

The success of the operon concept in describing the phenomenon of induction and repression in bacteria has provided a basis for research into analogous processes in higher organisms. However, extrapolation from bacterial to mammalian systems may not be justifiable in view of the large difference in complexity between the two systems. Prior to mitosis, the chromatin of mammalian cells undergoes structural modification and condenses to form chromosomes which are visible under the light microscope. In contrast to the situation in mammalian systems, bacterial DNA is not complexed with protein and does not form visible, compact



structures on mitosis. Such large differences in the complexity of mammalian and bacterial systems make it unlikely that the mechanisms of repression and induction of DNA, described by Jacob and Monod in bacterial systems operate in an identical fashion in mammalian cells.

Numerous studies have been reported, describing the repression of DNA caused by the binding of chromosomal proteins (Paul, Gilmour and Thomou, 1970; Dahmus and Bonner, 1970; Bekhor, Kung, and Bonner, 1969; Paul and Gilmour, 1968).

Difficulties in the interpretation of these studies have resulted in several different models of the repression of the mammalian genome being proposed. (Paul and Gilmour, 1968; Bekhor, Kung and Bonner, 1969). It is likely that a detailed understanding of the mechanisms of selective expression of DNA in mammalian cells will only be obtained when quantitative information is available on the nature and stoichiometry of nucleoprotein complexes. At present only limited data are available concerning this aspect of DNA-protein interaction. The work reported in this thesis describes the detailed characterization of the physiochemical properties of a discrete histone species and the interaction of this histone with various forms of DNA.

## 2. Structural Organisation of Chromatin

### 2.1 Components of Chromatin

The nature and relative amounts of the components of chromatin have been investigated by Bonner and Huang (1963), Marushige and Bonner (1966) and by Paul and Gilmour (1966, 1968). The major components of chromatin were identified as DNA, histones and non-histone protein, although estimates of the relative amounts of these components varied slightly.

Average relative amounts are shown in Table 1.

Component	% by Wt.
DNA	45
Histone	30
Non-histone protein	23

In addition to the major components of chromatin shown above, small amounts ( $<5\%$  by weight) of RNA were found in chromatin preparations. Recent evidence has suggested, however, that the presence of RNA in chromatin is an artefact of the method of preparation of chromatin (Heyden and Zachau, 1971).

Structural aspects of these individual components of chromatin will now be briefly discussed.

#### 2.1.1 DNA

Watson and Crick (1953) deduced from the X-ray diffraction studies of Wilkins, Stokes and Wilson (1953) that DNA in its native state exists in a right-handed double helical configuration, with two polynucleotide chains helically wound about a common axis. The purine and pyrimidine bases of the DNA project towards the interior of the double helix while the phosphate groups of the sugar-phosphate backbone of each strand are located on the exterior of the molecule. Adenine basis on one strand are linked by hydrogen bonds to thymine bases on the opposing strand, while cytosine bases are similarly linked with guanine bases. The sequence of bases on each

Average relative amounts are shown in Table 1.

Component	% by Wt.
DNA	45
Histone	30
Non-histone protein	23

In addition to the major components of chromatin shown above, small amounts ( $<5\%$  by weight) of RNA were found in chromatin preparations. Recent evidence has suggested, however, that the presence of RNA in chromatin is an artefact of the method of preparation of chromatin (Heyden and Zachau, 1971).

Structural aspects of these individual components of chromatin will now be briefly discussed.

#### 2.1.1 DNA

Watson and Crick (1953) deduced from the X-ray diffraction studies of Wilkins, Stokes and Wilson (1953) that DNA in its native state exists in a right-handed double helical configuration, with two polynucleotide chains helically wound about a common axis. The purine and pyrimidine bases of the DNA project towards the interior of the double helix while the phosphate groups of the sugar-phosphate backbone of each strand are located on the exterior of the molecule. Adenine basis on one strand are linked by hydrogen bonds to thymine bases on the opposing strand, while cytosine bases are similarly linked with guanine bases. The sequence of bases on each

polynucleotide chain is therefore complementary, that is, the order in which the bases occur in one chain automatically determines the order of bases in the other chain. In the B form of DNA, which is the form found in aqueous solution, the bases are perpendicular to the helix axis, the distance between each base-pair being  $3.4\text{\AA}$ . Two continuous helical grooves of different widths are located on the exterior of the molecule between the sugar-phosphate backbones of the polynucleotide strands. Most DNA molecules have a double helical configuration as described above, but single-stranded DNA molecules have been identified (e. g. the DNA from bacteriophage X 174). Hydrodynamic techniques have been used to distinguish between single-stranded and double-stranded DNA's. More detailed discussion of the hydrodynamic properties of DNA will be presented in Section 5.

#### 2.1.2 Histones

The fact that the basic amino acid residues of histones bind to the phosphate backbone of DNA and repress the DNA has stimulated research on the detailed characterization of these molecules. (Barr and Butler, 1963; Paul and Gilmour, 1966). Knowledge of the secondary and tertiary structures of histones is a prerequisite to the complete understanding of the structure of nucleohistone complexes. The relevance of studies on the structure of isolated histones may be affected, however, by the possibility that the procedures used

to isolate the histones from the nucleohistone complexes may alter the conformation of the histones. Indeed, Zubay and Doty (1959), Wagner (1970) and Simpson and Sober (1970) have shown that the complexing of histones to DNA causes alteration of the conformation of the histones. Information on the structure of isolated histones will nevertheless permit an understanding of such changes in the conformation of histones. Histones are small, basic proteins of molecular weight between 10,000 and 20,000 which contain no tryptophan and relatively high amounts of basic amino acid residues such as arginine and lysine (Stellwagen and Cole, 1969; Hnilica, 1967; DeReuck and Knight, 1964; Bonner and Ts'o, 1964). Early Studies on the fractionation and analysis of histones suggested that total cellular histone was composed of many individual species (Vendrely, Alfert, Matsudaira and Knoblock, 1958). More recent studies have employed preparative techniques in which proteolytic action could be rigorously controlled (Johns 1964; Starbuck, Mauritzen, Taylor, Saroja and Busch, 1968). With the introduction of sensitive analytical techniques such as poly-acrylamide gel electrophoresis (Fambrough and Bonner, 1969), it became apparent that the total number of discrete histone species was low, probably less than ten. The apparent multiplicity of histones detected in earlier work was attributed to proteolysis or the uncontrolled aggregation of histones.

The lack of any enzymic activity of histones has resulted in several systems of nomenclature being adopted. Currently the most widely used systems of nomenclature are based on chemical composition (Starbuck et al., 1968; Mauritzen, Starbuck, Saroja, Taylor and Busch (1967); DeLange, Fambrough, Smith and Bonner, 1968 a, b), or on the order of fractionation of histones by preparative methods (Johns, 1964; Luck, Rasmussen, Satake, and Tsvetikov, 1958). Histone classification can be inter-related using the molar lysine/arginine ratios of the histones as a standard basis for comparison (Hnilica (1967)) and is depicted below:-

Nomenclature of Busch	Nomenclature of Johns	Nomenclature of Luck	Lys/Arg
Very lysine rich	F <sub>1</sub> a	Ia Ib	15.8
Slightly Lysine rich	F <sub>2</sub>	IIb IIb <sub>2</sub>	2.23
Glycine Arginine rich	F <sub>2</sub> A <sub>1</sub>	IV	0.94
Arginine-lysine rich	F <sub>3</sub>	II	0.75

Histones have been isolated from sources as diverse as calf thymus and pea-bud seedlings (Marushige and Bonner 1966). The types and relative amounts of individual histone species isolated from different sources were found to be

constant. This lack of species or organ specificity of histones has been confirmed by the studies of Crampton, Stein and Moore (1957); DeLange, et al. (1968); Hnilica, Taylor and Busch, (1963) and Hnilica (1967). Only in one class of histones, the very lysine rich class, was a possible exception to the general lack of species specificity of histones found. Fambrough, Fujimura and Bonner (1968) reported that as pea seedlings mature, the level of this class of histones rises from low levels to the usual level. In general, however, it is currently widely held that histones show little species or organ specificity (Stellwagen and Cole, 1969).

Determinations of the amino acid sequence of several histone species have been carried out in an attempt to elucidate the molecular structure of the histones. The amino acid sequence of GAR histone has been determined using three different source materials - calf thymus (DeLange et al. (1968), Ogawa et al. (1969), pea seedlings (DeLange et al. (1968)) and Novikoff hepatoma (Wilson, Starbuck, Taylor, Jordan and Busch, (1970)). The amino acid sequences of GAR isolated from these source materials were found to be essentially identical, confirming the lack of species specificity of this type of histone molecule. The identical nature of the amino acid sequences of GAR from these source materials suggests that the histone molecule plays a vital biological role in vivo requiring strict evolutionary conservation of the amino acid sequences. The amino acid sequence

of slightly lysine rich histone has been determined by Iwai, Ishikawa and Hayashi (1970) and partial structural analysis and peptide sequencing of a fraction of the very lysine rich group of histones from rabbit thymus has been carried out (Bustin, Rall, Stellwagen and Cole, (1969)). Comparison of the amino acid sequences of the three histones so far determined reveals striking similarities although each histone has a unique overall sequence. The distribution of basic amino acids is not random; instead they are grouped in clusters, forming highly basic segments in the polypeptide chain. In both GAR and the <sup>slightly</sup>~~very~~-lysine rich histone, the basic residues are predominantly located at the amino terminal end of the protein, while in the very lysine rich histone, the carboxy-terminal end contains a high proportion of basic amino acid residues. This feature has led to the proposal that histones have positively charged 'sticky ends' which bind to the negatively charged phosphate residues of DNA, thus repressing segments of the DNA.

Sung and Dixon (1970) have constructed space filling models of the positively charged amino terminal end of GAR histone and found that this region of the histone can form an  $\alpha$ -helix of dimensions which permit binding to the large groove of DNA.

The function of histones as repressors of DNA will be further discussed in Section 3.1.



histones have been found to form non-covalent aggregates. (Edwards and Shooter, 1969a; 1970; Mauritzen et al., 1967; Johns 1968; Fambrough and Bonner, 1966; Hnilica 1967; Ui, 1957. With the discovery that histones contained irregularly spaced clusters of basic and hydrophobic residues, it was postulated that histone aggregation could take place in an ionic environment by the formation of hydrophobic bonds (DeReuck and Knight, 1964). Disulphide bridge formation has been suggested as an alternative mechanism of histone aggregation (Fambrough and Bonner, 1968; Neelin, 1968), and it is possible that through intermolecular disulphide bonds histones may aggregate covalently with themselves or with non-histone chromosomal proteins. Most histones contain only small numbers of cysteinyl residues, and some species contain none; it therefore appears unlikely that very large multicomponent aggregates may be formed by disulphide bridging. Nevertheless, the aggregates which are formed may have sufficient specificity to interact uniquely with individual genes. The presence of many histone-like species detected in early analytical work has been attributed in part to the aggregation of histones (Stellwagen and Cole, 1969).

Minor modification of the tertiary structure of histones has been shown to occur by the processes of phosphorylation of certain amino acid residues of the protein (Kleinsmith, Allfrey and

Mirsky, 1966; Stevely and Stocken, 1966).

Methylation (Tidwell, Allfrey and Mirsky, 1968; Burdon, 1971) and acetylation (Gershey, Vidali and Allfrey, 1968) of amino acid residues in histone species has also been reported. The implication of these discoveries in the function of histones as repressors will be discussed in Section 3.1.

### 2.1.3 Non-Histone Proteins

Non-histone proteins constitute a major component of chromatin (Paul and Gilmour, 1968; Bonner and Huang, 1963). Prior removal of histones from chromatin by extraction with acid allows preparation of non-histone proteins from the residual proteins by alkali-extraction. The low solubility of non-histone proteins in dilute aqueous buffers has, however, been a major obstacle to the fractionation and characterization of these proteins. Recently, Marushige, Brutlag and Bonner (1968) showed that non-histone proteins were soluble in buffers containing sodium-dodecyl sulphate (SDS). Preparations of non-histone proteins in such buffers were shown to be heterogeneous, with a minimum molecular weight of less than 20,000 daltons. Removal of the SDS caused the formation of large insoluble aggregates of non-histone proteins. The heterogeneous nature of preparations of non-histone proteins has been confirmed by the studies of Wang (1967) and Wang and Johns (1968) who showed that limited fractionation of the proteins could be achieved by

extraction with salt followed by chromatography on DEAE-cellulose. Unlike histones, the relative abundance of non-histone proteins in chromatin has been shown to be dependent on the type and physiological state of the starting material (Salser and Balis, 1966; Marushige and Ozaki, 1967).

The problems of solubility and fractionation of non-histone proteins have prevented detailed structural investigations of the type carried out on histone molecules. Nevertheless, non-histone proteins have been found to play an important role in the processes of selective repression of the mammalian genome (Paul and Gilmour, 1968; Paul, Gilmour and Thomou, 1970). The biological function of non-histone proteins in such processes will be discussed in Section 3.1.

#### 2.1.4 Chromosomal RNA (cRNA)

Small amounts of RNA have been detected in preparations of chromatin (Huang and Bonner, 1965; Paul and Gilmour, 1968; Bekhor, Kung, and Bonner, 1969;)

This RNA species, termed chromosomal RNA (cRNA), was found to be about 40 nucleotides long of which more than a quarter were dihydrouridylic acid residues. Huang (1967) showed that cRNA was covalently linked to a non-basic chromosomal protein and Bonner and Huang (1964) have postulated that cRNA linked to such an RNA-binding protein is implicated in the formation of a larger complex which contains 10-20 histone molecules.

A recent detailed examination of the methods used to prepare cRNA has, however, suggested that cRNA preparations are composed largely of RNA fragments formed by nuclease action on transfer RNA (tRNA) molecules (Heyden and Zachau, 1971). Clearly, further work is necessary to investigate this possibility that cRNA is a preparative artefact and to define its precise role in chromatin.

## 2.2 Nucleoprotein Structure

X-ray diffraction has been used by Zubay (1964) and Richards (1964) in the study of the structure of nucleoprotein complexes. The experimental data obtained were interpreted as indicating that nucleohistone is a sheet-like structure in which DNA molecules run in one direction and histone molecules traverse these parallel DNA strands at an angle of  $37^\circ$ , linking with the DNA in every second large groove. The model is shown below:-

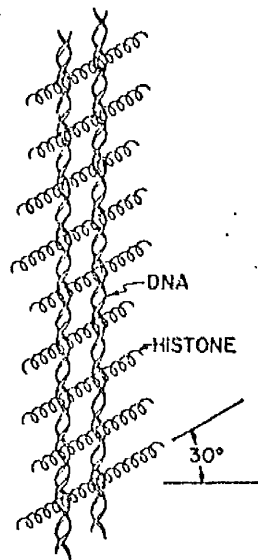


Fig. 4.—A model of oriented nucleohistone in the gel state. Histone bridges formed between DNA molecules lie parallel to the large groove of the DNA, with their long axis at an angle of  $60^\circ$  to the long axis of the DNA. Separation of the DNA molecules is sensitive to the amount of water present, but the spacing of the histone bridges is not. How many DNA molecules may be held together by the same histone bridges is unknown.

(Diagram taken from Zubay (1964)).

One attractive feature of the model proposed by Zubay (1964) is that if the histones are arranged on one side only of each DNA molecule, then a plausible mechanism is described for the maintenance of supercoiled structures which have been implicated in the formation of mitotic chromosomes (Pardon, Wilkins and Richards, 1967).

## 102 The Structure of Nucleohistones

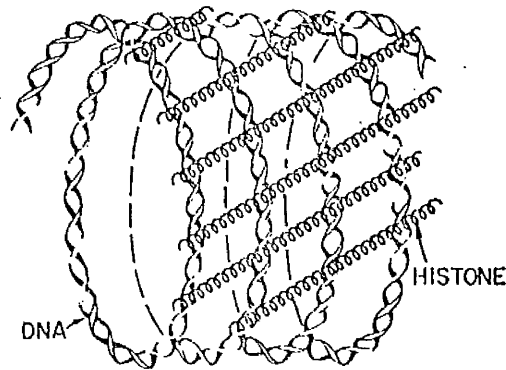


Fig. 6.—Diagram suggesting the function of histone bridges in chromosomes. DNA must form supercoils in mitotic chromosomes. It seems likely that the adjacent coils of the supercoiled DNA are held together by histone bridges. The dimensions of the supercoil are unknown.

(Diagram taken from Zubay (1964)).

An alternative model of the structure of nucleohistone predicts that the histone is wrapped in the large groove of one or perhaps two parallel DNA molecules (Sinsheimer, 1964). Such models have been substantiated by electron microscope studies of isolated chromosomes (Dupraw, 1966 a, b; Dupraw and Bahr, 1968). A model of chromosome structure based on these studies has been proposed by Dupraw (1965) in which the chromosomal unit is regarded as a single DNA-protein fibre which is repeatedly folded back on itself both longitudinally and transversely to make up the body of a chromatid.

13

The studies of Richards (1964) have indicated that the models of nucleohistone complexes described above may be over-simplified. X-ray studies carried out by Richards (1964) indicated the presence of a repeat unit of  $75\text{\AA}$ , but electron microscopy revealed a collection of fibres ranging from  $30\text{\AA}$  to  $200\text{\AA}$  in diameter.

Important information can be obtained about the site of binding of proteins to DNA by investigating the effect of the protein on the binding of small molecules such as dyes, whose interaction with DNA is well characterized. Actinomycin D and ethidium bromide are two such dyes. The chromophore of Actinomycin D molecules interacts with DNA by parallel insertion between two adjacent base residues, that is by intercalation (Muller and Crothers, (1968)). Ethidium bromide has also been shown to intercalate with DNA (Waring, 1965). Olins (1969) showed that the binding of  $F_1$  histones to DNA caused a reduction in the number of ethidium bromide molecules bound to DNA but did not affect the number of Actinomycin D molecules bound. Since both dyes intercalate with DNA it is difficult to rationalise these findings. Glucose residues attached to DNA by the action of  $\alpha$ -glucosyl transferase are located in the large groove of DNA and it was found that when  $F_1$  histones were bound to the DNA, glucosylation of the DNA was greatly reduced (Olins; 1969). It was therefore assumed by Olins that  $F_1$  histones bind to the large grooves of DNA.

Optical rotatory dispersion (ORD) and circular dichroism (CD) are powerful physical methods used for conformational studies of molecules in solution and are capable of providing data on the interaction of proteins with DNA (Wagner, 1970). Regions of ORD and CD spectra are

sensitive to changes in protein conformation and different regions of the spectra are sensitive to changes in the conformation of nucleic acids (Adler and Fasman, 1968). ORD and CD studies of nucleoprotein complexes can therefore distinguish the individual contributions from both the DNA and the protein to the overall conformation of the complex. Changes in one or both of the reactants in a nucleoprotein complex may be investigated by comparison of the combined spectra when the two components are unmixed, with that of the complex. Dissociated histones have been shown to have a low helix content which contrasts with the high helix content of histones in nucleoprotein complexes (Zubay and Doty, 1959; Wagner, 1970; Simpson and Sober, 1970). CD studies by Shih and Fasman (1970) of nucleoprotein complexes have shown that the normal B configuration of uncomplexed DNA is altered by the binding of chromosomal proteins. The structure of DNA in chromatin was found to be similar to that of the C form of DNA, the structure existing at low relative humidities, in which the bases are tilted. (Fasman, Schaffhausen, Goldsmith and Adler (1970)). Changes in the conformation of DNA caused by the binding of chromosomal proteins have been confirmed by the ORD and CD studies of Simpson and Sober (1970) and Tuan and Bonner (1969) and by the X-ray diffraction studies of Wilkins, Zubay and Wilson (1959) and Pardon et al. (1967). In contrast to these findings, however, Bram and Ris (1971) have shown that DNA in nucleoprotein complexes exists in the B form. Changes in DNA conformation have been found on complexing the DNA with poly-L-lysine (Cohen and Kidson, 1968; Leng and Felsenfeld, 1966). Inoue and Ando (1970 a, b) have reported conformational changes in DNA on complexing with clupeine, poly-arginine and poly-lysine. The interaction of polyamines with DNA has been studied by Liquori, et al. (1967)

using X-ray diffraction. It was found that the polyamines were attached to the DNA in the small groove.

Thermal denaturation studies have also been used to investigate nucleoprotein complexes. DNA-histone complexes have been shown to exhibit biphasic melting profiles, the first-step transition being due to the melting of free DNA segments and the second-step transition to that of the histone-complexed regions (Shih and Bonner, 1970; Olins, 1969). Accurate measurement of the first derivative curve of the absorbance melting profiles of DNA-F1 histone complexes have, however, suggested that there are several distinct transitions, indicating that the histone complexes to different stretches of DNA with different binding energies (Ansevin and Brown, 1971).

Useful information on the interaction of different histone fractions with DNA has been obtained from the order in which histones are dissociated from whole chromatin in preparative procedures. An advantage of this procedure is that investigation of the properties of the residual chromatin remaining after extraction of individual histone fractions may reveal the contribution of these fractions to the structure of whole chromatin. Titration of whole chromatin with acid removes histones in the order Ia, Ib, IIb, III and IV (Murray, 1964), with consequent decrease of the sedimentation coefficient of the chromatin. Murray, Bradbury, Crane-Robinson, Stephens, Haydon and Peacocke (1970) used salt to dissociate histones from chromatin and found that histone I was dissociated in 0.45M NaCl, histones V and I in 0.7M NaCl, histones IIb, V and I in 1.7M NaCl, and that all histones were removed in 2.0M NaCl. It was found that the removal of histones I and V from chromatin did not destroy its supercoiled structure but further removal of histones did and that histone I



10  
existed in the form of an extended polypeptide chain whereas other histones contained high helical contents in chromatin.

### 3. Biological Function of Chromatin

#### 3.1 The Nature of Gene Expression

DNA is the repository of genetic information in biological systems. Since selective repression of the mammalian genome may be brought about by the binding of specific repressors to the DNA, extensive research has been carried out to identify the specific repressors of the mammalian genome.

The basic nature of histones makes them likely candidates for the role of repressors and the multiplicity of histones detected by early fractionation studies suggested that individual histones could selectively repress a large number of genes. (Stedman and Stedman, 1950). The hypothesis that histones were the specific repressors of mammalian DNA was strengthened when it was shown that in vitro, histones decreased the ability of DNA to act as a priming template for DNA-dependent RNA synthesis (Huang and Bonner, 1962; Barr and Butler, 1963). The application of more rigorous fractionation and analytical procedures revealed, however, that the total number of discrete histone species was small and that no species-specificity of histones existed (Fambrough and Bonner, 1966). Consequently, it appeared unlikely that histones could selectively repress the large number of genes in the mammalian genome. The observation that individual isolated histone fractions did not bind to selective segments of DNA, but instead were capable of repressing the entire genome, provided additional evidence of the lack of specificity of the binding of histones to DNA.

(Huang, Bonner and Murray, 1964). Specificity might be conferred on histones by minor modification of their tertiary structure by the processes of phosphorylation, methylation or acetylation (Kleinsmith, et al., 1966; Stevely and Stocken, 1966; Tidwell et al., 1968; Gershey et al., 1968). It was suggested that the changes in the ionic charge properties of the proteins, caused by these processes would permit the selective removal or attachment of histones to DNA (Sung and Dixon, 1970). An attractive feature of this hypothesis is that the binding of histone to DNA could be regulated enzymically, through control of the histone modifying enzymes. The aggregation of histones is also of interest since the specificity required by genetic repressors might be obtained by relatively few histones in many combinations. However, no direct evidence is available to indicate that the increase in specificity conferred on histones by the processes of acetylation, phosphorylation and methylation or by aggregation enables the selective repression of the large number of genes in the mammalian genome.

Since histones by themselves do not selectively bind to specific parts of the genome it was postulated by Bekhor, Kung and Bonner (1969) that the combination of histones with cRNA species capable of binding to specific base sequences in DNA would enable direction of the histones to specifically repress certain genes. Evidence in support of this model was cited from studies on dissociated chromatin, the components of which were allowed to re-anneal under conditions permitting specific RNA-DNA interactions. It was found that in vitro transcription of such reconstituted chromatin produced RNA species similar to those produced by in vivo transcription of native chromatin. The experimental observations supporting

these conclusions were obtained from studies of the hybridization of both types of RNA species to DNA; it was found that the RNA produced from reconstituted chromatin competed with RNA from native chromatin on hybridization to complementary DNA species. This model of cRNA directing histones to specific sites on the genome will have to be re-examined in view of the possibility that cRNA preparations are contaminated by tRNA fragments (Heyden and Zachau, 1971).

The model of regulation of gene expression proposed by Bekhor, Kung and Bonner (1969) has not been supported by the experiments of Paul and co-workers (Paul and Gilmour, 1966, 1968; Gilmour and Paul, 1969; Paul, Gilmour and Thomou, 1970). Using an approach similar to that of Bekhor et al. (1969), Paul and Gilmour (1968) found that only when histones were complexed to DNA in the presence of non-histone chromosomal proteins were RNA species produced on in vitro transcription which were similar to RNA produced by the transcription in vivo of native chromatin, using competitive hybridization techniques to test the similarity of the RNA species. Paul, et al. (1970) have proposed a model of gene function which involves non-histone protein attaching specifically to those genes which are selectively transcribed, thus 'masking' such genes from the unspecific repression of histones bound to DNA.

The discrepancies between the evidence supporting the above models, one implicating cRNA and the other non-histone protein, are hard to rationalize. Stellwagen and Cole (1969) have suggested that the difficulties of interpretation of competitive hybridization data may cause the apparent inconsistencies.

Evidence that each of the above models of gene expression may be over-simplifications has been presented by Hoare and Johns (1970) and Johns and Hoare (1970), who showed that the physical state of chromatin affects its function. It was found that addition of histones to DNA caused increasing repression of the DNA up to a maximum point after which the addition of more histones decreased the amount of repression. The possibility that histones cause a decrease in the in vitro transcription of DNA by simple precipitation of the DNA can therefore be discounted. The results of Johns and Hoare (1970) also imply that after the points of maximum repression, addition of more histones to a nucleohistone complex may alter the conformation of the complex and allow more transcription of the DNA. Studies of the correlation of the physical state of chromatin, in terms of the nature of the precipitated chromatin, with the degree of repression have confirmed that the conformation and physical state of chromatin affects its function (Johns and Hoare, 1970; Hoare and Johns, 1970).

For these reasons, it appears likely that a satisfactory explanation of the nature of gene expression in mammalian cells will only be obtained by quantitative physicochemical investigation of the conformation of nucleoprotein complexes and the mechanisms of interaction of the various components of chromatin.

Mammalian chromatin is, however, a complex aggregation of several distinct macromolecular species and the determination of the physical structure of intact chromatin by current physicochemical techniques is therefore very difficult. One approach to this problem is to characterize in detail the physicochemical properties of isolated components

62

of chromatin. Meaningful interpretation of the nature of complexes of these components may then be possible. The use of model systems, such as poly-amino acids or small homogeneous DNA species, whose physicochemical properties have been characterized, is advantageous in such studies (Olins and Olins 1971). The experimental work described in this thesis (See Results Section) is concerned with the detailed physicochemical characterization of the Glycine Arginine Rich histone (GAR) and of GAR-DNA complexes.

#### 4. Association of Proteins

Since a major portion of the experimental characterization of GAR histone in this work is concerned with the self-association properties of the protein, a brief review of the physical approaches used in the study of associating protein systems will be presented.

Many proteins have been found to undergo self-association (e. g. lysozyme, Adams and Filmer, 1966); insulin, Jeffrey and Coates, 1966; oxyhaemoglobin; Schachman and Edelstein, 1966; chymotrypsin, Rao and Kegeles, 1958) and increasingly it is being realized that the function of proteins is dependent on its state of aggregation. The biological importance of associating protein systems has been demonstrated in the cases of allosteric enzymes (Monod, Wyman and Changeux, 1965) and virus coat assembly (Caspar and Klug, 1962).

Many physical techniques are available which can yield information on protein aggregation.

A major problem in the analysis of associating protein systems is that frequently the rates of equilibration between the associating species are such that the experimental method used disturbs the equilibrium (e. g. techniques involving moving boundaries of the

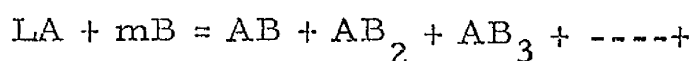
associating species). For this reason, one approach used frequently is that of simulation, that is, comparison of experimental data with predictions based on theory. The most commonly used techniques for the analysis of associating protein systems will be described.

#### 4.1 Light Scattering

Steiner (1952, 1953, 1954) developed equations enabling the evaluation of weight average molecular weights (q. v.) from light scattering studies of associating protein systems. An advantage of light scattering is that information on the shapes and sizes of complexes may be obtained. On the other hand, the amount of data obtainable from light scattering studies may be limited, since a single experiment yields only one value of molecular weight. Steiner (1952) used light scattering to investigate the aggregation of insulin at low pH. The presence of tetramers and higher polymers of insulin has also been detected by light scattering (Doty and Myers, 1953).

#### 4.2 Osmotic Pressure

The technique of osmometry has several features, which make it suitable for study of associating protein systems. The theory of osmometry is thermodynamically rigorous and the analytical procedures required to describe associating systems are simple. High speed osmometers allow the rapid evaluation of number-average molecular weight (q. v.). Nevertheless, only relatively few studies of associating systems by osmometry have been reported. Steiner (1954) derived theoretical equations enabling associating systems of the type:-



to be analyzed by osmometry. More recently, Adams et al. (1969) have extended Steiner's equations, to incorporate quantitative estimation of non-ideal effects (q. v.).

#### 4.3 Molecular Sieve Chromatography

Gel filtration techniques have been widely used as a biochemical tool for the fractionation and characterization of biological macromolecules. When dry particles of a cross-linked dextran are equilibrated with solvent, they swell to form a gel into which salt ions and other small molecules may diffuse freely while larger molecules are impeded from entering the gel by steric hindrance. Penetration of the gel is therefore dependent on molecular size and fractionation of macromolecules can be achieved on this basis. For small globular proteins the molecular weight is proportional to the molecular size. The molecular weights of such proteins can therefore be estimated from their elution positions using a calibrated gel filtration column. Andrews (1964) has demonstrated empirically that a linear relationship exists between the logarithm of the molecular weight of globular proteins and their elution volume. For fibrous, asymmetric proteins no such relationship exists, indicating that calibration of a gel filtration column using molecular weights is only valid for spherical proteins. A more rigorous method of calibration of gel filtration columns has been proposed by Steere and Ackers (1962), based on the Stokes radius,  $a$ , of standard proteins. Characterization of the gel filtration behaviour of an eluted macromolecule can be conveniently defined in terms of the molecular sieve coefficient,  $\sigma$ . Ackers (1964) has shown that  $\sigma$  may be calculated from the equation:-

$$\sigma = \frac{V_e - V_o}{V_i}$$

where  $V_e$  = the elution volume of the macromolecular species

$V_o$  = the void volume of the gel

$V_i$  = internal volume of the gel

Details of the method proposed by Ackers (1964) to calibrate a gel filtration column in terms of the Stokes radius,  $a$ , and the molecular sieve coefficient,  $\sigma$ , are given in Appendix 2(a).

In addition to the characterization of the molecular radius of discrete protein species, gel filtration analyses may be extended to the study of association protein systems. The fractionation of macromolecules on gel filtration columns may be considered analogous to the fractionation achieved by other transport methods, such as sedimentation velocity (q. v.). Mathematical analysis of associated protein systems derived for other transport methods can, therefore, be applied with only minor modification to gel filtration studies. The association of  $\alpha$ -chymotrypsin has been investigated by Winzor and Scheraga (1963, 1964) on gel filtration columns using mathematical treatments originally applied to sedimentation velocity experiments (Gilbert, 1959; Gilbert and Jenkins, 1956). The equilibrium of an associating system is concentration - dependent (Winzor and Nichol, 1965; Adams and Fujita, 1963). To enable gel filtration studies of associating protein systems to be carried out at constant concentration, Winzor and Scheraga, (1963) introduced the practice of applying large sample volumes to a gel filtration column so that the elution profile contains a plateau region in which the concentration equals that initially applied. For an associating system, the extreme concentration dependence of the molecular sieve coefficient arising as a result of the



association causes the trailing boundary of the plateau region to be diffuse (Ackers and Thompson, 1965). The centroid of such a boundary has been shown to move with constant velocity and the molecular sieve coefficient corresponding to the centroid has been defined as the weight average molecular sieve coefficient,  $\sigma_w$ , of the associating systems (Ackers and Steere, 1967). Mathematical theories based on the use of  $\sigma_w$  have been developed to analyse associating systems. (Ackers, 1967 a,b; 1968; 1970; Brumbaugh and Ackers, 1968; Zimmerman and Ackers, 1971).

In an extension of the basic theories of Ackers (1967), Chun, Kim, Stanley and Ackers, (1969) have shown that molecular sieve coefficient data from gel filtration experiments can be combined with molecular weight data from sedimentation equilibrium studies of associating protein systems (q.v.) to yield information on the shape of the aggregate. Details of their analysis are described in Appendix 2(b).

#### 4.4 Analytical Ultracentrifugation

Analytical ultracentrifugation is one of the most powerful analytical tools available for the study of biological macromolecules. Because of the importance of the technique, a brief review of the development of the instrument and of the theoretical analyses used in analytical ultracentrifugation will be presented.

The science of analytical ultracentrifugation was founded in the 1930's with the introduction by Svedberg of a turbine-driven ultracentrifuge equipped with Schlieren optics (Svedberg and Pedersen (1940)). Turbine driven instruments have since been superceded by commercially available electrically-powered ultracentrifuges capable of generating large centrifugal forces of up to 100,000g. A disadvantage

of the Schlieren optical system used in early machines was that large amounts (milligram quantities) of sample were required. The sensitivity of the instrument was considerably increased, however, by the use of optical systems based on the Rayleigh interference system, capable of analysing sedimenting species at concentrations as low as 250µg/ml (Klainer and Kegeles, 1956). Even greater sensitivity was provided by an absorption optical system and the automation of this optical system by Schachman, Gropper, Hanlon and Putney (1962) has represented a major technical advance. A photo-electric scanning system formed the basis of the automated system and recently equipment has become available to permit direct linkage of the scanning system with a computer, thus enabling large quantities of experimental data to be processed quickly and accurately.

As a result of these technical innovations, the ultracentrifuge has become a powerful analytical tool, prompting the concurrent development of theoretical analyses of ultracentrifugal processes. The principal application of the ultracentrifuge in early studies was the determination of the molecular weight of biological materials using the sedimentation diffusion method which involved separate experimental determination of the sedimentation coefficient,  $s$ , and the diffusion coefficient,  $D$ , of the macromolecule being studied.  $S$  was evaluated from the net rate of movement of a sedimenting boundary using the equation:-

$$S = \frac{1}{w t} \cdot \frac{d(\ln r)}{dt}$$

where  $w$  is the angular velocity

$t$  is time of sedimentation

$r$  is the distance of the boundary  
from the centre of rotation

$D$  was determined by establishing a synthetic boundary between a solution of the macromolecule and pure solvent and measuring the rate at which the two phases diffused into each other. Combination of  $S$  and  $D$  gave the Svedberg equation for the determination of molecular weight

$$M = \frac{RTs}{D(1 - \bar{V}_p \rho)}$$

where  $M$  is the molecular weight of the macromolecule

$R$  is the gas constant

$T$  is the absolute temperature

$\bar{V}$  is the partial specific volume of the macromolecule  
and  $\rho$  is the density of the solution

Determination of molecular weights of macromolecules by this sedimentation-diffusion method has now been largely superceded by the use of sedimentation equilibrium techniques. Sedimentation equilibrium is the equilibrium state achieved between the centrifugal force of sedimentation and the centripetal diffusion force and the technique is consequently thermodynamically rigorous. The basic equation of sedimentation equilibrium in a two component system, (Williams, Van Holde, Baldwin and Fujita, 1958) is:-

$$\frac{1}{c} \frac{dc}{dr} = \frac{M}{RT} \frac{(1 - \bar{V}_p)w^2 r}{\left(1 + c \left(\frac{d \ln y}{dc}\right)\right)}$$

where  $c$  = concentration of solution

$r$  = distance from centre of rotation

$\bar{V}$  = partial specific volume of the macromolecule

$\rho$  = density

T = absolute temperature

and R = the gas constant

$y_2$  is defined in terms of the activity and the concentration of the solution by  $y_2 = a_2/c_2$ . When the activity coefficient term in the above equation is omitted, the equation reduces to:-

$$M_{wapp} = \frac{2RT}{(1 - \bar{V}_\rho)\omega} \lambda \frac{d \ln c}{dr^2}$$

The photo-electric scanning system yields data in a form which permits direct evaluation of  $M_{wcellapp}$ , the whole cell weight average apparent molecular weight, using the gradient of a straight line fitted through a plot of  $\ln c$  vs.  $r^2$ . The apparent weight average molecular weight at each point in the  $\ln c$  vs.  $r^2$  data may be evaluated by fitting curves to successive groups of data points to obtain the gradient of the  $\ln c$  vs.  $r^2$  curve at each point.

The Rayleigh optical system has also been used in the sedimentation equilibrium determination of molecular weights of proteins but suffers from the disadvantage that since the concentration at any point in the cell is simply proportional to the number of Rayleigh fringes at that point, correlation of the number of fringes with absolute concentrations has to be separately determined. Yphantis (1964) has, however, described a form of the sedimentation equilibrium technique which enables a direct correlation of concentration with fringe number. By operating the ultracentrifuge at speeds higher than those normally used for the attainment of sedimentation equilibrium, the concentration of solute at the meniscus is reduced to zero and so provides a reference point in the cell where the concentration is known exactly. Separate correlation

of fringe number with concentration is therefore unnecessary. Archibald (1947) showed that after a short time of sedimentation there was no net transport of solute in the region of the meniscus or at the bottom of the cell, that is, the protein in these areas existed in a state of sedimentation equilibrium. The molecular weights of the macromolecules could therefore be evaluated by application of the sedimentation equilibrium equations to these areas. The 'Approach to Equilibrium' method of Archibald has the advantage that molecular weights can be determined quickly. The use of short columns in standard sedimentation equilibrium experiments has reduced substantially the time needed to attain equilibrium and so eliminates the need for the approach to equilibrium method.

The determination of the molecular weights of biological materials by ultracentrifuge techniques has been reviewed by Bowen (1970), Williams (1963) and Creeth and Pain (1967).

Numerous biological materials cannot be obtained as homogeneous discrete species whose molecular weight can be determined using the techniques described above. Heterogeneity may be a result of simple polydispersity or of self-association processes. Polydispersity in a macromolecular sample may be considered as the presence of distinct forms of the macromolecule between which no inter-conversion is possible. In an associating system, distinct macromolecular species are present in a dynamic equilibrium. Ultracentrifuge analyses are available to characterize both systems.

#### 4.4.1 Ultracentrifugal Analysis of Polydispersity

Sedimentation velocity ultracentrifugation is particularly useful for providing information about

the heterogeneity of sedimenting species.

Schumaker and Schachman (1957) introduced a distribution function  $g(s)$  to define the distribution of species of different sedimentation coefficients across a sedimenting boundary. They showed that the distribution function could be normalized by a process of summation and division to yield:-

$$g(s) = \frac{1}{c_o^{obs}} \frac{dc_o^{obs}}{dS_{20,w}} = \frac{\frac{\Delta C_o^{obs}}{\Delta S_{20,w}^o} \left(\frac{x}{x_o}\right)^3}{\sum \frac{\Delta C_o^{obs}}{\Delta S_{20,w}^o} \frac{x}{x_o}}$$

where  $\overline{\Delta S_{20,w}^o}$  is the average of the largest and smallest values of  $S_{20,w}^o$

$x$  is the distance from the axis of rotation

$x_o$  is the distance of the meniscus from the axis of rotation

The values of  $S_{20,w}^o$  were calculated at each point across the sedimenting boundary from the expression:-

$$S_{20,w}^o = \frac{(1 - v \rho_{20,w})}{(1 - v \rho)} \left( \frac{\eta}{\eta_{20,w}} \right) \frac{2.303}{w t} \log \frac{x}{x_o}$$

The above expression for  $g(s)$  assumes that the boundary spreading is due solely to the distribution of  $S$  values, in other words that there is no broadening of the sedimenting boundary due to diffusion, no effects of concentration and pressure dependencies of sedimentation coefficient. Creeth and Pain (1967) have pointed out that caution must be exercised in assessing derivative curves of a

3.

sedimenting boundary in terms of the degree of heterogeneity since there are several cases of associating systems where a single symmetrical pattern may be obtained. The review by Nichol, Bethune, Kegeles and Hess (1964) gives a full account of the theory and application of transport phenomena to the study of heterogeneous and chemically reacting systems.

#### 4. 4. 2 Ultracentrifugal Analyses of Associating Protein Systems

Sedimentation velocity experiments, successfully used by Schumaker and Schachman (1957) and Schumaker, Richards and Freer (1967) in the study of polydispersity of macromolecular samples, have also been used in the investigation of chemically reacting systems. For associating systems in which the reaction time is short relative to the period of the experiment, the theoretical analysis proposed by Gilbert (Gilbert, 1955, 1959; Gilbert and Jenkins, 1956, 1959) has made it possible to predict the shape of the sedimenting boundary and also enable estimation of the extent of the association and of the equilibrium constant involved. The Gilbert and Jenkins theory also predicts that, under certain circumstances, a single symmetrical boundary gradient curve may be observed when there are more than one sedimenting species present, illustrating the need for caution in interpretation of sedimentation profiles. The theory suffers from the disadvantage that certain restricting simplifications have been introduced

3.

and also from the fact that the pressures generated by the high speeds used in velocity centrifugation can affect the equilibrium of associating protein systems. (Fujita, 1956).

For these reasons, sedimentation equilibrium has been the method of choice for investigation of associating protein system and numerous mathematical methods have been developed to this end (Adams, 1964; Adams and Williams, 1964; Adams, 1965; Adams and Filmer, 1966; Adams, 1967 a, b, c; Sophianopoulos and Van Holde, 1964; Teller, Horbett, Richards and Schachman, 1969; Roark and Yphantis, 1969; Chun and Kim, 1970; Chun and Kim, 1969; Haschemeyer and Bowers, 1970).

Characterization of an associating protein system requires the elucidation of the species present and determination of the equilibrium constants of the formation of these species. Two general approaches have been adopted, one involving a direct evaluation of the molecular weight distributions of the polymer, the other requiring the evaluation of molecular weight averages (q. v.).

The former approach is the one developed by Haschemeyer and Bowers (1970). They have shown that discrete molecular weight distributions of associating protein systems in sedimentation equilibrium can be characterized when the concentration as a function of radial position is expressed as a sum of exponential terms and have described computer evaluation of such



expressions. Using simulated data, Haschmeyer and Bowers (1970) found that in the presence of realistic experimental errors, acceptable results were provided by the analysis. Scholte (1968) has also successfully applied the technique of fitting continuous molecular weight distribution to an exponential equation in the case of a polydisperse sample. The method of analysis of associating protein systems by fitting exponential equations to continuous molecular weight distributions is theoretically capable of describing accurately any type of association whereas, as is pointed out by Scholte (1968), molecular weight averages cannot, in theory, describe completely accurately a molecular weight distribution. The fact that the technique of describing molecular weight distribution in terms of an exponential equation is currently only applicable to thermodynamically ideal systems is, however, a limitation of the method. Non-ideal effects arise because of steric and electrostatic interaction of species in solutions and can be defined in terms of an empirical constant, the second virial coefficient, B, which relates the concentration of a molecular species to its activity by the equation:-

$$\ln y = BM_1 c$$

where  $M_1$  is the molecular weight of monomer species

$c$  is the concentration

$B$  is the virial coefficient

$y$  is the activity of the species

The methods of analysis of associating protein systems developed by Adams (1967) incorporate estimation of the second virial coefficient, in contrast to the methods using exponential expression of molecular weight distributions. Average molecular weights used in the method of Adams are defined:-

$$\text{Number average molecular weight, } M_n = \frac{\sum n_i M_i}{\sum n_i}$$

$$\text{Weight average molecular weight, } M_w = \frac{\sum n_i M_i^2}{\sum n_i M_i} =$$

$$= \frac{1}{c} \sum c_i M_i$$

$$\text{Z-average molecular weight, } M_z = \frac{\sum n_i M_i^3}{\sum n_i M_i^2} = \frac{1}{M_w} \times \frac{\sum c_i M_i^2}{\sum c_i M_i}$$

The molecular weight of monomer,  $M_1$ , is also used in the Adams method and can be estimated by extrapolation of a plot of  $M_{wapp}$  vs.  $c$  to zero concentration. It is possible that the use of such techniques may result in inaccurate values of  $M_1$  due to the difficulties of obtaining reliable experimental data at low concentrations. Rowe and Rowe (1970) have described a graphical method which allows accurate determination of  $M_1$  for systems showing a linear dependence of  $M_{wapp}$  on concentration. Estimates of  $M_1$  from alternative methods may indicate the reliability of the value of  $M_1$  obtained by the method of Rowe and Rowe (1970). One such method is sedimentation in concentrated solutions of guanidine hydrochloride which dissociates completely

any macromolecular complexes. A drawback of this method is that the protein may bind significant amounts of guanidine hydrochloride. Amino acid analyses may also be useful in terminations of  $M_1$ .

Adams defined special parameters, or molecular weight moments, in terms of  $M_{wapp}$ ,  $M_{napp}$ ,  $M_{zapp}$  and  $M_1$  and concentration  $c$ , and used these molecular weight moments to construct specific equations based on these of Steiner (1954).describing non-ideal associating systems. These equations can be solved for  $BM_1$  using the techniques of successive approximation. This value of  $BM_1$  may then be used to compare experimentally obtained values of molecular weight moments with those predicted by the theoretical equations. The best fit of calculated and experimental values identifies the type of association. Verification of the type of association may be achieved by generation of  $M_{wapp}$  vs.  $c$  plots, using the theoretical equations, and comparison with the original molecular weight data. The Adams theory of the analysis of associating protein systems is described in detail in Appendix 1.

The theories of Adams have been successfully applied to studies of the dimerization of lysozyme (Sophianopoulos and Van Holde, 1964; Adams and Filmer, 1966; Deonier and Williams, 1970), to studies of the association of myosin (Godfrey and Harrington, 1970 a, b) and of purines (Van Holde, Rossetti and Dyson (1969)).

Several authors have described extensions and minor modifications of the basic theory. (Roark and Yphantis, 1969; Chun et al., 1969; Chun and Kim, 1969; Teller (1970); Deonier and Williams (1970)). A particularly simple method of analyzing associating protein systems has been described by Chun and Kim (1970) based on the use of the weight fraction of monomer,  $f_1$ . They found that plots of  $M_w/M_1$  vs.  $f_1$ ,  $M_1/M_n$  vs.  $f_1$ ,  $M_w/M_1$  vs.  $1/\sqrt{f_1}$  and  $\frac{d(M_w/M_1)}{df_1}$  vs.  $\frac{d(M_1/M_n)}{df_1}$

generated theoretical curves for ideal associating systems. The Chun and Kim graphical method has the advantage of being very easily applied, although it is limited to consideration of ideal systems. For this reason, it is useful as a preliminary analysis to identify the type of association being studied.

The application of the theories of Adams and of Chun and Kim to the study of the self-association of GAR histone will be described in the Results Section of this thesis.

## 5. Hydrodynamic Characterization of DNA

The previous section has described methods used for the study of the physiochemical properties of proteins, which may be applied to the characterization of the histone components of chromatin. Knowledge of the physicochemical properties of DNA is also necessary to the understanding of the structure and function of nucleohistone complexes.

Mammalian DNA is very large and heterogeneous and is consequently difficult to characterize precisely. Sucrose density gradient centrifugation has been used by Schumaker, Richards and Freer, (1965) in an attempt to fractionate the DNA. They showed, however, that the DNA in fractions produced by this method still exhibited considerable heterogeneity. Estimation of the distribution function  $g(s)$  (Schumaker and Schachman, 1957) from boundary sedimentation velocity experiments was found to be useful in characterizing such heterogeneity. The large size of DNA has precluded the use of absolute methods of determination of molecular weight, such as sedimentation equilibrium and sedimentation-diffusion. Much effort has been devoted, therefore, to the establishment of 'relative' methods which could correlate the molecular weight of the DNA with its hydrodynamic behaviour.

Viscometry is a particularly useful hydrodynamic method for the characterization of DNA. The introduction of rotating cylinder viscometers which produce low shear stresses (Zimm and Crothers, 1962) is a significant technical improvement which has increased the accuracy of determination of the relative viscosity ( $\eta$ ), of DNA. Sedimentation velocity has also been used to characterize DNA. The introduction of the photo-electric scanning system (Schachman, 1963 a, b) enables the measurement of the sedimentation coefficient,  $s$ , of DNA, using only microgram amounts.

The absolute values of the molecular weight of DNA needed for the establishment of empirical relations of the molecular weight with  $S$  and ( $\eta$ ) have been obtained by using homogeneous preparation of viral DNA whose contour lengths may be measured directly in the electron microscope. The molecular weights of DNA preparations can also be estimated from a theoretical analysis of the width of a band of DNA at buoyant equilibrium in a density gradient (Schmid and Hearst, 1969).

32

The correlation of  $S$  and  $(\eta)$  with the molecular weight of DNA has been studied by Crothers and Zimm (1965) who deduced that the optimal empirical equation for native, double stranded DNA is:-

$$0.455 \log_{10} M = 1.819 + \log_{10} (S^{-2.7})$$

Correlation of  $S$  and  $\eta$  with the M. W. of DNA not only permits the rapid evaluation of the molecular weights of unknown DNAs but also yields information on structural parameters of the molecule. Such information has led to the conclusion that the double helix is a rigid rod over short distances, behaves like a weakly bending rod over several hundred angstroms and becomes very flexible over longer distances. (Bloomfield, 1968). Because of this behaviour, DNA has been described as a wormlike coil.

The heterogeneous nature of mammalian DNA has made detailed investigation of its hydrodynamic properties difficult. In contrast to mammalian DNA, circular DNA isolated from certain viruses is more homogeneous, thus permitting detailed characterization of its hydrodynamic properties. Because of a deficiency in the number of duplex turns, such circular DNA species adopt a supercoiled structure (Vinograd and Lebowitz, 1966). Release of the strain in these molecules by the introduction of single-stranded nicks causes them to form a relaxed circular duplex, which sediments at a slower rate than the supercoiled structures. The techniques of band sedimentation introduced by Vinograd, Bruner, Kent and Weigle (1963) have provided a convenient method for the comparison of the sedimentation properties of the two forms of circular viral DNA. Molecular weights of the DNA can be evaluated from the sedimentation coefficients of the two species using empirical equations derived for each form of the DNA by Gray, Bloomfield and Hearst (1967) and Hudson, Clayton and Vinograd (1968).

The formation of complexes of histones with the two forms of small circular DNA may provide a useful model system for analysis of the shape and conformation of mammalian chromatin.

6. Aim of Experimental Studies Carried Out

To allow meaningful interpretation of the physicochemical characterization of GAR-DNA complexes, the individual components of the nucleoprotein complex were studied separately. The properties of GAR histone were analyzed at different salt concentrations and pH. Shapes of the protein aggregates were studied using molecular sieve chromatography. To study the effects of binding different histone aggregates to DNA, the physicochemical properties of DNA-histone complexes were investigated, using different forms of DNA.

## MATERIALS AND METHODS



1. MATERIALS

1.1 Biochemicals

2X crystallized bovine serum albumin was obtained from Armour Pharmaceutical Co., Eastbourne, Sussex. Cytochrome C, ribonuclease A, lysozyme and haemoglobin were purchased from Sigma Chemical Co., St. Louis, Missouri, U.S.A. and a chymotrypsin was obtained from Seravac Laboratories, Maidenhead, England. Myoglobin and chymotrypsinogen were obtained from Mann Research Laboratories, New York, N.Y., U.S.A. Spermidine phosphate was purchased from Sigma Chemical Co.

1.2 Chemicals

CsCl (optical grade) was obtained from the Harshaw Chemical Co., Cleveland, Ohio, U.S.A. Urea (Ultra-pure grade) was purchased from Mann Research Laboratories, New York. All other chemicals were of 'ANALAR' grade and were obtained from British Drug Houses Biochemicals, Poole, Dorset.

1.3 Organic Chemicals

1.3.1 Stains

Amido Black was obtained from Edward Gurr and Sons, London, England.

1.3.2 Polyacrylamide gel reagents

Acrylamide was purchased from Koch-Light

Laboratories, Colnbrook, Bucks; N', N  
methylene bis-acrylamide from B. D. H.  
Laboratory Chemicals Division, Poole,  
Dorset, and N, N, N', N' tetramethylethylenediamine (TEMED) from Eastman Organic  
Chemicals, Rochester 3, New York, U.S.A.

#### 1.3.3 Intercalating Dyes

Ethidium bromide (EB) was obtained from  
Calbiochem, Los Angeles, U.S.A.

#### 1.4 Dialysis Tubing

Dialysis tubing used was Visking tubing sizes 8/32",  
18/32" and 36/32". The tubing was boiled five times in  
0.15M EDTA, pH 8.0 and five times in distilled water  
prior to use.

#### 1.5 Ultrafiltration

A Model 50 ultrafiltration cell (Amicon Industries,  
Inc., Cambridge, Mass., U.S.A.) was used for  
concentration of dilute histone solutions using a UM-2  
membrane with a molecular weight cut-off of 1000 under  
a pressure of 50 p. s. i. of nitrogen.

#### 1.6 Buffers

Dilute McIlvaine buffers of constant low ionic strength  
(0.005M) were prepared by direct weighing of the relevant  
constituents (Elving, Markowitz and Rosenthal, 1956).

Buffers were prepared as 10 times or 100 times concentrates,  
were sterilized by autoclaving and were stored at 4°C. The  
pH of the buffers was checked after dilution.

## 1.7 Materials for Column Chromatography

Sephadex G100, G25 and Blue Dextran 2000B were supplied by Pharmacia Fine Chemicals (U. K.) Ltd., London. Cellulose nitrate was obtained from B. D. H. Laboratory Chemicals Division, Poole, Dorset. The cellulose nitrate was suspended in 2XSSC and homogenized for about 1 min at top speed in an MSE Ato-mix to produce a fine slurry. A column of final height 4 inches was poured under gravity in a previously sterilized glass column of diameter 1" fitted with a sintered base. About 500ml of sterile 2XSSC was washed through the column prior to use to remove any UV-absorbing contaminants.

## 1.8 Biological Material

A plaque-purified strain of SV40 virus was supplied by Dr. J. Williams, Institute of Virology, Glasgow University.

Fresh calf thymus glands were obtained from the Veterinary Department, Corporation of Glasgow Markets Department and were immediately deep frozen and stored at  $-70^{\circ}\text{C}$  until used. In no case were glands stored for periods longer than 3 months.

Calf thymus DNA lot No. 71A was obtained from the Worthington Biochemical Corporation, Freehold, New Jersey, U. S. A.

African green monkey kidney cells (BSC-1) (Flow Laboratories Ltd., Irvine, Scotland) were grown in mono-layer cultures on glass in an atmosphere of 5%  $\text{CO}_2$  in air. Minimal Eagles medium supplemented with 10%

foetal calf serum (Flow Laboratories Ltd., Irvine, Scotland) was used as growth medium. Monolayer cultures of BSC-1 cells in plastic petri dishes (NUNC, Denmark, 90mm X 4mm) were infected with SV 40 virus as described by Rush, Eason and Vinograd (1971). Seven days after infection, cells were scraped from the dishes and the suspension was centrifuged at 1000g for 10 min at 4°C. The infected cell pellet was stored at -20°C.

## 2. METHODS

### 2.1 Purification of the Glycine Arginine Rich Histone

The Glycine Arginine rich (GAR) histone (histone IV in the nomenclature of De Lange et al. (1968)) was purified from calf thymus by the method of Starbuck et al. (1968). This method uses as a preliminary purification step the method of Johns (1964) to separate the histones of calf thymus chromatin into fractions of similar amino acid composition. 100g of calf thymus glands were thawed in 0.15M NaCl and attached fatty or muscle tissue was removed. The glands were partially minced by scissors and homogenized in 500ml ice-cold 0.15M NaCl in a Waring Blender for 5 min at full speed. The chromatin was pelleted by centrifugation at 1110g for 30 minutes in an MSE medium centrifuge at 4°C and was then washed five times by dispersing the chromatin in 400ml ice-cold 0.15M NaCl in a Waring Blender at half speed for 2 min, followed by centrifugation in an MSE medium centrifuge at 4°C for 15 min at 1100g. The washed pellet of chromatin was then dried by dispersing the chromatin in 400ml of ice-cold EtOH; H<sub>2</sub>O (90:10 by volume). The histones of the chromatin thus prepared were

fractionated by extraction with 400ml ice-cold 1.25N HCl: EtOH (1:4 by volume) in a rotating bottle at 4°C overnight, a procedure which selectively removed the arginine rich class of histones, comprising fractions  $F_3$  and  $F_2A$ . These two fractions were removed from the remaining insoluble chromatin by centrifugation at 1100g and were separated by dialysis against several changes of 100% EtOH at 4°C for 16h. The Arginine-lysine (AL) rich histone ( $F_3$  in the nomenclature of Johns (1964)) was precipitated by this treatment. Acetone precipitation of the soluble  $F_2A$  fraction as suggested by Johns (1964) was avoided because of the risk of degradation; instead the fraction containing histone  $F_2A$  was dialysed against several changes of 0.01M HCl and concentrated to a small volume on a Model 50 Ultrafiltration cell fitted with a UM2 membrane (molecular weight cut-off 1000). The histone fraction obtained by this method is heterogeneous (Starbuck et al., 1968; Johns, 1964); both GAR histone and arginine-lysine (AL) rich histone are present.

To ensure complete dissociation the crude histone fraction was left overnight at 4°C in 6M urea, 0.01M HCl. Separation of the two discrete molecular species present in the crude fraction was achieved by gel filtration chromatography on Sephadex G100, previously equilibrated with 0.01M HCl, as described by Starbuck et al. (1968). Separation of the two histone species which differ in molecular weight by about 6000 daltons, was achieved using two 100mm X  $2\frac{1}{2}$  cm diameter columns connected in series by a flow adaptor (Pharmacia Fine Chemicals (U. K.) Ltd.)). A perpex pump (LKB Scientific Instruments Ltd.)

was used to produce a constant flow rate of 12ml/h. Because of cross-contamination between the peaks corresponding to AL and GAR histones, peaks were pooled, concentrated by ultrafiltration and re-chromatographed. The resulting pure species of histone were then chromatographed separately on a 20cm X 1.5cm diameter column of Sephadex G25, previously equilibrated with 0.01M HCl, to remove any low molecular weight constituents. Pure GAR and AL stocks were rapidly frozen using a Drikold/ethanol freezing mixture and were stored at  $-70^{\circ}\text{C}$  till required.

## 2.2 Polyacrylamide gel electrophoresis of purified histone species

Analysis of purified histone species by polyacrylamide gel electrophoresis was carried out according to the method of Fambrough and Bonner (1969), which is based on the method of Reisfeld, Lewis and Williams (1962).

Stock solutions were made up as follows:-

### 1. Stock acrylamide solution

60g acrylamide	)	
4g bis-acrylamide	)	in 100ml $\text{H}_2\text{O}$

### 2. Stock TEMED solution

4ml pure TEMED	)	made up to
48ml 1N KOH	)	100ml by
17.2ml glacial acetic acid	)	distilled water

A gel solution was made by adding 2 vols. of stock TEMED to 1 vol. of stock acrylamide and adding 1 vol. of a freshly made solution of 1% ( $^{\text{W}}/\text{v}$ ) of ammonium persulphate (APS) in distilled water. The gel solution was poured into

4 $\frac{1}{2}$ " X  $\frac{1}{4}$ " diameter glass tubes and left for 30 min to allow polymerisation to take place. 0.4M glycine, pH 5.0 was used as electrode buffer. Histone samples in a volume of not greater than 0.2ml were made dense relative to the electrode buffer by the addition of a few crystals of solid sucrose and were applied directly to the top of the gel column through the electrode buffer using a 1ml syringe. Electrophoresis was carried out for 3 or 5h at a constant current of 3mA/gel, after which time the gels were removed from the glass tubes by rimming the tubes with a syringe needle. The gels were stained by immersion overnight in a 1% ( $^W/v$ ) solution of Amido black in 7% ( $^V/v$ ) acetic acid solution and were destained electrophoretically in a 7% ( $^V/v$ ) acetic acid solution.

### 2.3 Amino-acid analysis of purified histone species

Total amino acid analyses were carried out on a JEOLCO type JLC-5AH amino acid analyser (Japan Electronics and Optical Co., Ltd.). Histone samples were exhaustively dialysed against 0.01M HCl, lyophilized and hydrolyzed in constant boiling 6N HCl in sealed tubes at 110 $^{\circ}$ C for 20h. The HCl was removed by rotary evaporation under reduced pressure and the remaining hydrolyzate was dissolved in the starting buffer of the amino acid analyzer. Amounts of hydrolyzate applied were such that the amount of any individual amino acid was never greater than 100n moles. No corrections were made for hydrolytic losses. Amide N was not determined.

### 2.4 Isolation of intracellular SV40 DNA

Intracellular covalently closed SV40 DNA (form I) was

isolated from SV40-infected BSC-1 cells by the technique of selective alkaline denaturation as described by Rush, Eason and Vinograd (1971), which is based on that of Rush and Warner (1970). About 1g of frozen SV40-infected BSC-1 cells were suspended in 50ml of 0.1% (<sup>W</sup>/v) sodium dodecylsulphate, 0.15M EDTA (pH 8.0). The pH was adjusted to 12.2 by dropwise addition of 1N NaOH and was maintained at that pH at room temperature for 3 min with vigorous stirring. The pH was then adjusted to 7.5 by dropwise addition of 1N HCl and the precipitate thus formed was removed by centrifugation at 15,000g for 10 min at 4°C in an MSE 18 centrifuge. The resulting supernatant was then incubated at 80°C for 3 min with RNase at a final concentration of 10µg/ml. The precipitate formed was removed by centrifugation in an MSE 18 centrifuge at 4°C and the supernatant was concentrated by rotary evaporation under reduced pressure at 25°C to a final volume of about 20ml. The material was then chromatographed on a 100cm X 2½cm diameter Sephadex G100 column at 4°C, using 2 X SSC as eluting buffer. The Sephadex had previously been freed of contaminating nucleases by autoclaving. The eluate was collected in 5ml aliquots in sterile fraction collector tubes and the excluded volumes were pooled and passed through a nitrocellulose column which retained alkali-denatured, single-stranded material. The eluate contained closed circular duplex DNA and was concentrated by rotary evaporation at 25°C. Care was taken throughout the preparation to maintain sterility in order to minimize any nuclease contamination. Small amounts of circular duplex DNA with one or more single strand breaks (Form II DNA) were detected by band sedimentation in the



analytical ultracentrifuge (q. v.). The presence of Form II DNA is attributable to the introduction of single-stranded breaks into closed circular duplex DNA during the preparation. Closed circular duplex DNA and nicked circular DNA were resolved using CsCl-ethidium bromide equilibrium centrifugation. (Radloff, Bauer and Vinograd, 1967). DNA samples were centrifuged in CsCl gradients of initial density 1.55g/ml, containing 100µg/ml ethidium bromide for 40h at 20°C in an angle 40 rotor at 39,000 r.p.m. in a Spinco Model L Ultracentrifuge. Two fluorescent bands were visible on illumination of the tubes with ultraviolet light and were collected by direct tube puncture. Ethidium bromide was removed by extraction with a small amount of isoamyl alcohol. CsCl was removed by dialysis against SSC and the DNA samples were stored in sterile bijoux bottles at -20°C.

## 2.5 Preparation of GAR-DNA complexes

A convenient method for describing the relative amounts of DNA and histone used to form nucleoprotein complexes has been described by Shih and Bonner (1970), in which the molar concentration of the basic residues in the histone (Arg + Lys) is expressed as a fraction of the molar concentration of the phosphate residues present in the DNA to which the histone is bound. Alternatively, the composition of DNA-histone complexes may be described in terms of the relative weights of the macromolecular constituents.

GAR-DNA complexes were prepared at two pH values, 7.0 and 5.0, using the low ionic strength McIlvaine

type buffers described in Materials Section 1.6. Two methods were used to prepare GAR-DNA complexes - the salt gradient dialysis method described by Huang et al. (1964) and Olins et al. (1968) and by the method of direct mixing of the two constituents (Ansevin and Brown, 1971). Using the salt gradient dialysis method, samples of GAR and DNA in 0.7M NaCl at varying ratios of  $(\text{Arg} + \text{Lys})/\text{P}04^{\overline{=}}$ . The protein and DNA were mixed and dialyzed against 0.4M NaCl pH 7.0 for 4 hours. This was followed by dialysis for 1h against 0.15M NaCl and a further dialysis for 10h against 0.075M NaCl.

The method of directly mixing histone and DNA at low ionic strengths suffers from the disadvantage that precipitation of DNA occurs unless a low concentration of histones relative to DNA is used. The binding of histones at low  $(\text{Arg} + \text{Lys})/\text{P}04^{\overline{=}}$  was accomplished by the slow addition of histone solutions to DNA with vigorous agitation to avoid high local concentrations of histone.

## 2.6 Estimation of concentration of GAR histone solutions

The concentration of GAR solutions was determined from the value of the extinction coefficient at the wavelength of maximum absorbance (275nm). Experimental determinations of the extinction coefficient of GAR were obtained by exhaustive dialysis against distilled water followed by lyophilization. Accurately weighed amounts of lyophilized GAR protein were dissolved in accurately measured volumes of 0.01M HCl and the absorbance of the solutions read in an SP 500 spectrophotometer, with 0.01M HCl as a reference buffer. Several determinations were carried out and a mean value obtained.

A theoretical value of the extinction coefficient was determined from the amino acid composition of GAR by the method of Wetlaufer (1962).

## 2.7 Estimation of partial specific volume of GAR

Estimations of the partial specific volume of GAR were carried out using the technique of density perturbation sedimentation equilibrium in  $D_2O$  (Schachman and Edelstein (1966), Thomas and Edelstein (1971)). A series of sedimentation equilibrium experiments were performed in which the solvent density was varied by altering the amount of deuterium oxide ( $D_2O$ ) present. Objections to the theoretical validity of this approach have been raised by Reisler and Eisenberg (1969). Accordingly, a further estimation of the partial specific volume of GAR was made on the basis of a summation of the contributions to the overall partial specific volume, of the individual amino acids present in the protein molecule. The amino acid content of GAR protein as described by Starbuck et al. (1968) was used.

## 2.8 Analytical gel filtration chromatography

Analytical gel filtration chromatography was carried out on a Whatman 40cm X 1cm diameter glass column fitted with sintered end pieces or on a 6" X 3/8" diameter glass column. A slurry of Sephadex G100 (Pharmacia Inc., Uppsala, Sweden) was made in the appropriate buffer, "fines" were decanted and the slurry was degassed by partial evacuation. Equilibration was achieved by leaving the gel at room temperature overnight. The column was packed under gravity flow and the column was washed with several column volumes of buffer. Columns were run at

room temperature. Elution profiles were monitored using a LKB UVICORD flow absorptiometer (LKB Instruments Co., Uppsala, Sweden) equipped with a 277nm filter or by direct collection of 0.4ml fractions using a ISCO Model "T" fraction collector. The absorbance of the fractions was measured at 235nm in a UNICAM SP500 spectrophotometer. Calibration of the columns was carried out using the methods of Steere and Ackers (1969). Standard proteins used were cytochrome C, lysozyme, haemoglobin, and chymotrypsin, bovine serum albumin, myoglobin and chymotrypsinogen. The void volumes of the columns were determined from the elution volume of Blue Dextran 2000B and the internal volume was obtained from the elution volume of potassium dichromate. As described by Ackers (1967a, 1967 b) a more meaningful calibration of a column than a correlation of molecular weight with elution volume is the use of the Stokes radius,  $a$ , of the standard proteins. Values of  $a$ , the Stokes radius of the standard proteins used were taken from Tanford (1961). Values of  $\sigma$ , the molecular sieve partition coefficient as defined by Ackers (1967) were obtained from values of partition coefficient.

In order to study interacting protein systems using gel filtration techniques, large volumes of protein samples were applied to the Sephadex column, as described by Ackers and Thompson (1965). Large sample volumes ensure that on elution, a 'plateau' region is achieved at which the concentration of eluted protein is equal to that

of the applied sample. Initial sample volumes of 4ml - 10ml were routinely used to attain such constant elution concentrations. Values of the weight average partition coefficient,  $\sigma_w$ , at each of the plateau concentrations used were obtained from the trailing boundary of the plateau as described in Appendix 2.

## 2.9 Thermal Denaturation Studies

Melting profiles of DNA and DNA complexes were obtained using a UNICAM SP800 spectrophotometer equipped with an SP870 constant temperature cell accessory. Temperature measurements were made using a Pye "Scalamp" thermocouple galvanometer. Melting profiles were normally obtained at DNA concentration ranges corresponding to absorbances at 275nm of 0.6 - 1.0. Measurements of turbidity were monitored at 320nm.

## 2.10 Analytical Ultracentrifugation

All ultracentrifuge experiments were performed with a Spinco Model E analytical ultracentrifuge equipped with RTIC temperature control and a photoelectric scanning system. (Lamers, Putney, Steinberg and Schachman (1963)). Rotor speeds were controlled by an electronic rotor speed control system (Beckman Instruments Co.).

### 2.10.1 Two component equilibrium ultracentrifugation of GAR

All protein solutions for analysis were dialyzed overnight against the appropriate buffer to fulfil the requirements of Cassassa and Eisenberg (1964) concerning three component systems (Buffer ion, macromolecule, and solvent).

3.

The diffusate was used as a reference buffer. Experiments were performed with 12mm aluminium-filled epon double sector centrepieces. The sectors were loaded with protein solution and diffusate in the manner recommended by Adams (1967), using polyethylene syringe needles to minimize contact with metal. In all cases, the column heights in the solution sector were close to 0.3cm. No layering oils were used because of the possibility of interactions with the protein solution (Adams, 1967). Alignment of cells in the rotor was checked critically using a microscope aligning tool (Beckman Instruments Co.). Runs were allowed to proceed for at least 40h and usually longer. Scans were normally carried out at wavelengths which permitted measurable pen deflections to be recorded on the scanning system. The extinction coefficient of the protein at the scanning wavelength was used to relate absorbance to concentration of the protein using the calibration stair-steps produced by the scanning system.

#### 2.10.2 Analytical Band Sedimentation

Analytical band sedimentation runs were carried out by method of Vinograd, Bruner, Kent and Weigle (1963), using an aluminium-filled epon double sector band-forming centrepiece (Beckman Instruments Co.). 15 $\mu$ l of DNA solutions were introduced in the sample well and 0.35ml of bulk solvent (normally CsCl) in each sector. The rate of movement of the peak

maximum was used to calculate the sedimentation coefficient of the DNA. (Bruner and Vinograd, (1965).

### 2.10.3 Boundary sedimentation experiments

Experiments were carried out using 12mm aluminium-filled epon double sector centrepieces. During rotor acceleration, current to the drive was maintained at as constant a level as possible and the total time taken to obtain speed was noted. The time of any scan relative to the start of the run was always carefully noted.

## 2.11 Optical Rotatory Dispersion (ORD)

### 2.11.1 Determination of $\alpha$ -helix content of GAR histone

ORD spectra of GAR histone were obtained in three solvent conditions:- 0.075M NaCl/0.01M HCl, 0.15M NaCl, 0.01M HCl and 0.01M HCl. The concentration of histone used was such that the absorbance never exceeded 2.0.

ORD spectra were measured on a Bendix/Bellingham and Stanley Polarmatic G2 spectropolarimeter. The instrument was calibrated with sucrose (BDH-Analar grade) by the procedure of Yang and Samejima (1963).

### Treatment of ORD data

The rotation data were expressed in terms of

$[R]_{\lambda}$ , defined as:

$$[R]_{\lambda} = (\alpha)_{\lambda} \left( \frac{\bar{M}}{100} \right) \left( \frac{3}{n_{\lambda}^2 + 2} \right)$$

where  $[a]_{\lambda} = \frac{100 a_{\lambda}}{lc}$  and  $a_{\lambda}$  is the observed rotation in degrees

$l$  is the path length in decimetres of the col.,

$c$  is concentration in g/100ml

$\bar{M}$  is the mean amino acid residue weight which was determined for GAR from the amino acid composition of Starbuck et al. (1968) and was found to be 108.4. Rotations were reduced to the value they would have in vacuo, using the Lorentz correction factor  $\frac{3}{n_{\lambda}^2 + 2}$ ; where  $n_{\lambda}$  is the refractive index of the solvent. The variation of the refractive index of the solvent with wavelength, i. e. its dispersion, was taken into account in all measurements. The values of refractive indices at all wavelengths were approximated using the Sellmeir equation.

$$n^2 = 1 + \frac{a \lambda^2}{\lambda^2 - \lambda_v^2}$$

where  $n$  is the refractive index

$\lambda$  is the wavelength

and  $\lambda_v$  and  $a$  are coefficients to be determined.

The equation was solved for  $a$  and  $\lambda_v^2$  by substitution of known values of the refractive index at two wavelengths (Adler and Fasman, 1968).

The contribution to  $n_{\lambda}$  by the low protein concentrations used were assumed to be negligible.



The ORD spectra were analyzed by means of the Moffit-Yang and Schechter-Blout equations.

The Moffit-Yang equation is:

$$[R]_{\lambda} = \frac{a_o \lambda_o^2}{(\lambda^2 - \lambda_o^2)} + \frac{b_o \lambda_o^4}{(\lambda^2 - \lambda_o^2)^2}$$

$[R]_{\lambda} (\lambda^2 - \lambda_o^2) / \lambda_o^2$  was plotted against  $\lambda_o^2 / (\lambda^2 - \lambda_o^2)$  to yield  $a_o$  as the intercept and  $b_o$  as the slope. (Moffit and Yang, 1956).

$\lambda_o$  was assumed to be 212nm.

The Schechter-Blout equation is:

$$[R]_{\lambda} = \frac{A_{193} \lambda_{193}^2}{(\lambda^2 - \lambda_{193}^2)^2} + \frac{A_{225} \lambda_{225}^2}{(\lambda^2 - \lambda_{225}^2)}$$

To evaluate the coefficients  $A_{193}$  and  $A_{225}$   $[R]_{\lambda} (\lambda^2 - \lambda_{193}^2) / \lambda_{193}^2$  was plotted against  $\lambda_{225}^2 / (\lambda^2 - \lambda_{225}^2)$  and  $A_{225}$  calculated from the slope.  $A_{193}$  was calculated from the intercept of the above plot.

Helical contents were calculated according to Schechter and Blout (1964), and Schechter, Carver and Blout (1964). Helical contents are given by

$$H_{193} = (A_{193} + 750)/(36.5)$$

$$H_{225} = -(A_{225} + 60)/(19.9)$$

Using Moffit-Yang plots, assuming  $\lambda_o = 212\text{nm}$ , per cent helix is given by:

$$\% \text{ Helix} = -(b_o - 100)/8.00$$

The helix content of GAR was also measured by the method of Urnes and Doty (1961) from the experimentally obtained values of  $b_o$  using the equation:

$$\% \text{ Helix} = \frac{-b_o}{6.30}$$

## 2.12 Data Processing

Data processing and mathematical analyses were carried out using digital computer programmed in FORTRAN or ALGOL languages. Computers used were:-

UNIVAC 1108	-	National Engineering Laboratory, East Kilbride, Scotland.
ICL KDF9	-	University of Glasgow Computing Service, Glasgow.
DIGITAL PDP8L	-	Department of Biochemistry, University of Glasgow

## RESULTS

## RESULTS

In this section, the results of experimental investigations of the physico-chemical properties of one of the arginine-rich group of histones, the glycine-arginine rich histone (GAR), and of the properties of complexes formed between DNA and this discrete histone species will be described. Arginine-rich histones have been shown qualitatively to aggregate in salt conditions and it has been suggested that the presence of aggregates of these histones in vivo may affect the biological function of chromatin (Stellwagen and Cole, 1969; Edwards and Shooter, 1970). An initial aim of the present studies was to characterize the self-association properties of GAR histone on a rigorous, quantitative basis. Calf thymus was chosen as the source material of GAR histone preparations because of the relative abundance of the histone in this tissue. In addition, preparative techniques were available to enable the large-scale preparation of GAR in a discrete, homogeneous form from calf thymus tissue (Starbuck et al., 1968).

### 1. Purification and initial characterization of GAR histone from calf thymus tissue

Chromatin was prepared from calf thymus glands by homogenising approximately 100g of tissue in isotonic saline solution as described in Methods Section 2.1. The arginine rich class of histones ( $F_2A_1$ ) was isolated from the washed chromatin preparation by the selective extraction procedure of Johns (1964). Studies of the physico-chemical properties of such histone preparation have been carried out by Edwards and Shooter (1969) and have revealed that there are several discrete species of histones present. Current techniques for analysis and characterization of the physical properties of proteins generally require that the protein species be homogeneous. Accordingly, the arginine-rich class of histones obtained by the method of Johns (1964) was further purified by gel

filtration chromatography on Sephadex G100 as described in Methods Section 2. 1. The elution profile of a preparation of the  $F_2A_1$  class of histones on Sephadex G100 is shown in Fig. 1(a). It can be seen that the  $F_2A_1$  group of histones gives rise to 4 distinct peaks, one of which is eluted at a position close to the void volume. Starbuck et al. (1968) have obtained similar elution profiles and have shown by polyacrylamide gel electrophoresis that the peaks corresponding to fractions 119-130 and 150-168 are composed mainly of the arginine lysine rich histone (AL) and the glycine-Arginine rich histone (GAR) respectively, although there is minor cross-contamination between the peaks. Fractions 152-170 were pooled, concentrated and re-chromatographed. The resulting elution profile is shown in Fig. 1(b). Only one peak is obtained, eluting in a position similar to that of GAR. The fact that the peak is not symmetrical suggests that there may be some contamination by AL histone. Fractions 156-172 were pooled and aliquots containing about 20 $\mu$ g of protein were analyzed by polyacrylamide gel electrophoresis as described in Methods Section 2. 2. A typical gel is shown in plate 1. At the concentration of histone used, only one band is visible. Starbuck et al. (1968) obtained similar gel patterns and estimated that the histone was  $> 96\%$  pure. Prior to analysis, the preparation of GAR histone was chromatographed on Sephadex G25 to remove any low molecular weight contaminants not detected by polyacrylamide gel electrophoresis. The elution profile of GAR on G25 is shown in Fig. 1(c). Fractions 10-14 were pooled and concentrated.

Accurately weighed quantities of pure GAR protein were dissolved in known volumes of 0. 01M HCl and the absorbance measured. The average value of 4 estimations of the extinction coefficient obtained by this method was found to be 0. 397 with a standard deviation of  $\pm 0. 01$ . The extinction coefficient of pure GAR was also obtained

FIG 1 (a)

Elution profile of  $F_2A_1$  class of histones on a Sephadex G100 column 200cm X 2.5cm.

Histone fraction  $F_2A_1$  was isolated from 100g of calf thymus tissue by the selective extraction method of Johns (1964), as described in Methods Section 2.1. The proteins were dissociated in 6M urea/0.01M HCl for 36h at 4°C and applied to a 200 X 2.5cm Sephadex G100 column equilibrated with 0.01M HCl. 3ml fractions were collected and their absorbance at 275nm measured.

FIG 1 (b)

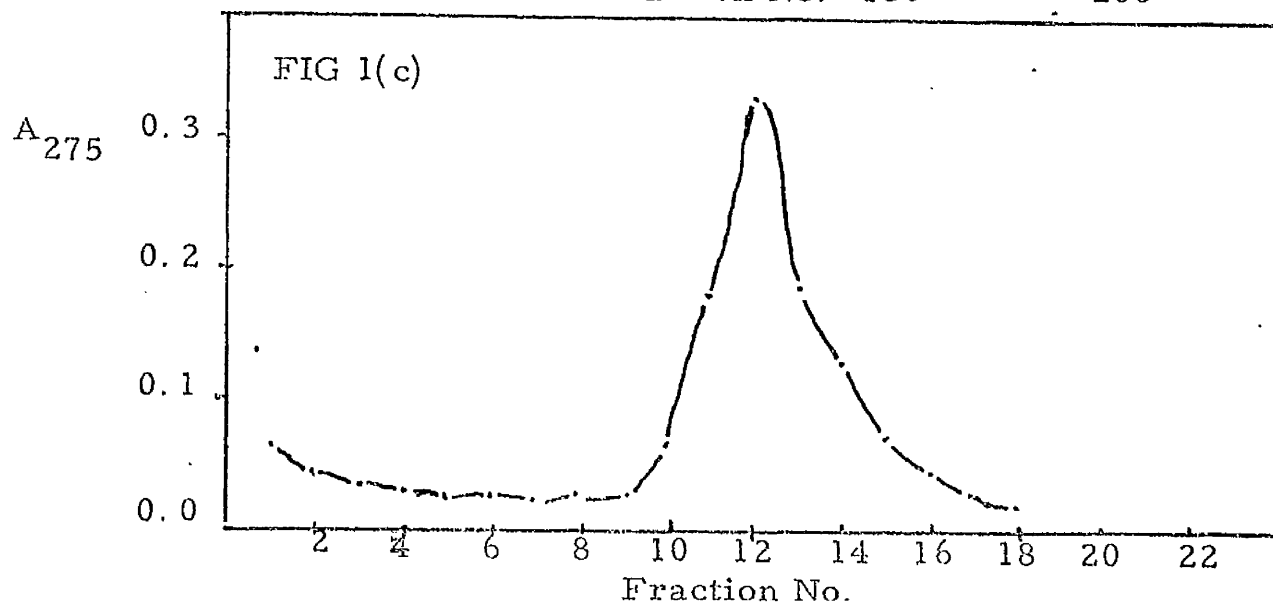
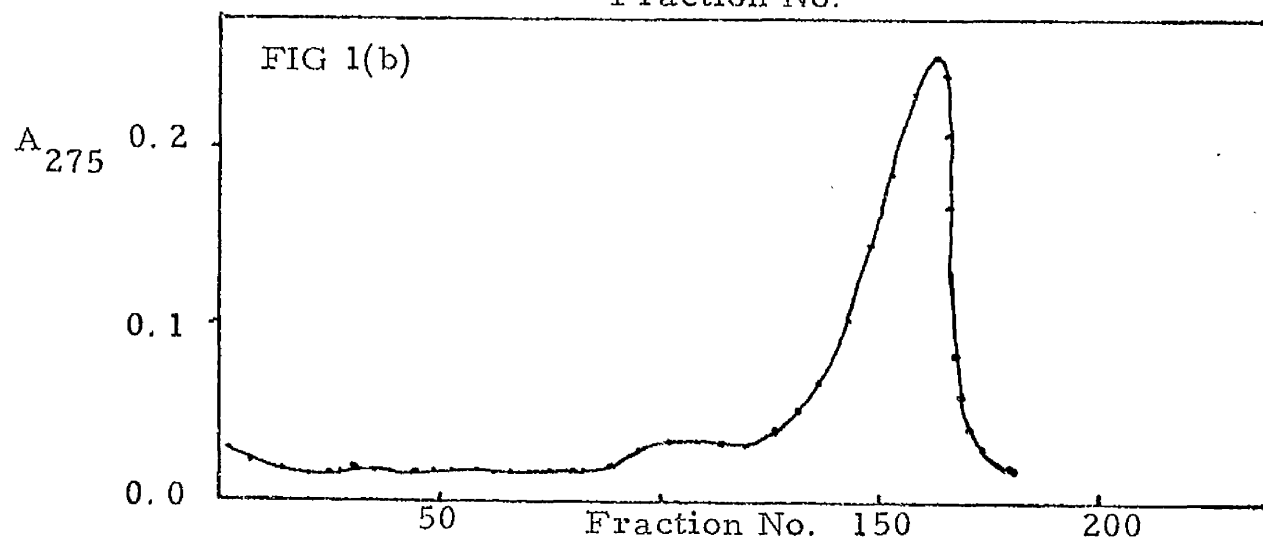
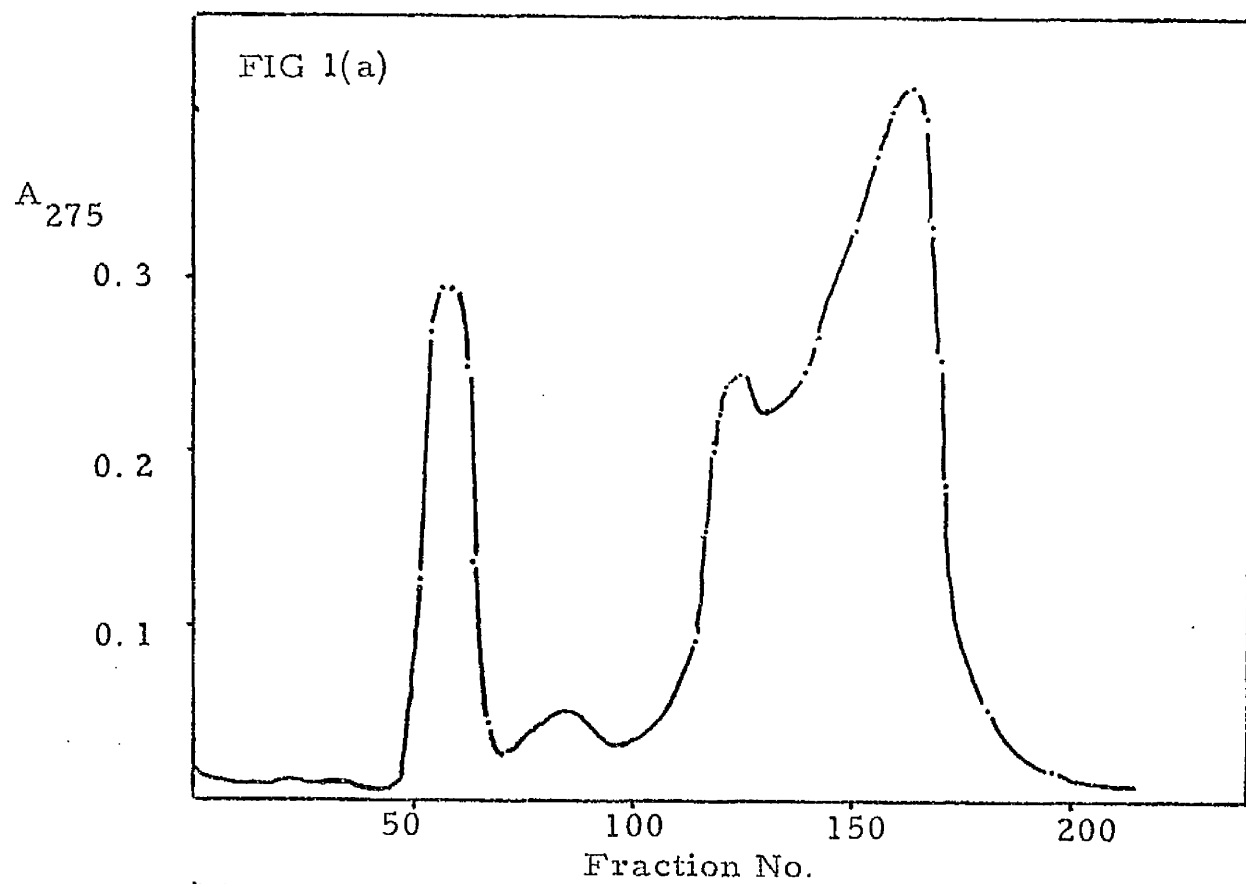
Elution profile of GAR histone on a 200 X 2.5cm G100 Sephadex column.

Histone fraction  $F_2A_1$  was chromatographed on a 200 X 2.5cm column of Sephadex G100 (Fig 1(a)). Fractions 150-168 were pooled, concentrated and re-chromatographed. 3ml fractions were collected and their absorbance at 275nm measured.

FIG 1 (c)

Elution profile of GAR histone on a 10 X 2.5cm Sephadex G25 column.

GAR was chromatographed on Sephadex G100 (Fig 1(b)), fractions 156-172 were pooled concentrated and re-chromatographed on a 10 X 2.5cm column of Sephadex G25. 2ml fractions were collected and their absorbance at 275nm measured.



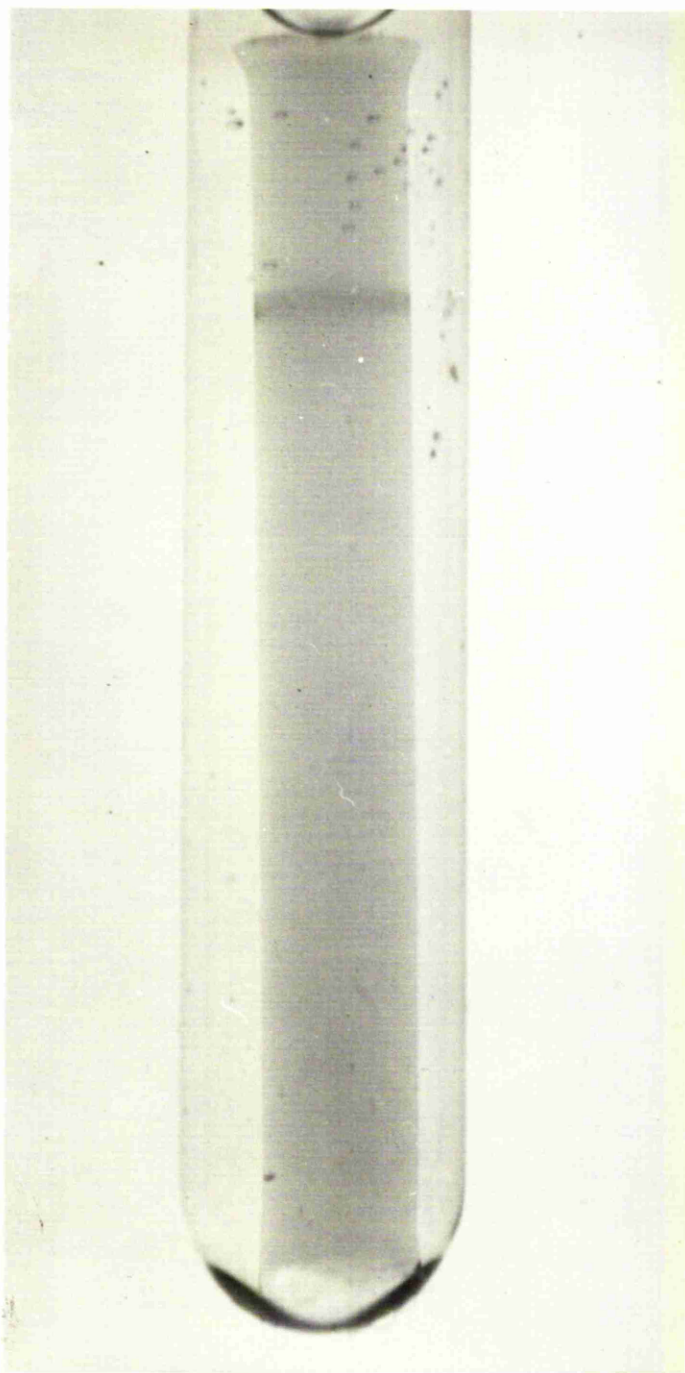
## PLATE 1

### POLYACRYLAMIDE GEL ELECTROPHORESIS OF GAR HISTONE

GAR histone was isolated from calf thymus by the method of Starbuck et al. (1968) as described in Methods Section 2.1. 0.2ml aliquots of GAR histone containing 20 $\mu$ g protein were applied to 7.5% polyacrylamide gels, with 0.4M glycine, pH 5.0 as electrode buffer. Electrophoresis was carried out for 3h at 3mA/gel. The gel was stained in 1% Amido Black and destained electrophoretically.



PLATE 1



from the absorbance of a solution whose concentration had been measured by the procedure of Lowry, Roseborough, Farr and Randall (1951), using standard solutions of BSA for calibration of the method, and found to be 0.236. The low value of the extinction coefficient obtained by this method compared to that obtained by the method of direct weighing is probably attributable to the abnormally low content of tyrosine residues in GAR histone, since the method of Lowry et al. (1953) is sensitive to the amount of tyrosine residues in a protein molecule. An additional check on the values of the extinction coefficient of GAR histone was provided by the calculation of the absorptivity of the GAR histone from its amino acid composition, according to the method of Wetlaufer (1962). The amino acid composition given by Starbuck et al. (1968) was used and the value of the extinction coefficient calculated to be 0.402. As pointed out by Wetlaufer (1962) this method is at best approximate, since local interactions between the amino acid residues of a polypeptide chain may affect significantly the absorptivity of the absorbing amino acid residues. The calculated absorbance of 0.402 at 275nm for a 1mg/ml solution of GAR nevertheless agrees well with the value of 0.397 obtained by the method of direct weighing, indicating that there is little secondary structure involving the amino acid chromophores (Wetlaufer, (1962)). The value of the extinction coefficient obtained by the method of direct weighing of GAR histone was used in all subsequent determinations of protein concentration. This value approximates to the extinction coefficient of 0.352 estimated for a 1mg/ml solution of whole histone at 275nm (Walker, 1965). The concentration of GAR histone was calculated from absorbance values at various wavelengths, using the UV spectrum of a solution of GAR of known concentration. The amino acid composition of GAR histone was estimated as described in Methods Section 2.3 and the average values of three separate determinations are tabulated in Table 2, along with the amino acid composition obtained by Starbuck et al.

TABLE 2

AMINO ACID ANALYSIS OF GAR HISTONE

Histone samples were exhaustively dialyzed against 0.01M HCl, lyophilized and hydrolyzed in 6M HCl at 110°C for 20h. Amino acid analyses were carried out on a JEOLCO type JLC 5. AH amino acid analyzer as described in Methods Section 2.3

The amino acid composition of GAR histone is compared with that obtained by Starbuck et al. (1968). Partial specific volume and mean residue weight of GAR were calculated from the individual contributions of the amino acids.

TABLE 2

Amino Acid	Moles % (Exptal)	Moles % Starbuck et al. (1968)	No. of residues	Specific Volume	Contribution to $\bar{v}$	Residue Weight	Contribution to M. R. W.
Lys	9.7	9.8	9	0.82	0.0803	128.17	12.5606
His	2.16	2.2	2	0.67	0.0065	137.14	3.0472
Arg	11.2	13.0	12	0.70	0.0910	156.18	20.303
Asp	6.06	5.4	5	0.60	0.0314	115.08	6.2140
Thr	6.02	6.8	6	0.70	0.0476	101.10	6.8750
Ser	3.97	2.4	2	0.63	0.0151	87.07	2.0896
Glu	8.5	6.7	6	0.66	0.0422	129.11	8.6503
Pro	1.0	1.0	1	0.76	0.0076	97.11	0.9711
Gly	13.8	16.8	16	0.74	0.1292	57.05	9.5844
Ala	10.6	7.8	7	0.74	0.0577	71.07	5.5430
Cys	0.0	0.0	0	0.61	0.000	103.14	0.0000
Val	6.7	7.7	7	0.75	0.0577	99.13	7.6330
Met	1.0	1.0	1	0.75	0.0075	131.19	1.3119
Ile	5.7	5.3	5	0.90	0.0477	113.15	5.9969
Leu	9.3	8.5	8	0.90	0.0705	113.15	9.6172
Tyr	3.3	3.1	3	0.71	0.0220	163.17	5.0584
Phe	1.6	2.0	2	0.77	0.0154	147.17	2.9430
Trp	N.D.	0.0	0	0.74	0.0	186.20	0.0000
					$\bar{v} = 0.7294$	MRW = 1084	

(1968). It can be seen that the histone molecule has a high arginine and glycine content although the experimentally obtained values are somewhat lower than those obtained by Starbuck et al. (1968). A significant feature of the amino acid composition is the high lysine content, which with the high arginine content accounts for the basic nature of the protein. The basic amino acids, lysine, arginine and histidine comprise about 23% of the total amino acids and four amino acids (lysine, arginine, glycine and leucine) constitute over 40% of the total amino acids. The number of each amino acid residue per protein molecule calculated by Starbuck et al. (1968) on a basis of a protein molecular weight of 10,600 is shown in Table 2. This molecular composition was used to calculate the individual contribution of each amino acid to the overall partial specific volume of the protein, using the values of Cohn and Edsall (1943) for the specific volume of each amino acid (Table 2). A value of 0.7294 was obtained for  $\bar{v}$ . Estimation of the molecular weights of a protein by ultracentrifugal analyses are dependent on the values of  $\bar{v}$  used; for this reason, a reliable value is essential. At present, however, there is no simple yet completely accurate method available for the determination of  $\bar{v}$ . Goodrich, Swinehart, Kelly and Reithel (1969) have pointed out that since  $\frac{dp}{dc} \approx 1 - \bar{v}\rho$ , evaluation of the partial specific volume term in the sedimentation equilibrium equation may be obtained by measuring the change in density of dialyzed proteins with respect to concentration. Such a procedure is laborious although satisfactory results have been reported using this method (Goodrich and Reithel (1970)). The technique of density perturbation sedimentation equilibrium introduced by Schachman and Edelstein (1966) and Thomas and Edelstein (1971) is probably the simplest of all available methods for the determination of  $\bar{v}$ . Sedimentation equilibrium experiments on solutions of GAR histone in 0.01M HCl/D<sub>2</sub>O yielded a value of 0.715 for  $\bar{v}$ , calculated

by the method of Schachman and Edelstein (1966). Because of objections to the theoretical validity of this technique (Reisler and Eisenberg, 1969), the value of  $\bar{v}$  calculated from the amino acid composition of GAR determined by Starbuck et al. (1968) was used in all subsequent ultracentrifugal analyses. Current methods for the analysis of associating protein systems using ultracentrifugal techniques make the assumption that the partial specific volume of all interacting species is the same (Adams, 1967 c). In such cases, the accuracy of  $\bar{v}$  is not crucial, since the characteristics and type of association will be correctly identified although the absolute values of molecular weights may be in error because of inaccuracies in  $\bar{v}$ .

The mean residue weight (M. R. W.) of GAR histone was calculated using the amino acid analysis obtained by Starbuck et al. (1968).

Values of the individual contribution of each amino acid to the overall M. R. W. are shown in Table 2. A value of 108.4 for M. R. W. of GAR was calculated.

## 2. Analytical gel filtration chromatography of GAR histone

Analytical gel filtration chromatography provides a powerful, yet technically simple method for obtaining information concerning the size and shapes of macromolecules. To obtain such data on GAR histone, analytical gel filtration chromatography was carried out on Sephadex G100 as described in Methods Section 2.8. Since Edwards and Shooter (1969) have shown that histone fraction  $f_{2a_1}$  exists in an unaggregated state in salt-free conditions, the column was equilibrated with 0.01M HCl. Sample volumes of about 0.5 ml were applied; the elution volumes, Stokes radii and molecular weights of the standard proteins used to calibrate the column are shown in Table 3. The elution volumes of BSA and lysozyme were arbitrarily selected to calibrate the column as described in Appendix 2(a).

TABLE 3

ANALYTICAL GEL FILTRATION CHROMATOGRAPHY OF GAR  
HISTONE

0.5ml samples of GAR histone were chromatographed on a 40cm X 1cm Sephadex G100 column equilibrated with 0.01M HCl and the elution profile monitored at 275nm by an UVICORD flow absorptometer. Standard proteins were also chromatographed and the Stokes radius,  $a$ , of GAR was calculated from the elution volumes and Stokes radius of BSA and lysozyme using the calibration procedure described in Appendix 2(a).

Table 3

Protein	Elution Volume (ml)	Molecular Sieve Coefft. ( $\sigma$ )	Stokes radius, a, $\text{\AA}$	M. W.
Bovine Serum Albumin	18.05	0.196	36.1	65000
Chymotrypsin	25.5	0.413	24.0	21500
Chymotrypsinogen	24.8	0.392	24.5	23650
Cytochrome C	28.6	0.500	19.0	12400
Haemoglobin	19.50	0.238	39.8	64000
Lysozyme	28.70	0.506	20.6	13930
Myoglobin	25.60	0.415	18.8	18800
Ribonuclease A	28.65	0.504	19.2	12640
	( $V_0$ )			
Blue Dextran	11.31	-	-	-
	( $V_i$ )			
Potassium Dichromate	34.40	-	-	-
GAR	27.85	0.480	20.53	10000



62

The Stokes radius of GAR histone was determined from the equation

$$a = 5.25 + 32.6\sigma$$

where  $a$  is the Stokes radius of the eluted species

and  $\sigma$  is the molecular sieve coefficient (Appendix 2(a)).

The Stokes radius of GAR was found to be  $20.53\text{\AA}$ . Although the estimation of molecular weights from gel filtration data has been demonstrated by Ackers (1964) and Chun et al. (1969) to be inaccurate because of molecular asymmetry, Andrews (1965) has shown empirically that an approximately linear relationship exists between elution volume and  $\log_{10}(\text{Molecular Weight})$ . The elution volumes and  $\text{Log}(\text{Molecular Weights})$  of the standard proteins used are shown in Fig. 2(a). It may be seen that for these proteins, a linear relationship between  $V_e$  and  $\text{Log}(\text{MW})$  does exist. The straight line does not, however, pass through the elution volume of GAR histone. This may indicate some molecular asymmetry in GAR histone, but it is possible that the salt-free conditions with which the column was equilibrated may have caused aggregation or changes in the conformation of the proteins used for calibration, thus affecting the calibration curve.

Gel filtration chromatography fractionates molecules on the basis of molecular size and consequently, in the case of asymmetric molecules, correlation of molecular weights with elution volumes may not be accurate. A more rigorous method for describing the gel filtration behaviour of macromolecules is to correlate the Stokes radius,  $a$ , of an eluting species with its elution volume. Porath (1963) has found that a linear relationship exists between the cube root of the molecular sieve coefficient and the Stokes radius of eluted species. Fig. 2(b) shows the relationship between the cube root of the molecular sieve coefficient,  $\sigma^{\frac{1}{3}}$ , of the standard proteins used for the

FIG 2 (a)

ANALYTICAL GEL FILTRATION CHROMATOGRAPHY OF GAR  
HISTONE

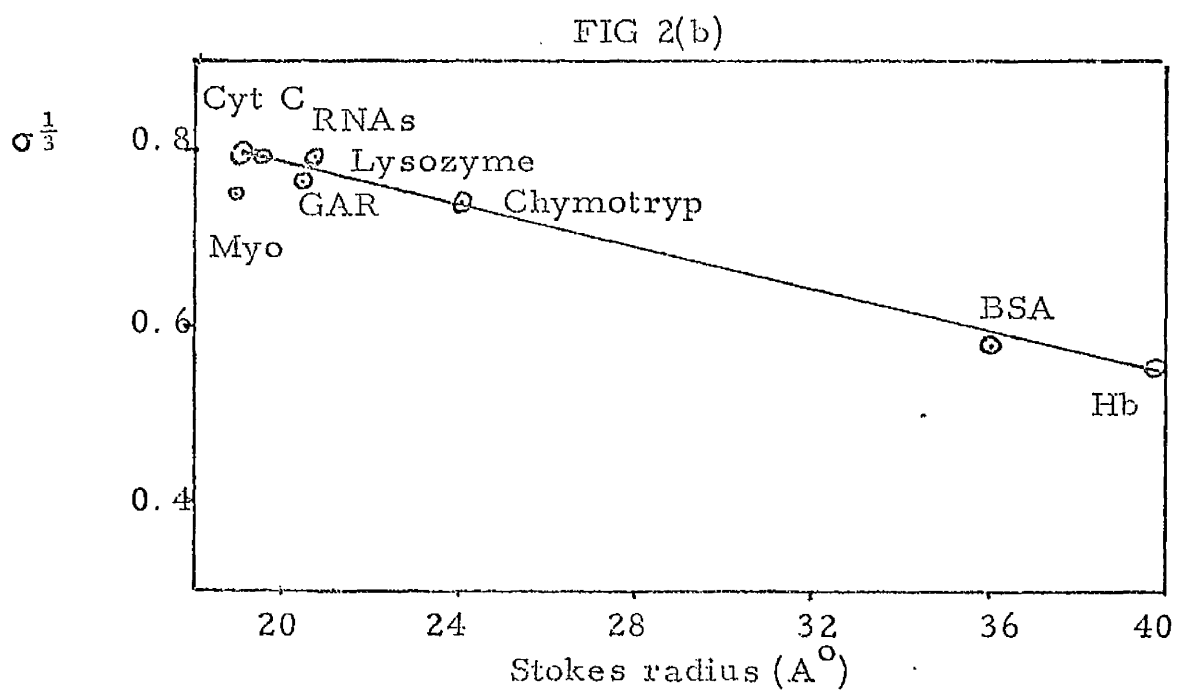
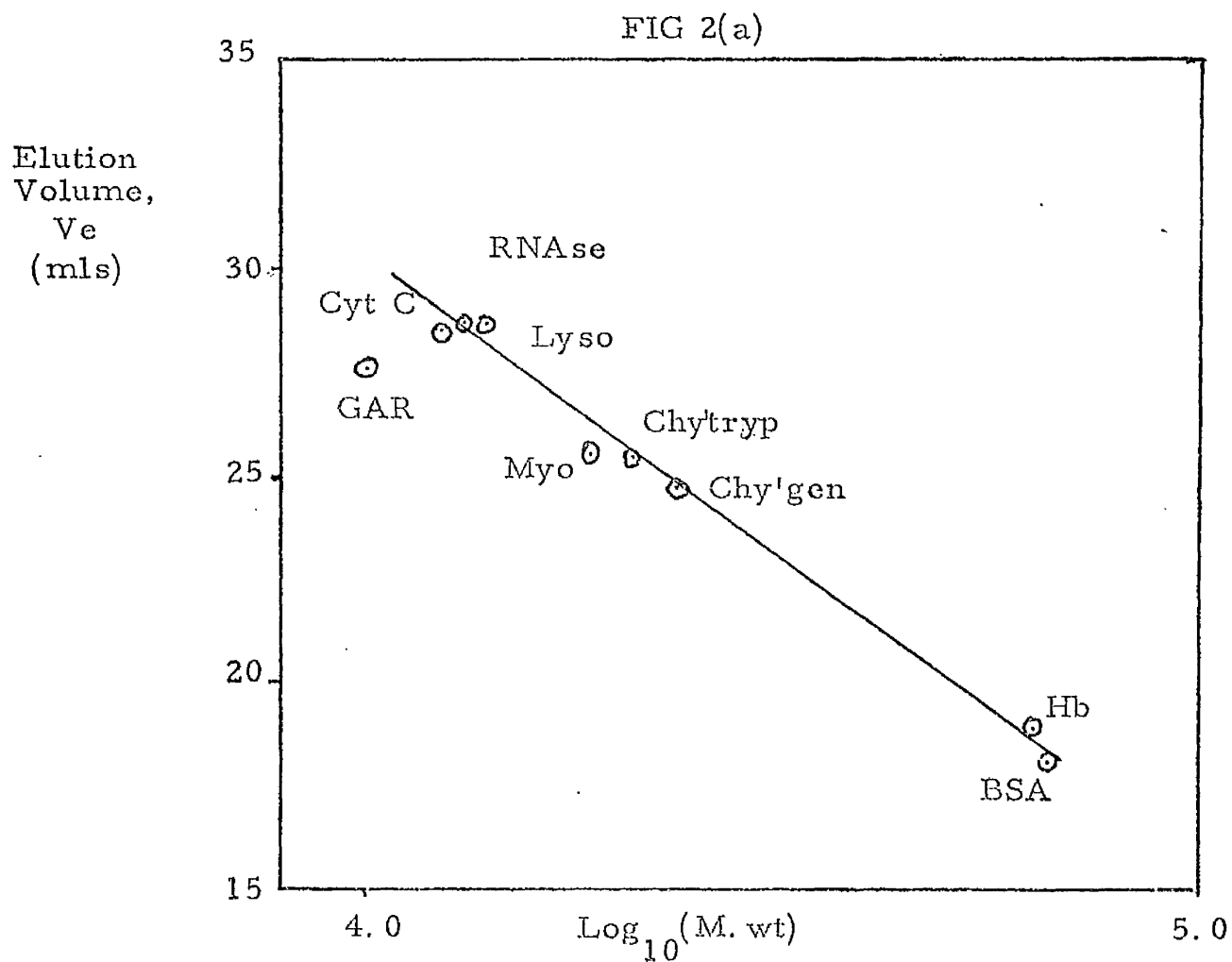
0.5ml aliquots of GAR histone were chromatographed on a 40cm X 1cm diameter Sephadex G100 column equilibrated with 0.01M HCl and the elution profile monitored on a LKB UVICORD flow absorptiometer. The elution volumes of the following standard proteins were also measured:- cytochrome C, ribonuclease A, lysozyme, myoglobin, chymotrypsin, chymotrypsinogen, haemoglobin and bovine serum albumin.

FIG 2 (b)

ANALYTICAL GEL FILTRATION CHROMATOGRAPHY OF GAR  
HISTONE

0.5ml aliquots of GAR histone were chromatographed on a 40cm X 1cm diameter Sephadex G100 column equilibrated with 0.01M HCl. The void volume,  $V_o$ , and the internal volume,  $V_i$ , of the column were estimated from the elution volumes of Blue Dextran and potassium dichromate respectively. The column was calibrated using the Stokes radii and elution volumes of BSA and lysozyme as described in Appendix 2(a). Values of the molecular sieve coefficient,  $\sigma$ , for the calibrating proteins were calculated from their elution volumes using the expression:-

$$\sigma = \frac{V_e - V_o}{V_i}$$



calibration of the gel filtration column and their Stokes radius,  $a$ . With the exception of myoglobin, it is found that all the data points lie on a straight line. The Stokes radius of GAR was calculated from the molecular sieve coefficients and Stokes radii of BSA and lysozyme as described in Appendix 2(a). Effectively this calibration procedure assumes the existence of a linear relationship between the Stokes radius and the molecular sieve coefficients of the two proteins used. It is therefore to be expected that a linear relationship exists between GAR, BSA and lysozyme in Fig. 2(b). The validity of the column calibration based on BSA and lysozyme is confirmed by the fact that the data points for the other standard proteins used also fall on this line. It is therefore reasonable to conclude that GAR histone can be represented as a spherical protein of Stokes radius  $20.53\text{\AA}$ .

To analyze associating systems of GAR on gel filtration columns, it is necessary to evaluate the molecular sieve coefficients of oligomers of GAR (Appendix 2(b)). Values of  $\sigma_i$ , the molecular sieve coefficient of  $i$ -mers of GAR histone, were calculated as described in Appendix 2(b) according to two extreme models of molecular shape, compact and linear aggregation. The values of  $\sigma_i$  calculated for these forms of molecular complexes are shown in Table 4. For linear complexes of more than 6 monomeric species, the values of  $\sigma_i$  are so small that experimental resolution of higher aggregates would be unattainable. Gel-filtration analysis of GAR complexes of more than 6 monomeric units is therefore difficult using Sephadex G100 but could be carried out on gels of larger pore size. In the present studies, gel filtration analyses of GAR complexes were carried out on G100, the mathematical interpretations of the data being limited to the consideration of aggregates of not more than 6 monomeric units.

TABLE 4

MOLECULAR SIEVE COEFFICIENTS OF COMPLEXES OF GAR  
HISTONE

The molecular sieve coefficient of unaggregated GAR histone was obtained from chromatography on Sephadex G100 equilibrated with 0.01M HCl. Molecular sieve coefficients of aggregates of GAR histone were calculated for both linear and compact aggregation as described in Appendix 2(b). Equations used were:-

Compact aggregation  $\sigma_i = \text{erfc} (a, i^{\frac{1}{3}} - a_o) / b_o$

Linear aggregation  $\sigma_i = \text{erfc} ((f/f_o) a, i^{\frac{1}{3}} - a_o) / b_o$

For linear aggregation, values of  $f/f_o$  were calculated from the ratio of length to diameter of the aggregates using the equations of Perrin (1936) as described in Appendix 2(b).

TABLE 4

i	$\frac{a}{b}$	$\frac{f}{f_o}$ App. 2(b)	$\sigma_i$ Linear Aggregates	$\sigma_i$ Compact Aggregates
1	0.8165	-	0.4760	0.4760
2	1.6330	1.022	0.3583	0.3583
3	2.4495	1.074	0.2495	0.2903
4	3.2660	1.131	0.1703	0.2351
5	4.0825	1.188	0.0952	0.1947
6	4.8990	1.243	0.0745	0.1638
7	5.7155	1.296	0.0517	0.1394
8	6.5320	1.347	0.0297	0.1198
9	7.3485	1.396	0.0184	0.1036
10	8.1650	1.443	0.0115	0.0902
11	8.9815	1.488	0.0065	0.0793
12	9.7980	1.532	0.0038	0.0697
13	10.6145	1.575	0.0021	0.0616
14	11.4310	1.616	0.0016	0.0547
15	12.2475	1.657	0.0007	0.0487
16	13.0690	1.696	0.0004	0.0434

Sedimentation equilibrium analysis of GAR histone was carried out as described in Methods Section 2.10.1 in two different solvent conditions, 0.075M NaCl/0.01M HCl and 0.15M NaCl/0.01M HCl. All runs were carried out using UV optics at a speed of 26,000 rpm at 20°C. The apparent weight average molecular weights ( $M_{wapp}$ ) of GAR histone in 0.075M NaCl/0.01M HCl obtained from seven separate sedimentation equilibrium experiments are shown as a function of concentration in Fig. 3, and  $M_{wapp}$  values obtained from eight separate sedimentation equilibrium experiments in 0.15M NaCl/0.01M HCl are shown in Fig. 4. It may be seen that under both solvent conditions,  $M_{wapp}$  increases with concentration. This may be attributable to either the presence of an associating protein system or to polydispersity within the sample. Cassman and Schachman (1971) have pointed out that only in an associating system is the value of  $M_{wapp}$  at any particular concentration independent of the starting concentration of the equilibrium run. Comparison, at a single concentration, of  $M_{wapp}$  values evaluated from  $\ln c$  vs.  $r^2$  data obtained from separate sedimentation equilibrium experiments at different initial concentration thus enables distinction between polydispersity and associating protein systems. It can be seen from Figs. 3 and 4 that at any single concentration the values of  $M_{wapp}$  from separate sedimentation equilibrium experiments are similar, indicating the presence of reversibly associating protein systems. In principle, values of  $M_{wapp}$  from separate sedimentation equilibrium runs should form a continuous curve when plotted against concentration but in practice, discontinuities of the type shown in Figs. 3 and 4 are common (Adams and Filmer, 1966; Albright and Williams, 1968; Deonier and Williams, 1970; Kelly and Reithel, 1971). Such discontinuities have been attributed to pressure effects at the extremities of the sedimenting column (Deonier and Williams, 1970). The discontinuous

FIG. 3

APPARENT WEIGHT AVERAGE MOLECULAR WEIGHTS OF GAR  
HISTONE IN 0.075M NaCl/0.01M HCl

Samples of GAR histone at different initial concentrations were dialyzed exhaustively against 0.075M NaCl/0.01M HCl and centrifuged at 26,000 rpm for at least 36h at 20°C in an AN-G rotor in a Beckman Model E analytical ultracentrifuge equipped with absorption optics. Apparent weight average molecular weights ( $M_{wapp}$ ) were determined from computer evaluation of the gradient of  $\ln c$  vs.  $r^2$  data. The gradient at each point in the  $\ln c$  vs.  $r^2$  data was evaluated by fitting a quadratic polynomial to successive and overlapping sets of 5 data points on the  $\ln c$  vs.  $r^2$  curve, and differentiating the polynomial analytically. Concentrations were estimated from absorbance measurements using the relationship:-

$$1\text{mg/ml} \quad \equiv \quad 0.397 \text{ O.D. units at } 275\text{nm}$$

A third degree polynomial was fitted to the data and constrained to pass through  $M_{wapp} = 10,600$  at  $C = 0$

————— Experimental  $M_{wapp}$  curves  
————— Best fitting curve



$\Delta_{wapp}$   
 $\times 10^{-3}$ )

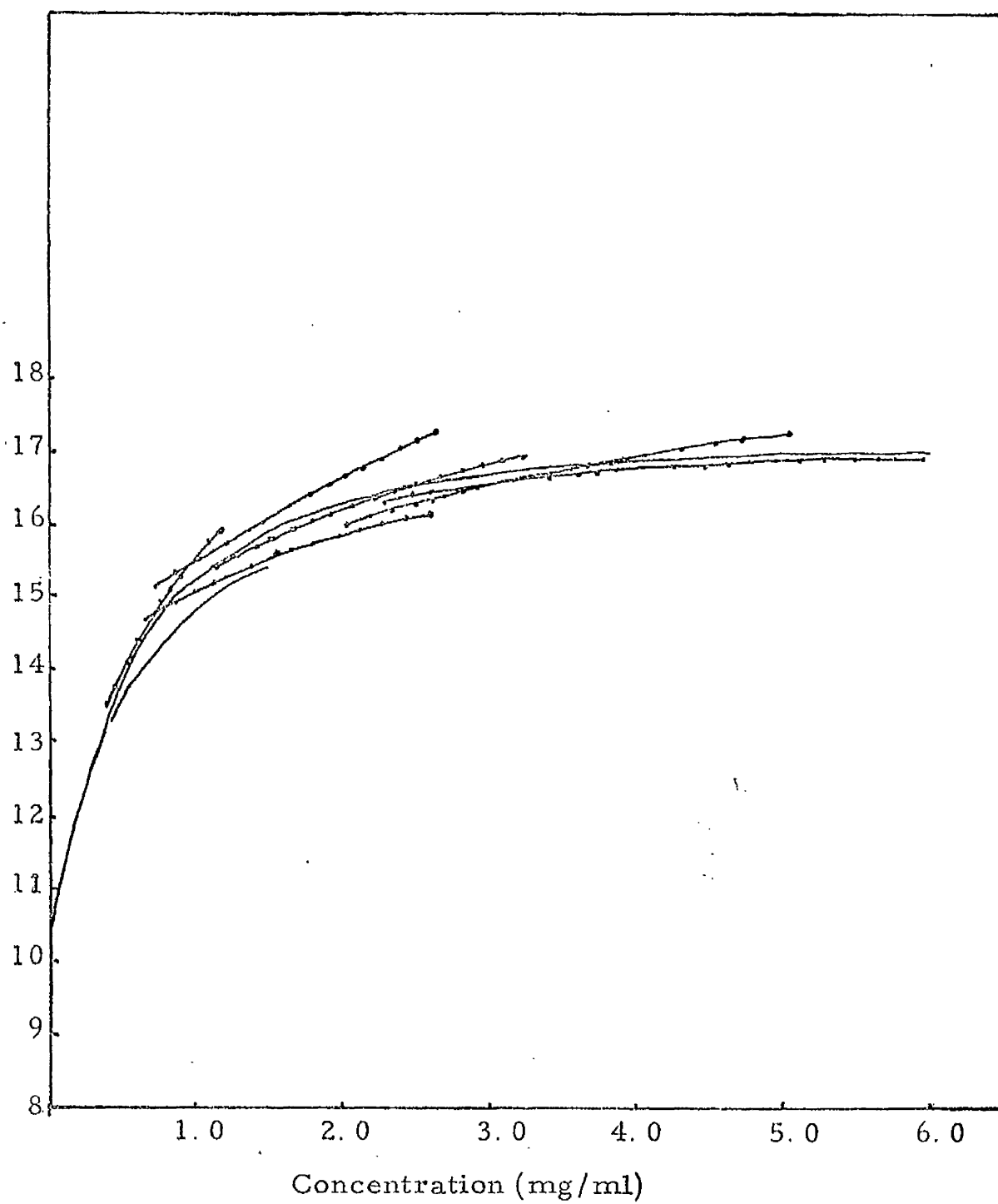


Fig 3

FIG. 4

APPARENT WEIGHT AVERAGE MOLECULAR WEIGHTS OF GAR  
HISTONE IN 0.15M NaCl/0.01M HCl

Samples of GAR histone at different initial concentrations were dialyzed exhaustively against 0.15M NaCl/0.01M HCl and centrifuged at 26,000 rpm for at least 36h at 20°C in an AN-G rotor in a Beckman Model E analytical ultracentrifuge, equipped with absorption optics. Apparent weight average molecular weights ( $M_{wapp}$ ) were determined from computer evaluation of the gradient of  $\ln c$  vs.  $r^2$  data. The gradient at each point in the  $\ln c$  vs.  $r^2$  data was evaluated by fitting a quadratic polynomial to successive and overlapping sets of 5 data points on the  $\ln c$  vs.  $r^2$  curve and differentiating the polynomial analytically. Concentrations were estimated from absorbance measurements, using the relation  $1\text{mg/ml} \approx 0.397 \text{ O.D. units at } 275\text{nm}$ .

A third degree polynomial was fitted to the data and constrained to pass through  $M_{wapp} = 10600$  at  $C = 0$ .

———— Experimental  $M_{wapp}$  values  
———— Best fitting curve

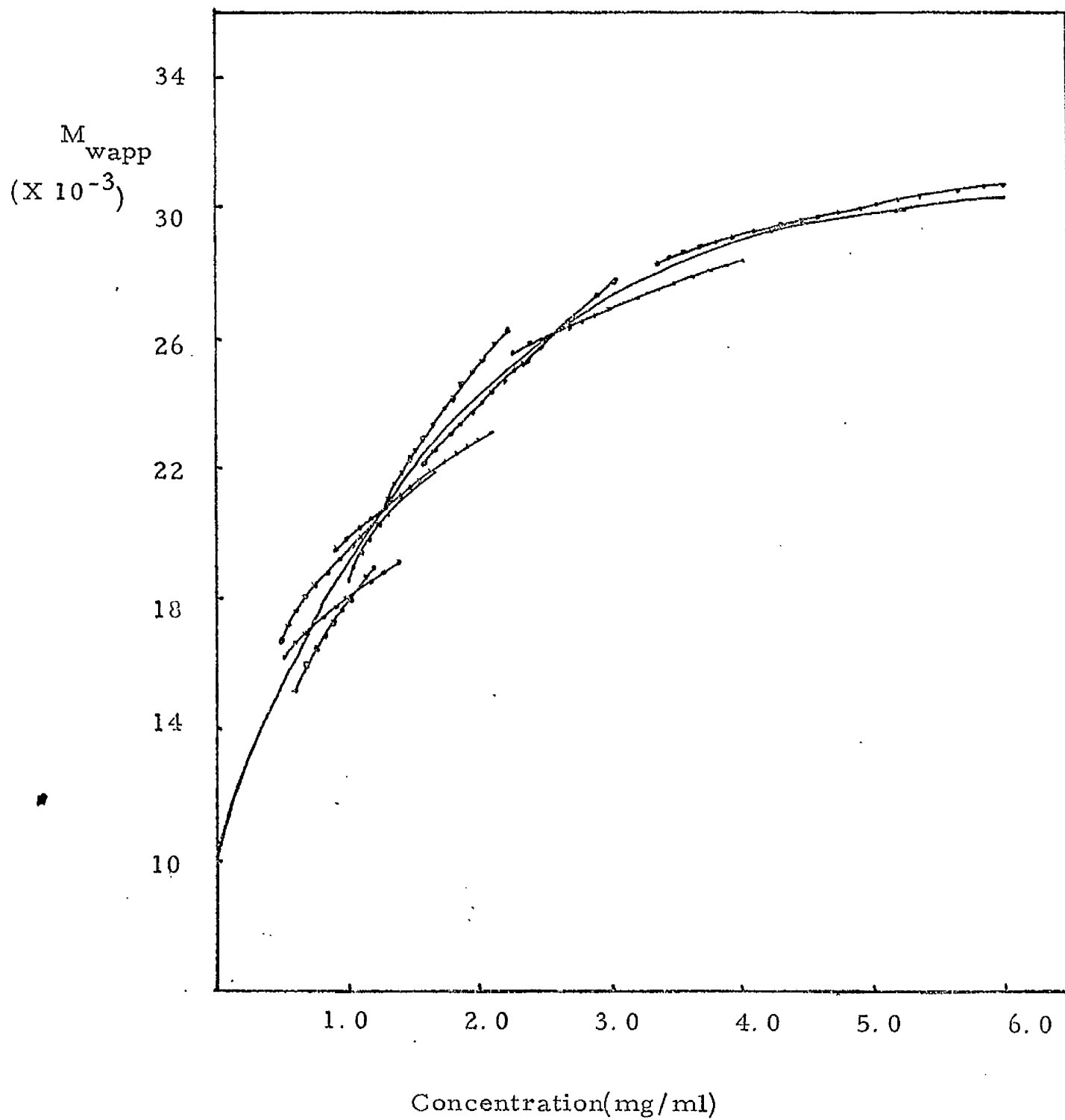


Fig. 4

molecular weight data shown in Figs. 3 and 4 were processed by the construction of a continuous interpolation curve using numerical techniques of curve-fitting by the method of least squares. (Adams, 1967 c; Godfrey and Harrington, 1970 a, b). A third degree polynomial relating  $M_{wapp}$  to  $C$  was considered adequate to describe the data of Figs. 3 and 4. It was found that both fitted curves intersected the ordinate at a value of  $M_{wapp}$  slightly higher than the monomer molecular weight  $M_1$ , of 10,600 calculated from the amino acid analysis of GAR. These discrepancies illustrate the difficulties of extrapolating accurately the weight average molecular weight data describing associating protein systems, to infinite dilution. In part, these difficulties can be ascribed to the problems of obtaining accurate molecular weight data at low concentrations. In the particular case of GAR histone, the relatively low extinction coefficient of the protein makes accurate measurement of  $M_{wapp}$  at low concentrations difficult when absorption optics are used. It is also possible that inaccurate values of  $M_1$  may arise from the use of unweighted polynomial curve-fitting. Using this type of curve-fitting it is possible that the preponderance of data at higher concentrations adversely affects the ability of the fitted curve to represent accurately the experimental data at lower concentrations. This effect may be overcome by using weighted polynomial curve-fitting in which each set of data points is assigned a weighting factor directly proportional to the accuracy with which the data were determined experimentally. In the present studies, no such weighted curve-fitting procedure was available. Even with weighted curve-fitting procedures, accurate determination of  $M_1$  for associating protein systems is difficult. However, a number of simple graphical procedures are available which allow, in some cases, more accurate extrapolation of  $M_{wapp}$  data to zero concentration. Fig. 5(a) shows plots of the reciprocal

## FIG 5

### ESTIMATION OF MONOMER MOLECULAR WEIGHTS OF GAR HISTONE

Sedimentation equilibrium analyses of GAR histone in 0.075M NaCl/0.01M HCl and 0.15M NaCl/0.01M HCl were carried out as described in Methods Section 2.10.1, at various initial concentrations. Whole cell apparent weight average molecular weights ( $M_{wcellapp}$ ) were evaluated from the gradient of the best straight line through the  $\ln c$  vs.  $r^2$  data.

$\Delta$ ————— $\Delta$  0.075M NaCl/0.01M HCl  
 $\circ$ ————— $\circ$  0.15M NaCl/0.01M HCl

Fig. 5(a) The reciprocal of  $M_{wcellapp}$  is plotted as a function of initial concentration.

Fig. 5(b) The logarithm of  $M_{wcellapp}$  is plotted as a function of initial concentration.

Fig. 5(c) Rowe and Rowe (1970) plots of data from one single sedimentation run.  $\ln c$  vs.  $r^2$  data were smoothed by fitting of a quadratic polynomial to the data and values of Z and T were evaluated using a PDP8/L computer as described by Rowe and Rowe (1970).

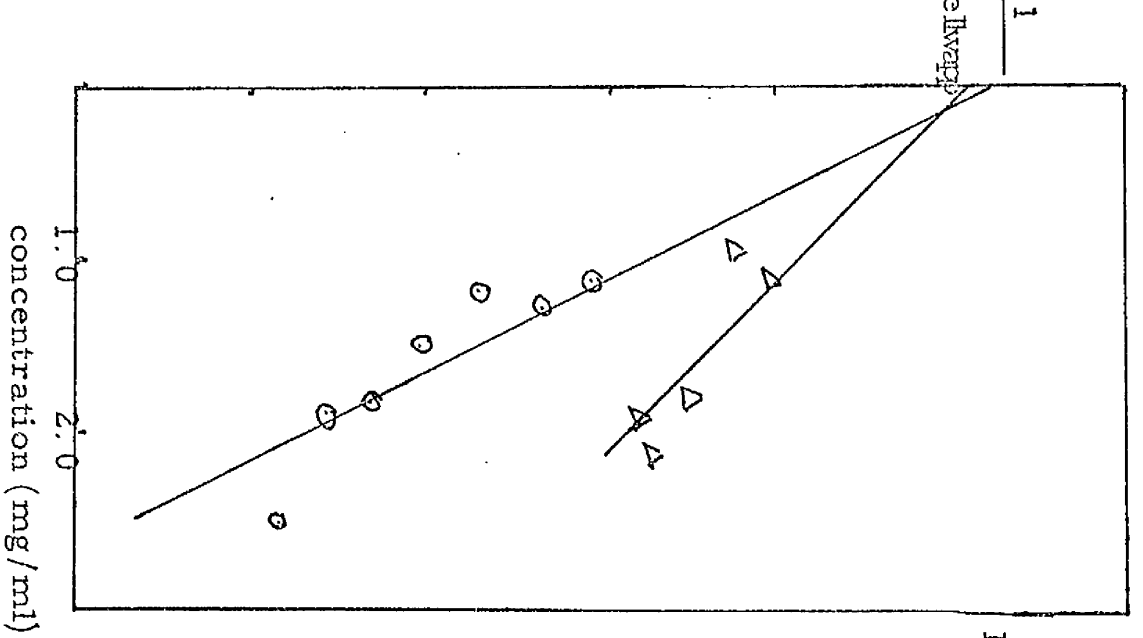


Fig. 5(a)

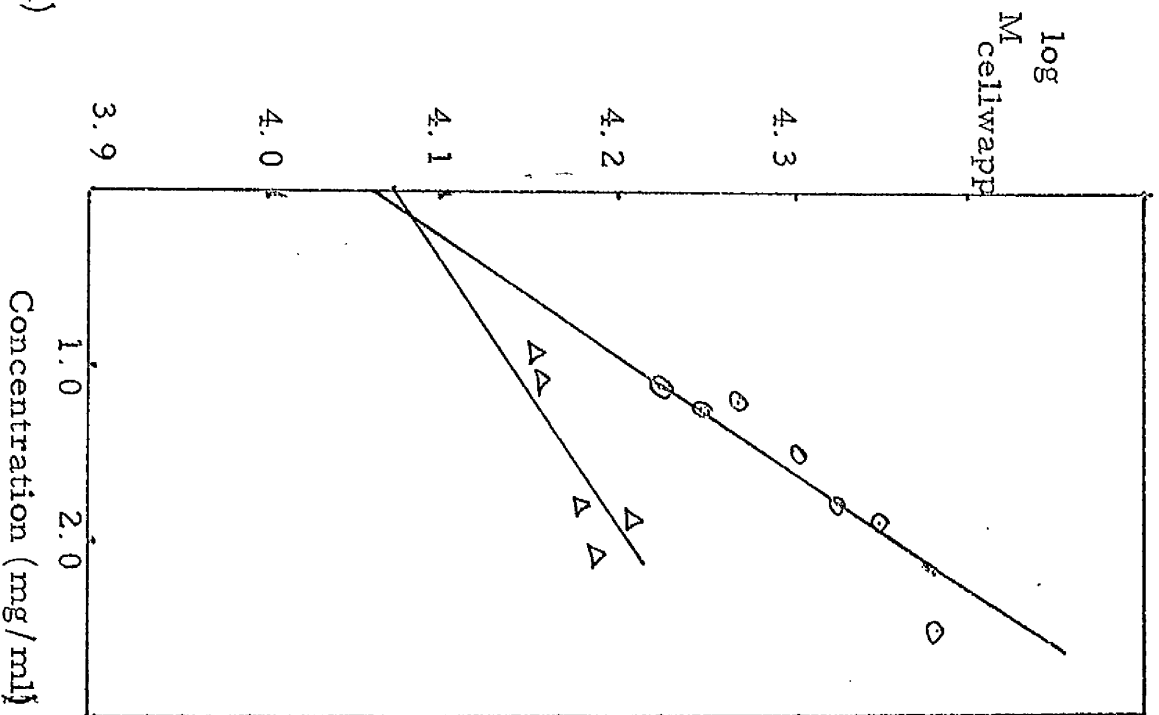


Fig. 5(b)

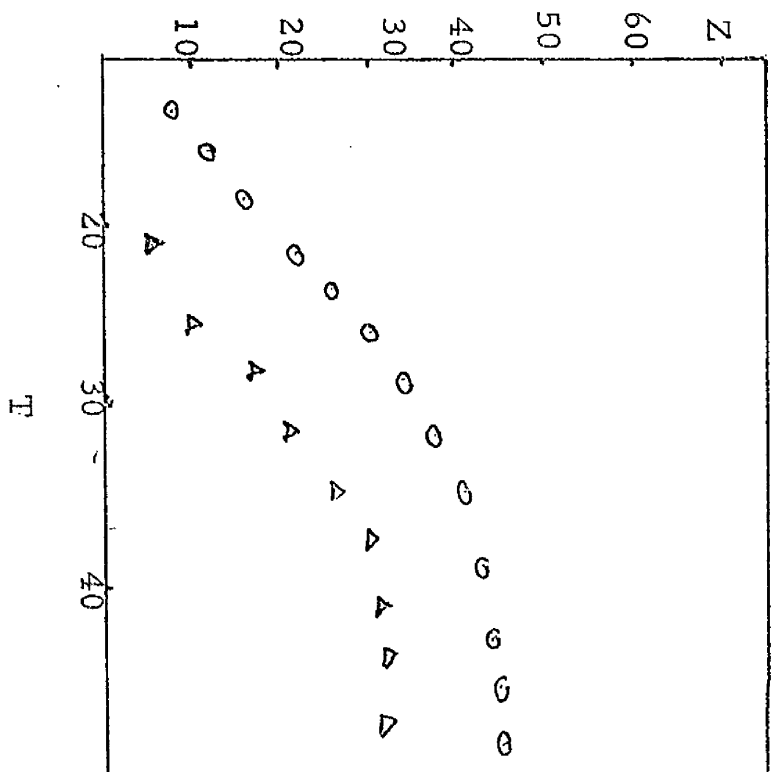


Fig. 5(c)

of the whole cell weight average molecular weight  $M_{wcellapp}$ , as a function of initial concentration. For associating systems, such plots are generally curved. Values of  $1/M_{wcellapp}$  for each of the separate sedimentation equilibrium experiments used to construct Figs. 3 and 4 formed distinct curves, and accordingly only values of  $M_{wcellapp}$  obtained from sedimentation equilibrium experiments with starting concentrations less than 2.5mg/ml were processed, to allow linear extrapolation through the data. Best-fitting straight lines through the data are shown in Fig. 5(a) and yielded values of  $M_1$  of 12390 and 12090 in 0.075M NaCl/0.01M HCl and 0.15M NaCl/0.01M HCl respectively. The lack of a good fit to the data is probably due to the inaccuracies involved in the estimations of  $M_{wcellapp}$  by fitting a straight line to non-linear  $\ln c$  vs.  $r^2$  data. Fig. 5(b) shows plots of  $\log_{10} M_{wcellapp}$  vs. concentration. Again because of non-linearity at high concentrations, only data from runs with starting concentrations less than 2.5mg/ml were processed. Best-fitting straight lines through the data are shown in Fig. 5(b) and yielded  $M_1$  values of 11850 and 11750 in 0.075M NaCl/0.01M HCl and 0.15M NaCl/0.01M HCl respectively. These values of  $M_1$  are higher than the value of monomer molecular weight obtained from amino acid analysis, and further illustrate the difficulties of obtaining monomer molecular weights of associating systems. Recently, Rowe and Rowe (1970) have derived equations which enable more accurate evaluation of  $M_1$  from a single sedimentation equilibrium run. They defined the functions  $Z = \frac{\left[ \ln c \right]_{c_i}^{c_j}}{\left[ c \right]_{c_i}^{c_j}}$  and

$$T = \frac{\left[ r^2 \right]_{r_i}^{r_j}}{\left[ c \right]_{c_i}^{c_j}}$$

and showed that the gradient of a plot of  $Z$  as a function

of  $T$  may be used to calculate  $M_1$ . Plots of  $Z$  as a function of  $T$ , evaluated for a single sedimentation equilibrium run are shown in Fig. 5(c). It can be seen that in both 0.075M NaCl/0.01M HCl and 0.15M NaCl/0.01M HCl,  $Z - T$  plots for GAR histone are non-linear, indicating polydispersity with respect to molecular weight (Rowe and Rowe, 1970). In the case of the electrophoretically pure GAR histone this polydispersity is due to associating processes. Regression lines through the data gave values for  $M_1$  of 10,800 and 11200 in 0.075M NaCl/0.01M HCl and 0.15M NaCl/0.01M HCl respectively.

The graphical methods depicted in Fig. 5 a, b, c all yield different values of  $M_1$ , with the method of Rowe and Rowe (1970), (Fig. 5(c)) yielding values of  $M_1$  closest to that obtained from the amino acid analysis. In view of the significant non-linearity of the  $Z - T$  plots, however, the accuracy of the determinations of the gradient of these plots may be limited and consequently, it is possible that the agreement of the values of  $M_1$  obtained by this method with that given by amino acid analysis is fortuitous. For this reason the value of  $M_1$  used in the present studies was that based on amino acid analysis, namely 10,600 daltons. Several ultracentrifugal analyses of associating protein systems have shown that extrapolated  $M_{wapp}$  data at  $C = 0$  does not agree with the monomer molecular weight estimated by alternative methods such as amino acid analysis. (Kelly and Reithel, 1971; Godfrey and Harrington, 1970 a, b; Albright and Williams, 1968; Deonier and Williams, 1970). These authors have attributed the inconsistency to inaccuracies in the  $M_{wapp}$  data at low concentrations and have artificially constrained the best-fitting curve through the  $M_{wapp}$  vs. conc. data to pass through  $M_1$ , the monomer molecular weight obtained by amino acid analysis. Such a procedure was adopted in the present studies; the best-fitting curves through the  $M_{wapp}$



vs.  $c$  data assuming  $M_1 = 10600$  are shown in Figs. 3 and 4. The apparent weight average molecular weight data represented in Figs. 3 and 4 were used to calculate the parameters required for the analysis of associating protein systems developed by Adams (1967a), as described in Appendix 1. Data processing was performed on a UNIVAC 1108 computer programmed in FORTRAN. The computer program was extensively tested using standard data of Adams and Filmer (1966), Sophianopoulos and Van Holde (1964) and Albright and Williams (1968). In all cases, the computed results were in complete agreement with the results quoted by these authors.

The values of  $M_{napp}$  obtained from the processing of  $M_{wapp}$  data (Appendix 1) are shown in Fig. 6(a) and plots of  $M_1/M_{wapp}$  and  $M_1/M_{napp}$  are shown in Fig. 6(b). The values of the molecular weight moments  $M_1/cM_{wapp}$  and  $cM_1/M_{napp}$  and of the parameters  $\alpha$  and  $f_1$ , which were used in the Adams-type analysis are shown in Table 5. The graphical procedure of Chun and Kim (1970) for the analysis of associating protein systems is a useful preliminary to the more detailed and rigorous treatment of Adams, since the type of association may be identified graphically by comparison of the experimental data with those predicted theoretically. In the analysis of Chun and Kim (1970) reduced molecular weight moments are used which are defined as:

$$(M_{wapp})' = M_{wapp}/M_1 \text{ and } (M_{napp})' = M_{napp}/M_1$$

Fig. 7(a) shows plots of  $(M_{wapp})'$  vs.  $1/(M_{napp})'$  which characterize theoretical ideal associating systems of the monomer- $n$ -mer type for  $1 \leq n \leq 8$ , the standard graph describing an ideal indefinite association and also the experimentally obtained data for GAR in 0.075M NaCl/0.01M HCl and 0.15M NaCl/0.01M HCl. For GAR in 0.075M NaCl/0.01M HCl, it can be seen that the experimental data fit most closely the standard curve for an ideal monomer-dimer type of association. At values of  $1/(M_{napp})' \leq 0.6$ , there is a slight downturn of the experimental data away from the predicted curve. This slight deviation, which occurs in the high concentration

$M_{WAPP}$  AND  $M_{NAPP}$  OF GAR HISTONE IN 0.075M NaCl/0.01M HCL

AND 0.15M NaCl/0.01M HCl

Apparent weight average molecular weights ( $M_{wapp}$ ) of GAR histone were obtained from sedimentation equilibrium analyses at different starting concentrations. Best-fitting curves through the experimental  $M_{wapp}$  data were constrained to pass through the value of the monomer molecular weight of GAR (10600 daltons) as estimated from amino acid analysis.  $M_{napp}$  values were calculated from  $M_{wapp}$  data using the relationship:

$$\int_0^c \frac{M_1}{M_{wapp}} = \frac{cM_1}{M_{napp}}$$

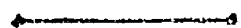


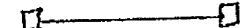
	$M_{wapp}$ of GAR in 0.15M NaCl/0.01M HCl
	$M_{napp}$ of GAR in 0.15M NaCl/0.01M HCl
	$M_{wapp}$ of GAR in 0.075M NaCl/0.01M HCl
	$M_{napp}$ of GAR in 0.075M NaCl/0.01M HCl

FIG 6(b)

$M_1/M_{APP}$  OF GAR HISTONE IN 0.075M NaCl/0.01M HCl and 0.15M  
NaCl/0.01M HCl

$M_{wapp}$  of GAR histone were evaluated from sedimentation equilibrium experiments at different starting concentration and  $M_{napp}$  values calculated using the expression:

$$\int_0^c \frac{M_1}{M_{wapp}} = \frac{cM_1}{M_{napp}}$$

Best-fitting curves through the  $M_{wapp}$  data were constrained to pass through  $M_1 = 10600$  daltons.





	$M_1/M_{napp}$ of GAR histone in 0.075M NaCl/0.01M HCl
	$M_1/M_{wapp}$ of GAR histone in 0.075M NaCl/0.01M HCl
	$M_1/M_{napp}$ of GAR histone in 0.15M NaCl/0.01M HCl
	$M_1/M_{wapp}$ of GAR histone in 0.15M NaCl/0.01M HCl

FIG 5(a)

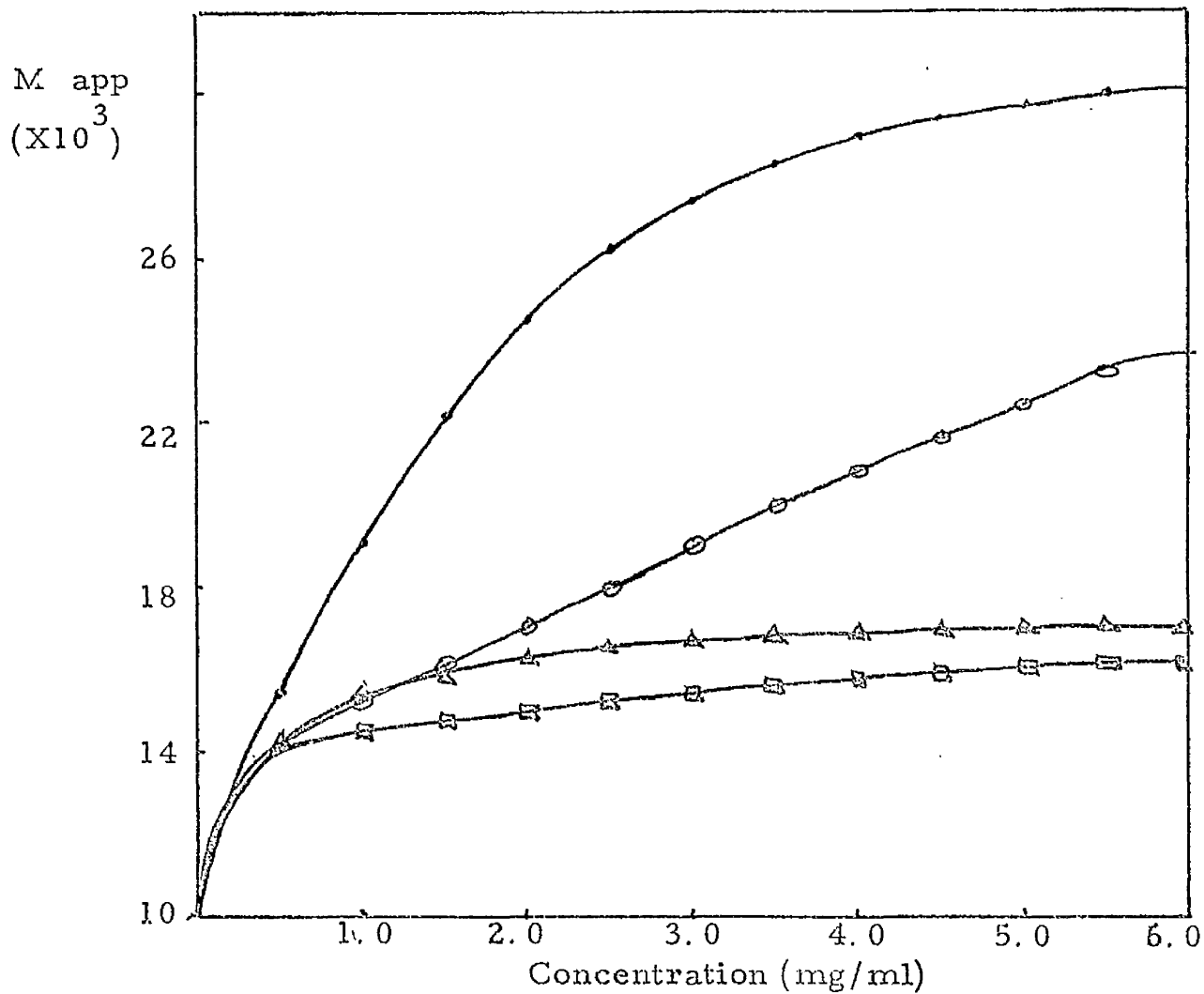


Fig. 6(b)

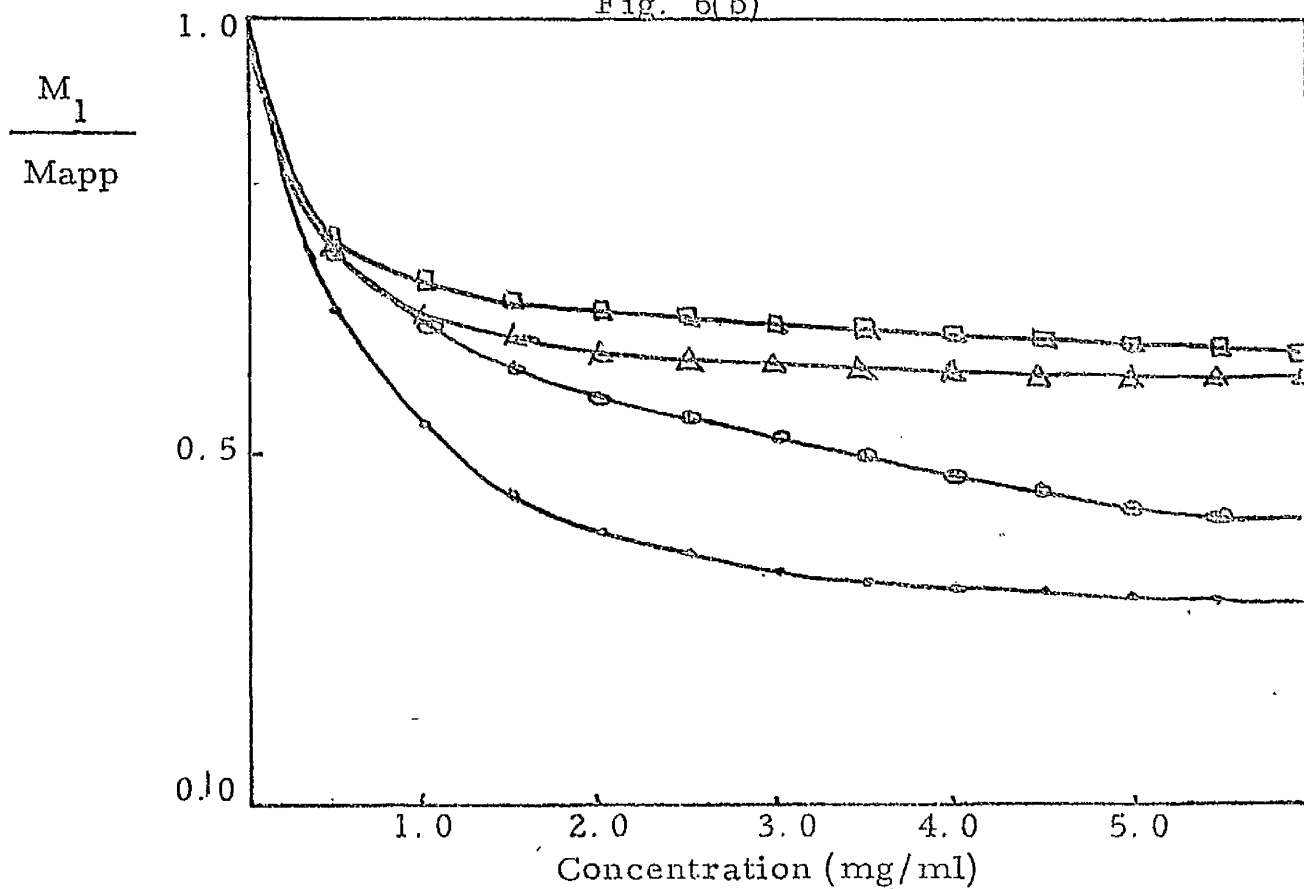


TABLE 5

ANALYSIS OF SELF-ASSOCIATION OF GAR HISTONE IN 0.075M  
NaCl/0.01M HCl and 0.15M NaCl/0.01M HCl BY ADAMS THEORY

The  $M_{wapp}$  vs.  $c$  data (Figs. 3 and 4) obtained from ultra-centrifugal analysis of GAR histone in 0.075M NaCl/0.01M HCl and 0.15M NaCl/0.01M HCl was processed by computer to evaluate:-

$f_1$ ,  $a$ ,  $M_1/cM_{wapp}$  and  $cM_1/M_{napp}$  as described in Appendix 1.

Equations used were:-

$$a = c \exp \int_0^c \left( \frac{M_1}{M_{wapp}} - 1 \right) \frac{1}{c} dc$$

$$\frac{cM_1}{M_{napp}} = \int_0^c \frac{M_1}{M_{wapp}} dc$$

$$f_1 = \exp \int_0^c \left( \frac{M_1}{M_{wapp}} - 1 \right) \frac{1}{c} dc$$

TABLE 5

conc. mg/ml	0.01M HCl/0.075M NaCl				0.15M NaCl/0.01M HCl			
	$\alpha$	$\frac{M_1}{cM_{wapp}}$	$\frac{cM_1}{M_{napp}}$	$f_1$	$\alpha$	$\frac{M_1}{cM_{wapp}}$	$\frac{cM_1}{M_{napp}}$	$f_1$
0.5	0.384	1.436	0.356	0.768	0.386	1.534	0.364	0.771
1.0	0.620	0.666	0.699	0.620	0.616	0.551	0.688	0.616
1.5	0.786	0.428	1.031	0.524	0.762	0.308	0.960	0.508
2.0	0.920	0.314	1.354	0.460	0.862	0.208	1.203	0.431
2.5	1.043	0.248	1.668	0.417	0.937	0.156	1.418	0.375
3.0	1.165	0.204	1.977	0.388	0.999	0.125	1.610	0.333
3.5	1.291	0.174	2.280	0.369	1.056	0.104	1.786	0.302
4.0	1.420	0.152	2.581	0.355	1.108	0.089	1.950	0.277
4.5	1.550	0.134	2.880	0.344	1.159	0.077	2.110	0.258
5.0	1.673	0.121	3.179	0.335	1.707	0.069	2.271	0.241
5.5	1.779	0.110	3.480	0.323	1.256	0.062	2.438	0.227
6.0	1.855	0.101	3.783	0.309	1.286	0.057	2.619	0.214

range of the data, may be a result of non-ideal effects. For GAR in 0.15M NaCl/0.01M HCl it may be seen that in the low concentration range, that is, for values of  $1/(M_{\text{napp}})'$  greater than 0.7, the experimental data are barely distinguishable from the theoretical plots describing monomer-dimer or indefinite association. At higher concentrations the experimental data do not correspond to any of the standard curves. In Fig. 7(b), theoretical plots of  $(M_{\text{wapp}})'$  vs. the weight fraction of monomer,  $f_1$ , are depicted for ideal monomer-n-mer association where  $1 < n < 5$ . The experimental data obtained for GAR in 0.075M NaCl/0.01M HCl, approximate best to the standard curve for monomer-dimer association, while the data obtained in 0.15M NaCl/0.01M HCl do not satisfactorily agree with any of the standard curves. It can be seen that for both sets of experimental data there is a deviation from linearity at a value of  $f_1$  of approximately 0.75. In general, errors in the Chun and Kim graphical procedure may arise from non-ideal effects or from errors introduced in the numerical processes used to generate the data. In the case of Fig. 7(b) it seems likely that the small deviations observed in the experimental data at  $f_1 \approx 0.75$  are a result of the latter source of error. At this value of  $f_1$ , the concentration is low and it is therefore to be expected that non-ideal effects will be small. Moreover, at this low concentration range it can be seen from Figs. 3 and 4 that in both experimental conditions, apparent weight average molecular weights increase markedly with concentration. In this range of sharply increasing  $M_{\text{wapp}}$  values as a function of  $c$ , there is therefore a possibility that the integration procedures used to evaluate  $M_{\text{napp}}$  and  $f_1$  may introduce errors which give rise to the small deviation of Fig. 7(b). The same argument of small numerical errors introduced by integration at low concentration can be employed to explain the deviations shown by the experimental data in Fig. 7(d) where plots of  $1/(M_{\text{napp}})'$

FIG 7

Analysis of association of GAR in 0.075M NaCl/0.01M HCl and 0.15M NaCl/0.01M HCl by the graphical method of Chun and Kim (1970). Experimental values of  $(M_{wapp})'$ ,  $(M_{napp})'$  and  $f_1$  were determined from the  $M_{wapp}$  data of Fig.3,4 as described in Appendix 1.

\_\_\_\_\_ Theoretical curves  
 o-----o GAR histone in 0.15M NaCl/0.01M HCl  
 v-----o GAR histone in 0.075M NaCl/0.01M HCl

FIG 7(a)

Theoretical curves of  $(Mw)'$  vs.  $1/(Mn)'$  for ideal monomer-n-mer associations were constructed using the relationship  $(Mw)' = -n \frac{1}{(Mn)'} + n + 1$  and for ideal indefinite association using the relationship  $(Mw)' = 2 (Mn)' - 1$

FIG 7(b)

Theoretical curves of  $(Mw)'$  vs.  $f_1$  were constructed for ideal monomer-n-mer associations using the relationship  $(Mw)' = -(n-1)f_1 + n$ .

FIG 7(c)

Theoretical curves of  $(Mw)'$  and  $(Mn)'$  vs.  $(f_1)^{-\frac{1}{2}}$  were constructed for ideal indefinite associations using the relationships  $(Mw)' = 2 (f_1)^{-\frac{1}{2}} - 1$  and  $f_1 = 1/(Mn')^2$

FIG 7(d)

Theoretical curves of  $(1/Mn)'$  vs.  $f_1$  were constructed for ideal monomer-n-mer associations using the relationship  $1/(Mn)' = (1 - \frac{1}{n}) f_1 + \frac{1}{n}$  and for ideal indefinite association using the relationship  $f_1 = \frac{1}{(Mn)'}^2$

□ ——— □  $(Mwapp)'$  vs.  $f_1^{-\frac{1}{2}}$ , 0.15M NaCl, 0.01M HCl  
 Δ ——— Δ  $(Mnapp)'$  vs.  $f_1^{-\frac{1}{2}}$ , 0.15M NaCl, 0.01M HCl  
 • ——— •  $(Mwapp)'$  vs.  $f_1^{-\frac{1}{2}}$ , 0.075M NaCl, 0.01M HCl  
 o ——— o  $(Mnapp)'$  vs.  $f_1^{-\frac{1}{2}}$ , 0.075M NaCl, 0.01M HCl

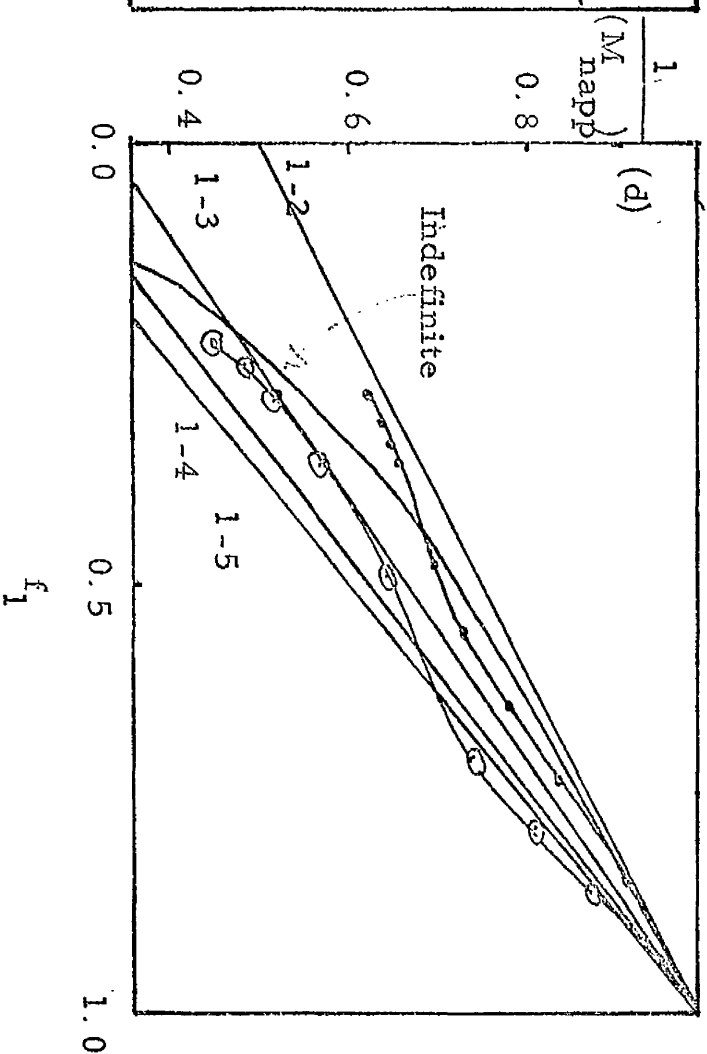
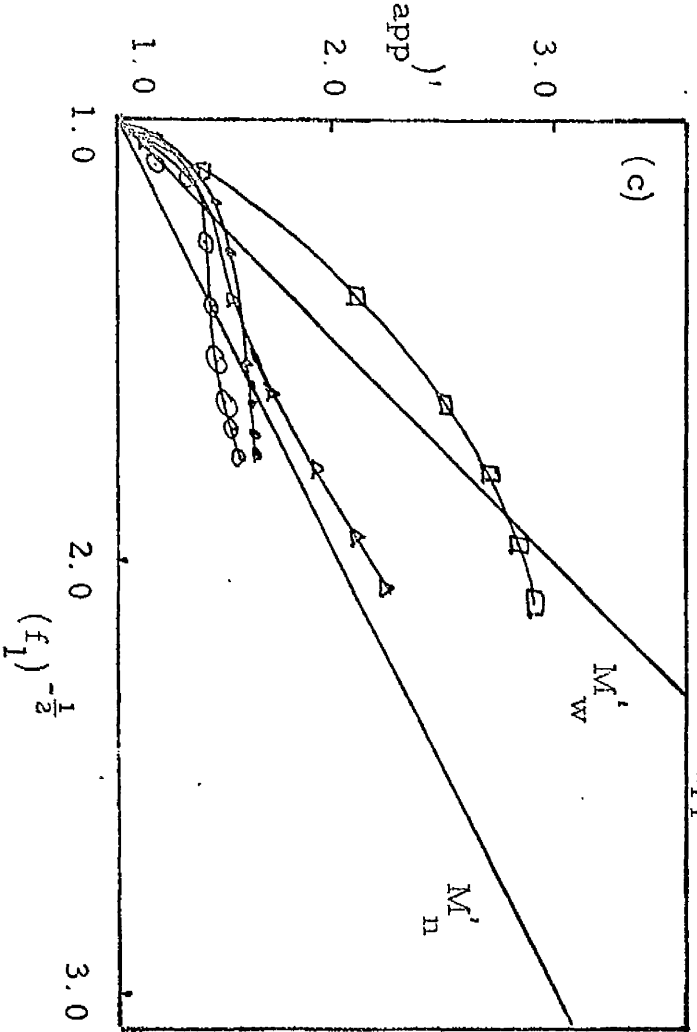
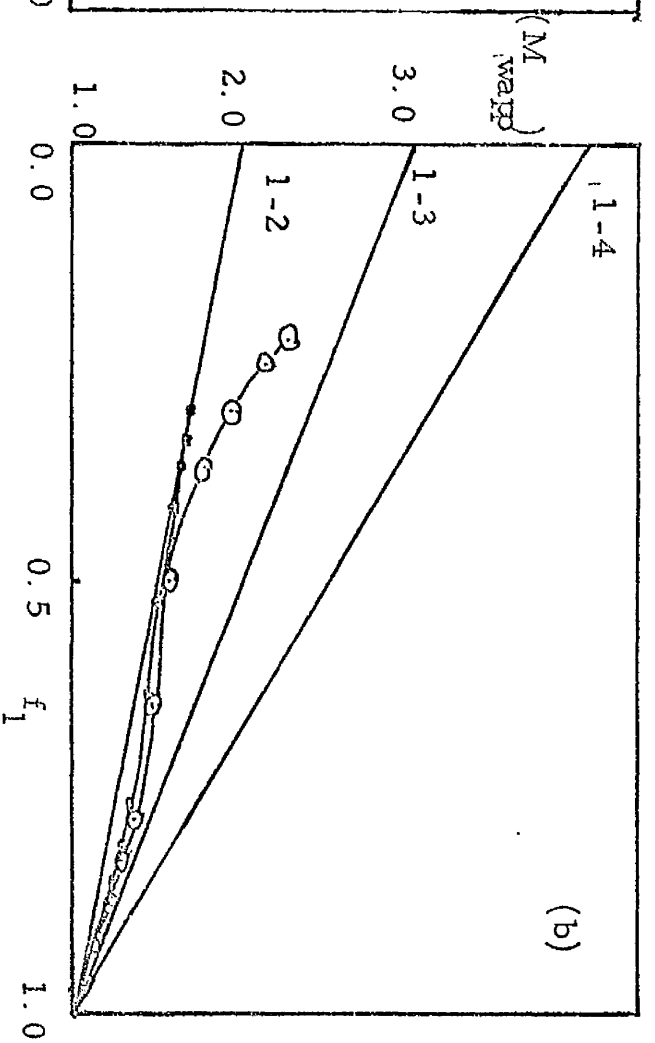
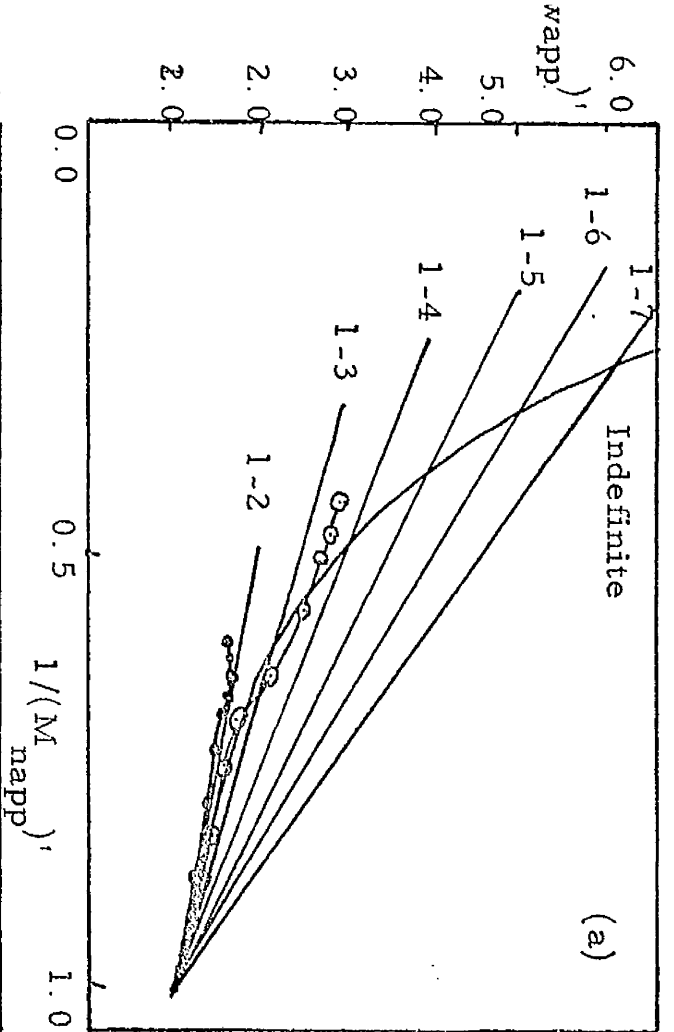


FIG. 7



vs.  $f_1$  are depicted for ideal monomer-n-mer associations and for indefinite association. In plots of this kind, errors introduced by integration affect the parameters of both axes, which may account for the larger deviations in Fig. 7(d). At high concentrations,  $f_1 < 0.5$ , it can be seen that the experimental data obtained in 0.075M NaCl/0.01M HCl approximate best to the monomer-dimer standard graph while in 0.15M NaCl/0.01M HCl the experimental data initially coincide with the standard monomer-trimer curve but deviate from this curve at higher concentrations. This deviation, coupled with the fact that Figs. 7(a) and 7(b) do not show agreement between the experimental data in 0.15M NaCl/0.01M HCl and standard curves for monomer-trimer makes it seem unlikely that the association of GAR histone in these solvent conditions can be adequately described by a monomer-trimer or indeed by any monomer-n-mer association or indefinite association. A more reliable test of indefinite association is provided by comparison of theoretical plots of  $(M_{wapp})'$  and  $(M_{napp})'$  vs. the reciprocal of the square root of the weight fraction of monomer  $f_1^{-\frac{1}{2}}$ , with experimental data. For GAR in 0.075M NaCl/0.01M HCl, neither of the experimental curves of  $M_{wapp}$  or  $M_{napp}$  vs.  $(f_1)^{-\frac{1}{2}}$  approximated to the theoretically predicted curves for indefinite association (Fig. 7(c)). The experimental curves of  $M_{app}$  vs.  $(f_1)^{-\frac{1}{2}}$  for GAR in 0.15M NaCl/0.01M HCl were closer to the theoretical curves but did not agree satisfactorily with either. Overall, it therefore appears from Fig. 7 that while the association of GAR histone in 0.075M NaCl/0.01M HCl may be described with reasonable accuracy by a monomer-dimer association, the association of GAR in 0.15M NaCl/0.01M HCl is not satisfactorily described by monomer-n-mer or by indefinite associations. The possibility that the data obtained in 0.15M NaCl/0.01M HCl may describe an association of the general monomer-m-mer-n-mer type was tested by comparing the experimental data with the theoretical curves for association of the general type monomer-dimer-n-mer.

The derivative of  $(M_{wapp})'$  with respect to  $f_1$ ,  $\frac{d(M_{wapp})'}{df_1}$  is plotted against the derivative of  $(1/M_{napp})'$  with respect to  $f_1$ ,  $\frac{d(1/(M_{napp})')}{df_1}$  in Fig. 8(a). It can be seen that for GAR in 0.075M NaCl/0.01M HCl, the experimental data do not agree with any of the predicted curves for monomer-dimer-n-mer association; for GAR in 0.15M NaCl, there appears to be some agreement between the experimental curve and the predicted curve for a monomer-dimer-tetramer association. It can be seen that there is a 'tail' on the experimental curve which is probably due to errors introduced in the numerical processing of the data, since the evaluation of both  $\frac{d(M_{wapp})'}{df_1}$  and  $\frac{d(1/(M_{napp})')}{df_1}$  involve the potentially error-producing process of differentiation. Most of the experimental points lie between the predicted curves for monomer-dimer-trimer and monomer-dimer-tetramer but are closer to the monomer-dimer-tetramer curve. Fig. 8(b) shows that there is no agreement between the experimental data in both conditions and theoretical curves for monomer-trimer-n-mer.

From the graphical analysis of Chun and Kim represented in Figs. 7 and 8, the following tentative conclusions were made. Although no unequivocal determination of the type of association of GAR in 0.075M NaCl/0.01M HCl and 0.15M NaCl/0.01M HCl was possible, nevertheless the Chun and Kim analysis indicated the most likely modes of association to be monomer-dimer in 0.075M NaCl/0.01M HCl and monomer-dimer-tetramer in 0.15M NaCl/0.01M HCl. The discrepancies between the experimental data and the predicted curves arise from one or both of two possible sources, namely, errors in the numerical processing of the data or from deviations from thermodynamic ideality. The theories of Adams (1967b) however, incorporate quantitation of non-ideal effects. For these reasons, it seems that the optimal use of the ideal graphical procedure of Chun and Kim (1970) is as a preliminary process prior

## FIG 8

### ANALYSIS OF ASSOCIATION OF GAR HISTONE IN 0.075M NaCl/0.01M HCl and 0.15M NaCl/0.01M HCl BY THE GRAPHICAL METHOD OF CHUN AND KIM (1970)

Experimental values of  $(M_{wapp})'$ ,  $(M_{napp})'$ ,  $f_1$  were evaluated from the  $M_{wapp}$  vs.  $c$  data of Figs. 3, 4 as described in Appendix 1. Differentiation of  $(M_{wapp})'$  and  $1/(M_{napp})'$  with respect to  $f_1$  was carried out by fitting a third degree polynomial and differentiating analytically.

—————	Theoretical curves
○————○	GAR histone in 0.15M NaCl/0.01M HCl
●————●	GAR histone in 0.075M NaCl/0.01M HCl

### FIG 8(a)

Theoretical curves for ideal monomer-dimer-n-mer association were constructed using the relationship:

$$\frac{d(M_w)'}{df_1} = -2n \cdot \frac{d(1/(M_n)')}{df_1} + n-1$$

### FIG 8(b)

Theoretical curves for ideal monomer-trimer-n-mer associations were constructed using the relationship:

$$\frac{d(M_w)'}{df_1} = -3n \cdot \frac{d(1/(mn)')}{df_1} + n-1$$

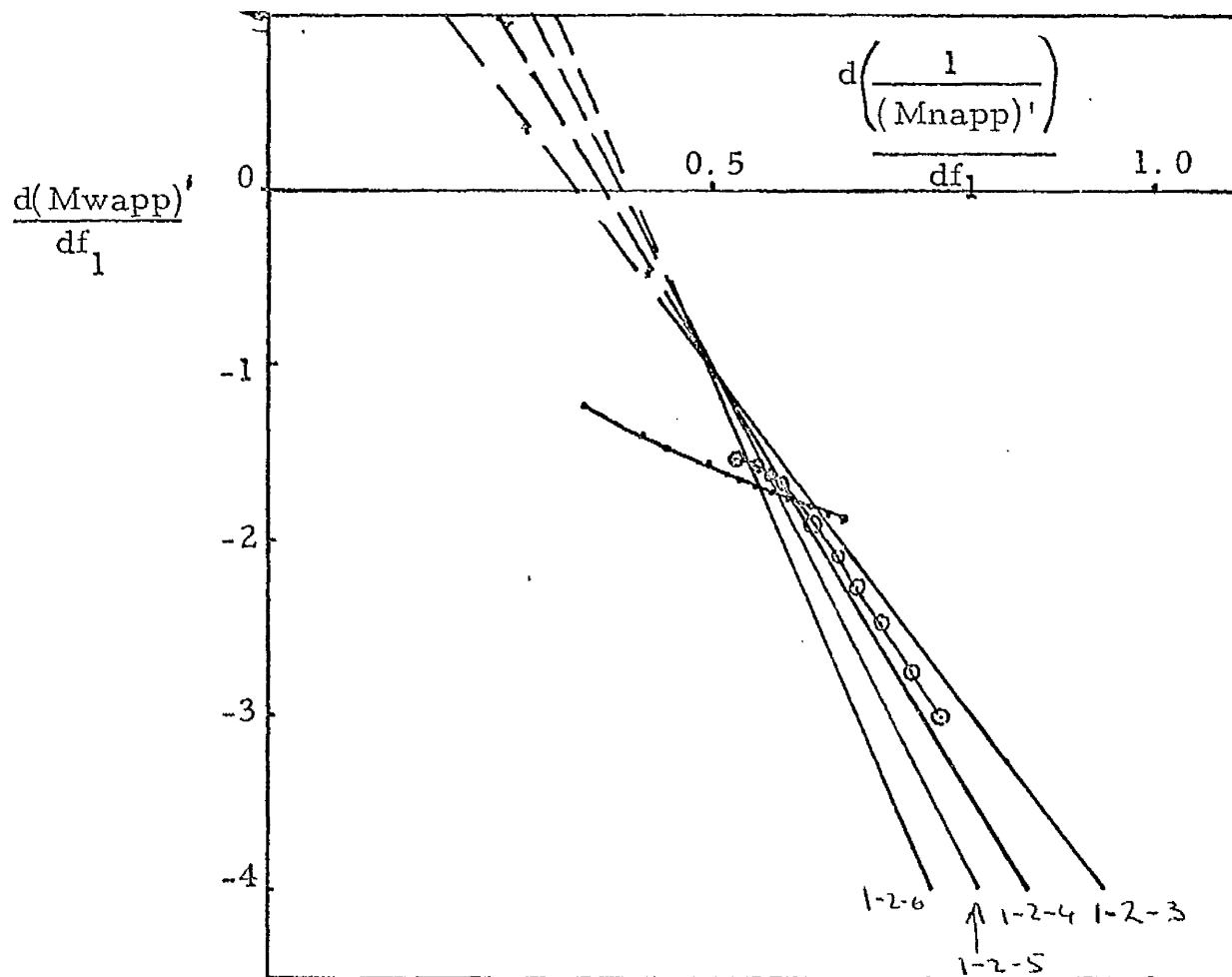


Fig. 8(a)

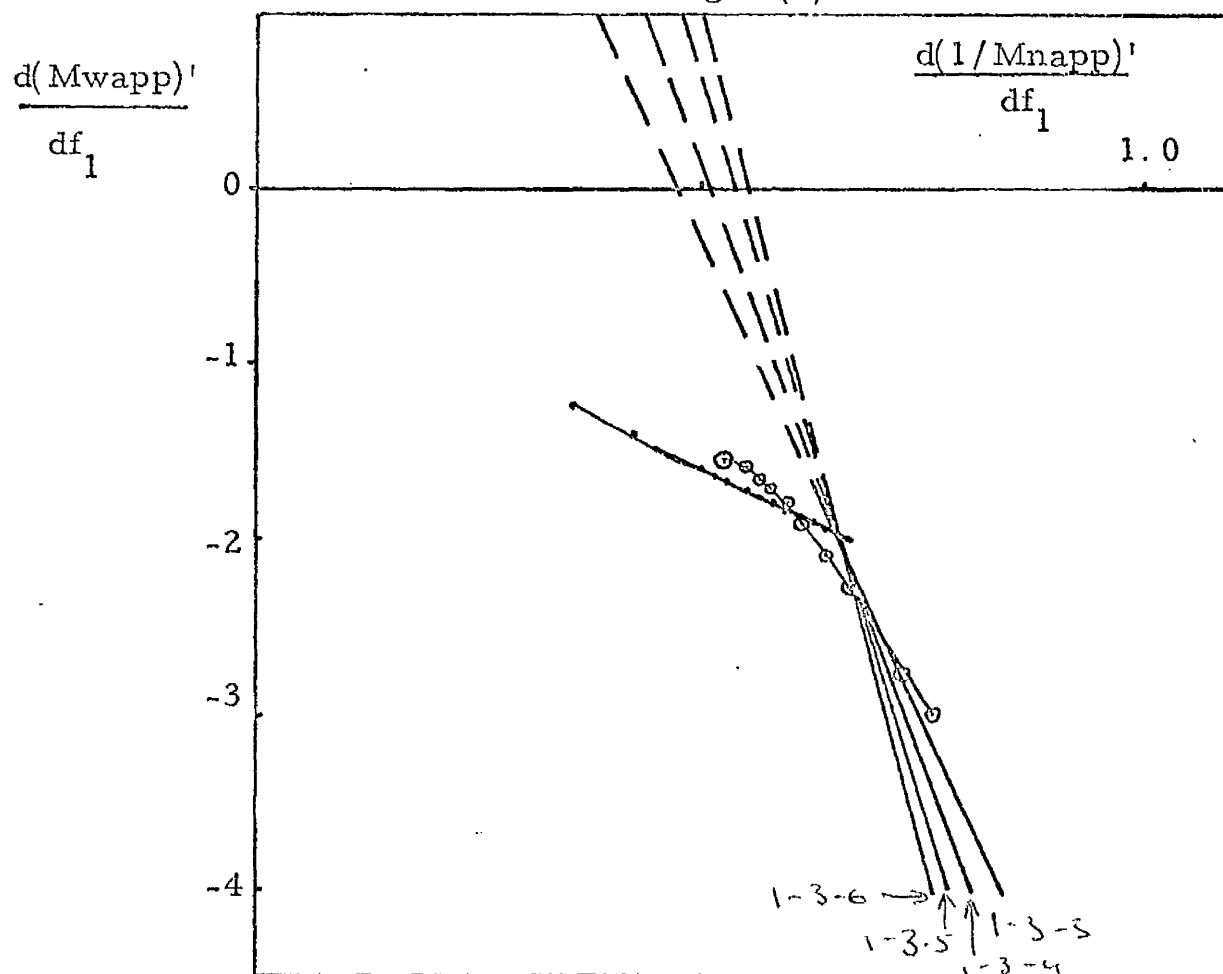


Fig. 8(b)

- to more rigorous analysis.

Used in this context, the procedure of Chun and Kim (1970) may limit the number of different association models to be tested by the more rigorous analyses.

The experimental data describing GAR in 0.075M NaCl /0.01M HCl and 0.15M NaCl/0.01M HCl were analyzed by the procedures of Adams using the tested computer program referred to earlier.

Initial analysis of the experimental  $M_{wapp}$  data of GAR in 0.075M NaCl/0.01M HCl, was carried out using the techniques of successive approximation to find values of  $BM_1$  which satisfied equation No. 1.1 in Appendix 1. Table 6 lists these values of  $BM_1$  which satisfy best the Adams equation for a monomer-n-mer association with  $2 \leq n \leq 10$ , at four different concentrations. Only in the case of monomer-dimer association, is the best value of  $BM_1$  approximately constant at the concentrations used, suggesting that this is the type of association involved. The values of  $BM_1$  obtained for this type of association are small, an average of about 0.006ml/mg. Similar techniques were used to determine the best value of  $BM_1$  using Adams equation (No. 1.2, Appendix 1), for indefinite association. At the four concentrations used in this analysis, no consistency was observed in the  $BM_1$  values obtained for this type of association. (Table 7). The implication of the existence of a monomer-dimer type of association with small  $BM_1$  suggested that a complete analysis of the association by the methods of Adams be carried out assuming this type of association. Using a value of 0.006ml/mg for  $BM_1$  the equations (Nos. 1.3 and 1.4, Appendix 1) describing a monomer-dimer association were evaluated at several different concentrations (Table 8).

TABLE 6

ANALYSIS OF SELF-ASSOCIATION OF GAR HISTONE IN 0.075M

NaCl/0.01M HCl

$M_{wapp}$  as a function of  $c$  was determined from sedimentation equilibrium analyses and values of the parameter,  $\alpha$  and  $M_{wapp}$  were obtained by computer analysis of the  $M_{wapp}$  data. (Appendix 1). Successive approximation techniques were used to determine best-fitting values of  $BM_1$  for monomer-n-mer association using the equations:-

$$n c^{-(n-1)} \alpha \exp(-BM_1 C) (M_1/M_{wapp} - BM_1 c) - c = 0$$

TABLE 6

C mg/ ml	BM <sub>1</sub> For Discrete Association (ml/mg)								
	1-2	1-3	1-4	1-5	1-6	1-7	1-8	1-9	1-10
1.5	.008	.1119	.1909	-	-	-	-	-	-
3.5	.005	.0539	.0839	.1019	.1139	.1230	.1290	.1340	.138
4.5	.006	.043	.066	.079	.088	.095	.099	.104	.107
5.5	.004	.036	.054	.065	.073	.078	.082	.085	.088

TABLE 7

ANALYSIS OF SELF-ASSOCIATION OF GAR HISTONE IN 0.075M

NaCl/0.01M HCl

$M_{wapp}$  as a function of  $c$  was determined from the sedimentation equilibrium analyses and values of the parameters,  $a$  and  $M_{napp}$  were obtained by computer analysis of the  $M_{wapp}$  data (Appendix 1). Successive approximation techniques were used to determine best-fitting values of  $BM_1$  for indefinite association using the equation:-

$$(2/\rho - 1) (M_1/M_{wapp} - BM_1 c) - 1 = 0$$

where  $\rho = M_1/M_{napp} - BM_1 c/2$



TABLE 7

Concentration (mg/ml)	BM <sub>1</sub> for Indefinite Association
1.5	-0.0004
3.0	0.0040
4.5	0.0130
5.5	0.0280

TABLE 8

ANALYSIS OF SELF-ASSOCIATION OF GAR HISTONE IN 0.075M  
NaCl/0.01M HCl USING ADAMS THEORY (APPENDIX 1)

Values of  $M_{wapp}$  of GAR as a function of  $c$  were determined by sedimentation equilibrium and the parameters,  $\Psi$ ,  $cM_1/M_{napp}$ ,  $M_1/cM_{wapp}$  were evaluated from the  $M_{wapp}$  vs.  $c$  data (Appendix 1). Modes of association are tested by comparison of experimental data with those calculated using the theories of Adams (Appendix 1).

Equations used were:

- a)  $2 cM_1/M_{napp} - c = a \exp(-BM_1 c) + BM_1 c^2$
- b)  $2 cM_1/M_{napp} - c = \Psi + 2 (M_1/c M_{wapp} - BM_1) + BM_1 c^2$
- c)  $6 cM_1/M_{napp} - 5c = 2 a \exp(-BM_1 c) + 3BM_1 c^2 - 1/(M_1/cMw - BM_1)$
- d)  $30 cM_1/M_{napp} - 19c = 12 a \exp(-BM_1 c) + \Psi + 15 BM_1 c^2$
- e)  $8 cM_1/M_{napp} - 6c = 3 a \exp(-BM_1 c) + 4 BM_1 c^2 - 1/(M_1/cMw - BM_1)$
- f)  $24 cM_1/M_{napp} - 26c = 6 a \exp(-BM_1 c) + 12 BM_1 c^2 - \Psi - 9/(M_1/cMw - BM_1)$
- g)  $3 cM_1/M_{napp} - c = \Psi + 3/(M_1/cMw - BM_1) + 3/2 (BM_1 c^2)$

TABLE 8

Mode	Eq. used	BM <sub>1</sub> used	Data Value	<sup>c</sup> Cold. Value	Conc. (mg/ml)
M-D	a	0.006	0.70	0.91	2.0
	a	0.006	0.95	1.20	3.0
	a	0.006	1.358	1.775	5.0
	b	0.006	0.840	0.920	2.5
	b	0.006	1.26	1.33	4.5
M-D-Tr	c	0.006	-1.876	-1.358	2.0
	c	0.006	-3.15	-2.60	3.0
	d	0.006	-5.92	-5.09	5.0
	d	0.006	2.51	2.70	2.5
	d	0.006	0.90	1.30	4.5
M-D-Tet	e	0.006	-2.2	-1.456	3.0
	e	0.006	-4.78	-3.32	5.0
	f	0.006	0.45	0.62	2.0
	f	0.006	30.6	31.5	3.0
M-Tr	g	0.006	2.92	7.98	3.0

It was found that there was approximate agreement between the experimental and calculated values of the equations, indicating that a monomer-dimer association correctly describes the association of GAR histone in 0.075M NaCl/0.01M HCl. Additional verification of the type of association involved was provided by comparison of the experimental data with those calculated by equations 1.6 and 1.7 (Appendix 1), describing a monomer-dimer-trimer type of association and by equations 1.8 and 1.9 of Appendix 1, describing a monomer-dimer-tetramer association. As pointed out by Adams and Filmer (1966) and Godfrey and Harrington (1970a, b) a monomer-dimer association is a special case of both monomer-dimer-trimer and monomer-dimer-tetramer associations. A monomer-dimer type of association can be regarded as a monomer-dimer-trimer association with  $K_3 = 0$  and as a monomer-dimer-tetramer association with  $K_4 = 0$ . As can be seen from Table 8, there is approximate agreement between the experimental and calculated values of the equations describing monomer-dimer-trimer and monomer-dimer-tetramer associations, using a value of 0.006ml/mg for  $BM_1$ . The lack of exact agreement between experimental and calculated data for the cases of monomer-dimer, monomer-dimer-trimer and monomer-dimer-tetramer associations can only be accounted for by experimental error in the initial evaluation of molecular weights or by the introduction of numerical errors in the subsequent processing of the data. The most likely source of error in the numerical processing of the data is the evaluation of  $\psi$ , which requires numerical differentiation techniques. It was considered that in view of the relatively small amount of data being processed, standard techniques of numerical differentiation were potentially error-producing. Differentiation was therefore accomplished by fitting a polynomial to the data and differentiating the polynomial by analytical techniques. Extension of the range of concentration used in the initial evaluation of  $M_{wapp}$  to both higher and lower concentrations would also improve the analysis. Comparison of the experimental and calculated values of the equation describing a

monomer-trimer type of association (Equation 1.5 of Appendix 1) is also indicated in Table 8. It can be seen that there is complete disagreement between the experimental and calculated data for this type of association, the extent of the difference between the calculated and experimental values being much greater than those for monomer-dimer, monomer-dimer-trimer and monomer-dimer-tetramer associations, which are probably due to slight errors in numerical processing. Since a monomer-trimer association is not a special case of a monomer-dimer association, no agreement is expected between calculated and experimental values of the monomer-trimer association if the real mode of association is monomer-dimer. Overall, the data of Fig. 8 indicate the likelihood of a monomer-dimer association best describing the association of GAR histone in 0.075M NaCl/0.01M HCl and accordingly the value of  $K_2$ , the equilibrium constant of the monomer-dimer association was calculated using a value of 0.006ml/mg for  $BM_1$ , as described in Appendix 1.  $K_2$  was found to be 2.203ml/mg. To eliminate the possibility that the mode of association had been falsely assigned, theoretical values of  $1/M_{wapp}$  vs.  $c$  were generated for a monomer-dimer association with  $K_2 = 2.203\text{ml/mg}$ . Generation of theoretical  $M_{wapp}$  data was accomplished as recommended by Adams (1967 c), using the equation:-

$$\frac{M_1}{M_{wapp}} = \frac{M_1}{M_w} + BM_1 c \quad \text{where } M_w \text{ is given by the}$$


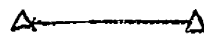
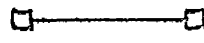
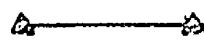
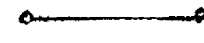
equation  $M_w = \frac{M_1}{c} (c_1 + 2K_2 c_1^2)$ . For each value of  $c$  (the total concentration),  $c_1$  is obtained from the quadratic  $K_2 c_1^2 + c_1 - c = 0$ . Thus it can be seen that the generation of theoretical  $M_1/M_{wapp}$  vs.  $c$  data for a given association is completely independent of any parameters used in the Adams' type of analysis and is therefore independent of any possible numerical errors introduced in the evaluation of these parameters. Comparison of theoretical curves of  $M_1/M_{wapp}$  vs.  $c$  with the original experimental values thus provides a rigorously valid method of verifying the mode of association (Adams, 1967 b). In Fig. 9(a), the original

FIG 9(a)

EFFECT OF VARIATION OF  $BM_1$  ON MONOMER-DIMER ASSOCIATION

WITH  $K_2 = 2.2031\text{ml/mg}$

Values of  $M_1/M_{\text{wapp}}$  were predicted for a monomer-dimer association with  $K_2 = 2.2031\text{ml/mg}$  as described in Appendix 1.

	$BM_1 = 0.10\text{ml/ug}$
	$BM_1 = 0.01\text{ml/mg}$
	$BM_1 = 0.005\text{ml/mg}$
	$BM_1 = 0.01\text{ml/mg}$
	$BM_1 = 0.10\text{ml/mg}$



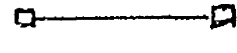
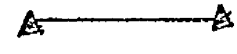
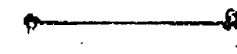
Data obtained experimentally for GAR in 0.075M NaCl/  
0.01M HCl are shown as . . .

FIG 9 (b)

EFFECT OF VARIATION OF  $BM_1$  ON MONOMER-DIMER-TETRAMER

ASSOCIATION WITH  $K_2 = 0.169\text{ml/mg}$  and  $K_4 = 1.237\text{ml/mg}$

Values of  $M_1/M_{\text{wapp}}$  were predicted for a monomer-dimer-tetramer association with  $K_2 = 0.169\text{ml/mg}$  and  $K_4 = 1.237\text{ml/mg}$  as described in Appendix 1.

	$BM_1 = 0.10\text{ml/mg}$
	$BM_1 = 0.01\text{ml/mg}$
	$BM_1 = 0.005\text{ml/mg}$
	$BM_1 = 0.01\text{ml/mg}$
	$BM_1 = 0.10\text{ml/mg}$

Data obtained experimentally for GAR in 0.15M NaCl/0.01M  
HCl are shown as . . .

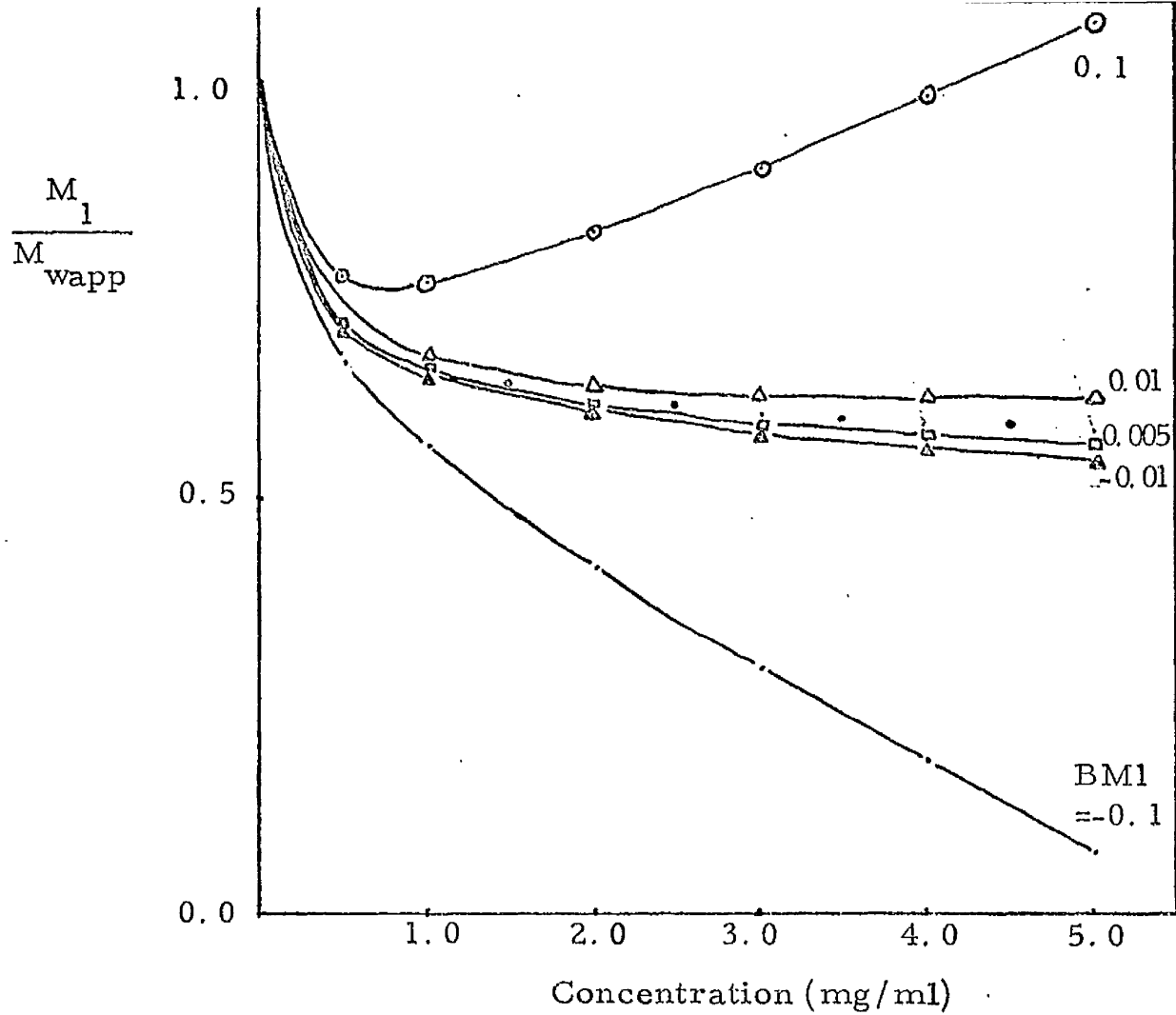


Fig. 9(a)

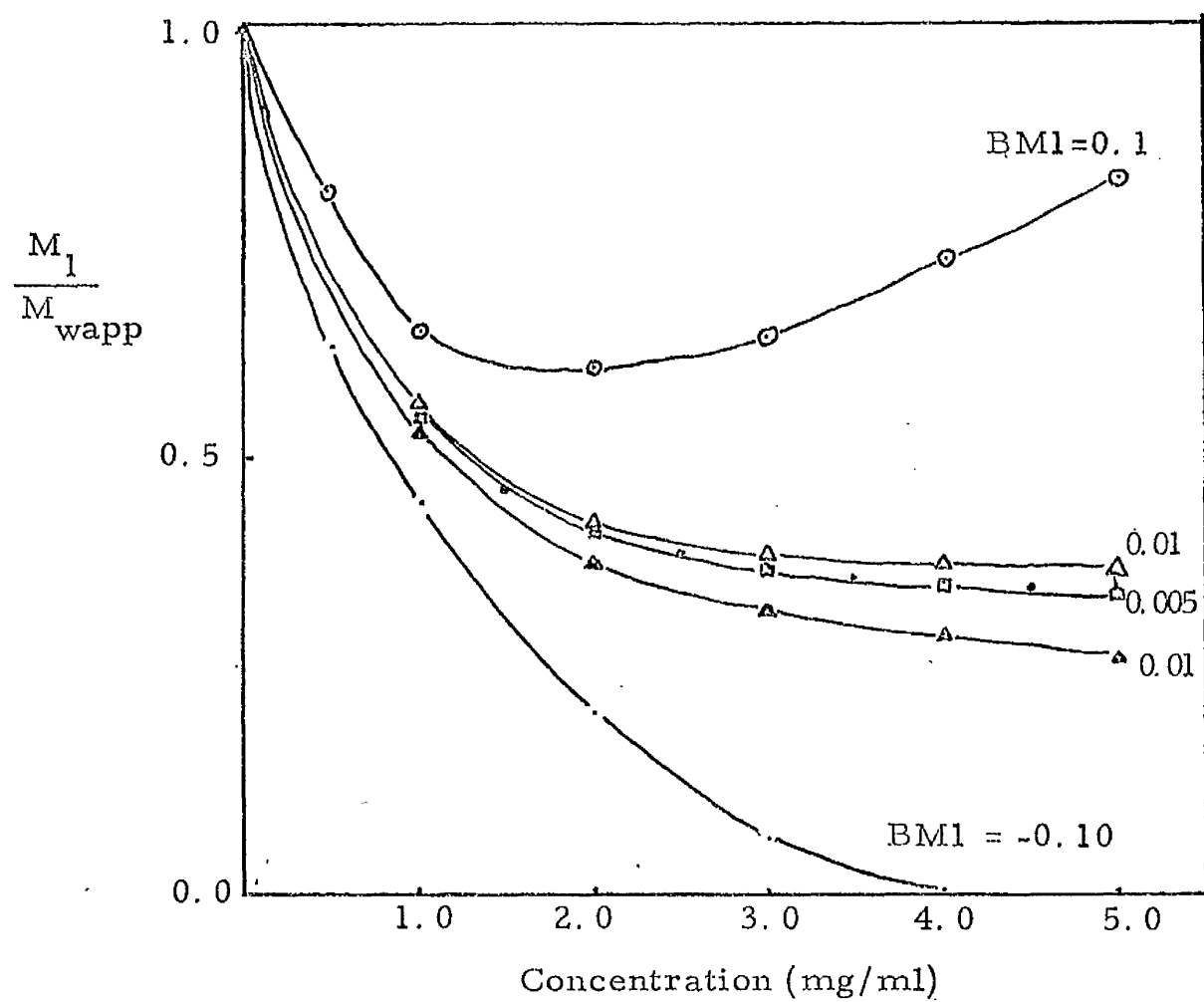


Fig. 9(b)

experimental values of  $M_1/M_{wapp}$  are seen to agree closely with those predicted for a monomer-dimer association with  $K_2 = 2.203 \text{ ml/mg}$  ( $2.081 \times 10^{-3} \text{ l/mole}$ ) and  $BM_1 = 0.006 \text{ ml/mg}$ , thus verifying that this mode of association accurately describes the association of GAR histone in  $0.075 \text{ M NaCl}/0.01 \text{ M HCl}$ . Also shown in Fig. 9(a) are the predicted curves of  $M_1/M_{wapp}$  vs.  $c$  for a variety of  $BM_1$  values. The free-energy change,  $\Delta G$ , for the dimerization of GAR histone in  $0.075 \text{ M NaCl}/0.01 \text{ M HCl}$  was calculated using the equation  $\Delta G = -RT \ln K$  and found to be  $-5.86 \text{ K cal/mole}$ . This value of  $\Delta G$  is of the same order of magnitude as values of  $\Delta G$  calculated for other associating systems (e.g.  $-6.02 \text{ K cal/mole}$  for the dimerization of  $\beta$ -lactoglobulin (Kelly and Reithel, 1971)).

Since the graphical procedure of Chun and Kim suggested that the association of GAR in  $0.15 \text{ M NaCl}/0.01 \text{ M HCl}$  could possibly be described in terms of a monomer-dimer-tetramer association, this type of association was tested using the more rigorous analysis of Adams. Values of  $BM_1$  were calculated using equation 1.1 of Appendix 1 for monomer-n-mer association by successive approximation techniques (Table 9). For associations of the monomer-n-mer type it can be seen that there is no consistency in the calculated  $BM_1$  values at the three concentrations used, thus effectively eliminating monomer-n-mer as the type of association involved. Also shown are the calculated  $BM_1$  values using equation 1.2 of Appendix 1 for indefinite association. No consistency of  $BM_1$  values at the three concentrations used is observed. Values of  $BM_1$  calculated for monomer-dimer-tetramer association using equation 1.8 of Appendix 1 were found to be consistent at the three concentrations used. (Table 9). The value of  $0.004 \text{ ml/mg}$  for  $BM_1$  was therefore used in a detailed analysis of the experimental data by the procedure of Adams. (Table 10). It can be seen that there is very good agreement between the calculated and experimental values of equations 1.8 and 1.9 of Appendix 1 describing monomer-dimer-tetramer associations. For monomer-dimer association, using equations 1.3 and



TABLE 9

ANALYSIS OF SELF-ASSOCIATION OF GAR HISTONE IN 0.15M NaCl/  
0.01M HCl

Values of  $M_{wapp}$  as a function of  $c$  were determined from sedimentation equilibrium analyses and values of the parameters  $a$  and  $M_{wapp}$  were obtained by computer analysis of the  $M_{wapp}$  data (Appendix 1). Successive approximation techniques were used to determine best-fitting values of  $BM_1$  for monomer- $n$ -mer association (Table 7(a)) and for indefinite association (Table 7(b)), using the equations:-

$$nc - (n-1) a \exp(-BM_1 c) (M_1/M_{napp} - BM_1 c) - c = 0$$

$$\text{and } (2/\rho - 1) (M_1/M_{napp} - BM_1 c) - 1 = 0$$

$$\text{where } \rho = M_1/M_{napp} - BM_1 c/2$$

TABLE 9

Conc. mg/ml	BM <sub>1</sub> for Monomer-n-mer ml / mg										BM <sub>1</sub> for indefinite ml/mg	BM <sub>1</sub> for M-D-Tet. ml/mg
	1-2	1-3	1-4	1-5	1-6	1-7	1-8	1-9	1-10			
1.5	0.010	.025	.050	.130	.138	.163	.181	.196	.200	0.167	0.005	
3.5	.000	.005	.012	.031	.043	.051	.058	.063	.067	0.073	0.004	
4.5	-0.005	.001	.002	.017	.027	.035	.040	.044	.048	0.059	0.004	

1.4 of Appendix 1, there are large differences in the calculated and experimental data. Also, for monomer-trimer association the calculated and experimental values of equation 1.5 of Appendix 1 do not agree closely. For monomer-dimer-trimer associations the differences between the calculated and experimental values of equations 1.6 and 1.7 are smaller than those for monomer-dimer and monomer-trimer association but are considerably larger than the differences between the calculated and experimental data for monomer-dimer-tetramer association. It should be noted that unlike the case of monomer-dimer association, which is a sub-set of monomer-dimer-tetramer and monomer-dimer-trimer associations, a monomer-dimer-tetramer association is not, conversely, a sub-set of a monomer-dimer association or of a monomer-dimer-trimer association. This distinction is clearly made by Adams (1967 a) and explains the inconsistency of  $BM_1$  values in Table 9 for monomer-dimer and monomer-tetramer associations. On this basis, the close agreement between calculated and experimental data for only the monomer-dimer-tetramer association (Table 10) suggests this mode of association as best describing the association of GAR in 0.15M NaCl/0.01M HCl. Calculated values of the equations describing monomer-dimer-trimer, monomer-dimer and monomer-trimer associations are unlikely to agree with the experimental values using a value of 0.004ml/mg for  $BM_1$  if the mode of association is monomer-dimer-tetramer. The approximate agreement between calculated and experimental values for the monomer-dimer-trimer equations (Table 10) is less close than that for the monomer-dimer-tetramer association. Overall, the data of Table 10 indicate the possibility of a monomer-dimer-tetramer association describing correctly the association of GAR in 0.15M NaCl/0.01M HCl and accordingly the values of  $K_2$  and  $K_4$ , the equilibrium constants describing the monomer-dimer-tetramer association were calculated as described in Appendix 1.  $K_2$  was found to be 0.169ml/mg and  $K_4$  1.237ml/mg. Rigorous confirmation of the assigned mode of association is, however, only achieved by comparison of the original  $M_1/M_{wapp}$  vs. c data with that

TABLE 10

ANALYSIS OF SELF-ASSOCIATION OF GAR HISTONE IN 0.15M NaCl/  
0.01M HCl USING THE THEORY OF ADAMS

Values of  $M_{wapp}$  of GAR as a function of  $c$  were determined by sedimentation equilibrium and the parameters  $\alpha$ ,  $\Psi$ ,  $c M_1/M_{napp}$ ,  $M_1/cM_{wapp}$  were evaluated from the  $M_{wapp}$  vs.  $c$  data (Appendix 1). Modes of association are tested by comparison of experimental data with those calculated using the theories of Adams (Appendix 1).

Equations used were:

- a)  $2 cM_1/M_{napp} - c = \alpha \exp(-BM_1 c) + BM_1 c^2$
- b)  $2 cM_1/M_{napp} - c = \Psi + 2/(M_1/cM_{wapp} - BM_1) + BM_1 c^2$
- c)  $8 cM_1/M_{napp} - 6c = 3 \alpha \exp(-BM_1 c) + 4 BM_1 c^2 - 1/(M_1/cM_w - BM_1)$
- d)  $24 cM_1/M_{napp} - 26c = 6 \alpha \exp(-BM_1 c) + 12 BM_1 c^2 - \Psi - 9/(M_1/cM_w - BM_1)$
- e)  $6 cM_1/M_{napp} - 5c = 2 \alpha \exp(-BM_1 c) + 3BM_1 c^2 - 1.0/(M_1/cM_w - BM_1)$
- f)  $3 cM_1/M_{napp} - c = \Psi + 3/(M_1/cM_w - BM_1) + \frac{3}{2} BM_1 c^2$
- g)  $30 cM_1/M_{napp} - 19c = 12 \alpha \exp(-BM_1 c) + \Psi + 15 BM_1 c^2$

TABLE 10

Mode	Eq. used	BM <sub>1</sub> used	Data Value	Calcd Value	Conc. (mg/ml)
M-D	a	0.004	0.406	0.872	2.0
	a	0.004	0.220	1.023	3.0
	b	0.004	-0.458	-1.54	5.0
	b	0.004	0.420	0.13	1.5
M-D-Tet	c	0.004	-2.37	-2.313	2.0
	c	0.004	-5.11	-5.164	3.0
	c	0.004	-11.87	-10.30	5.0
	d	0.004	-15.95	-16.51	1.5
M-D-Tr	e	0.004	-2.77	-3.142	2.0
	e	0.004	-5.35	-6.182	3.0
	g	0.004	0.30	1.95	1.5
M-Tr	f	0.004	1.80	5.30	5.0

generated from the equations describing the association. Generation of theoretical  $M_1/M_{wapp}$  vs.  $c$  data was carried out for a monomer-dimer-tetramer association using the equation:-

$$\frac{M_1}{M_{wapp}} = \frac{M_1}{M_w} + BM_1 c$$

$$\text{where } \frac{M_1}{M_w} = \frac{M_1 (c_1 + 2 K_2 c_1^2 + 4 K_4 c_1^2)}{c}$$

At each value of  $c$  (the total concentration), values of  $c_1$  were estimated by Newton-Raphson solution of the equation

$$K_4 c_1^2 + K_2 c_1^2 + c_1 - c = 0. \quad \text{The predicted values of } M_1/M_{wapp}$$

are therefore completely independent of the parameters used in the Adams analysis and are unaffected by any possible error in the evaluation of these parameters. Comparison of the generated  $M_1/M_{wapp}$  data with the experimental data is therefore a rigorous test of the postulated mode of association. Fig. 9(b) shows that there is close agreement between the original experimental  $M_1/M_{wapp}$  vs.  $c$  data and those generated theoretically for a monomer-dimer-tetramer association with  $K_2 = 0.169\text{ml/mg}$  and  $K_4 = 1.237\text{ml/mg}$  and  $BM_1 = 0.004\text{ml/mg}$ . This confirms that a monomer-dimer-tetramer type of association correctly identifies the association of GAR in 0.15M NaCl/0.01M HCl. Also shown in Fig. 9(b) are the theoretical  $M_1/M_{wapp}$  data for monomer-dimer-tetramer associations with  $K_2 = 0.169\text{ml/mg}$  and  $K_4 = 1.237\text{ml/mg}$ , for a variety of  $BM_1$  values.

From each of the equilibrium constants,  $K_2 = 0.169\text{ml/mg}$

( $1.59 \times 10^{-3}$  l/mole) and  $K_4 = 1.237 \text{ ml/mg}$  ( $1.168 \times 10^{-3}$  l/mole), the free energy changes,  $\Delta G$ , of the association were computed using the equation  $\Delta G = -RT \ln K$  and were found to be -5.47 K cal/mole and -5.52 K cal/mole respectively for the monomer-dimer and dimer-tetramer equilibria. These values of  $\Delta G$  are of the same order of magnitude as those described for other associating protein systems (e.g. -5.32 K cal/mole for the dimerization of insulin (Jeffrey and Coates, 1966)).

#### 4. Gel Filtration Analyses of the Association of GAR

The analyses of the association properties of GAR in 0.15M NaCl/0.01M HCl and 0.075M NaCl/0.01M HCl described above, are all based on molecular weight data, so no indication is given of the shape of complexes formed. Analyses of the association of GAR histone were therefore carried out by the gel filtration techniques described in Methods Section 2.8 using columns equilibrated with the same solvent as used in the ultracentrifugal analyses, 0.075M NaCl/0.01M HCl and 0.15M NaCl/0.01M HCl. Large sample volumes (up to 10ml) of GAR histone were applied to the column to produce a plateau region in the elution profile. Values of  $\sigma_w$ , the weight average molecular sieve coefficient were calculated from the trailing boundary by the method described by Ackers and Steere, (1967) (See Appendix 2(b)). Values of  $\sigma_w$  were calculated for several different plateau concentrations and are tabulated in Tables 11 and 12.

For the association of GAR histone in 0.075M NaCl values of  $f_1$  obtained from the ultracentrifugal analysis of the protein (Table 5) were substituted in equation 1 of Appendix 2(b) along with the values of  $\sigma_i$  predicted for complexes of GAR with  $i \leq 6$  according to two extremes of molecular shape. (Table 4). A KDF-9 computer programmed in ALGOL was used to calculate theoretical  $\sigma_w$ 's as a function of

TABLE 11

ANALYSIS OF THE SELF-ASSOCIATION OF GAR HISTONE IN 0.075M  
NaCl/0.01M HCl BY GEL FILTRATION CHROMATOGRAPHY

GAR histone was chromatographed on Sephadex G100 columns equilibrated with 0.075M NaCl/0.01M HCl using sample volumes of 4-10ml. Values of  $\sigma_w$  were calculated from the elution volume of the centroid of the trailing boundary of the plateau region as described in Appendix 2(b). Simson's rule was used as the method of integration to locate the centroid of the trailing boundary, which is that point where the area beneath the trailing boundary equals the area above the trailing boundary up to an extension of the plateau region (See Appendix 2(b)). Values of  $\eta$ , required for the gel-filtration analysis of monomer-dimer-n-mer, were evaluated using the equation:-

$$\eta = \frac{\int_0^c \sigma_w C dc}{\frac{2}{c}}$$



TABLE 11

conc. mg/ml	$\sigma_w$	$\sigma_w C$	$\int_0^c \sigma_w c dx$	$c^2$	$\eta = \frac{\int_0^c \sigma_w C}{c^2}$
1.50	0.450	0.675	0.454	2.25	0.201
2.70	0.420	1.133	1.525	7.29	0.2095
3.27	0.386	1.270	2.099	10.68	0.196
4.42	0.382	1.682	3.685	19.52	0.189

TABLE 12

ANALYSIS OF THE SELF-ASSOCIATION OF GAR HISTONE IN 0.15M  
NaCl/0.01M HCl BY GEL FILTRATION CHROMATOGRAPHY

GAR histone was chromatographed on a Sephadex G100 column equilibrated with 0.15M NaCl/0.01M HCl, using sample volumes of 4-10ml. Values of  $\sigma_w$  were calculated from the elution volume of the centroid of the trailing boundary of the plateau region as described in Appendix 2(b). Simson's rule was used as the method of integration to locate the centroid of the trailing boundary which is that point where the area beneath the boundary equals the area above the trailing boundary up to an extension of the plateau region (See Appendix 2(b)). Values of  $\eta$ , required for the gel-filtration analysis of monomer-dimer-n-mer, were evaluated using the equation:-

$$\eta = \frac{\int_0^c \sigma_w C dc}{\frac{c^2}{2}}$$

TABLE 12

$C$ (mg/ml)	$\sigma_w$	$\sigma_w \cdot c$	$\int_0^c \sigma_w c dc$	$c^2$	$\eta = \frac{\int_0^c \sigma_w C dc}{c^2}$
1.65	0.348	0.573	0.474	2.22	0.174
2.15	0.320	0.688	0.816	4.62	0.177
2.90	0.295	0.856	1.378	8.41	0.164
4.25	0.260	1.105	2.63	18.05	0.145

concentration for the monomer-n-mer association with  $n \leq 6$ . The computer program had previously been tested using standard data of Chun et al. (1969). The predicted curves are plotted in Figs. 10(a) and 10(b), and show that the experimental values of  $\sigma_w$  agree most closely with the curve predicted for monomer-dimer association. As expected for monomer-n-mer associations with  $n \leq 3$ , the predicted values of  $\sigma_w$  at high concentration are lower for linear association than for the corresponding compact association. The curves corresponding to linear and compact monomer-dimer associations are identical.

A directly analogous procedure using equation 3 of Appendix 2(b) was employed to generate predicted curves for indefinite associations of linear and compact shapes for GAR in 0.075M NaCl/0.01M HCl. The experimental data do not fit either of the theoretical curves (Fig. 10(c)), confirming that indefinite association does not adequately describe the association of GAR in 0.075M NaCl/0.01M HCl. It can be seen from Fig. 10(c) that the experimental data do not lie between the two predicted curves, eliminating the possibility that the experimental data represented an indefinite association of a shape intermediate between the two extreme models of shape, linear and compact.

The procedure of Chun et al. (1969) and Chun and Kim (1969) using gel filtration techniques for the analysis of associating protein systems combines information obtained from gel-filtration studies with data (in particular, values of  $f_1$ , the weight fraction of monomer), derived from molecular weights obtained in the ultracentrifuge. It is significant that no attempt is made to derive  $f_1$  or molecular weights from the gel-filtration data; values of  $f_1$  obtained in the analytical ultracentrifuge in the same solvent conditions in which the gel filtration studies are carried out, are simply combined with the gel-filtration data. This necessity for combining data obtained by one

GEL FILTRATION ANALYSIS OF GAR IN 0.075M NaCl/0.01M HCl

Approx. 10ml samples of GAR were chromatographed on a 40cm X 1cm Sephadex G100 column, equilibrated with 0.075M NaCl/0.01M HCl. Values of  $\sigma_w$  were calculated from the trailing boundary of the plateau regions in the elution profiles as described in Appendix 2(b). Theoretical curves of  $\sigma_w$  vs.  $c$  were constructed as described in Appendix 2(b) using  $f_1$  values obtained from ultracentrifugal analysis (Table 4).

FIG 10(a)

Theoretical curves were constructed for ideal monomer-n-mer associations using values of  $\sigma_i$  calculated for linear aggregation (Table 4), using equation 1 of Appendix 2(b).

—————	Theoretical Curves
○————○	GAR histone in 0.075M NaCl/0.01M HCl

FIG 10(b)

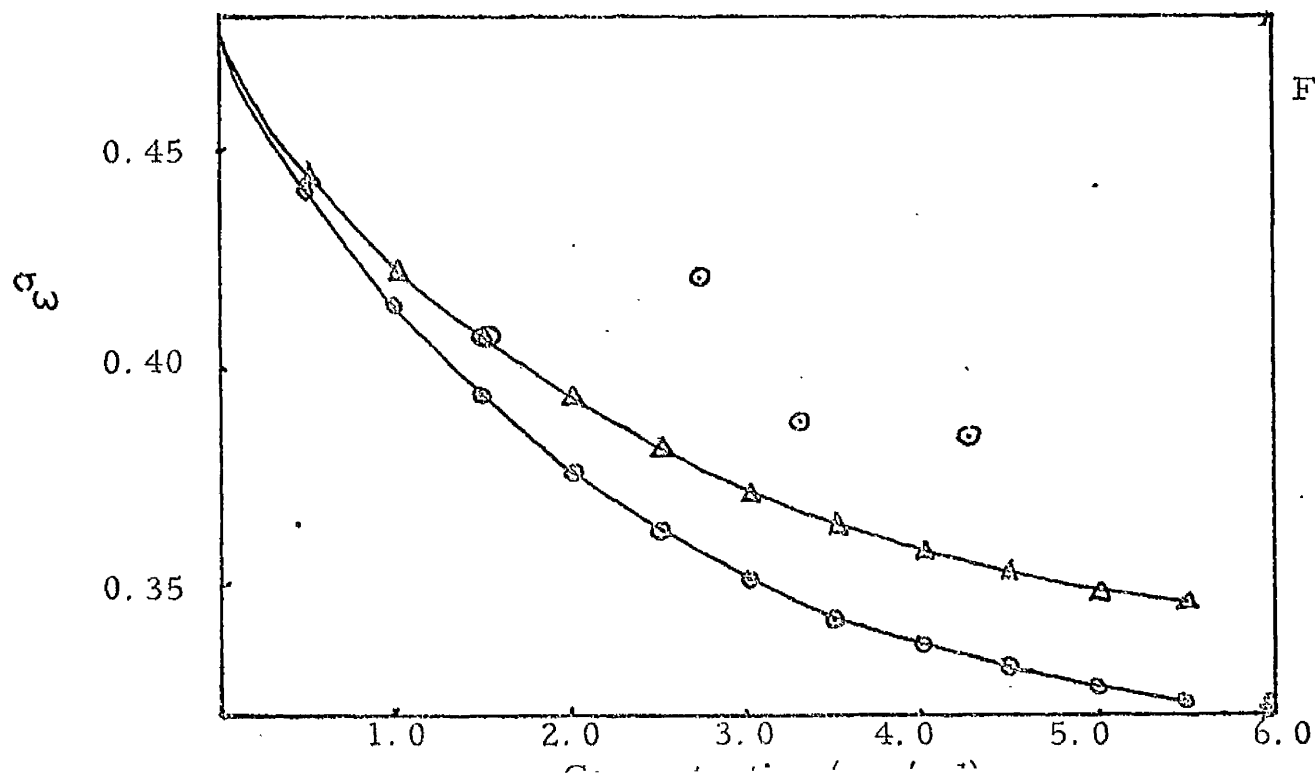
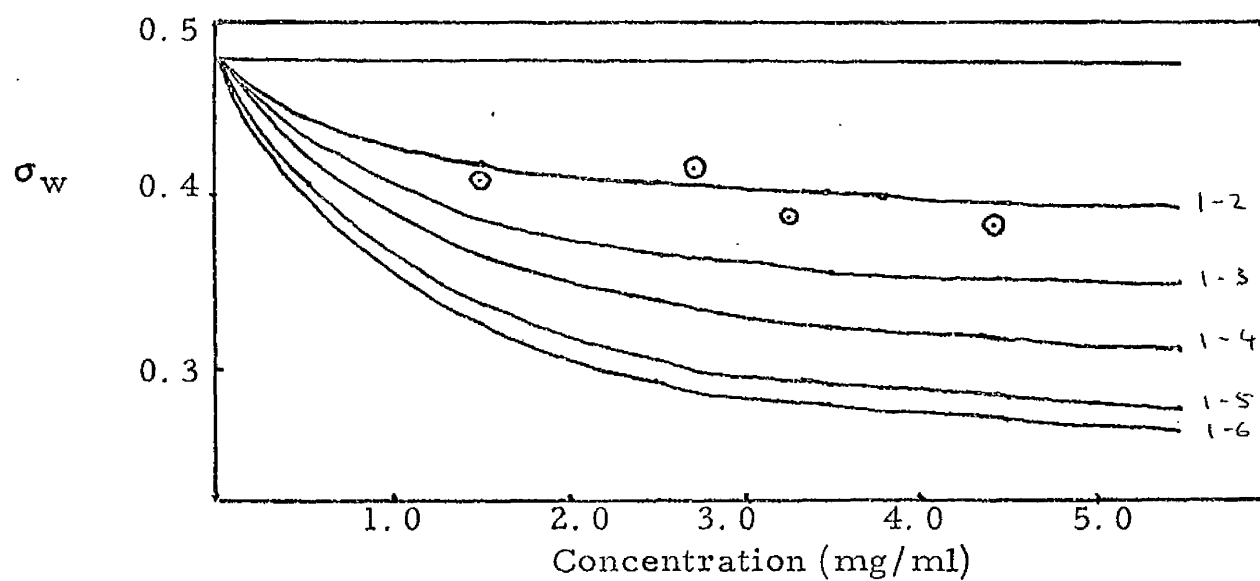
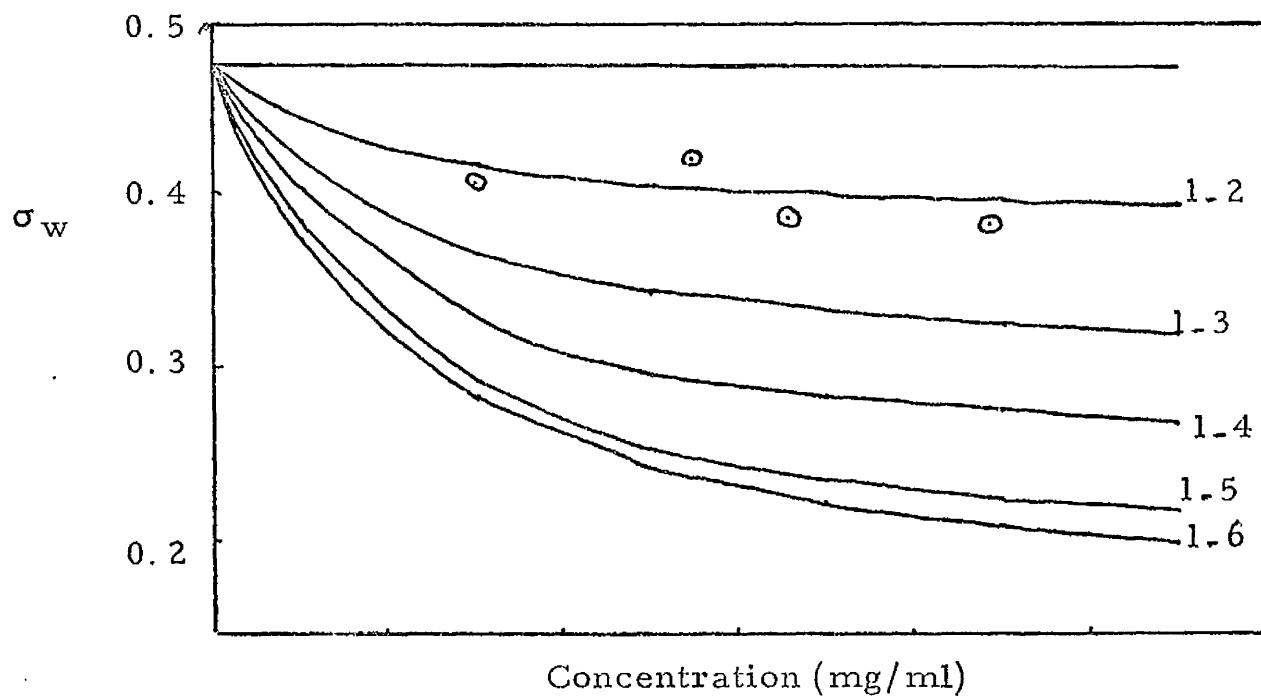
Theoretical curves were constructed for ideal monomer-n-mer association using values of  $\sigma_i$  calculated for compact aggregation.

—————	Theoretical curves
○————○	GAR histone in 0.075M NaCl/0.01M HCl

FIG 10(c)

Theoretical curves were constructed for ideal indefinite association, using equation 3 of Appendix 2(b).

○   ○   ○	GAR histone in 0.075M NaCl/0.01M HCl
△————△	Compact indefinite association
○————○	Linear indefinite association



technique with those from another technique represents the major drawback of the analysis of Chun et al. (1970). Despite the fact that the ultracentrifugation and gel-filtration are carried out under the same solvent conditions, it is possible that small sources of errors unique to each technique may affect the combination of these two sets of data. For example, pressure effects in sedimentation may affect the accuracy of derived values of  $f_1$  and thus errors may be introduced when these data are combined with the gel filtration data, in which pressure effects are absent. Nevertheless, it has been demonstrated clearly by Chun et al. (1969) that the approach using the two techniques of ultracentrifugation and gel-filtration is vastly superior to the method in which molecular weights are estimated empirically from gel-filtration studies.

As described in Appendix 2(b), the method of Chun et al. (1970) for analyzing monomer-m-mer-n-mer associations was modified for ease of computation. Instead of substituting values of  $f_1$  obtained from ultracentrifugal studies into the gel-filtration equation and generating theoretical curves of  $\sigma_w$  vs.  $c$  in a manner analogous to that used above for monomer-n-mer and indefinite association, it was found more convenient to generate standard curves of  $f_1$  vs.  $c$  from the gel filtration values of  $\sigma_w$ . The test of the existence of a particular mode of monomer-m-mer-n-mer association is therefore comparison of predicted and experimental curves of  $f_1$  vs.  $c$ . For the association of GAR in 0.075M NaCl/0.01M HCl the experimental values of  $\sigma_w$  (Table 4) were substituted into Equation 2 of Appendix 2(b) and theoretical curves of  $f_1$  vs.  $c$  were evaluated by computer, for comparison with the experimental values of  $f_1$  obtained from analytical ultracentrifugation and tabulated in Table 5. The values of  $\eta = \int_0^c \sigma_w c dc$ , required for this procedure were calculated by integration of  $\sigma_w$  as a function of  $c$ . (Table 11).

Using the experimentally obtained values of  $\sigma_w$  and  $\eta$  together with the predicted values of  $\sigma_i$  (Table 4), theoretical curves of  $f_1$  vs.  $c$  were generated and are shown in Figs. 11 a and b for monomer-dimer-n-mer associations according to the two shape models, compact and linear. Fig. 11(a) demonstrates that the experimental values of  $f_1$  obtained from ultracentrifuge analysis under the same conditions do not agree satisfactorily with the predicted curves for compact monomer-dimer-n-mer association. At low concentrations ( $<1.5\text{mg/ml}$ ) it can be seen that the experimental curve coincides with the predicted curve for monomer-dimer-trimer association. This may be due to the fact that there are no points between  $C = 0$  and  $c = 1.5\text{mg/ml}$  on the predicted curves and the exact position of the curve in this concentration range is uncertain. The lack of points in this concentration range is a consequence of the generation of the predicted curves from  $\sigma_w$  data, rather than the generation of predicted curves of  $\sigma_w$  vs.  $c$  from  $f_1$  data, which are available over the whole concentration range. Similarly, Fig. 11b, demonstrates that although there is agreement at low concentrations between the experimentally obtained data and the predicted curve for a linear monomer-dimer-trimer aggregation, there is no satisfactory overall agreement between the experimental data and the standard curves. Again, the exact positions of the predicted curves at concentrations less than  $1.5\text{mg/ml}$  are unknown because of the lack of data points in this region.

Complete gel filtration analysis of the association of GAR in  $0.075\text{M NaCl}/0.01\text{M HCl}$  therefore confirms the results of the ultracentrifugal studies, since correlation between experimental data and predicted curves only occurs in the case of a monomer-dimer association.

Gel filtration analyses were also carried out on GAR in  $0.15\text{M NaCl}$ ,  $0.01\text{M HCl}$ . The values of  $\sigma_w$  obtained are shown in



## FIG 11

### GEL FILTRATION ANALYSIS OF GAR IN 0.075M NaCl/0.01M HCl

Approximately 10ml samples of GAR were chromatographed on a 40cm X 1cm Sephadex G100 column, equilibrated with 0.075M NaCl/0.01M HCl. Values of  $\sigma_w$  were calculated from the trailing boundary of the plateau regions in the elution profiles as described in Appendix 2(b). Theoretical curves of  $f_1$  vs.  $c$  were constructed using equation 2 of Appendix 2(b).

#### FIG 11(a)

Theoretical curves of  $f_1$  vs.  $c$  were constructed for ideal monomer-dimer-n-mer associations using values of  $\sigma_i$  calculated for compact aggregation (Table 4).

○————○

Theoretical curves

△————△

Experimental curves obtained from  
ultracentrifuge analysis of GAR in  
0.075M NaCl/0.01M HCl

#### FIG 11(b)

Theoretical curves of  $f_1$  vs.  $c$  were constructed for ideal monomer-dimer-n-mer associations using values of  $\sigma_i$  calculated for linear aggregation (Table 4).

○————○

Theoretical curves

△————△

Experimental curves obtained from  
ultracentrifugal analysis of GAR in  
0.075M NaCl/0.01M HCl

Fig. 11(a)

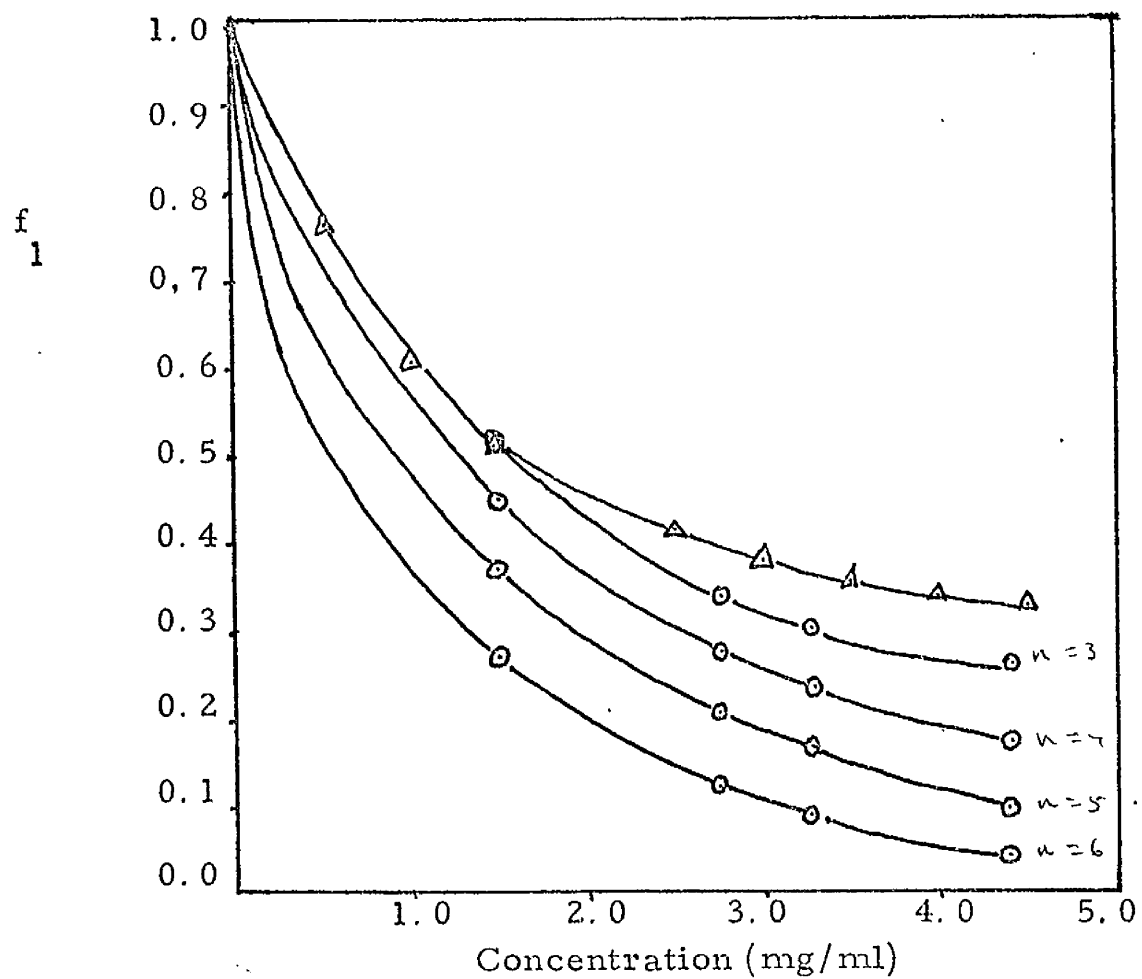
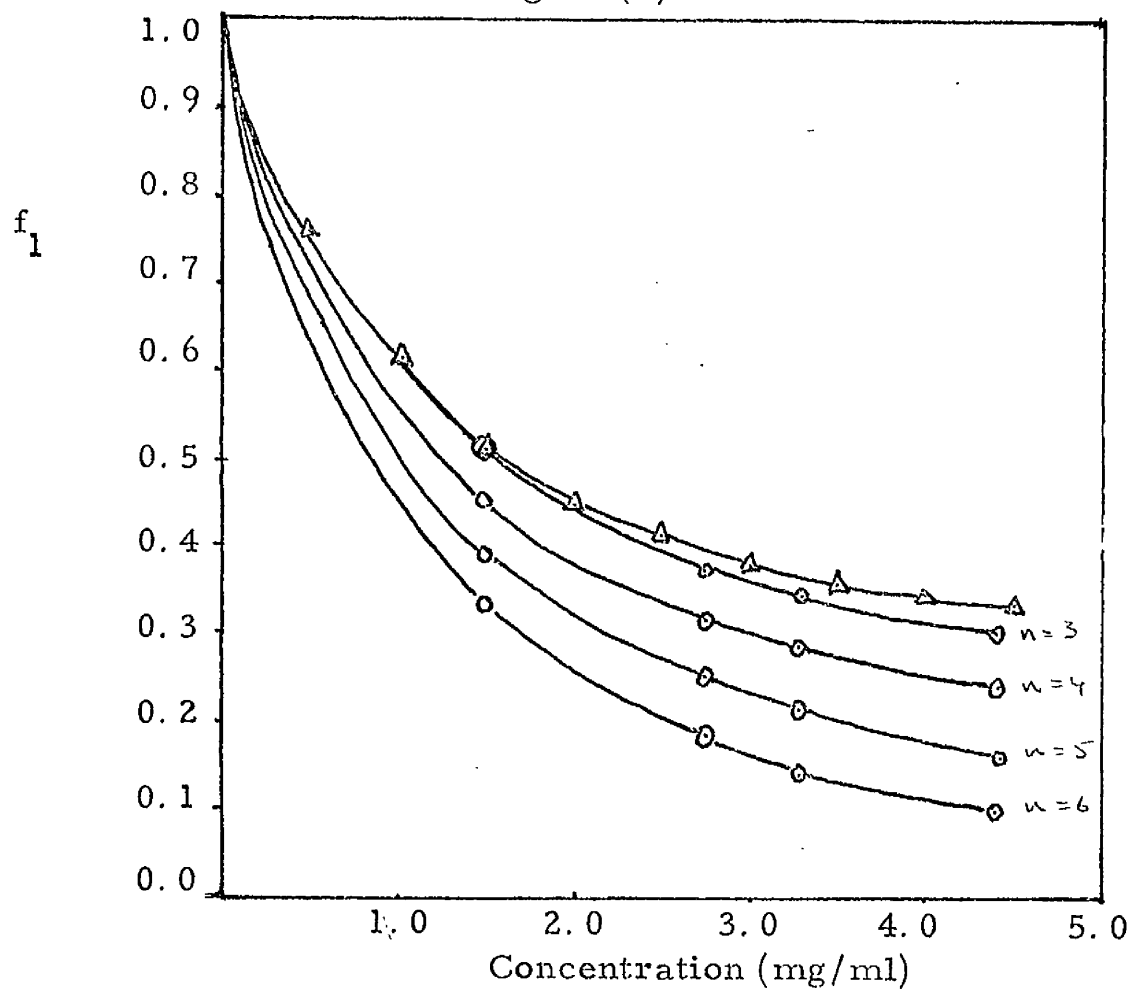


Fig. 11(b)

Table 12. Using the values of  $f_1$ , shown in Table 5, which were obtained by ultracentrifugal analysis, theoretical curves for ideal compact and linear association of the monomer-n-mer type were generated using equation 1 of Appendix 2b. Comparison of the experimental and theoretical curves are shown in Figs. 12(a),(b). It may be seen that there is little agreement between theoretical and experimental curves. A similar procedure was used to generate theoretical curves of  $\sigma_w$  vs.  $c$  for compact and linear ideal indefinite association, using equation 3 of Appendix 2(b). (Fig. 12(c)). No agreement is observed between theoretical and experimental curves. When equation 2 of Appendix 2(b) is used to generate curves of  $f_1$  vs.  $c$  from experimental values of  $\sigma_w$  (Table 12) and the theoretical values of  $\sigma_i$  (Table 4), it can be seen (Figs. 13 a, b) that the values of  $f_1$  vs.  $c$  obtained experimentally by ultracentrifugation agree reasonably with the curves predicted for a linear monomer-dimer-trimer association and a compact monomer-dimer-tetramer association. The values of  $\eta$  required for the generation of the theoretical curves were evaluated from integration of the curve of  $\sigma_w$  vs.  $c$  (Table 12). The inability of the analysis to distinguish unambiguously between linear monomer-dimer-trimer associations and compact monomer-dimer-tetramer associations is probably due to the similarity in size of a linear trimer and a compact tetramer which is reflected in the similarity of their predicted  $\sigma_i$ 's of 0.2495 and 0.2351 respectively. Since ultracentrifugal analysis had clearly implicated a monomer-dimer-tetramer type of association the possibility, suggested by the gel filtration analysis, that a linear-monomer-dimer-trimer association was involved, was discounted. It was therefore concluded that GAR histone undergoes a monomer-dimer-tetramer association in which the complex formed is of a compact shape, similar to a tetrahedron.

##### 5. Effect of pH on the association of GAR histone

One aim of these studies is to investigate the nucleoprotein

GEL FILTRATION ANALYSIS OF GAR IN 0.15M NaCl/0.01M HCl

4-10ml samples of GAR were chromatographed on a 40cm X 1cm Sephadex G100 column, equilibrated with 0.15M NaCl/0.01M HCl. Values of  $\sigma_w$  were calculated from the trailing boundary of the plateau regions in the elution profiles as described in Appendix 2(b). Theoretical curves of  $\sigma_w$  vs.  $c$  were constructed as described in Appendix 2(b) using  $f_1$  values obtained from ultracentrifugal analysis (Table 5).

FIG 12(a)

Theoretical curves were constructed for ideal monomer-n-mer associations using values of  $\sigma_i$  calculated for linear aggregation (Table 4), using Equation 1 of Appendix 2(b)



 Theoretical curves  
 GAR histone in 0.15M NaCl/0.01M HCl

FIG 12(b)

Theoretical curves were constructed for ideal monomer-n-mer associations using values of  $\sigma_i$  calculated for compact aggregation (Table 4), using Equation 1 of Appendix 2(b)




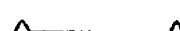

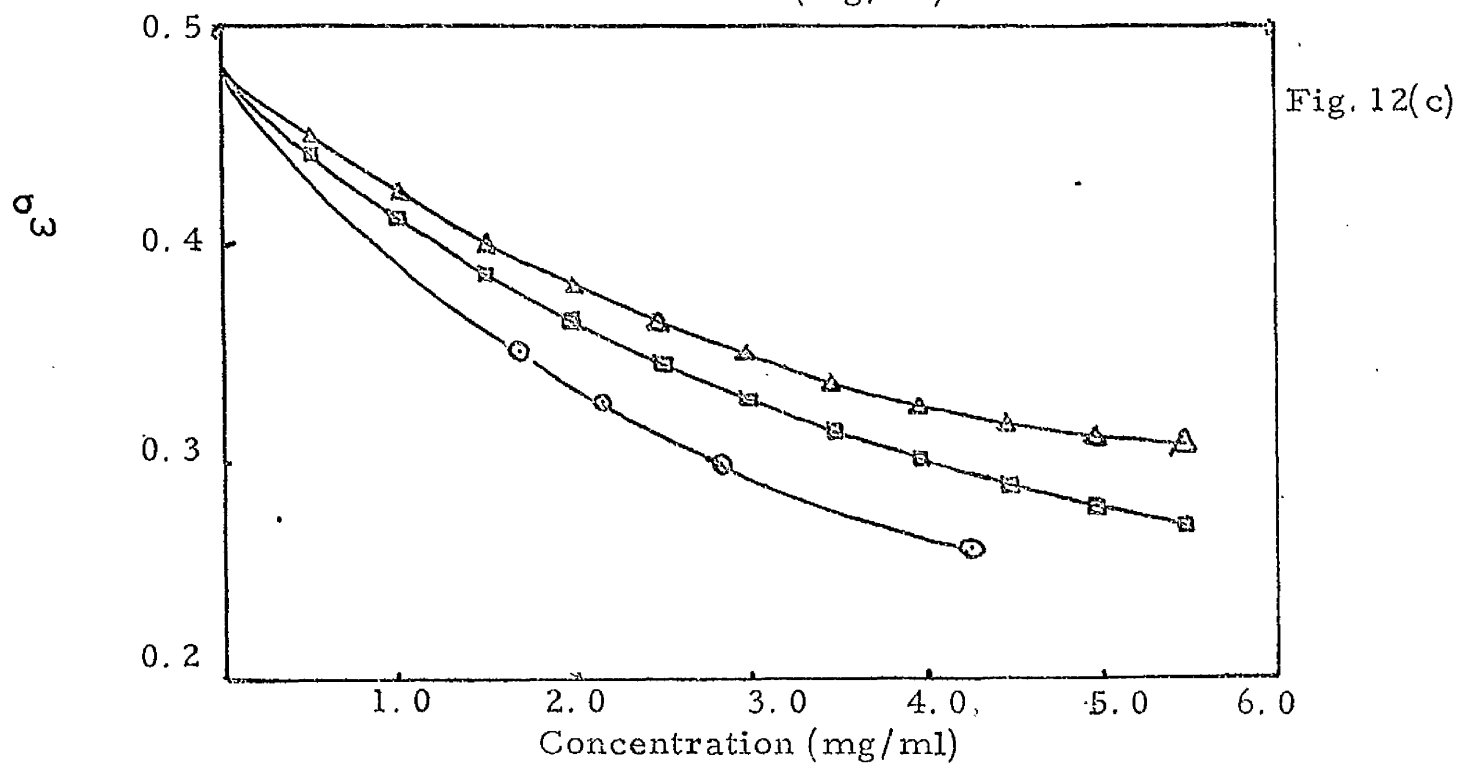
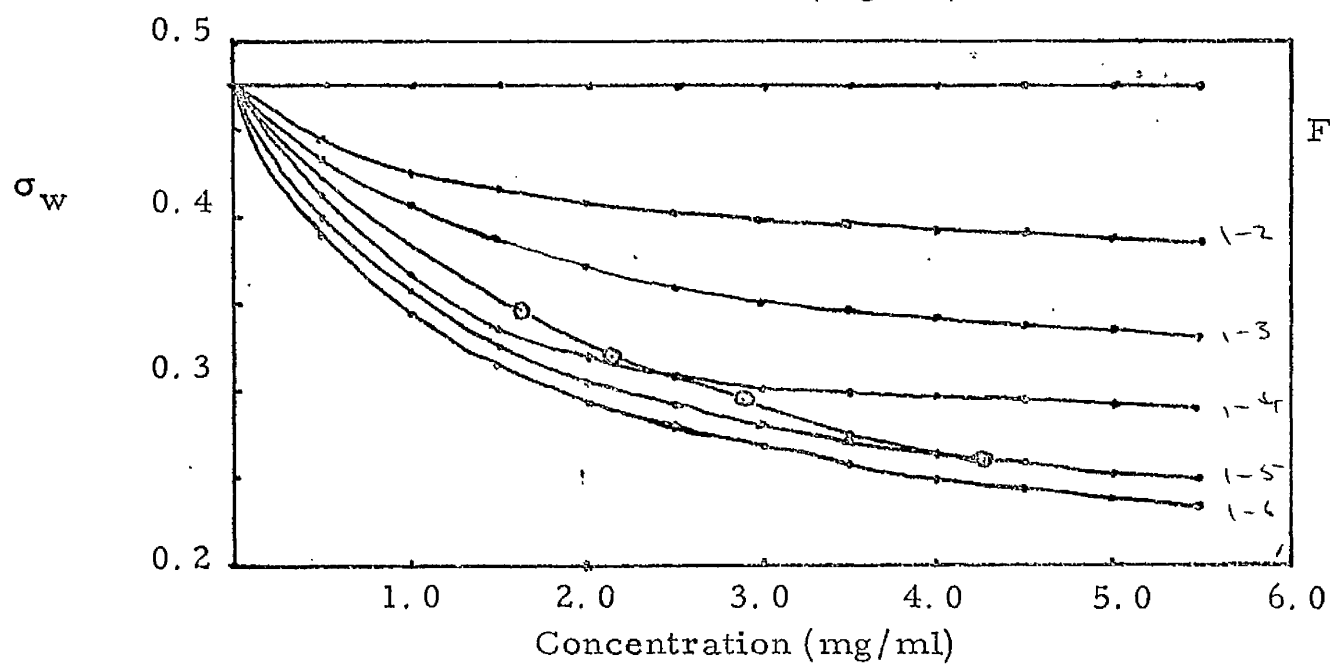
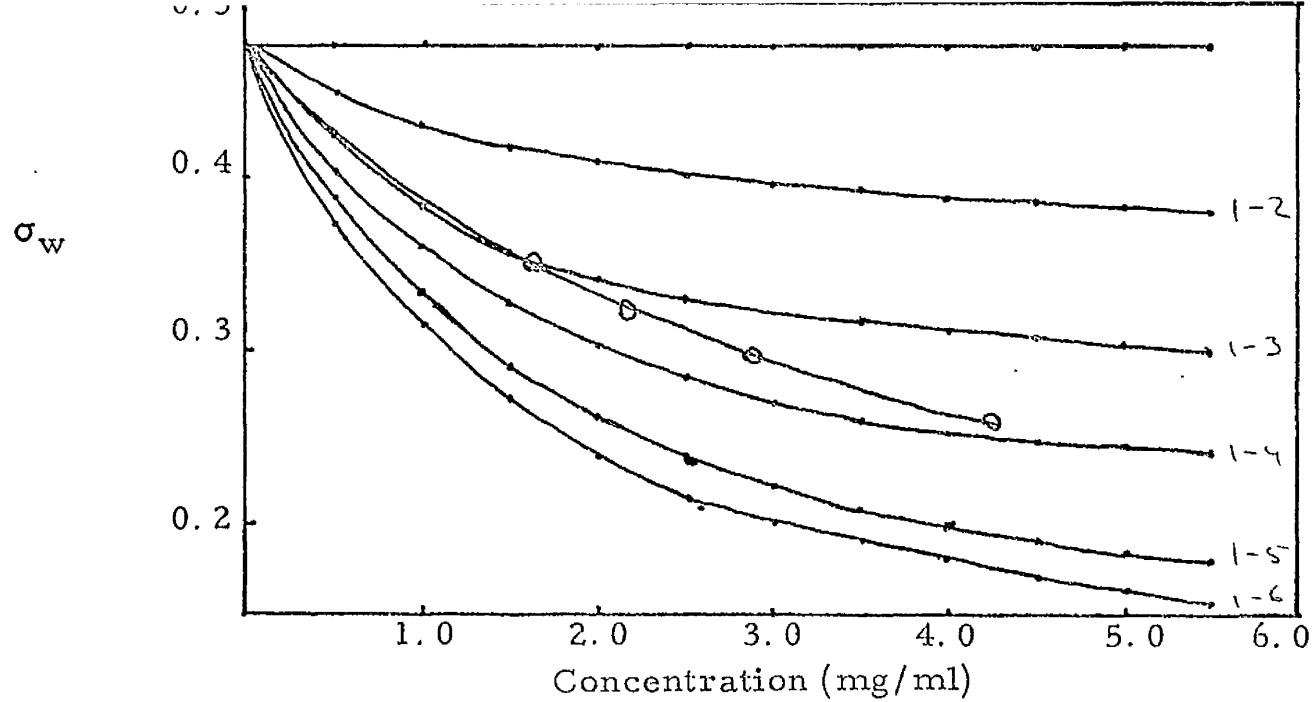
 Theoretical curves  
 GAR histone in 0.15M NaCl/0.01M HCl

FIG 12(c)

Theoretical curves were constructed for ideal indefinite association, using Equation 3 of Appendix 2(b).

 GAR histone in 0.15M NaCl/0.01M HCl  
 Compact indefinite association  
 Linear indefinite association



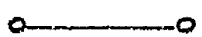

### FIG 13

#### GEL FILTRATION ANALYSIS OF GAR IN 0.15M NaCl/0.01M HCl

4-10ml samples of GAR were chromatographed on a 40cm X 1cm Sephadex G100 column, equilibrated with 0.15M NaCl/0.01M HCl. Values of  $\sigma_w$  were calculated from the trailing boundary of the plateau regions in the elution profiles as described in Appendix 2(b). Theoretical curves of  $f_1$  vs.  $c$  were constructed using equation 2 of Appendix 2(b).

#### FIG 13(a)

Theoretical curves of  $f_1$  vs.  $c$  were constructed for ideal monomer-dimer-n-mer associations, using values of  $\sigma_i$  calculated for compact aggregation (Table 4).

	Theoretical curves
	Experimental curve obtained from ultracentrifugal analysis of GAR in 0.15M NaCl/0.01M HCl

#### FIG 13(b)

Theoretical curves of  $f_1$  vs.  $c$  were constructed for ideal monomer-dimer-n-mer associations using values of  $\sigma_i$  calculated for linear aggregates (Table 4).


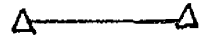
	Theoretical curves
	Experimental curve obtained from ultracentrifugal analysis of GAR in 0.15M NaCl/0.01M HCl

Fig. 13(a)

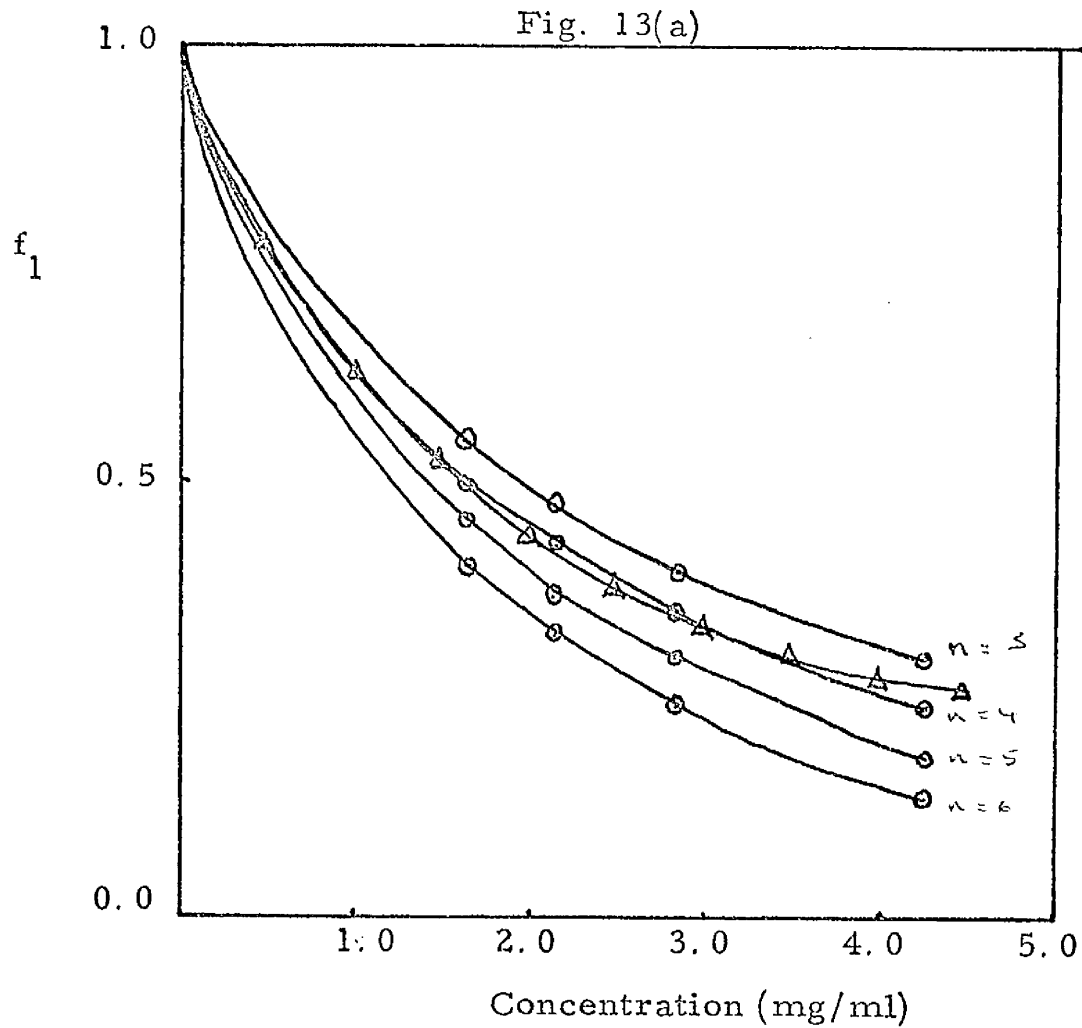
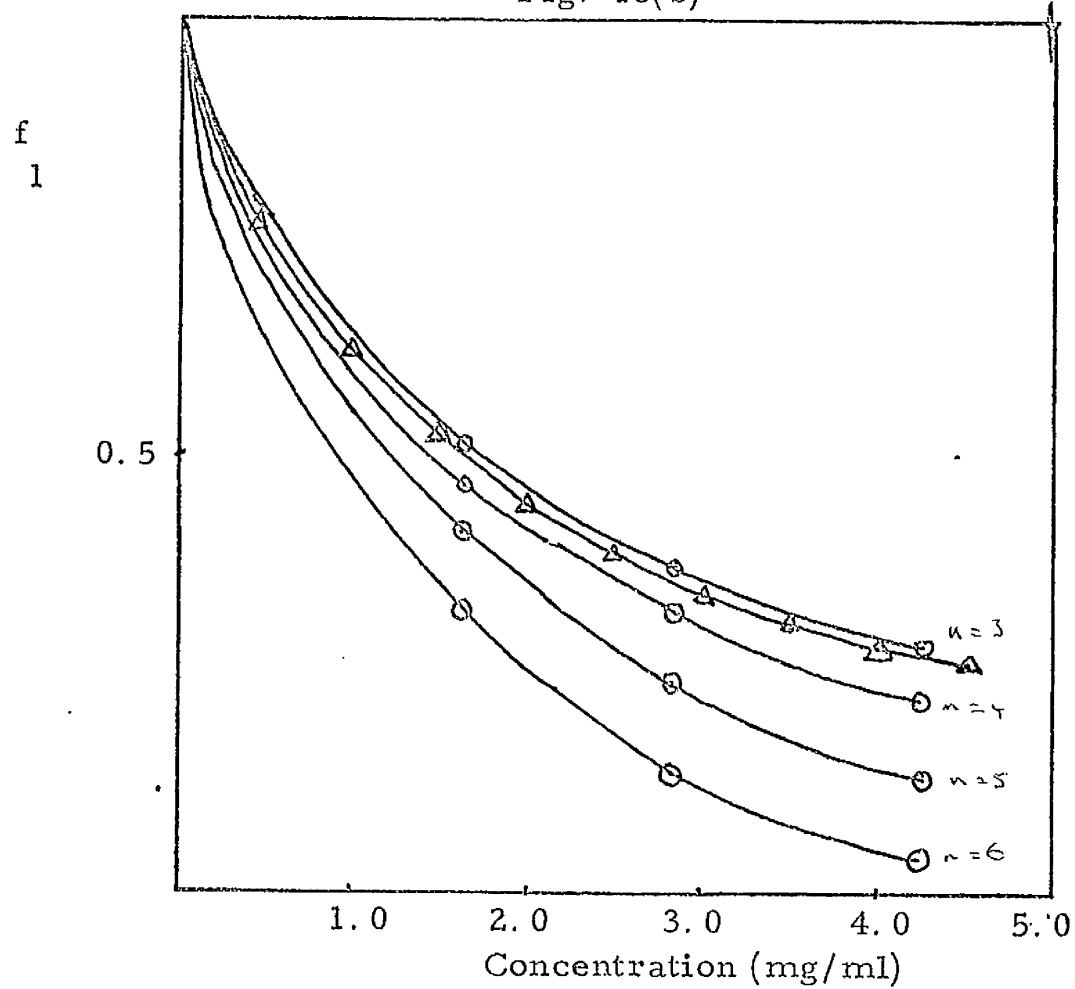


Fig. 13(b)



complexes formed by the interaction of GAR and DNA. Since these nucleoprotein complexes are generally formed experimentally at pH values near neutrality, ultracentrifugal studies on pure GAR histone were carried out to investigate the type of association of GAR histone at higher pH values. The preliminary ultracentrifugal analysis of Edwards and Shooter (1969) on the aggregation of  $F_2A_1$  histone fractions had shown that the state of aggregation was independent of pH in the range 1-7. The graphical analysis of Chun and Kim (1970) of the association of GAR in 0.075M NaCl/0.01M HCl and 0.15M NaCl/0.01M HCl had suggested that the modes of association in these conditions were monomer-dimer and monomer-dimer-tetramer, respectively. These suggestions were confirmed by the more detailed analysis of Adams. Accordingly, the graphical procedure of Chun and Kim was again used to study the association at higher pH values. Dilute low ionic strength McIlvaine type buffers were used for these studies and Fig. 14(a) shows the values of  $M_{wapp}$  obtained from sedimentation equilibrium experiments carried out on GAR histone in 0.075M NaCl, pH 5.0 and 0.075M NaCl, pH 7.0. As in the analysis of the association of GAR histone in 0.075M NaCl/0.01M HCl, the value of  $M_1$ , the monomer molecular weight was taken to be 10600, as calculated from the amino acid analysis. The best-fitting curve through the  $M_{wapp}$  data was constrained to pass through  $M_1$  at  $c = 0$  and is shown in Fig. 14(a). For each pH value, three separate sedimentation equilibrium experiments were carried out. A large concentration range (from about 0.5mg/ml to 5.0mg/ml) is nevertheless covered by these three sedimentation equilibrium studies and it can be seen from Fig. 14(a) that a single continuous curve can be drawn through the data without large deviations between the best-fitting curve and the experimental data. Possible errors introduced because of the relatively small number of separate sedimentation equilibrium studies used to described the associations



FIG 14(a)

ASSOCIATION OF GAR HISTONE IN 0.075M NaCl, pH 5.0 and  
0.075M NaCl, pH 7.0

Preparation of GAR histone at different initial concentrations were exhaustively dialyzed against 0.075M NaCl, pH 5.0 and 0.075M NaCl, pH 7.0 and centrifuged at 26,000 rpm for at least 36h at 20°C in an AN-G rotor in a Beckman Model E analytical ultracentrifuge, equipped with absorption optics. Apparent weight average molecular weights ( $M_{wapp}$ ) were determined from computer evaluation of the gradient of  $\ln c$  vs.  $r^2$  data. A third degree polynomial was fitted to the data using a least squares curve-fitting procedure and constrained to pass through  $M_1 = 10600$ .

- GAR histone in 0.075M NaCl, pH 5.0
- GAR histone in 0.075M NaCl, pH 7.0
- Best-fitting curve

FIG 14(b)

ANALYSIS OF ASSOCIATION OF GAR IN 0.075M NaCl, pH 5.0 AND  
0.075M NaCl, pH 7.0 BY THE GRAPHICAL PROCEDURE OF CHUN  
AND KIM (1970)

Experimental values of  $(M_{wapp})'$ ,  $(M_{napp})'$  and  $f_1$  were determined from the  $M_{wapp}$  data of Fig. 14(a) as described in Appendix 1. Theoretical curve for an ideal monomer-dimer association was constructed using the relationship:

$$(M_w)^1 = -f_1 + 2$$

- Theoretical curve
- Experimental curve for GAR in 0.075M NaCl, pH 5.0
- Experimental curve for GAR in 0.075M NaCl, pH 7.0

Fig. ( 14 (a)

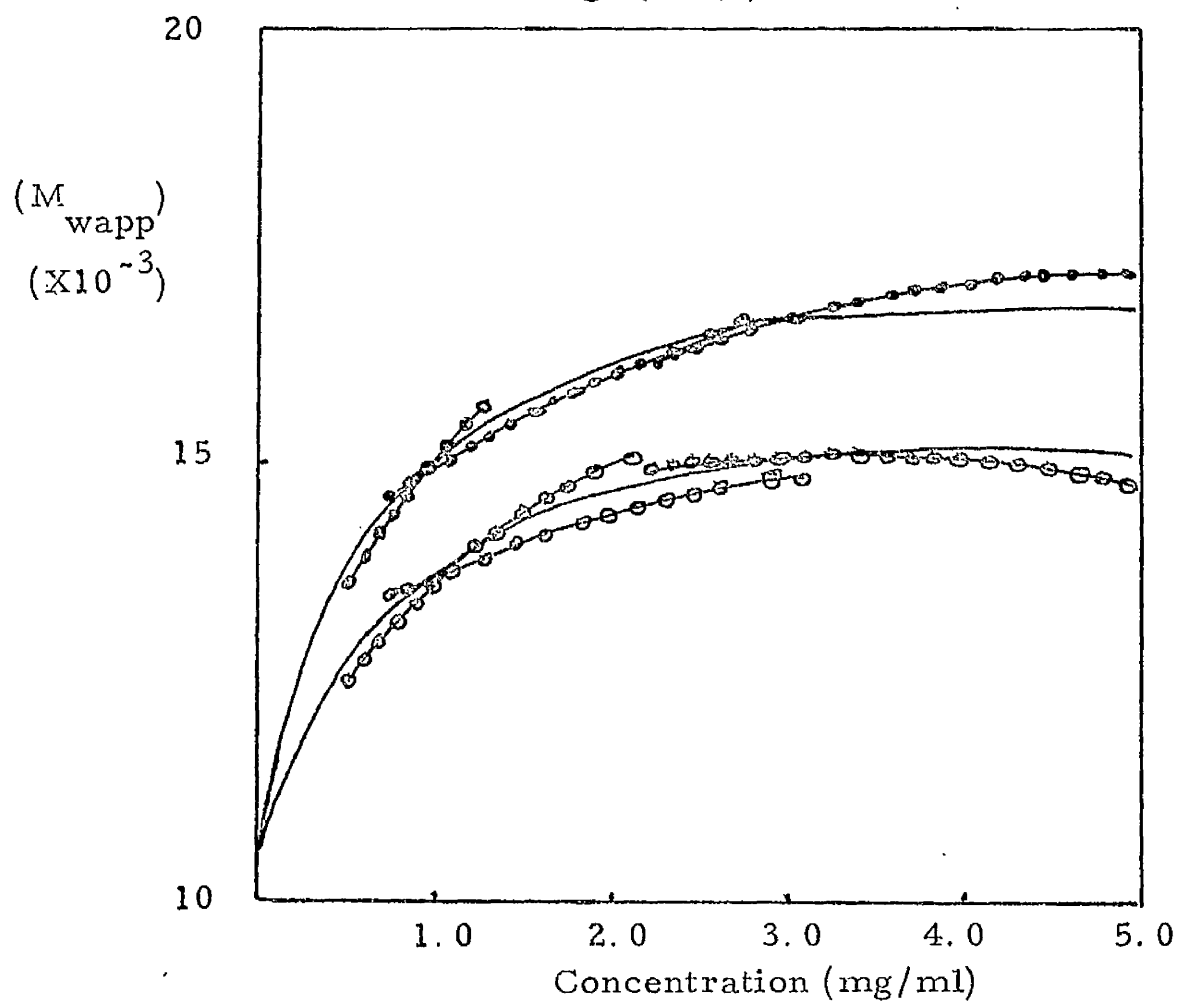
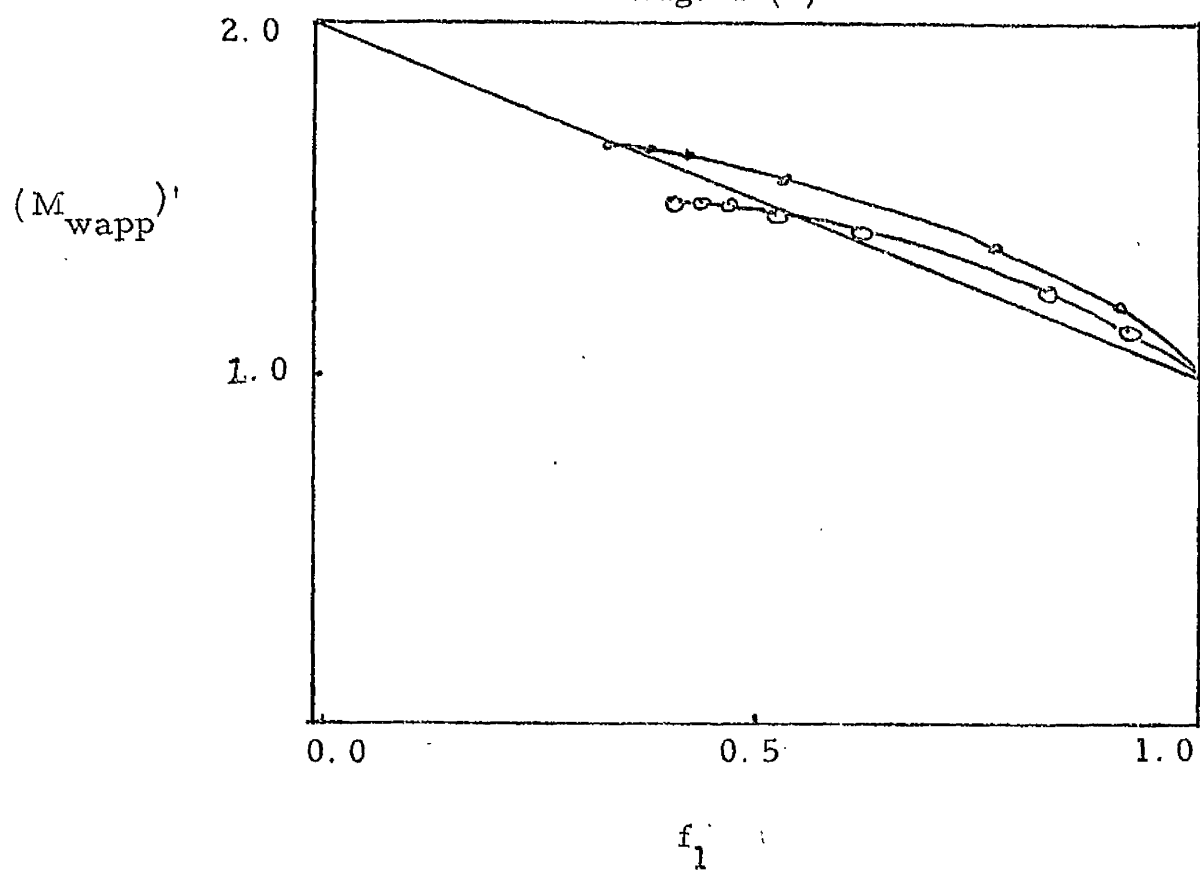


Fig. 14(b)



are therefore likely to be small. Although the absolute values of  $M_{wapp}$  for GAR in 0.075M NaCl, pH 5.0 are different from those in 0.075M NaCl, pH 7.0, the  $M_{wapp}$  vs.  $c$  curves are broadly similar in both cases. Fig. 14(b) shows close agreement between both sets of experimental data and the predicted plot of  $(M_{wapp})'$  vs.  $f_1$  for a monomer-dimer association. The experimental data form a curve over the whole concentration range, with a slight downward deviation at high concentrations. This may be due to non-ideal effects. Fig. 15(a) confirms that a monomer-dimer association satisfactorily describes the experimental data. Plots of  $(M_{wapp})'$  vs.  $1/(M_{napp})'$  for experimental data obtained in both 0.075M NaCl pH 5.0 and pH 7.0 agree well with the standard monomer-dimer curve. Ideal indefinite association is shown in Fig. 15(c) to be inadequate as a description of the experimental association. None of the experimental plots of  $(M_{app})'$  vs.  $(f_1)^{-\frac{1}{2}}$  agree with the standard curves for indefinite association. Similarly Fig. 15(b), effectively eliminates monomer-dimer-n-mer associations. Plots of  $d(M_{wapp})'/df_1$  vs.  $d(1/M_{napp})'/df_1$  for the experimental data do not agree with the standard curves for monomer-dimer-n-mer associations. In Fig. 15(d), it can be seen that at higher concentrations, that is at  $f_1 < 0.5$ , plots of  $1/(M_{napp})'$  vs.  $f_1$  of the experimental data approximate best to the standard plot describing a monomer-dimer association. At low concentrations, small deviations from linearity are observed, similar to those observed in the Chun and Kim analysis of the association of GAR in 0.075M NaCl/0.01M HCl and 0.15M NaCl/0.01M HCl. The deviations are probably due to errors introduced in the integration processes used to derive  $f_1$  and  $M_{napp}$ . While the Chun and Kim (1970) graphical analysis does not permit completely unambiguous identification of the mode of association and is less rigorous than the procedure of Adams, nevertheless graphical analysis of the self-association of GAR histone

ANALYSIS OF ASSOCIATION OF GAR IN 0.075M NaCl, pH 5.0 AND 0.075M NaCl, pH 7.0 BY THE GRAPHICAL PROCEDURE OF CHUN AND KIM (1970)

Experimental values of  $(M_{wapp})'$ ,  $(M_{napp})'$  and  $f_1$  were calculated from  $M_{wapp}$  data of Fig. 14(a) as described in Appendix 1.

- Theoretical curves
- GAR histone in 0.075M NaCl, pH 7.0
- GAR histone in 0.075M NaCl, pH 5.0

FIG 15(a)

Theoretical curves of  $(M_w)'$  vs.  $1/(M_n)'$  for ideal monomer-n-mer associations were constructed using the relationship:

$$(M_w)' = -n \frac{1}{(M_n)'} + n + 1 \text{ and for ideal indefinite association using the relationship: } (M_w)' = 2 (M_n)' - 1$$

FIG 15 (b)

Theoretical curves for ideal monomer-dimer-n-mer associations were constructed using the relationship:

$$\frac{d(M_w)'}{df_1} = -2 \frac{d(1/(M_n)')}{df_1} + n - 1$$

FIG 15(c)

Theoretical curves of  $(M_w)'$  and  $(M_n)'$  vs.  $(f_1)^{-\frac{1}{2}}$  were constructed for ideal indefinite associations using the relationship:

$$(M_w)' = 2 (f_1)^{-\frac{1}{2}} - 1 \text{ and } f_1 = 1/(M_n)'^2$$

- Experimental  $M_{wapp}$ , GAR in 0.075M NaCl, pH 5.0
- △————△ Experimental  $M_{napp}$ , GAR in 0.075M NaCl, pH 5.0
- Experimental  $M_{wapp}$ , GAR in 0.075M NaCl, pH 7.0
- Experimental  $M_{napp}$ , GAR in 0.075M NaCl, pH 7.0

FIG 15(d)

Theoretical curves of  $1/(M_n)'$  vs.  $f_1$  for ideal monomer-n-mer association were constructed using the relationship:

$$1/(M_n)' = (1 - \frac{1}{n}) f_1 + 1/n \text{ and for ideal indefinite association using the relationship: } f_1 = \left( \frac{1}{(M_n)'} \right)^2$$

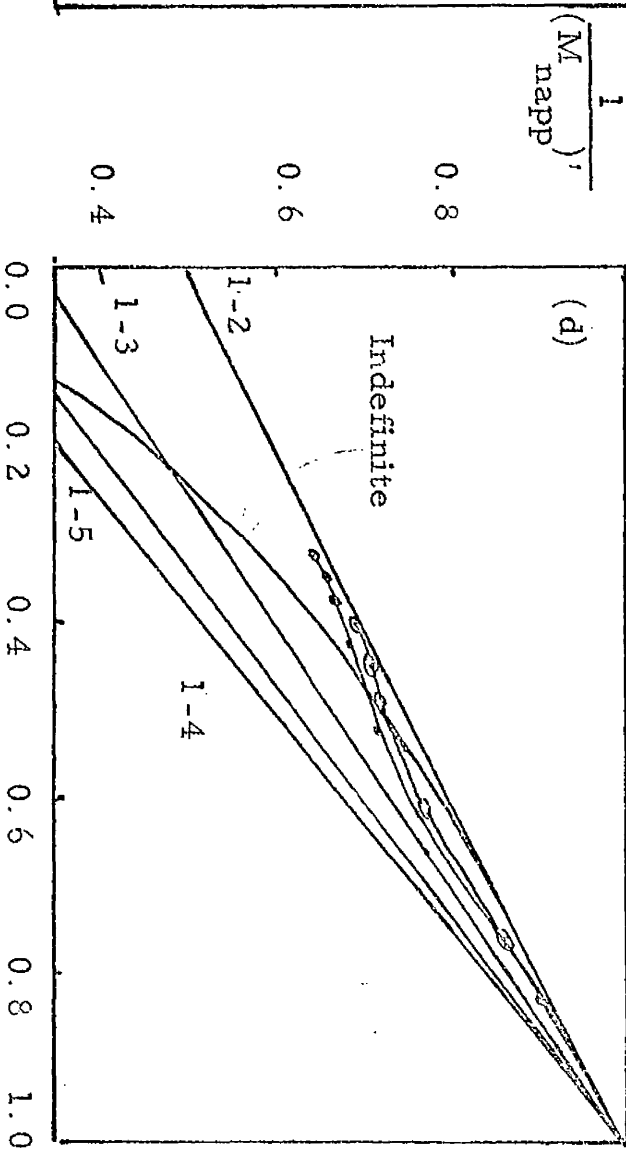
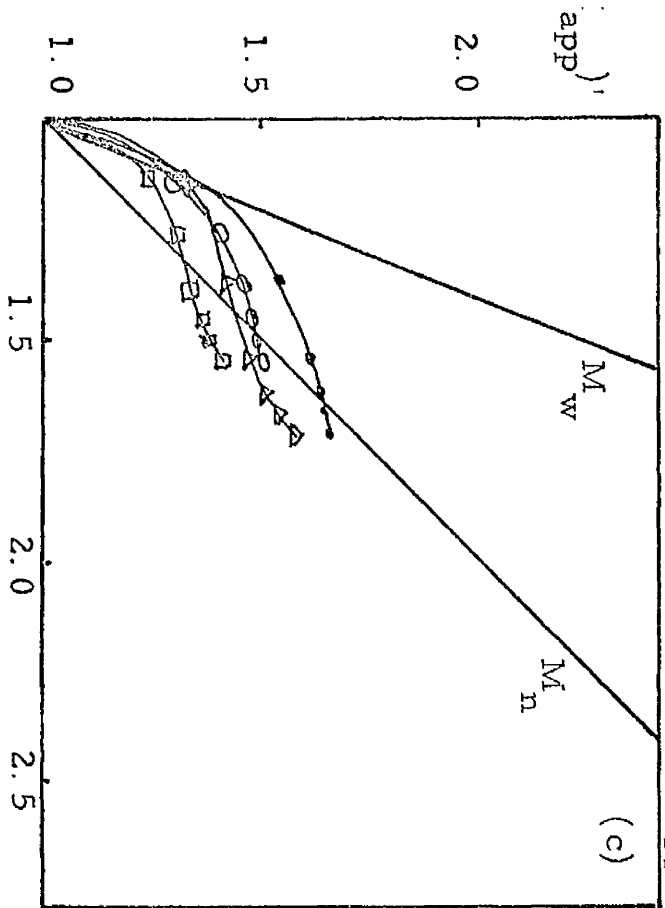
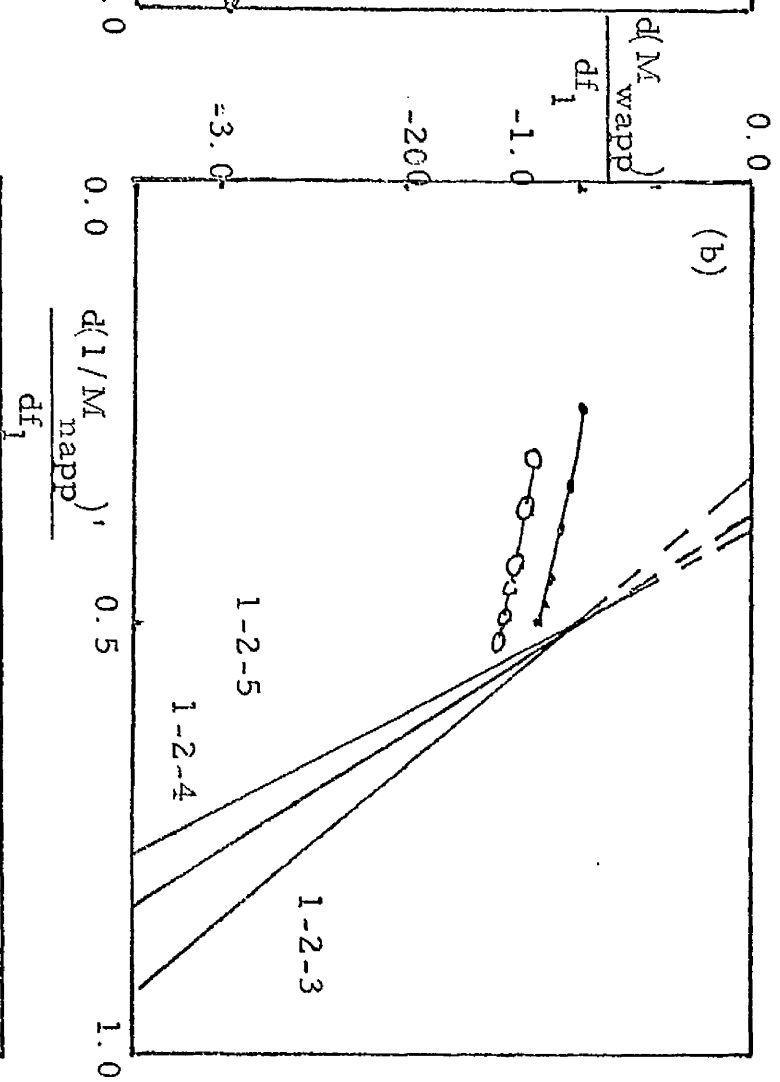
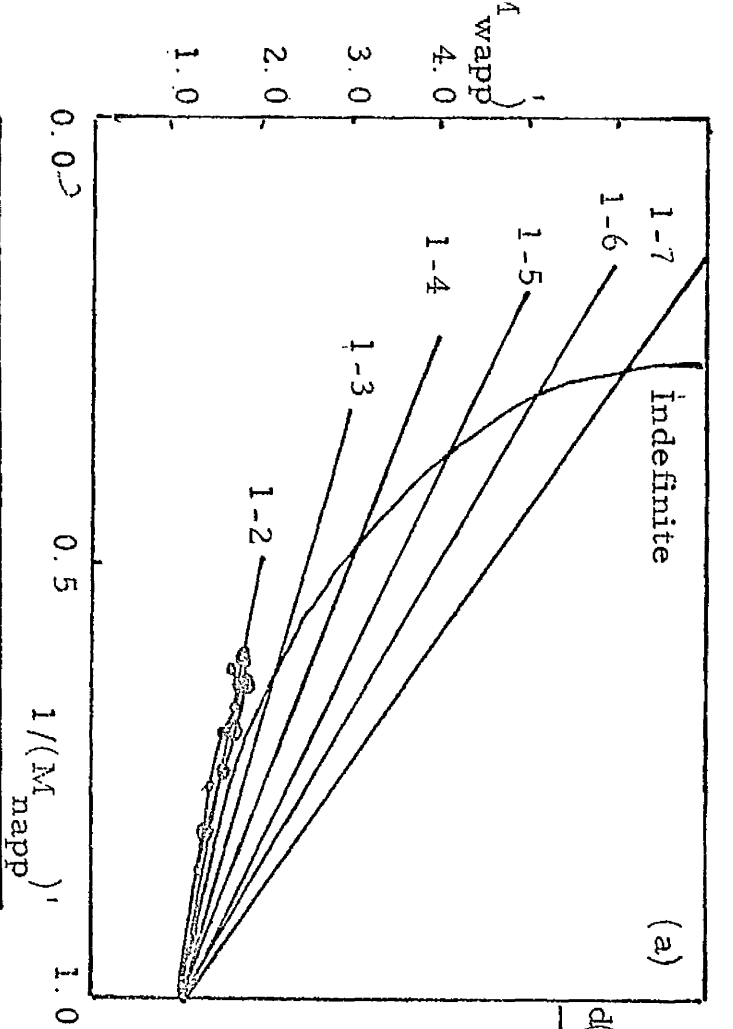


Fig. 15

in 0.075M NaCl, pH 5.0 and 7.0 suggested that the most likely mode of association in both conditions was monomer-dimer. The differences in the  $M_{wapp}$  vs.  $c$  curves (Fig. 14(a)) for the two solvent conditions are probably due to differences in the equilibrium constant governing the association, or in the virial coefficient,  $BM_1$ . The association of GAR histone in 0.15M NaCl at pH 5.0 and 7.0 were also analyzed by the graphical procedure of Chun and Kim (1970). Fig. 16(a) shows the  $M_{wapp}$  vs.  $c$  data obtained in these conditions. For each solvent condition, only two separate sedimentation equilibrium runs were carried out but these span a large range of concentration. The best-fitting third-order polynomials through the data, constrained to pass through the monomer molecular weight ( $M_1$ ) as determined by amino acid analysis (10,600 daltons) are also shown in Fig. 16(a). It can be seen that these best-fitting curves adequately represent the experimental data, suggesting that errors introduced because of the lack of many separate sedimentation equilibrium experiments may be minimal. In Fig. 16(b) plots of  $(M_{wapp})'$  vs.  $f_1$  for the experimental data are compared with standard graphs representing monomer-n-mer associations. No agreement between experimental and theoretical graphs is observed. In Fig. 17(a), an agreement is apparent between the experimental plots of  $(M_{wapp})'$  vs.  $1/(M_{napp})'$  and the theoretical graphs depicting monomer-n-mer association. At low concentrations, the experimental curves show an inflection point, similar to that described in the association of GAR histone in 0.15M NaCl/0.01M HCl. The explanations, of numerical error introduced in the processes of integration of the  $M_{wapp}$  curve at its steepest regions, and of thermodynamic non-ideality, which were proposed in the case of 0.15M NaCl/0.01M HCl, probably also hold at pH 5.0 and pH 7.0. Fig. 17(b) demonstrates that the experimental plots of  $d(M_{wapp})'/df_1$  vs.  $d(1/M_{napp})'/df_1$  approximate best to the standard graph depicting

FIG 16(a)

SELF-ASSOCIATION OF GAR HISTONE IN 0.15M NaCl, pH 5.0 AND  
0.15M NaCl, pH 7.0

Preparations of GAR histone at different initial concentrations were exhaustively dialyzed against 0.15M NaCl, pH 5.0 and 0.15M NaCl, pH 7.0 and centrifuged at 26,000 rpm for at least 36h at 20°C in an AN-G rotor in a Beckman Model E analytical ultracentrifuge equipped with absorption optics. Apparent weight average molecular weights ( $M_{wapp}$ ) were determined from computer evaluation of the gradient of  $\ln c$  vs.  $r^2$  data. A third degree polynomial was fitted to the data using a least squares curve-fitting procedure constrained to pass through  $M_1 = 10600$

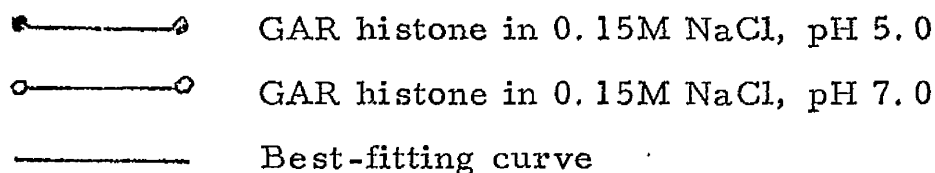


FIG 16(b)

ANALYSIS OF SELF-ASSOCIATION OF GAR IN 0.15M NaCl, pH 5.0 AND  
0.15M NaCl, pH 7.0 BY THE GRAPHICAL PROCEDURE OF CHUN AND  
KIM (1970)

Experimental values of  $(M_{wapp})'$ ,  $(M_{napp})'$  and  $f_1$  were determined from the  $M_{wapp}$  data of Fig. 16(a) as described in Appendix 1. Theoretical curves for ideal monomer-n-mer associations were constructed using the relationship  $(M_w)^1 = -(n-1)f_1 + n$

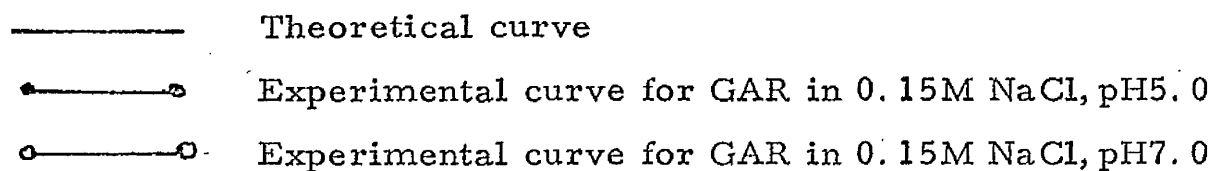


Fig 16(a)

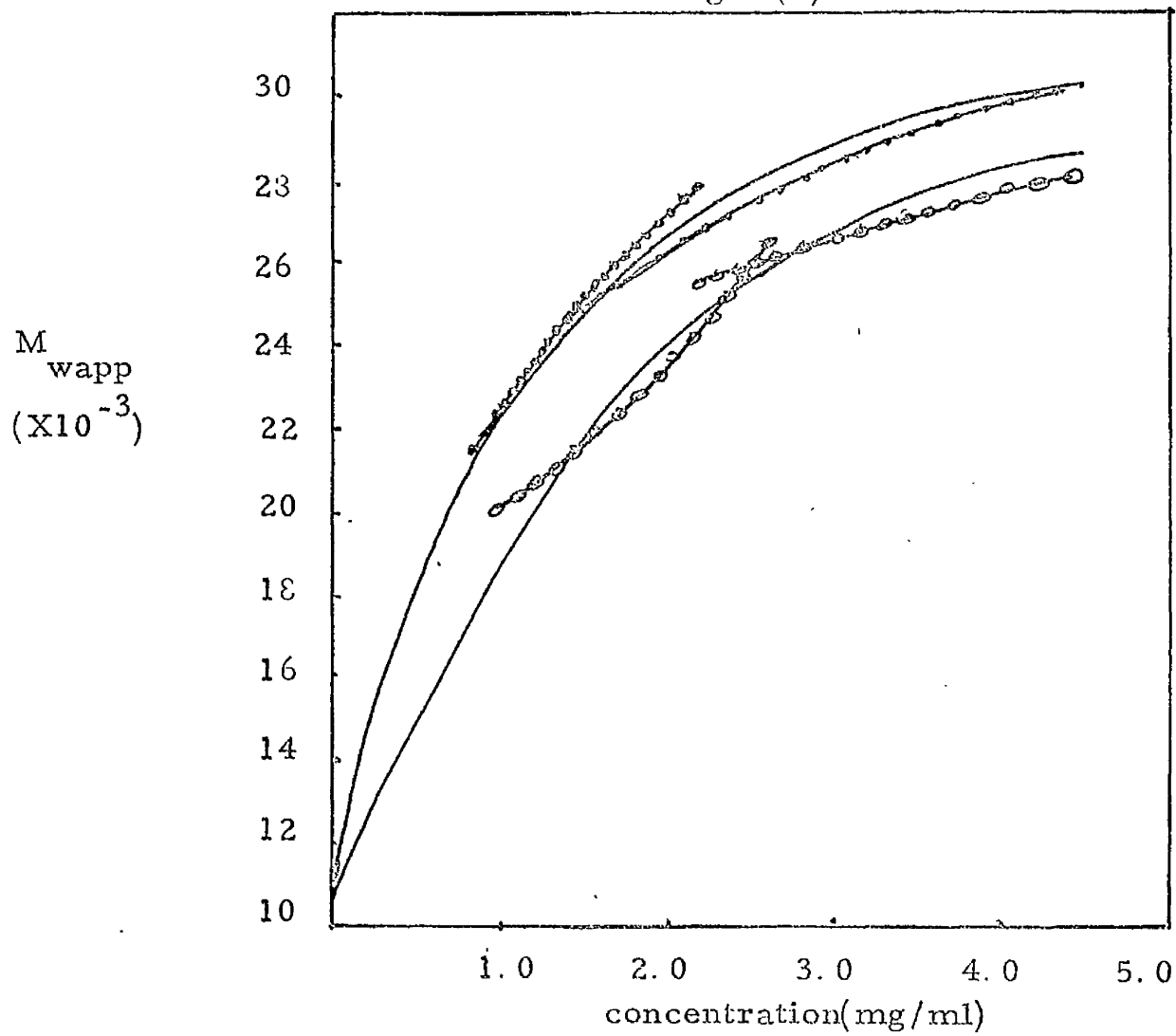
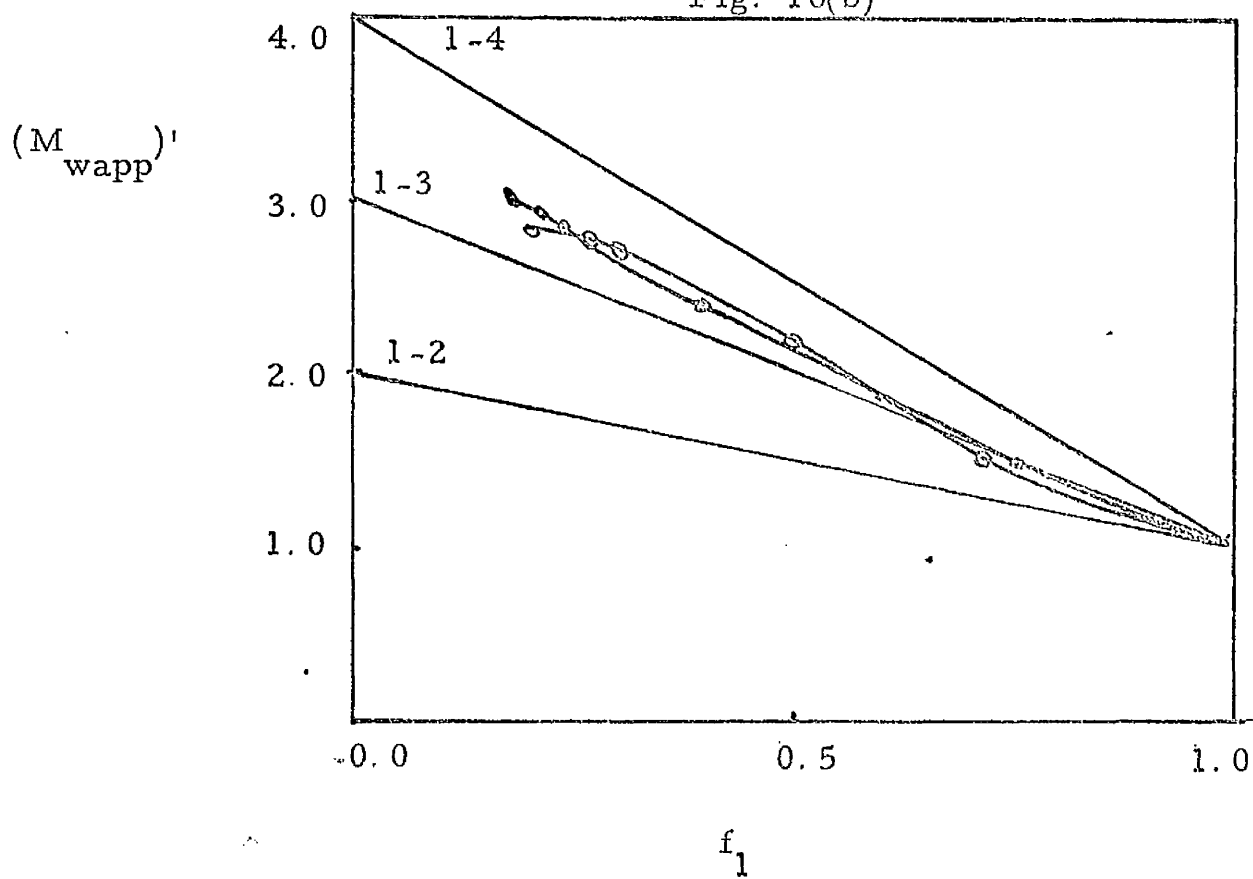


Fig. 16(b)





ANALYSIS OF SELF-ASSOCIATION OF GAR IN 0.15M NaCl, pH 5.0  
AND 0.15M NaCl, pH 7.0 BY THE GRAPHICAL PROCEDURE OF  
CHUN AND KIM (1970)

Experimental values of  $(M_{wapp})'$ ,  $(M_{napp})'$  and  $f_1$  were calculated from  $M_{wapp}$  data of Fig. 16(a) as described in Appendix 1.

———— Theoretical curves  
 ○——○ GAR histone in 0.15M NaCl, pH 7.0  
 ●——● GAR histone in 0.15M NaCl, pH 5.0

FIG 17(a)

Theoretical curves of  $(M_w)'$  vs.  $1/(M_n)'$  were constructed for ideal monomer-n-mer associations using the relationship  $(M_w)' = -n 1/(M_n)' + n + 1$  and for ideal indefinite association using the relationship  $(M_w)' = 2 (M_n)' - 1$ .

FIG 17(b)

Theoretical curves for ideal monomer-n-mer associations were constructed using the relationship:

$$d(M_w)' / df_1 = -2n d(1/(M_n)') / df_1 + n - 1$$

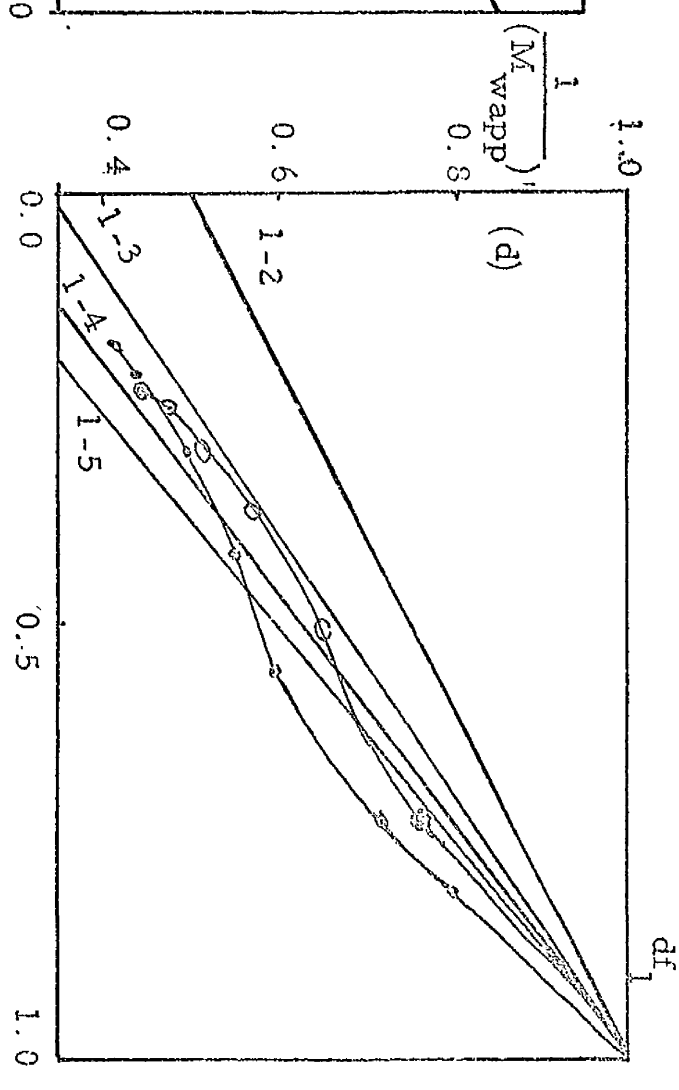
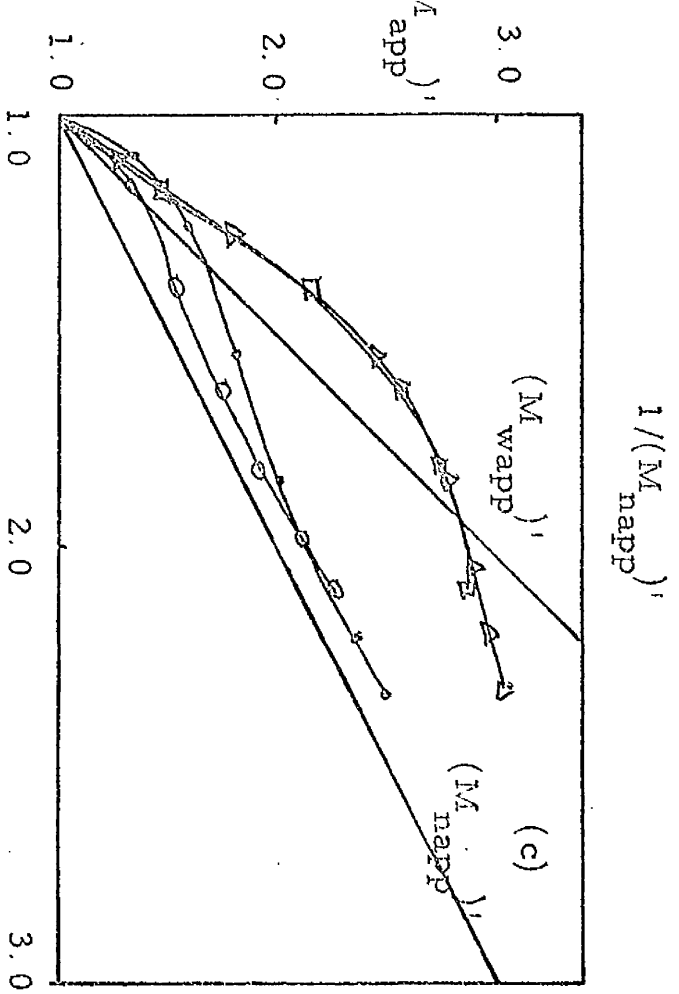
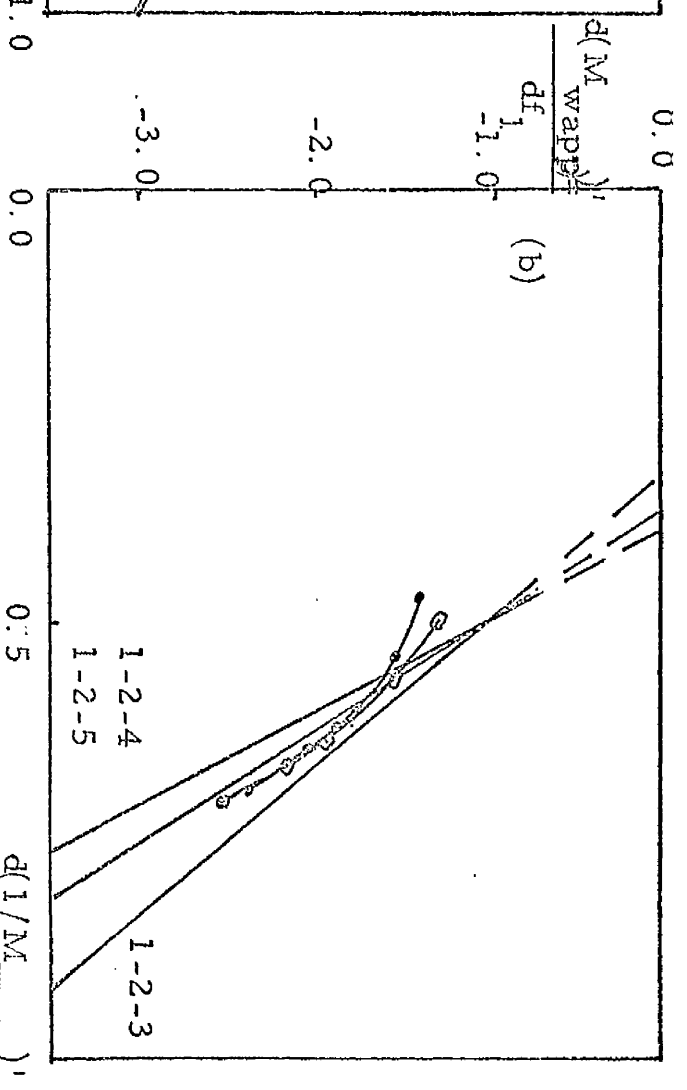
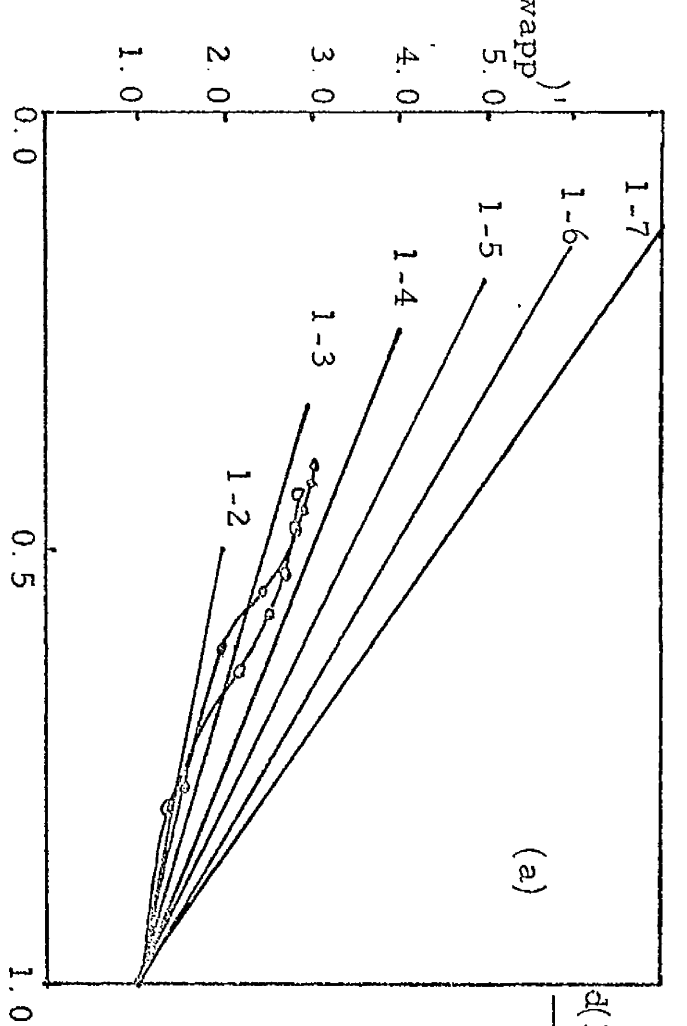
FIG 17(c)

Theoretical curves of  $(M_w)'$  and  $(M_n)'$  vs.  $(f_1)^{-\frac{1}{2}}$  were constructed for ideal indefinite association using the relationship  $(M_w)' = 2 (f_1)^{-\frac{1}{2}} - 1$  and  $f_1 = 1/(M_n)'^2$

○——○ Experimental  $M_{napp}$ , GAR in 0.15M NaCl, pH 5.0  
 △——△ Experimental  $M_{wapp}$ , GAR in 0.15M NaCl, pH 5.0  
 ○——○ Experimental  $M_{napp}$ , GAR in 0.15M NaCl, pH 7.0  
 □——□ Experimental  $M_{wapp}$ , GAR in 0.15M NaCl, pH 7.0

FIG 17(d)

Theoretical curves of  $1/(M_n)'$  vs.  $f_1$  were constructed for ideal monomer-n-mer associations using the relationship  $1/(M_n)' = (1-1/n) f_1 + 1/n$  and for ideal indefinite association using the relationship  $f_1 (1/(M_n)')^2$



$$(f_1)^{-\frac{1}{2}}$$

Fig. 17

$f_1$

monomer-dimer-tetramer association. Again at low concentrations there are marked downward curvatures. The possibility of indefinite association being involved is discounted by comparison of the experimental plots of  $(M_{app})'$  vs.  $(f_1)^{-\frac{1}{2}}$  with the standard graphs for indefinite association (Fig. 17(c)). Fig. 17(d) illustrates that the experimental data are not adequately described by monomer-n-mer associations. The experimental data in Fig. 17(d) do not agree with any of the standard graphs. Marked deviation from linearity may be seen in the experimental data at low concentrations. These deviations are similar to those found in the association of GAR in 0.15M NaCl/0.01M HCl which were attributed to numerical errors introduced in the data processing. It appears that plots of  $1/(M_{wapp})'$  vs.  $f_1$  are particularly sensitive to these errors.

While conclusions regarding the mode of association, drawn from the Chun and Kim (1970) type of analysis must be considered with some slight reservation because of the ideal nature of the analysis and because of the possibility of the introduction of numerical errors, nevertheless the graphical analyses of the association of GAR histone in 0.15M NaCl, pH 5.0 and 7.0, depicted in Figs. 16(b) and 17, indicate that the most likely description of the association may be in terms of a monomer-dimer-tetramer association. Within the limitations imposed by these reservations, it therefore appears that the modes of association detected in 0.075M NaCl/0.01M HCl and 0.15M NaCl/0.01M HCl are unaltered at pH 5.0 and 7.0, at the same salt concentrations.

## 6. ORD Analysis of GAR histone

The associations of GAR-histone described above, were further analyzed using ORD to determine whether the formation of complexes of GAR caused an alteration in the secondary structure of

the protein. Optical rotatory dispersions were measured, using light in the visible range, under different conditions, 0.15M NaCl/0.01M HCl, 0.075M NaCl/0.01M HCl and 0.01M HCl as described in Methods Section 2.11. ORD data were processed on a DIGITAL PDP8/L computer using a tested program kindly supplied by Mr. D. S. Lochead, Department of Biochemistry, University of Glasgow. Schechter-Blout and Moffitt-Yang plots, which can provide information on the secondary structure of protein in solution, were constructed as described in Methods Section 2.11 and are represented in Fig. 18(a),(b). Fig. 18(a) shows that the gradients of the best straight line through the data obtained in 0.075M NaCl/0.01M HCl and 0.15M NaCl/0.01M HCl are approximately equal while the gradient of the best-fitting straight line through the data obtained in 0.01M HCl is much smaller. The Moffitt-Yang plots shown in Fig. 18(b) also reveal that the gradients of best-fitting straight lines through the data obtained in 0.075M NaCl/0.01M HCl and 0.15M NaCl/0.01M HCl are similar while the gradient through the data obtained in salt-free conditions is much smaller. The gradients and intercepts of these plots (Figs. 18 a and b) are shown in Table 13, and the values were used to calculate the helix contents of GAR histone in the different solvent conditions. % helix contents were estimated from the Schechter-Blout parameters,  $A_{193}$  and  $A_{225}$ , as described in Methods Section 2.11. Helical contents were also calculated from the Moffitt-Yang parameter,  $b_0$ , by the methods of Schechter, Carver and Blout (1964) and Urnes and Doty (1961). Helical contents calculated by these methods are shown in Table 14. For GAR in salt-free conditions, the method using the  $A_{225}$  coefficient of the Schechter-Blout plots and the Urnes and Doty (1961) method using  $b_0$  of Moffitt-Yang plots yielded small negative values of helix content.

## FIG 18

ORD OF GAR IN 0.01M HCl, 0.075M NaCl/0.01M HCl and 0.15M NaCl/  
0.01M HCl

ORD spectra were obtained as described in Methods Section 2.11 and were analyzed by means of the Schechter-Blout and Moffitt-Yang equations. Best fitting straight lines were constructed through the experimental points using the method of least squares.

### FIG 18(a)

Schechter-Blout plots of the data

□ — □	GAR in 0.01M HCl
△ — △	GAR in 0.075M NaCl/0.01M HCl
○ — ○	GAR in 0.15M NaCl/0.01M HCl

### FIG 18(b)

Moffitt-Yang plots of the data

□ — □	GAR in 0.01M HCl
△ — △	GAR in 0.075M NaCl/0.01M HCl
○ — ○	GAR in 0.15M NaCl/0.01M HCl

Fig. 18(a)

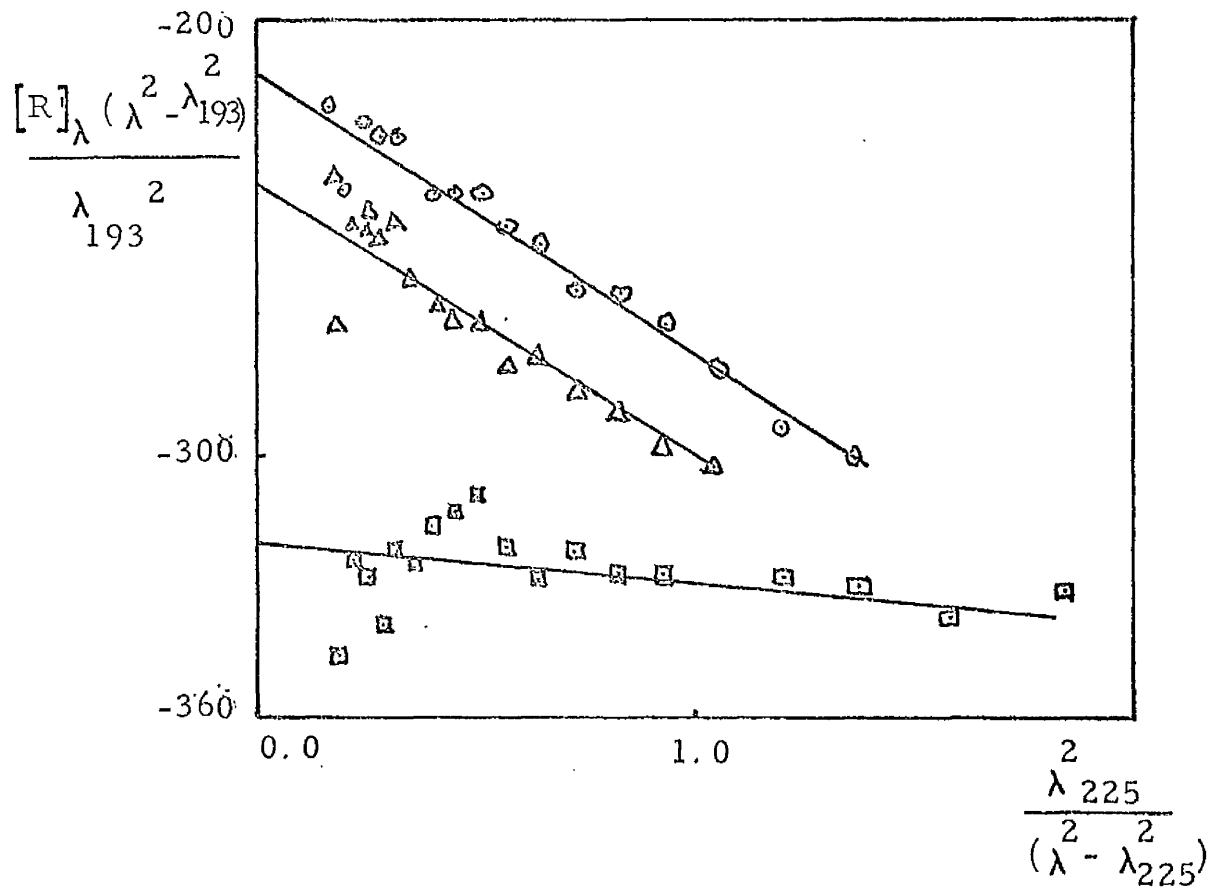


Fig. 18 (b)

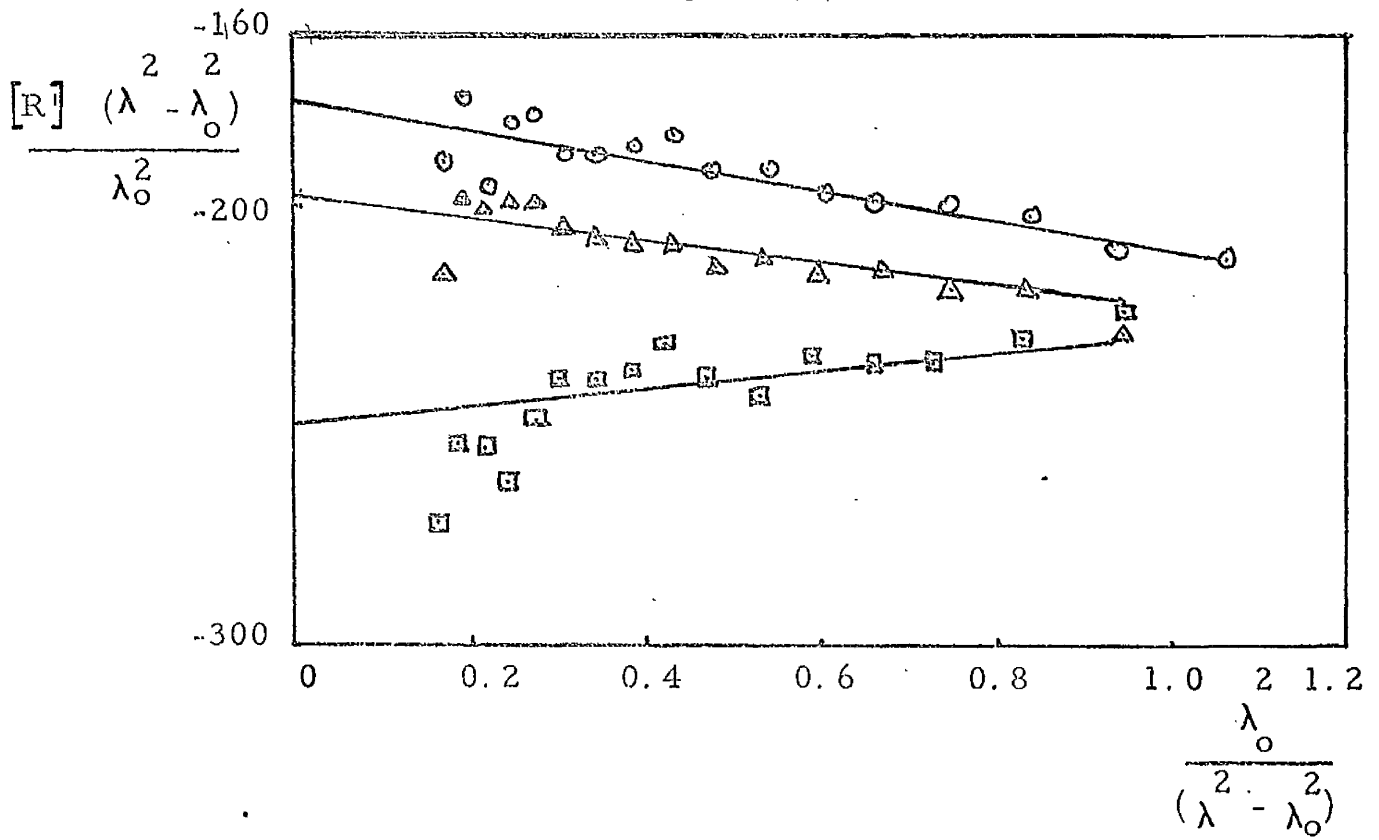


TABLE 13

OPTICAL ROTATORY PARAMETERS FOR GAR HISTONE

ORD spectra of GAR were obtained as described in Methods Section 2.11. Parameters were estimated from Schechter-Blout plots and Moffitt-Yang plots (Figs. 17 (a, b)).

TABLE 13

Solvent	$A_{193}$	$A_{225}$	$b_o$	$a_o$
0.01M HCl	-320	-10	+21	-249
0.01M HCl/ 0.075M NaCl	-212	-64	-33	-177
0.01M HCl/ 0.15M NaCl	-228	-62	-26	-196



TABLE 14

HELIX CONTENT OF GAR HISTONE

Helix contents of GAR histone were calculated from the optical rotatory parameters of Table 13 using the following equations:-

$$H_{193} = (A_{193} + 750)/(36.5)$$

$$H_{225} = -(A_{225} + 60)/(19.9)$$

$$\% \text{ Helix} = -(b_o - 100) / 8.0$$

$$\% \text{ Helix} = -b_o / 6.30$$

TABLE 14

Solvent	% Helix by various methods			
	A <sub>193</sub>	A <sub>225</sub>	b <sub>o</sub>	Urnes/ Doty b <sub>o</sub>
0.01M HCl	11.84	-2.51	9.77	-3.33
0.01M HCl/ 0.075M NaCl	14.74	0.20	16.62	5.24
0.01M HCl/ 0.15M NaCl	14.54	0.10	15.75	4.12

The estimation of helical contents by ORD methods is an empirical procedure, all methods currently available being based on a calibration system using completely random coil structures and synthetic polypeptides containing 100%  $\alpha$ -helix. Experimental values between these two extremes are expressed as a percentage of a completely helical structure. On this basis, negative values of helix content are therefore impossible in principle. Experimental determinations of helix content using ORD are at best only accurate to within  $\pm 5\%$  (Tomimatsu and Gaffield, 1965). Within experimental error, the negative values of helix content found in the case of GAR histone in salt-free conditions using the  $A_{225}$  coefficient of the Schechter-Blout plots and the Urnes and Doty (1961) method using  $b_0$  of the Moffitt-Yang plots, could therefore represent small positive helical contents. The small positive gradient of the best-fitting straight line through the Moffitt-Yang plots of the data for GAR in salt-free conditions is also hard to rationalize except on the basis of experimental error. Evaluation of helix content by the method of Urnes and Doty (1961) using  $b_0$  has been shown to be less reliable than estimates based on the methods of Schechter et al. (1964) using  $b_0$ . (Tomimatsu and Gaffield, 1965). Helical contents estimated by the latter method agree reasonably with those calculated using  $A_{193}$ , both methods indicating low helix contents in GAR histone in salt-free conditions. (Table 14). Helix contents in 0.075M NaCl and 0.15M NaCl are slightly greater than that in salt-free conditions but not by more than the minimum experimental error of  $\pm 5\%$ , so from these studies one cannot unambiguously state that salt increases the helicity of GAR histone. For all conditions examined, large differences in the helix content calculated from  $A_{193}$  and from  $A_{225}$  coefficients were found indicating the presence in GAR histone of secondary structures (for example, hydrophobic bonds and hydrogen bonds and  $\beta$ -sheet structures) other than random coils and helices. (Schechter and Blout, 1964).

The analyses of the association of GAR histone by ultracentrifugation, gel-filtration and ORD, as described above provide quantitative information on the association process. The remainder of the experimental work described in this thesis is concerned with studies of the binding of GAR to DNA and the effect of the association of GAR histone on its interaction with DNA.

These studies initially used calf thymus DNA (C. T. DNA) and to permit meaningful interpretations of the properties of CT-DNA-GAR complexes, some physico-chemical properties of the DNA alone were investigated.

## 7. Characterization of C. T. DNA

Mammalian DNAs are generally of high molecular weight and are frequently heterogeneous with respect to their sedimentation properties. The procedure described by Schumaker and Schachman (1957) to analyze the distribution of sedimentation coefficients across a sedimenting boundary is particularly useful for the characterization of heterogeneous DNA species. The distribution of sedimentation coefficients across a sedimenting boundary  $g(s)$  of C. T. DNA in 0.15M NaCl, pH 5.0 was calculated by the method of Schumaker and Schachman (1957) using a PDP8/L computer. The  $g(s)$  distribution is shown in Fig. 19(a) and can be seen to encompass a wide range of  $s$  values, from 13s to 33s, indicating that the DNA is heterogeneous. The distribution is asymmetric with a larger proportion of sedimenting species of high sedimentation coefficients. The value of the ordinate,  $g(s)$ , gives a measure of the relative number of species of DNA with a given  $s$  value. The values of the molecular weight of the DNA corresponding to the range of sedimentation coefficients covered by the  $g(s)$  plot were obtained using the empirical equation of Crothers and Zimm (1965) relating the sedimentation coefficient of linear duplex DNA to its molecular weight:-

$$0.445 \log_{10} M = 1.819 + \log_{10} (s - 2.7)$$

HETEROGENEITY OF C. T. DNA

Solutions containing 25µg/ml of C. T. DNA were centrifuged at 20°C in an AN-D rotor in a Beckman Model E analytical ultracentrifuge at 44,000 rpm. Sedimentation coefficients across the sedimenting boundary were calculated using the equation:

$$S_{20,w} = \frac{(1 - v \rho_{20,w})}{(1 - v \rho)} \cdot \left( \frac{\eta}{\eta_{20,w}} \right) \frac{2.303}{w_t^2} \cdot \log \left( \frac{x}{x_o} \right)$$

The distribution  $g(s)$  of sedimentation coefficients across the sedimenting boundary was calculated by the method of Schumaker and Schachman (1957) using the equation:

$$g(s) = \frac{\frac{\Delta C_o^{obs}}{\Delta x} \cdot \left( \frac{x}{x_o} \right)^3}{S_{20,w}^o \sum \frac{\Delta C_o^{obs}}{\Delta x} \cdot \left( \frac{x}{x_o} \right)^3}$$

HETEROGENEITY OF C. T. DNA

Using the equation of Crothers and Zimm (1965),  $S = 2.7 + 0.0157 X (M.W.)^{0.447}$ , molecular weights were calculated from  $S_{20,w}^o$  values across a sedimenting boundary of DNA (Fig. 19(a)). The molecular weights are plotted against the  $g(s)$  values corresponding to the  $S_{20,w}$  values from which they were derived.

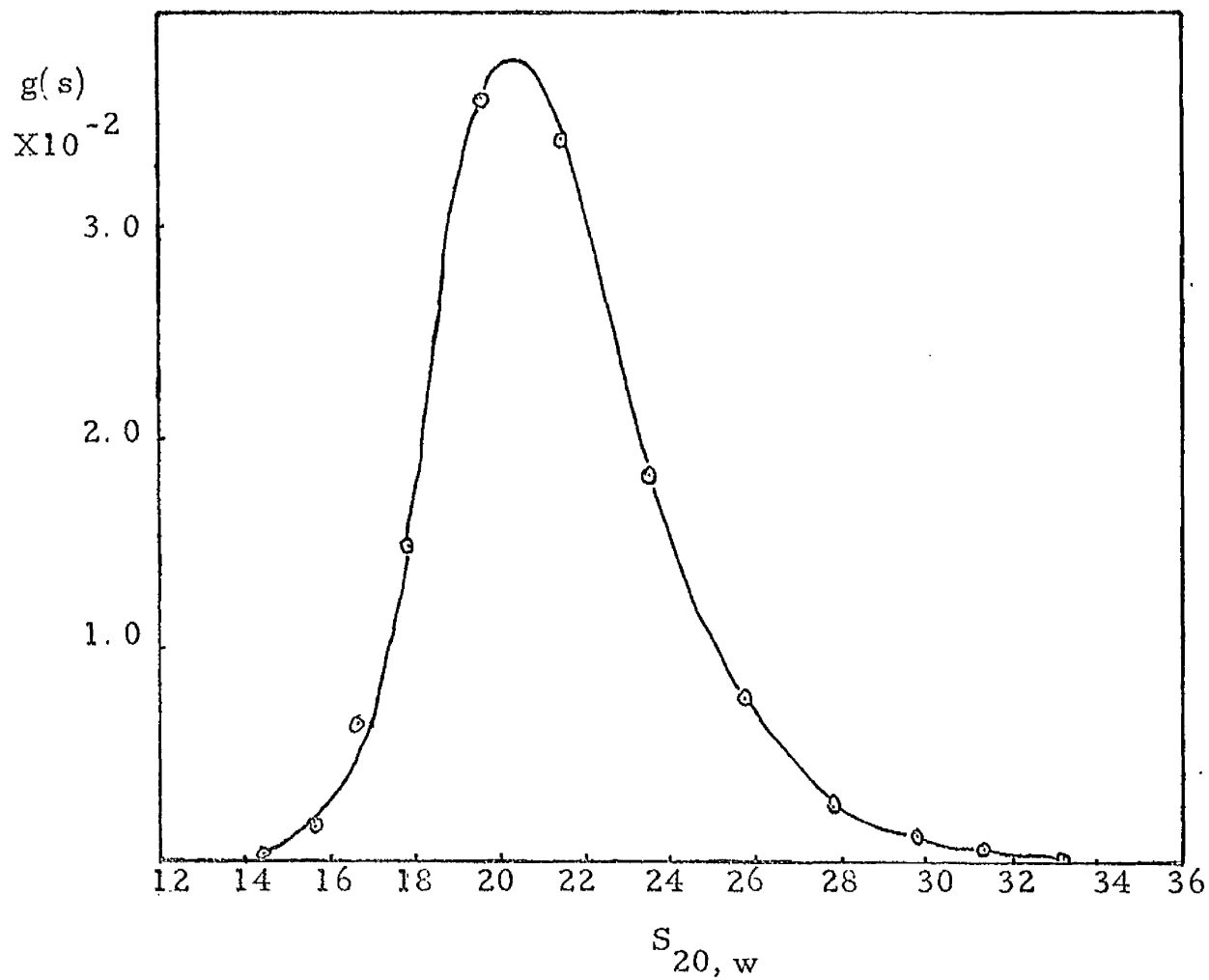
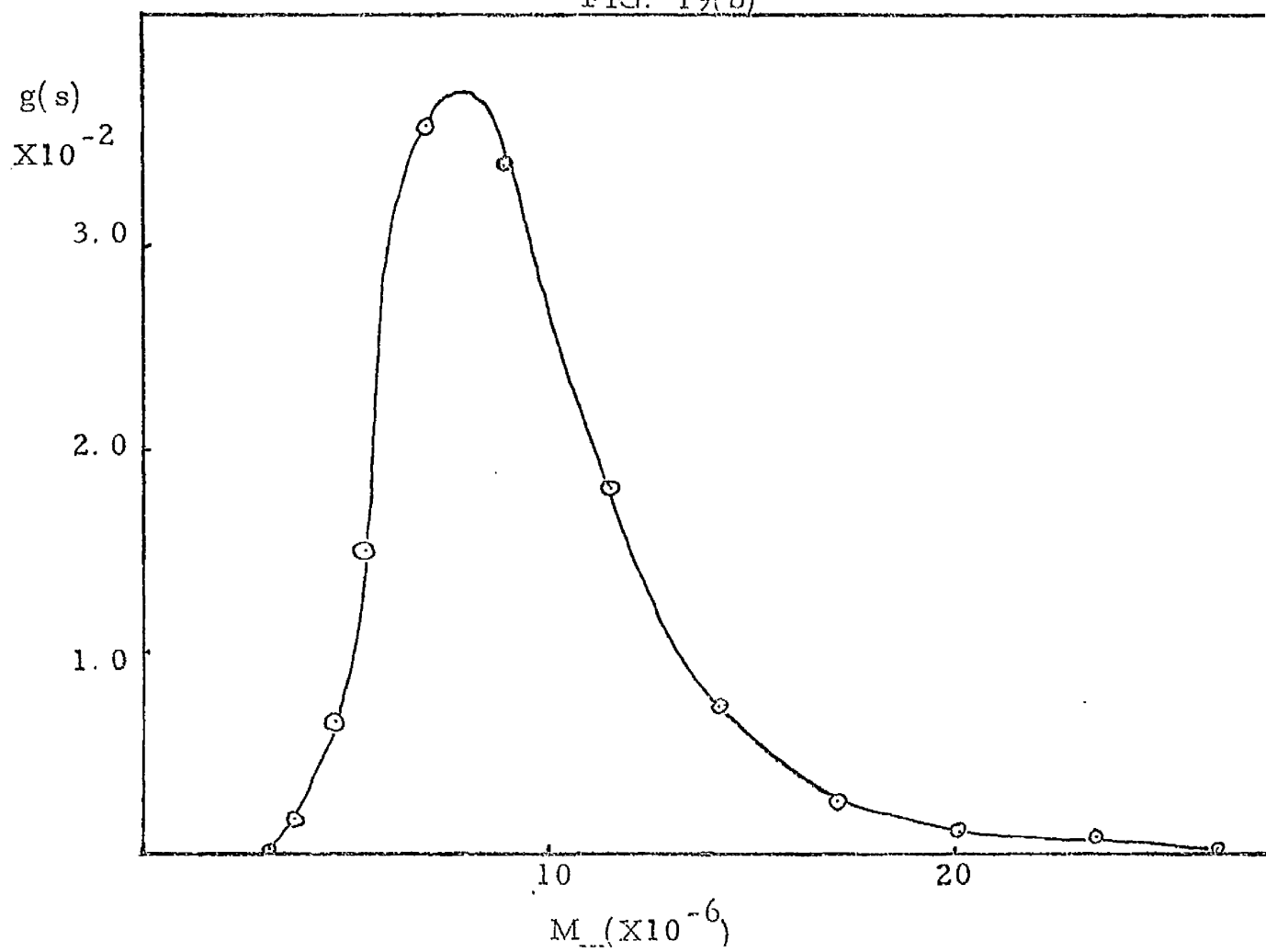


FIG. 19(b)



The values of the molecular weight of the C. T. DNA evaluated from the sedimentation coefficients shown in the  $g(s)$  plot are depicted in Fig. 19(b). Molecular weights in this Figure are plotted against the  $g(s)$  value corresponding to the sedimentation coefficient from which the molecular weights were derived. Although  $g(s)$  values are customarily used to indicate the distribution of sedimentation coefficients of a heterogeneous sedimenting boundary,  $g(s)$  values are a measure of the relative number of species present in a sedimenting population, and  $g(s)$  can therefore be used to indicate the distribution of molecular weights. Fig. 19(b) demonstrates that the distribution pattern of molecular weights is slightly different from the distribution of sedimentation coefficients shown in Fig. 19(a), with the molecular weight distribution being slightly more skewed towards the higher molecular weight region. This emphasis towards higher molecular weight values is a direct consequence of the exponential nature of the empirical equation of Crothers and Zimm (1965), used to evaluate the molecular weights of the DNA from its sedimentation coefficients. Since  $g(s)$  represents the relative amount of a particular species in a heterogeneous population,  $g(s)$  values can be considered as directly proportional to the concentration of the particular species in the population. Accordingly, the value of  $M_w$ , the weight average molecular weight can be evaluated for the heterogeneous population of DNA using the basic equation for  $M_w$ :-

$$M_w = \frac{\sum c_i M_i}{\sum c_i}$$

The value of  $M_w$  for the distribution of C. T. DNA shown in Fig. 19(b) was calculated to be  $8.2 \times 10^6$  daltons. It can be seen that the value of  $M_w$  does not correspond to the maximum of the distribution. The fact that the distribution of sedimentation coefficients (Fig. 19(a)) is different from the distribution of molecular weights (Fig. 19(b)), precludes the evaluation of a weight average sedimentation coefficient

from the distribution of sedimentation coefficients and the subsequent evaluation of a molecular weight corresponding to this value of a weight-average sedimentation coefficient.

The heterogeneity of C. T. DNA shown by the distribution of sedimentation coefficient  $g(s)$  in Fig. 19(a) was confirmed by band sedimentation of C. T. DNA through 1.2M NaCl as described in Methods Section 2.10.2. A typical trace is shown in Fig. 20. A sedimentation profile is indicated which is broadly similar to the  $g(s)$  distribution but differs slightly in having a slightly greater predominance of sedimenting species of higher  $s$  value. This minor discrepancy may be explained in terms of the concentration dependence of sedimenting species, which in general, predicts a decrease in the sedimentation coefficient with increasing concentration. In boundary sedimentation (Fig. 19) the leading edge of the boundary penetrates a zone containing a finite concentration of DNA, the concentration effect thus effectively lowering the sedimentation coefficients of this part of the boundary. In contrast, the leading species in band sedimentation penetrate a zone composed of the bulk solvent, 1.5M NaCl, of zero DNA concentration. Effectively, the sedimentation coefficients of this part of the boundary are therefore slightly greater than those of the corresponding species in boundary sedimentation.

The characterization of the C. T. DNA provided by the  $g(s)$  distribution and the band sedimentation data provides a basis for the investigation of GAR histone - DNA complexes.

## 8. Analysis of GAR histone - C. T. DNA complexes

### 8.1 Thermal denaturation studies

Thermal denaturation studies of nucleoprotein complexes can provide useful qualitative information on the



FIG. 20

BAND SEDIMENTATION OF C. T. DNA

15 $\mu$ l of C. T. DNA in SSC were introduced into the sample well of a Vinograd type III double sector band-forming centrepiece, containing 0.35ml of CsCl (density 1.320g/ml) as bulk solvent. Sedimentation was carried out at 20<sup>o</sup> C at 40,000 rpm in AN-D rotor. The scanning wavelength was 265nm.

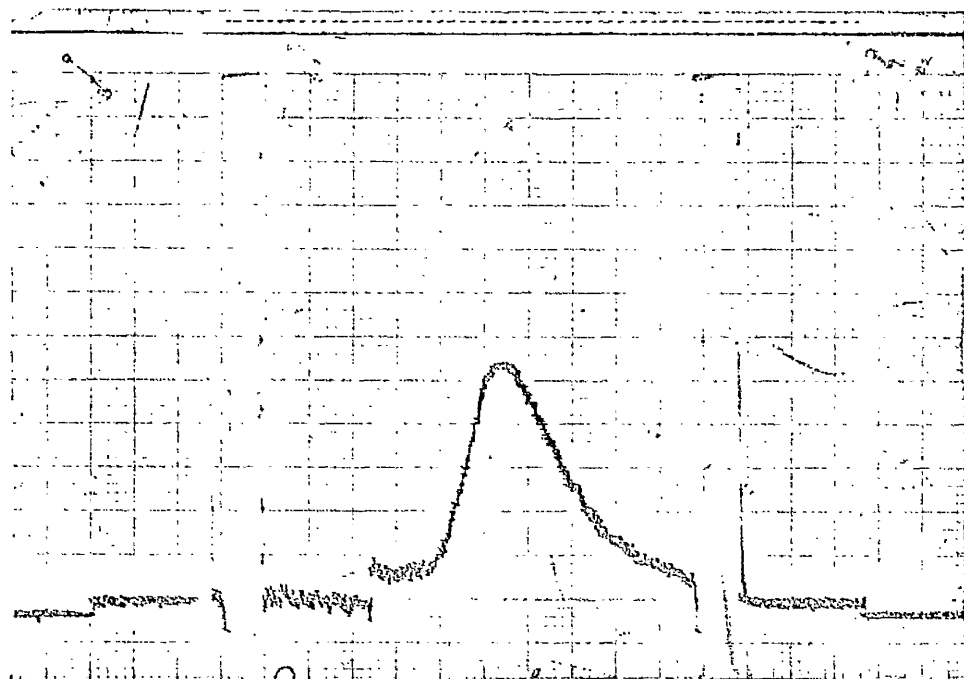


FIG. 20

interaction of proteins with DNA. Binding of histones to DNA stabilizes the double helix against thermal denaturation (Olins, 1969; Shih and Bonner, 1970) and histone-DNA complexes are therefore characterized by melting temperatures considerably higher than those of free DNA. In certain solvent conditions, the increased melting temperature due to the histone-DNA complex may be greater than 100°C and therefore be unable to be measured because of boiling. For this reason, thermal denaturation studies of histone-DNA complexes are frequently carried out in solvent conditions which lower the melting temperature of both free DNA and DNA-histone complexes. In the present studies, EDTA at a concentration of  $2.5 \times 10^{-4}$  M was used to lower melting temperatures to within a measurable range. EDTA presumably achieves this effect by chelation of cations which stabilize the double helix.

Formation of DNA-histone complexes can be achieved by two methods, the salt gradient dialysis method of Huang et al. (1964) or by the method of direct addition of histones to DNA (Ansevin and Brown, 1971). In both methods, precipitation of the DNA may occur if a high ratio of histone to DNA is used. The nomenclature system of Shih and Bonner (1970) (Methods Section 2.5) can be used to describe the relative amounts of DNA and histone. Complexes of GAR histone and C. T. DNA were formed using the salt-gradient dialysis method of Huang et al. (1964) at various ratios of  $(\text{Arg} + \text{Lys})/\text{Po}_4$ . Absorbance melting profiles of these complexes in  $2.5 \times 10^{-4}$  M EDTA, pH 5.0 were carried out as described in Methods Section 2.5. The melting profiles shown in Fig. 21(a), demonstrate that the melting of the nucleoprotein complex is characterized by a biphasic melting profile, with one transition at approximately the same temperature as that of free DNA and a second transition about 30-40°C higher. In the complex formed at an  $\text{Arg} + \text{Lys}/\text{Po}_4$  ratio of 0.35, the second transition is not clearly indicated but can be

## FIG 21

### THERMAL DENATURATION OF GAR - C. T. DNA COMPLEXES

Fig. 21(a) C. T. DNA - GAR complexes were prepared by the salt-gradient dialysis method of Huang et al. (1964) at several (Arg + Lys)/ $P\theta_4$  ratios and were diluted with the final buffer to an absorbance value between 0.7 and 2.0 absorbance units at 260nm. Thermal denaturation was followed as described in Methods Section 2.9, using a UNICAM SP500 spectrophotometer.

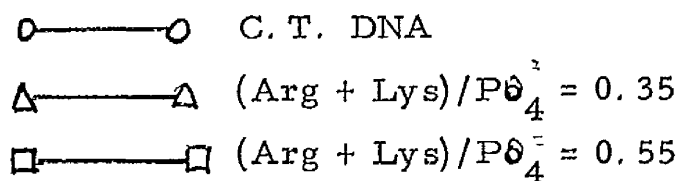


Fig. 21(b) C. T. DNA - GAR complexes were prepared by the direct addition of GAR to DNA in 0.075M NaCl, pH 5.0 +  $2.5 \times 10^{-4}$  M EDTA at various ratios of histone to DNA, as described in Methods Section 2.5.

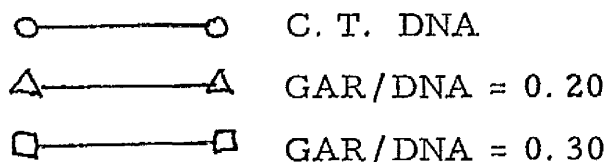


Fig. 21(c) C. T. DNA - GAR complexes were prepared by the direct addition of GAR to DNA in a dilute McIlvaine type phosphate buffer, of ionic strength  $<0.01$ , at pH 5.0.

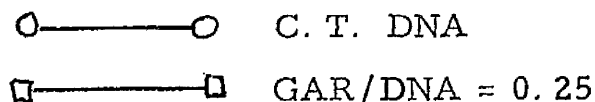


Fig. 21(a)

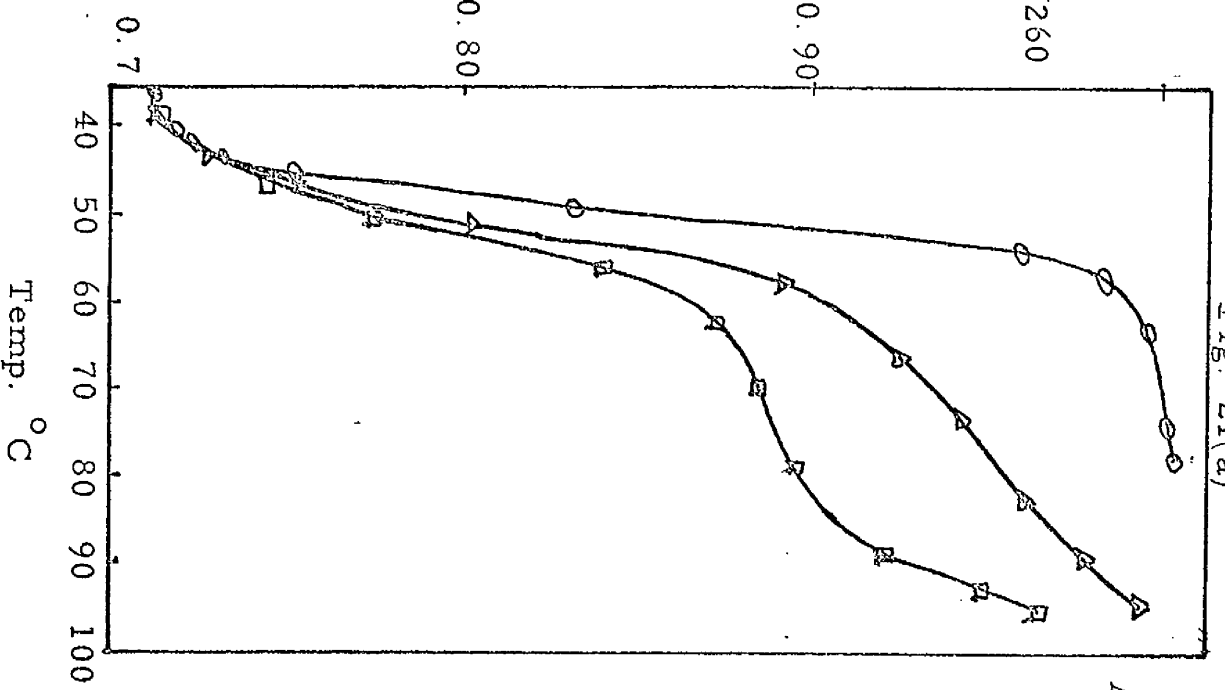


Fig. 21(b)

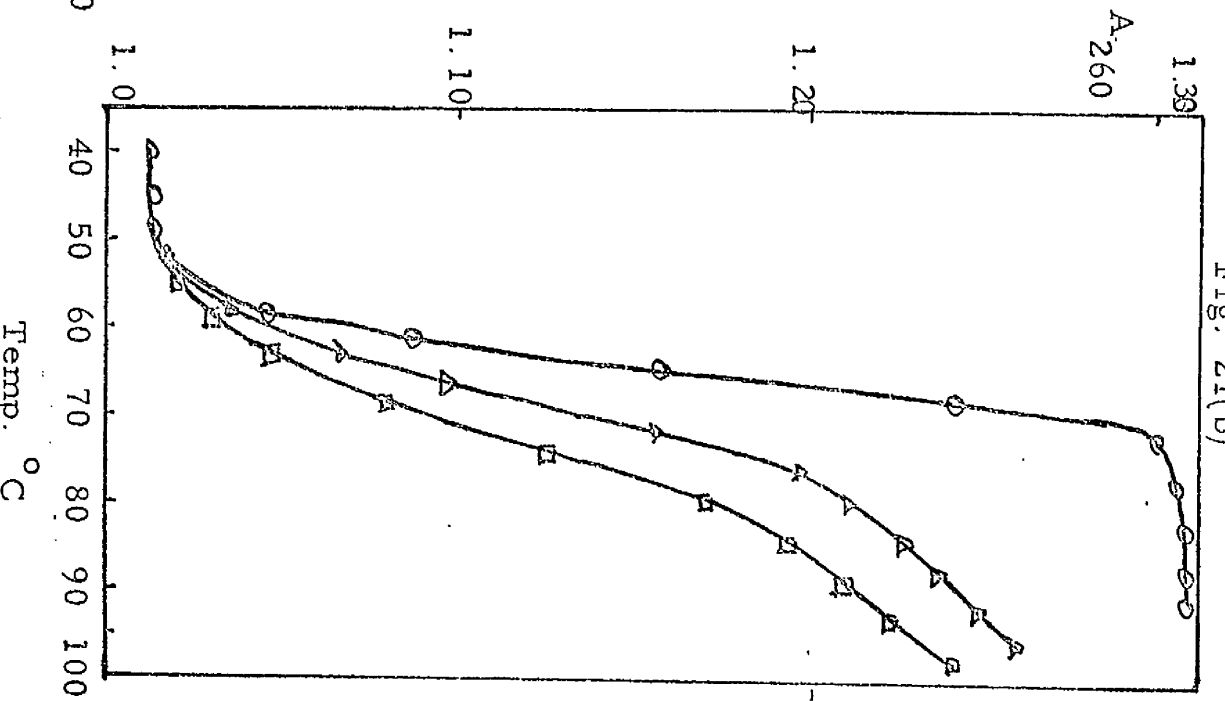
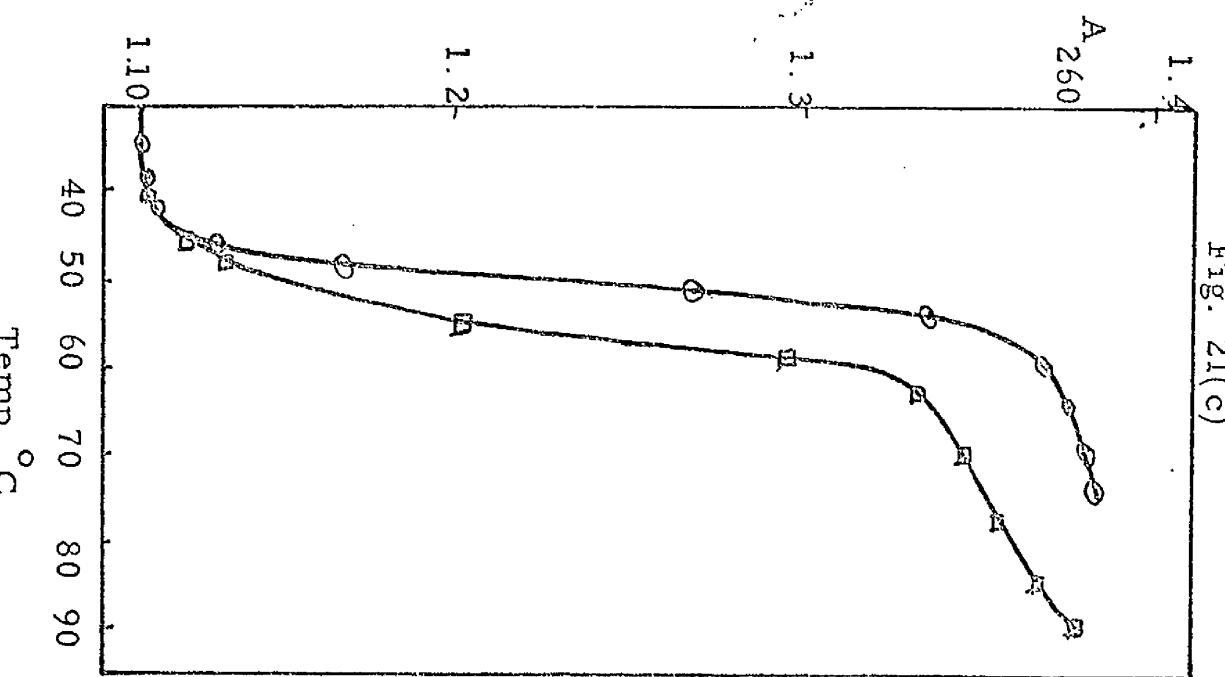


Fig. 21(c)



qualitatively estimated to occur over approximately the same range as that of the complex formed at an  $(\text{Arg} + \text{Lys}) / \text{Po}_4$  ratio of 0.55. It can be seen from Fig. 21(a), that the first transition in the biphasic melting profile of the nucleoprotein complex does not correspond exactly with that of free DNA, but instead is less sharp and occurs at a slightly higher temperature. This effect is more pronounced with a complex of a higher  $\text{Arg} + \text{Lys} / \text{Po}_4$  ratio. Fig 21(b), shows the melting profiles of nucleoprotein complexes prepared by the direct addition of histones to DNA at various ratios by weight of histone/DNA in 0.075M NaCl, pH 5.0 X  $2.5 \times 10^{-4}$  M EDTA. Assuming that the EDTA does not significantly affect the self-association of GAR histone, the protein exists in these conditions in a monomer-dimer equilibrium.

The validity of the assumption that EDTA does not affect the state of aggregation of GAR can only be verified experimentally. Nevertheless, the present studies on the association of GAR as well as those of Edwards and Shooter (1970) on crude  $\text{F}_2\text{A}_1$  histone fractions have indicated that the aggregation of the arginine-rich histone is dependent only on salt concentration and it therefore appears unlikely that EDTA which chelates divalent cations, will affect the aggregation. However, in the lack of any direct experimental proof, the assumption that EDTA does not affect the aggregation of GAR is entirely arbitrary. It can be seen that the complexing of histone to DNA under these conditions causes part of the DNA to melt at a higher temperature than that of free DNA. The exact melting temperature of the nucleoprotein complex cannot be accurately ascertained because of the high temperatures involved. It may be seen that free DNA in 0.075M NaCl, pH 5.0, +  $2.5 \times 10^{-4}$  M EDTA melts at a higher temperature than free DNA in  $2.5 \times 10^{-4}$  M EDTA, pH 5.0 (Fig. 21(a)). This is almost certainly due to the stabilizing influences of the salt ions on the double helix. Fig. 21(c) shows the

melting profile of a GAR histone-DNA complex formed by the direct addition of histone to DNA at a weight ratio of 0.25 in  $2.5 \times 10^{-4}$  M EDTA, pH 5.0. The studies of Edwards and Shooter (1969a) have shown that in salt free conditions, the  $F_2A_1$  class of histones exists in an unaggregated state. The melting profile of DNA-GAR histones complex in these conditions is similar to the melting profile of DNA-GAR complexes prepared by the salt-gradient dialysis method of Huang et al. (1964) (Fig. 21(a)), indicating that the method of preparation of the complexes does not affect significantly their melting properties. As in the complexes prepared by salt-gradient dialysis, the first transition of the biphasic melting profile of GAR histone-DNA complexes prepared by direct addition is not exactly equivalent to the melting profile of free DNA, being instead more diffuse and occurring at a higher temperature.

#### Sedimentation analyses of GAR histone C. T. DNA complexes

Complexes of C. T. DNA with GAR histone were prepared at pH 5.0 by the salt-gradient dialysis method of Huang et al. (1964) and were analyzed by band sedimentation through deuterium oxide. Deuterium oxide was used to provide a stabilizing density gradient through which the sedimenting nucleoprotein complex can migrate. Salt solutions cannot be used for this purpose since dissociation of the protein from the complex occurs in high salt conditions. Values of the sedimentation coefficients across the sedimenting band were calculated using the equation:

$$S = \frac{2.303}{2w} \log \frac{x}{x_0} \quad \text{where } x_0 \text{ is the radial distance of the meniscus.}$$

The distribution of sedimentation coefficients across the sedimenting zone is shown in Fig. 22(a). The effect of deuteration of the replaceable hydrogen atoms in the complex was not taken into account. Deuteration may affect the equilibrium position of associating protein systems and may also affect the binding of proteins to DNA. It can be seen from Fig. 22(a) that the complex is heterogeneous with respect to sedimentation coefficient, having an  $S_{20,w}$  value distribution maximum

FIG 22

HETEROGENEITY OF C. T. DNA - GAR HISTONE COMPLEXES

Fig. 22(a) C. T. DNA - GAR histone complexes were prepared by the method of salt gradient dialysis as described in Methods Section 2.5 and were analyzed by band sedimentation through 100% D<sub>2</sub>O. Values of the sedimentation coefficients across the sedimenting band were calculated using the equation:

$$S = \frac{2.303}{w^2 X} \cdot \log \left( \frac{X}{X_o} \right)$$

S values are plotted against the pen height in cm at each point throughout the sedimenting band.

Fig. 22(b) C. T. DNA - GAR complexes were prepared by the method of salt-gradient dialysis as described in Methods Section 2.5 and were analyzed by boundary sedimentation.

Values of g(s), the distribution of sedimentation coefficients across the sedimenting boundary are plotted as a function of the sedimentation coefficient at each point in the boundary.

⊖ ——— ⊕      Complex formed in pH 7.0, GAR/DNA = 0.2  
— — — — —      Complex formed in pH 5.0, GAR/DNA = 0.2



FIG. 22(a)

Pen Height  
(cm)

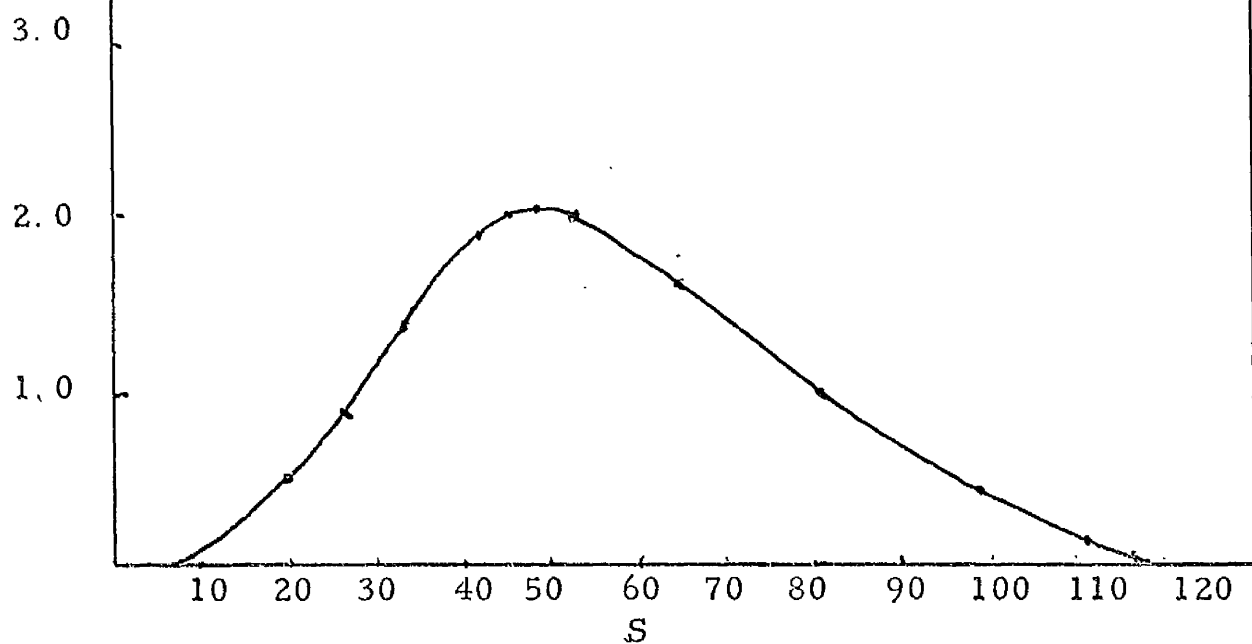
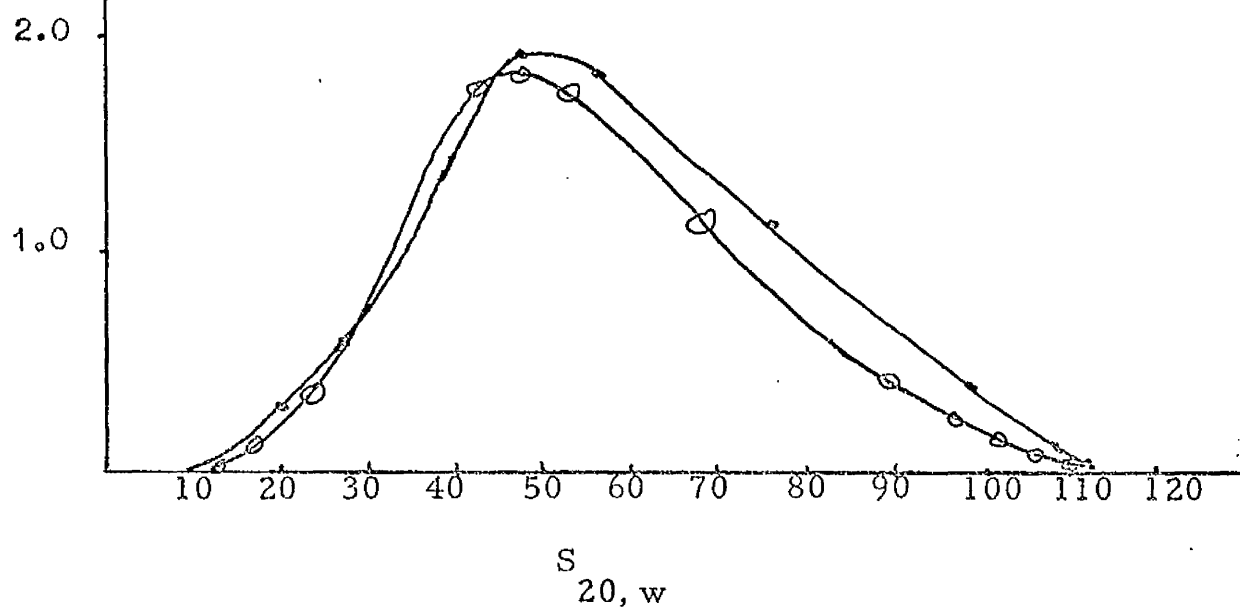


FIG. 22(b)

$g(s)$   
 $\times 10^{-2}$



at around 50 s, that is about 29 s units greater than that of pure C. T. DNA. The distribution of sedimentation coefficients,  $g(s)$ , of the complex was also estimated from boundary sedimentation experiments and is shown in Fig. 22(b). The distribution is broadly similar to that shown in Fig. 22(a) obtained by band sedimentation, indicating that the deuteration of histone-DNA complex does not affect significantly its sedimentation properties. Also shown in Fig. 22(b), is the  $g(s)$  distribution of complexes formed by salt-gradient dialysis at pH 7.0. It can be seen that changes in pH over this range do not significantly alter the sedimentation coefficient distribution.

For GAR histone-DNA complexes formed by the method of direct addition of the histones to the DNA, the number of histone molecules bound per DNA molecule was calculated using the approach used by Steinberg and Schachman (1966) to estimate the number of molecules of methyl orange bound to BSA. In their method, sedimentation velocity experiments were carried out on mixtures of BSA and methyl orange, with methyl orange in excess. Because of their large size, complexes of BSA and methyl orange sedimented rapidly, leaving unbound methyl orange behind. From estimates of the constituent sedimentation coefficients of the interacting species the number of methyl orange molecules bound per BSA molecule was calculated. Similar experiments were carried out in the present studies of GAR histone C. T. DNA complexes but the method involving constituent sedimentation coefficients was not used. Instead the approach adopted in the present studies was to add known concentrations of one component, either histone or DNA, to excess known amounts of the second component and carry out sedimentation velocity experiments on the mixture using UV absorption optics. The rationale behind this approach is that the GAR-histone-DNA complexes will sediment rapidly and leave behind a 'supernatant' region comprising excess unbound component whose concentration may be estimated from its absorbance. Using the original concentration of both reactant and the final concentration of the unbound

excess component, the stoichiometry of the histone-DNA complex may be determined in a manner directly analogous to that used to calculate the number of ligands bound to a macromolecule in equilibrium dialysis experiments (Klotz, 1946, 1953; Klotz, Walker and Pivan, 1946). It is evident that equilibrium dialysis experiments cannot be directly carried out on GAR-histone-DNA interacting systems because of the sizes of the molecules involved. The sedimentation velocity analogue of equilibrium dialysis described above has, in principle, several advantages over normal dialysis methods. The sedimentation coefficient distribution of the sedimenting complex may be estimated from a  $g(s)$  analysis. In addition, the sedimentation properties of the excess, unbound component in the 'supernatant' region can be directly analyzed, again by measuring the  $g(s)$  distribution.

Initially, experiments were carried out with C. T. DNA in excess and adding small amounts of GAR histone. The experiments were carried out under three solvent conditions, 0.075M NaCl, pH 5.0, in which GAR histone was shown to exist most probably in a monomer-dimer equilibrium; 0.15M NaCl, pH 5.0 in which GAR probably existed in a monomer-dimer-tetramer equilibrium; and 0.4M NaCl, pH 5.0. Although the aggregation properties of GAR were not accurately known at this latter salt concentration, it was nevertheless considered desirable to extend the range of salt concentration studied to 0.4M NaCl for the following reasons. The principle of the salt-gradient dialysis method of preparation of histone-DNA complexes involves initial mixing of the two components at salt concentrations in which there is likely to be little binding. Subsequent gradual reduction of the salt concentration results in a condition in which binding of histones to DNA is balanced by their dissociation from DNA, that is, the binding is readily reversible. Under these conditions, histone molecules might be expected to combine with and dissociate from the DNA until a 'preferred' binding takes place, that is, the histone combines with a segment of the DNA molecule whose

chemical structure is such that the attractive forces between the DNA and the histone are stronger than the forces tending to dissociate the complex. DNA-histone complexes formed in such conditions might therefore have distinctive properties as a result of the 'preferred' binding. Since the exact salt concentration at which reversible binding of GAR histone to C. T. DNA occurs is unknown, the range of salt concentration used in the present studies was extended to 0.4M NaCl, despite the fact that no detailed knowledge of the aggregation properties of the histone in these conditions is available. Edwards and Shooter (1969) have measured the sedimentation coefficient of the heterogeneous histone fraction  $F_2A_1$ , and shown that the sedimentation coefficient increases with increasing salt concentrations. Within the reservations imposed by the use of heterogeneous histone fractions and the use of sedimentation coefficient as a measure of aggregation, the results of Edwards and Shooter (1969) suggest that in 0.4M NaCl, GAR histone exists in a more aggregated form than in 0.15M NaCl.

GAR histone and C. T. DNA solutions were dialyzed extensively against the appropriate buffer and mixed at various ratios by weight of GAR to DNA, with DNA in excess, as described in Methods Section 2.5. A representative trace of the sedimentation profile of the complex in 0.4M NaCl, pH 5.0 is shown in Fig. 23(a). Only one heterogeneous boundary was present so that neither discrete species of complex nor free DNA could be distinguished. In this case, the concentration of the remaining unbound DNA cannot be estimated, thus preventing calculations of the stoichiometry of the complex formation. The sedimentation coefficient distribution  $g(s)$  across the sedimenting boundary was measurable. Fig. 23(b) illustrates the  $g(s)$  distribution of the complexes in 0.075M NaCl pH 5.0, 0.15M NaCl, pH 5.0 and 0.4M NaCl, pH 5.0. It can be seen that the distributions are very broad and in all cases encompass the  $g(s)$  distribution of free DNA (Fig. 19(a)). In 0.4M NaCl, the  $g(s)$  maximum is approximately 57 s, while the corresponding maxima for 0.15M NaCl

FIG 23(a)

HETEROGENEITY OF GAR-HISTONE-C. T. DNA COMPLEXES

Preparations of GAR histone and C. T. DNA were dialyzed extensively against 0.4M NaCl, pH 5.0.

Complexes of GAR histone and C. T. DNA were prepared by the method of direct addition (Methods Section 2.5), at a histone to DNA ratio of 0.1. The complex was centrifuged at 10,000 rpm in an AN-G rotor in a Beckman Model E analytical ultracentrifuge equipped with UV optics and a photo-electric scanning device, using light of wavelength 265nm.

FIG 23(b)

DISTRIBUTION OF SEDIMENTATION COEFFICIENTS OF GAR-HISTONE  
C. T. DNA COMPLEXES

Preparations of GAR histone and C. T. DNA were dialyzed against buffers of 0.075M NaCl, pH 5.0, 0.15M NaCl, pH 5.0 and 0.4M NaCl, pH 5.0. Complexes of GAR histone and C. T. DNA were prepared by the method of direct addition (Methods Section 2.5), at low histone to DNA ratios. The complexes were centrifuged at 10000 rpm at 20°C in an AN-G rotor in a Beckman Model E analytical ultracentrifuge equipped with absorption optics. g(s) distributions were calculated using the equation of Schumaker and Schachman (1957):-

$$g(s) = \frac{\frac{\Delta c_o^{obs}}{\Delta S_{20,w}^o} \left( \frac{x}{x_o} \right)^3}{S_{20,w}^o \sum \frac{\Delta c_o^{obs}}{\Delta S_{20,w}^o} \left( \frac{x}{x_o} \right)^3}$$

$\longleftrightarrow$  0.4M NaCl  
 $\circ - \circ$  0.15M NaCl  
 $\Delta - \Delta$  0.075M NaCl

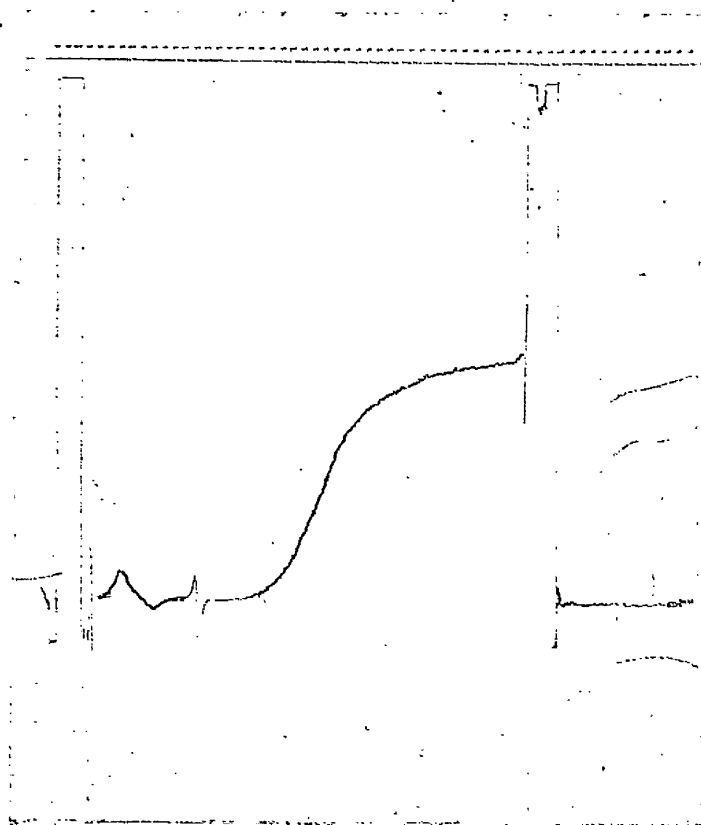


Fig. 23(a)

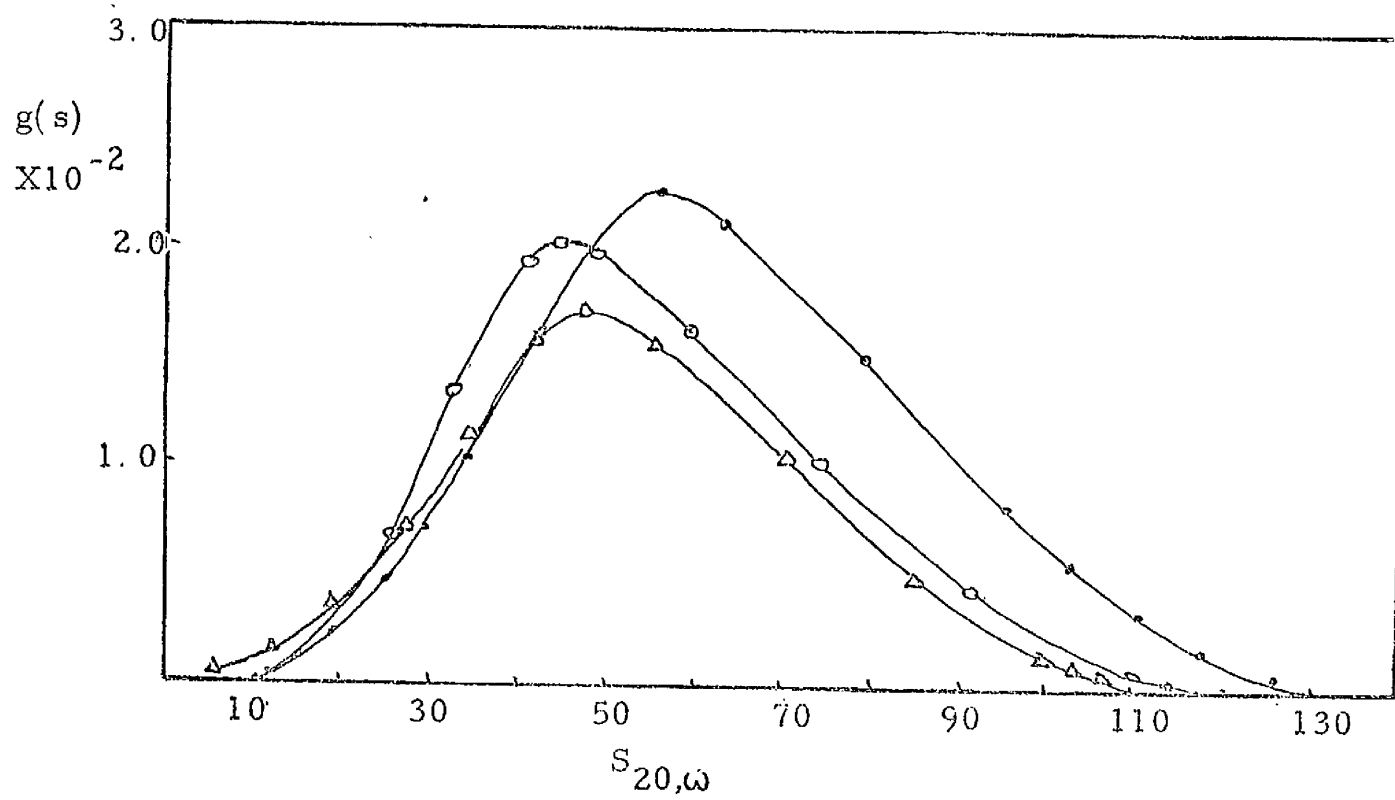



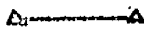

Fig. 23(b)

and 0.075M NaCl are approximately 42 s and 48 s respectively. The distribution of sedimentation coefficients in 0.4M NaCl has a higher proportion of material sedimenting with greater sedimentation coefficients. The  $g(s)$  distributions are broadly similar to those exhibited by complexes prepared by the salt-gradient dialysis method at pH 5.0 and pH 7.0 (Fig. 22(b)), indicating that the method of preparation of the complexes and the pH at which they are prepared do not affect the sedimentation coefficient distributions. These results confirm the thermal denaturation data which do not show any significant difference between complexes prepared by different methods. The ultracentrifuge analyses of pure GAR reported earlier indicated that in 0.075M NaCl the protein existed in a monomer-dimer equilibrium and in a monomer-dimer-tetramer equilibrium in 0.15M NaCl. Complexes of C. T. DNA with GAR in these different aggregation states show similar  $g(s)$  distributions (Fig. 23(b)). However, the  $g(s)$  distribution of the complexes formed in 0.4M NaCl, pH 5.0 shows a slight shift to higher  $s$  values compared with those of complexes in 0.075M NaCl and 0.15M NaCl. Although detailed analysis of the aggregation state of GAR histone in 0.4M NaCl was not carried out, the work of Edwards and Shooter (1969) indicates that the protein exists in a more aggregated state than in 0.15M NaCl, that is, the protein forms species higher than tetramer in 0.4M NaCl. It is possible that the higher  $s$  values of the complex formed in 0.4M NaCl are a result of the more aggregated state of the protein.

Since the complexes formed by the direct addition of histones to excess DNA at low histone-DNA ratios, were so heterogeneous as to prevent determination of the concentration of unbound DNA, thus preventing calculation of the stoichiometry of the complexes, analogous experiments were carried out using excess histone and adding known amounts of C. T. DNA. At high ratios of histone to DNA, however, the DNA is precipitated by the histone and the resulting nucleoprotein complex sediments so quickly as to prevent accurate measurement of its sedimentation coefficient.

AMOUNTS OF GAR HISTONE BOUND TO C. T. DNA

Preparations of GAR histone and C. T. DNA were dialyzed against 0.075M NaCl, pH 5.0, 0.15M NaCl, pH 5.0 and 0.4M NaCl, pH 5.0. Small varying concentrations of a solution of DNA of concentration 0.28mg/ml were added to known excess concentrations of GAR histone in a total volume of 0.4ml. Complexes were sedimented at 30000 rpm in an AN-G rotor at 70°C in a Beckman Model E ultracentrifuge equipped with UV optics. The wavelength of the light used was 275nm. The number of moles of GAR histone bound to a known concentration of C. T. DNA was estimated from the absorbance of the remaining unbound GAR histone. In all conditions the molecular weight of GAR histone was taken as 10600 and that of DNA as  $8.2 \times 10^6$  daltons.

	0.075M NaCl, pH 5.0
	0.15M NaCl, pH 5.0
	0.4M NaCl, pH 5.0



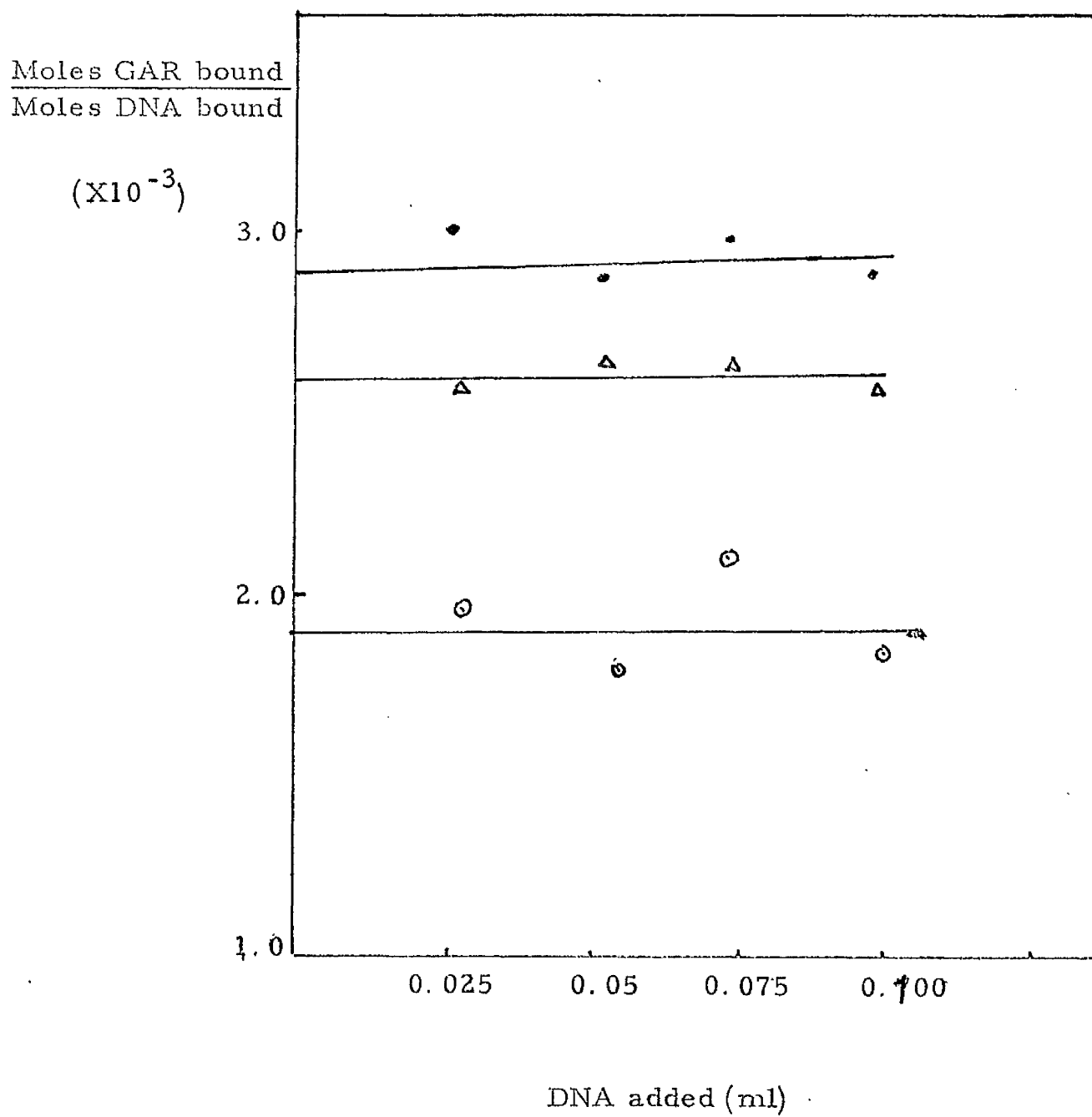


Fig. 24

Nevertheless, determination of the stoichiometry of these complexes can still be calculated, since the concentration of unbound excess histone molecules can be measured from the absorbance of the supernatant. Varying amounts of C. T. DNA were added to known excess amounts of GAR histone in three different solvent conditions: 0.075M NaCl, pH 5.0; 0.15M NaCl, pH 5.0; and 0.4M NaCl, pH 5.0. The number of histone molecules bound to a single molecule of C. T. DNA was calculated using the known initial amounts of both components and the amount of unbound histone. For the calculation, the molecular weight of the C. T. DNA was taken as the weight average molecular weight ( $8.2 \times 10^6$  daltons) estimated from the distribution across a sedimenting boundary of molecular weights which were, in turn, obtained from the  $g(s)$  distribution of sedimentation coefficient across a sedimenting boundary (Figs. 19a, b). The implications of using a single molecular weight to describe a heterogeneous population in studies on the binding of proteins to DNA will be discussed later. The molecular weight of GAR histone in the calculation was taken as the monomer molecular weight based on amino acid analysis, namely, 10600 daltons and the significance of using the monomer molecular weight will also be discussed in the Discussion Section. Fig. 24 depicts the ratio of the number of moles of GAR bound to the number of moles of DNA bound, as a function of the amount of DNA added, for all three conditions. The best-fitting straight lines through the data are also shown. Although there is a certain amount of scatter in the data, it can be seen that the data lie on approximately horizontal lines indicating that the number of individual histone molecules bound to each DNA molecule is independent of the amount of DNA added. The fact that the ratio of moles of histone bound to moles of DNA bound is independent of amount of DNA added indicates that there exists a direct proportionality of histone bound to DNA available, despite the fact that the DNA is heterogeneous. From the data of Fig. 24, it can be inferred that all species of the heterogeneous population of DNA

bind GAR histone. If only one species of DNA of a particular size and base sequence were capable of binding GAR histone then the remaining unbound DNA would be detected in the ultracentrifuge as a boundary sedimenting at a rate equivalent to that of free DNA (Fig. 19a). It was found experimentally, however, that the 'supernatant' remaining after the sedimentation of the complex migrated in the centrifugal field at a very low rate, less than 3 s, indicating that the supernatant was composed of histone. These results are consistent with the fact that these experiments were carried out in conditions of excess histone. It can be seen from Fig. 24 that the ratio of moles of GAR bound to moles of DNA bound is affected by the salt concentration at which the complex is formed. Most molecules are bound per DNA molecule of molecular weight  $8.2 \times 10^6$ , in 0.075M NaCl, slightly fewer in 0.15M NaCl and fewer in 0.4M NaCl. Table 15 shows the number of GAR histone molecules bound to C. T. DNA in the salt conditions used, assuming a value of  $8.2 \times 10^6$  for the molecular weight of the C. T. DNA. A subsidiary experiment was carried out in which spermidine phosphate at a final concentration of 0.1mM was added to the dialyzed C. T. DNA preparations. Varying amounts of the DNA-spermidine mixtures were then added to known, excess amounts of GAR histone. The number of GAR molecules bound was calculated as described above and found to be effectively the same as the number bound in the absence of spermidine phosphate. Table 15 also shows the contribution of the protein component of the nucleoprotein complex to the overall molecular weight of the complex, calculated on the basis of the number of GAR molecules bound to the DNA, using a value of 10600 for the molecular weight of one GAR histone molecule. The heterogeneity of C. T. DNA makes the interpretation of the sedimentation properties of GAR histone - C. T. DNA complexes difficult. To minimize the analytical problems caused by the heterogeneity of the DNA, studies were

TABLE 15

ESTIMATION OF AMOUNT OF GAR HISTONE BOUND TO C. T. DNA

Preparations of GAR histone and C. T. DNA were dialyzed exhaustively against buffers of 0.075M NaCl, pH 5.0, 0.15M NaCl, pH 5.0 and 0.4M NaCl, pH 5.0. Aliquots of varying known concentrations of DNA were added to known excess amounts of GAR histone and the mixtures were centrifuged at 6000 rpm in an AN-G rotor in a Beckman Model E analytical ultracentrifuge equipped with UV optics. The wavelength of the light used was 275nm.

The amount of GAR histone bound to known amounts of C. T. DNA was estimated from the absorbance of the histones remaining unbound in the 'supernatant'. The molecular weight contribution of the bound GAR histone was estimated from the number of molecules bound, using a value of 10,600 for the molecular weight of each histone molecule. The molecular weight of the complex was estimated by adding the weight average molecular weight of the DNA ( $8.2 \times 10^6$  daltons) to the total molecular weight of the histones bound to the DNA.

TABLE 15

Salt Conc.	No. of GAR molecules bound $\times 10^{-3}$	mol. wt. contri- bution by GAR ( $\times 10^{-6}$ )	Total mol. wt. of complex ( $\times 10^{-6}$ )
0.40	1.9	20.1	28.3
0.150	2.59	27.4	35.6
0.075	2.84	28.5	36.7

carried out using small viral DNA which is more homogeneous than mammalian DNA.

## 9. Preparation and Characterization of SV40 DNA

Covalently closed circular SV40 DNA was prepared from SV40 infected BSC-1 cells as described in Methods Section. Band sedimentation of the preparation of SV40 DNA through CsCl of density 1.320g/ml (Fig. 25(a)) revealed that the preparation was contaminated by a small amount of nicked circular DNA sedimenting with a lower sedimentation coefficient than the covalently closed DNA. The supercoiled circular DNA and relaxed circular DNA were resolved using the CsCl-ethidium bromide equilibrium centrifugation technique of Radloff, Bauer and Vinograd (1967), described in Methods Section 2.10.2. The absorbance profile obtained after harvesting the gradient is shown in Fig. 26(b). Fractions 30-36, containing only closed circular DNA were pooled and concentrated as were fractions 41-48 containing nicked circular DNA. Band sedimentation of these preparations of SV40 DNA through CsCl of density 1.320g/ml revealed that both preparations were essentially pure (Figs. 26(a), 26(b)), although the preparation of singly nicked circular DNA was contaminated with a small amount of non-sedimenting material. The preparations of supercoiled SV40 DNA and relaxed circular SV40 DNA sedimented with  $S_{20,w}$  values of 21.2 and 16.8 respectively. The molecular weight of each form of SV40 DNA was calculated from the experimental values of  $S_{20,w}$  using the empirical equations of Gray, Bloomfield and Hearst, (1967) and Hudson, Clayton and Vinograd (1968). Covalently closed circular SV40 DNA was found to have a molecular weight of  $3.05 \times 10^6$  daltons and relaxed circular SV40 DNA was found to have a molecular weight of  $2.97 \times 10^6$  daltons, confirming that the two species of DNA are merely different physical forms of the same DNA.

FIG. 25(a)

ANALYTICAL BAND SEDIMENTATION OF SV40 DNA

Preparations of SV40 DNA isolated from SV40-infected BSC-1 cells as described in Methods Section 2.4 were analyzed by band sedimentation as described in Methods Section 2.10.2. 15 $\mu$ l of DNA solutions were introduced into the sample well of a double band-forming centrepiece with 0.35ml of CsCl (density 1.320g/ml) as bulk solvent. Runs were carried out at 40,000 rpm and the scanning wavelength was 265nm.

FIG. 25(b)

FRACTIONATION OF CLOSED CIRCULAR SV40 DNA AND NICKED  
CIRCULAR SV40 DNA

DNA samples were centrifuged in CsCl of density 1.55g/ml, containing 100 $\mu$ g/ml ethidium bromide for 40h at 20<sup>o</sup>C in an angle 40 rotor at 39,000 rpm in a Spinco Model L ultracentrifuge. 5-drop fractions were collected by direct tube puncture. Ethidium bromide was removed by extraction with isoamyl alcohol. CsCl was removed by dialysis against SSC and absorbance of the fractions measured at 259nm in a UNICAM SP500 spectrophotometer.

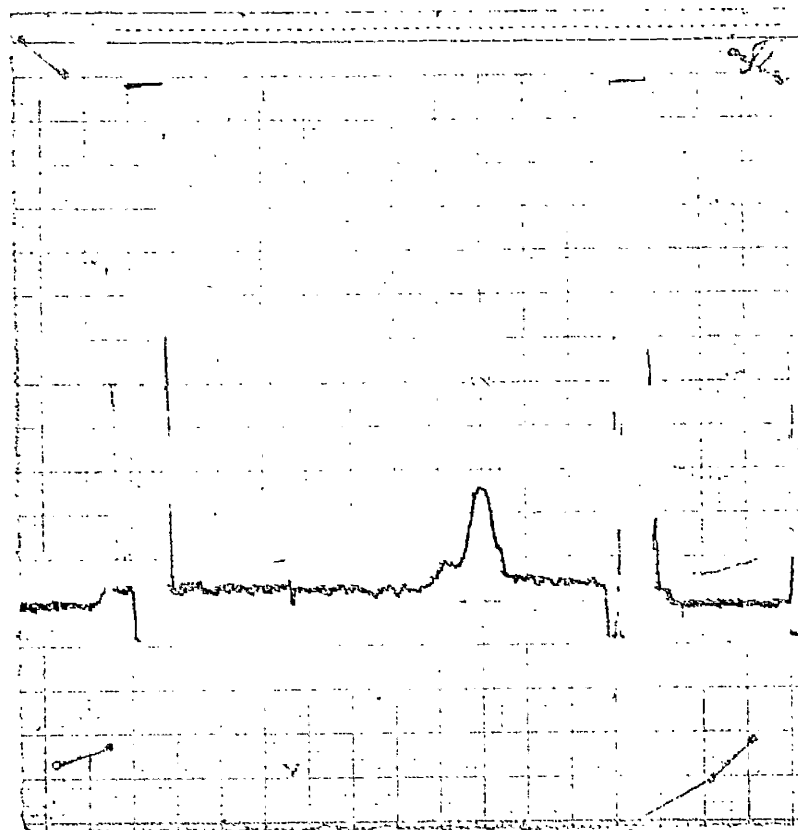


Fig. 25(a)

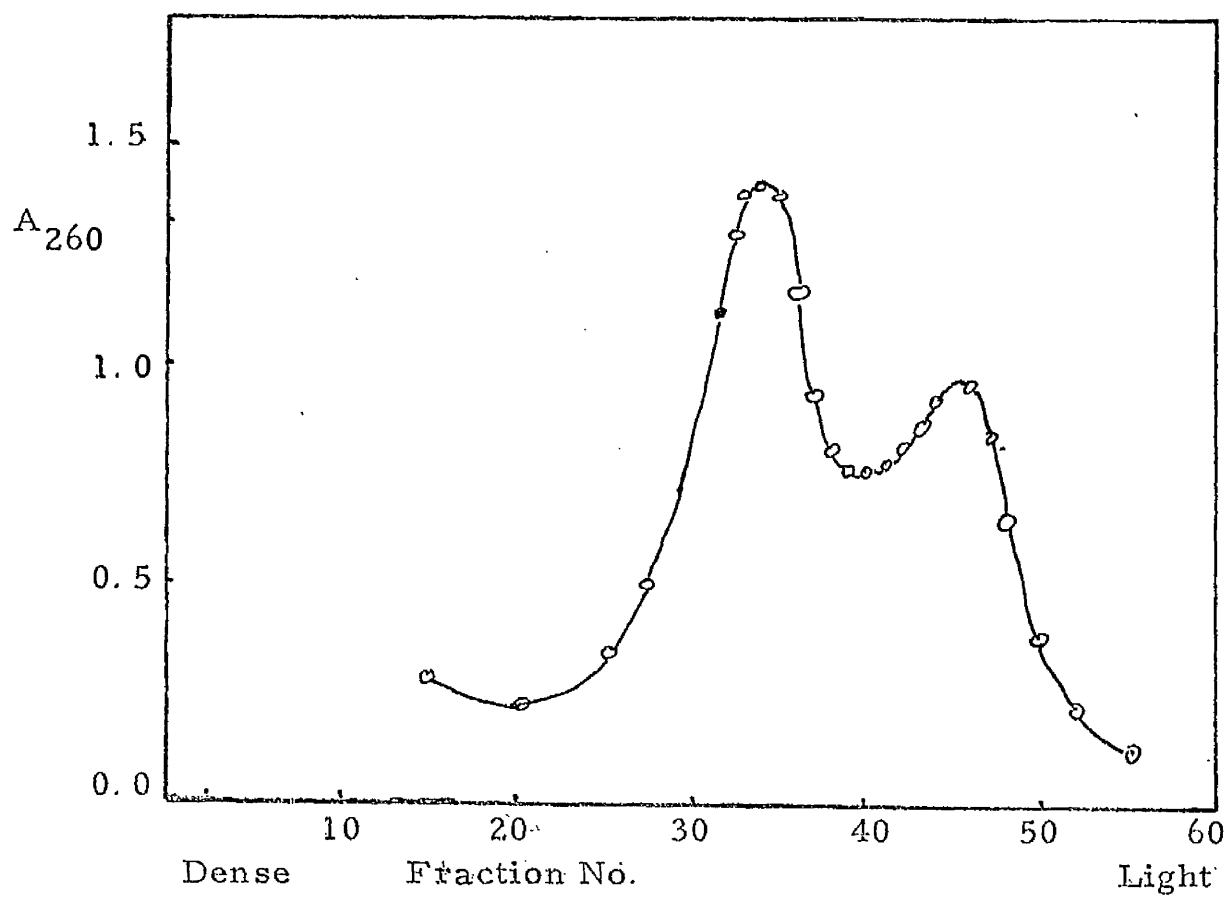


Fig. 25 (b)



FIG. 26(a)

BAND SEDIMENTATION OF CLOSED CIRCULAR SV40 DNA

Closed circular SV40 DNA was obtained from SV40-infected BSC-1 cells as described in Methods Section 2.4 and freed from contamination by nicked circular SV40 DNA by CsCl-ethidium bromide density gradient centrifugation. 15 $\mu$ l aliquots of the purified closed circular SV40 DNA in SSC were introduced into the sample well of a double sector band forming centrepiece with 0.35ml CsCl (density 1.320g/ml) as bulk solvent. Centrifugation was carried out at 40,000 rpm at 20°C. Scanning wavelength was 265nm.

FIG. 26(b)

ANALYTICAL BAND SEDIMENTATION OF NICKED CIRCULAR SV40  
DNA

SV40 DNA was prepared from SV40-infected BSC-1 cells and nicked circular SV40 DNA was freed from contamination by closed circular SV40 DNA by CsCl-ethidium bromide density gradient centrifugation. 15 $\mu$ l aliquots of the purified nicked circular SV40 DNA in SSC were introduced in the sample well of a double sector band forming centrepiece with 0.35ml CsCl (density 1.320g/ml) as bulk solvent. Centrifugation was carried out at 40,000 rpm at 20°C. Scanning wavelength was 265nm.

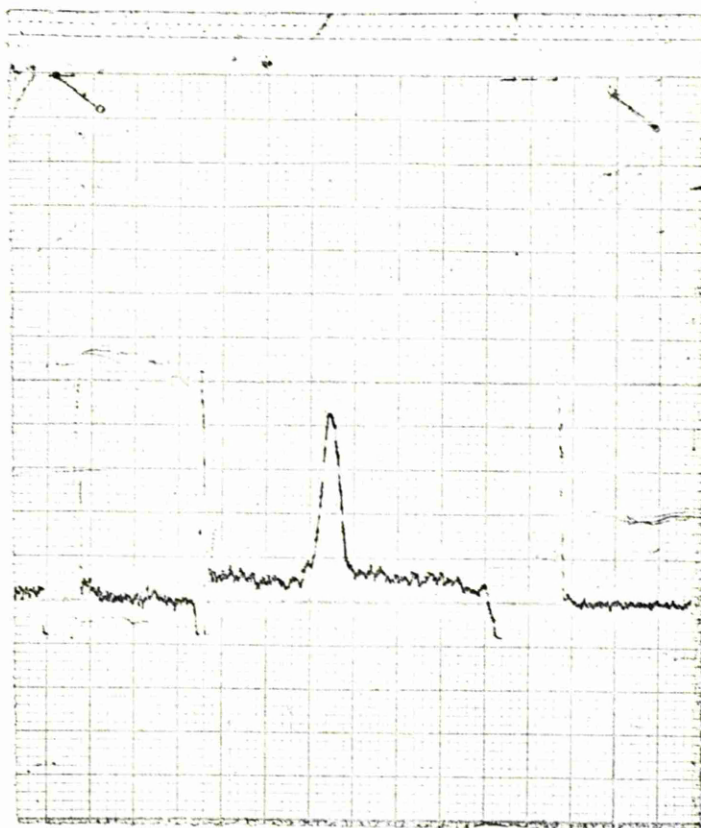


FIG. 26 (a)

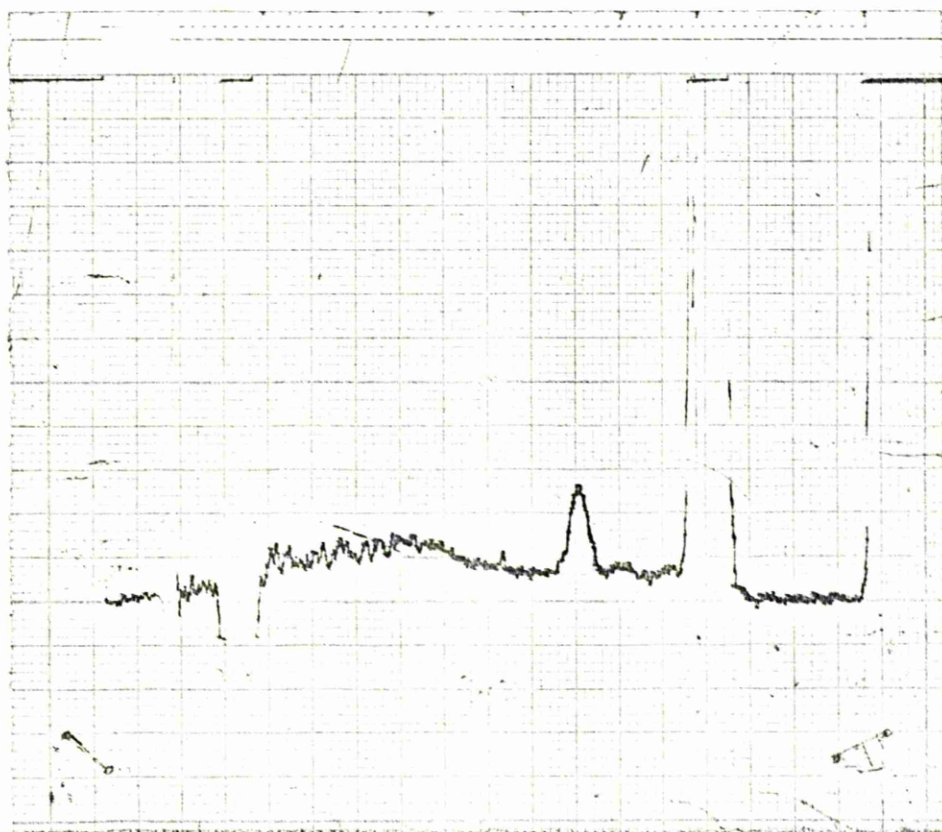


FIG. 26(b)

Studies of the formation of GAR histone-C. T. DNA complexes revealed that the complex formed was very heterogeneous with respect to sedimentation coefficient, thus making detailed investigation of the binding process difficult. Since both forms of SV40 DNA have been shown to be almost completely homogeneous, studies of the binding of GAR histone to SV40 DNA were carried out to allow detailed analysis of the binding process. Complexes were formed by the direct addition of the two components in two solvent conditions, 0.15M NaCl, pH 5.0 and 0.075M NaCl, pH 5.0. Small varying amounts of GAR histone were added to known excess amounts of both forms of SV40 DNA and the complexes formed were analyzed by boundary sedimentation, using absorption optics. To permit the analysis of high concentration of DNA, the ultracentrifuge was operated at several wavelengths. Representative traces are shown in Figs. 27(a) and 27(b). Fig. 27(a) illustrates the trace obtained in 0.15M salt by the addition of 10 $\mu$ l of a stock solution of GAR (0.38mg/ml) to excess supercoiled SV40 DNA, to a final volume of 1ml. Fig. 27(b) illustrates the trace obtained in 0.15M salt by the addition of 10 $\mu$ l of a stock solution of GAR (0.4 mg/ml) to excess relaxed circular SV40 DNA to a final volume of 1.0ml. In both cases the major sedimenting boundary represents unbound excess DNA and the shoulder represents DNA-histone complexes. Estimates of the concentrations of unbound DNA can thus be obtained from the absorbance of the free DNA. Using this value of the amount of unbound DNA, together with the amount of GAR and DNA originally added, the amount of histones bound to the DNA can be estimated. Fig. 28, shows the ratio of GAR bound to supercoiled SV40 DNA bound as a function of the amount of histone added in both 0.075M NaCl, pH 5.0 and 0.15M NaCl, pH 5.0 and Fig. 29 shows the corresponding data for relaxed circular SV40 DNA. It can be seen that at higher concentration of added GAR, the ratio of histone bound to DNA bound becomes approximately constant and is independent of the amount of GAR added. These experiments were always carried out in conditions of excess DNA, and so such an effect

SEDIMENTATION OF GAR HISTONE SV40 DNA COMPLEXES

Preparations of GAR histone and both supercoiled and relaxed circular SV40 DNA were dialyzed against 0.075M NaCl, pH 5.0 and 0.15M NaCl, pH 5.0. Small varying amounts of GAR histone were added to known excess amounts of SV40 DNA in a total volume of 1.0ml. Mixtures were centrifuged in an AN-G rotor at 20°C in a Beckman Model E analytical ultracentrifuge equipped with UV optics and a photo-electric scanning device. Wavelength of the light used was generally 265nm but for higher concentrations of DNA, higher wavelengths of ~~265nm~~ were used. Fig. 27(a) shows a typical trace obtained on centrifuging a mixture of supercoiled SV40 DNA in 0.15M NaCl, pH 5.0 to which 10µl of a stock solution of GAR histone, concentration 0.38mg/ml had been added to a final volume of 1.0ml. Fig. 27(b) shows a typical trace obtained on centrifuging a mixture of relaxed circular SV40 DNA in 0.15M NaCl, pH 5.0 to which 10µl of a stock solution of GAR concentration 0.41mg/ml had been added to a final volume of 1.0ml.

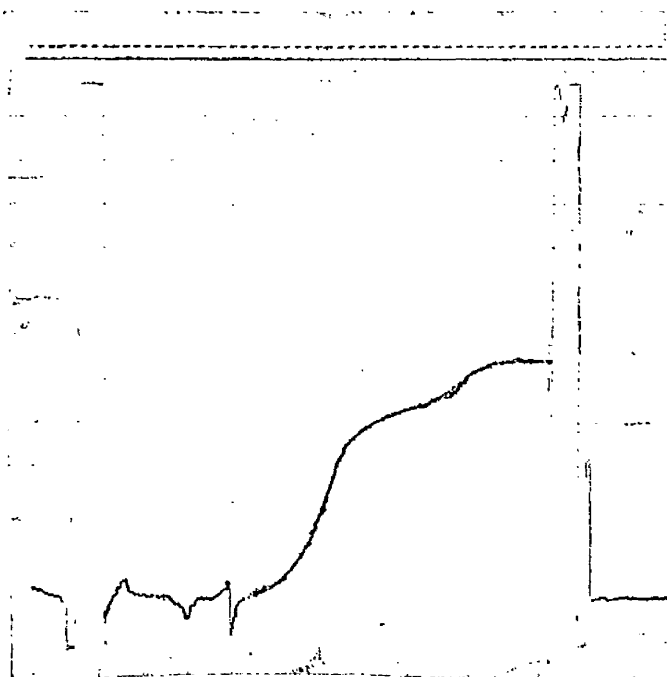


Fig. 27(a)

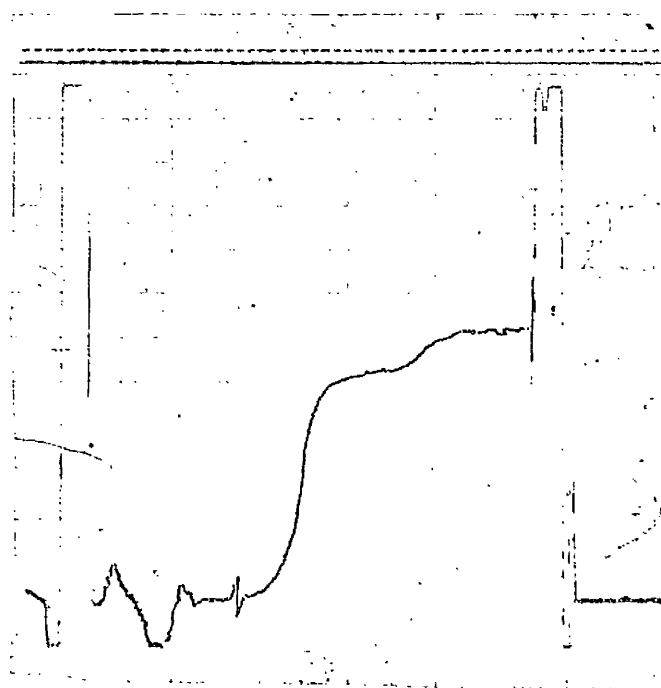


Fig. 27(b)

BINDING OF GAR HISTONE TO SUPERCOILED SV40 DNA

Preparations of GAR histone and closed circular SV40 DNA were dialyzed against 0.075M NaCl, pH 5.0 and 0.15M NaCl, pH 5.0. Small varying amounts of a solution of GAR histone of concentration 0.38mg/ml were added to known excess amounts of closed circular SV40 DNA in a total volume of 1.0ml, with vigorous agitation as described in Methods Section 2.5. Aliquots were sedimented in an AN-G rotor at 20°C in a Beckman Model E analytical ultracentrifuge equipped with absorption optics and a photo-electric scanning device. The wavelength of the light used was generally 265nm but for higher concentrations of DNA, higher wavelengths were used. Runs were carried out at 20000 rpm. Blanks were run with no histone added. The amounts of DNA to which the known amounts of GAR histone were bound were estimated from the absorbance of the boundary corresponding to the remaining, free unbound DNA. The data are expressed as the ratio of moles of GAR bound to DNA bound as a function of the amount of added histone. The molecular weight of GAR histone was taken as 10600 in both salt conditions and the molecular weight of the DNA was taken as  $3.0 \times 10^6$ .

○——○ 0.075M NaCl, pH 5.0  
△——△ 0.15M NaCl, pH 5.0

Moles GAR bound  
Moles DNA bound  
( $\times 10^{-2}$ )

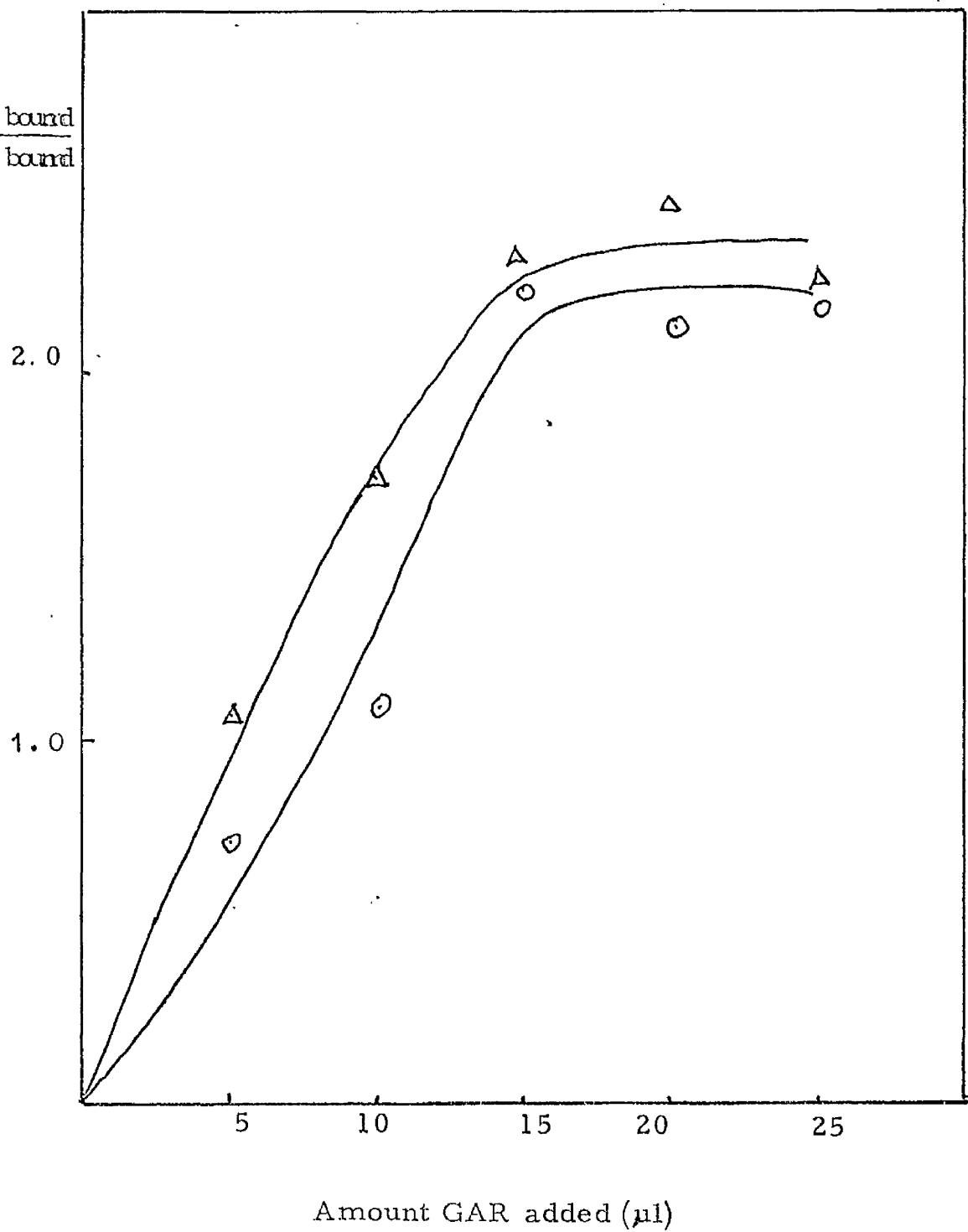


Fig. 28

BINDING OF GAR HISTONE TO RELAXED CIRCULAR SV40 DNA

Preparations of GAR histone and relaxed circular SV40 DNA were dialyzed against 0.075M NaCl, pH 5.0 and 0.15M NaCl, pH 5.0. Small varying amounts of a solution of GAR histone of concentration 0.41mg/ml were added to known excess amounts of relaxed circular SV40 DNA in a total volume of 1.0ml with vigorous agitation as described in Methods Section 2.5. Aliquots were sedimented in an AN-G rotor at 20°C in a Beckman Model E analytical ultracentrifuge equipped with absorption optics and a photo-electric scanning device. The wavelength of the light used was generally 265nm but for higher concentrations of DNA, higher wavelengths were used. Runs were carried out at 20,000 rpm. Blanks were run with no histone added. The amount of DNA to which the known amounts of GAR histone were bound was estimated from the absorbance of the boundary corresponding to the remaining free, unbound DNA. The data are expressed as the ratio of moles of GAR bound to DNA bound as a function of the amount of added histone. The molecular weight of GAR histone was taken as 10600 in both salt conditions and the molecules weight of the DNA was taken as  $3.0 \times 10^6$ .

○—○ 0.15M NaCl, pH 5.0

△—△ 0.075M NaCl, pH 5.0



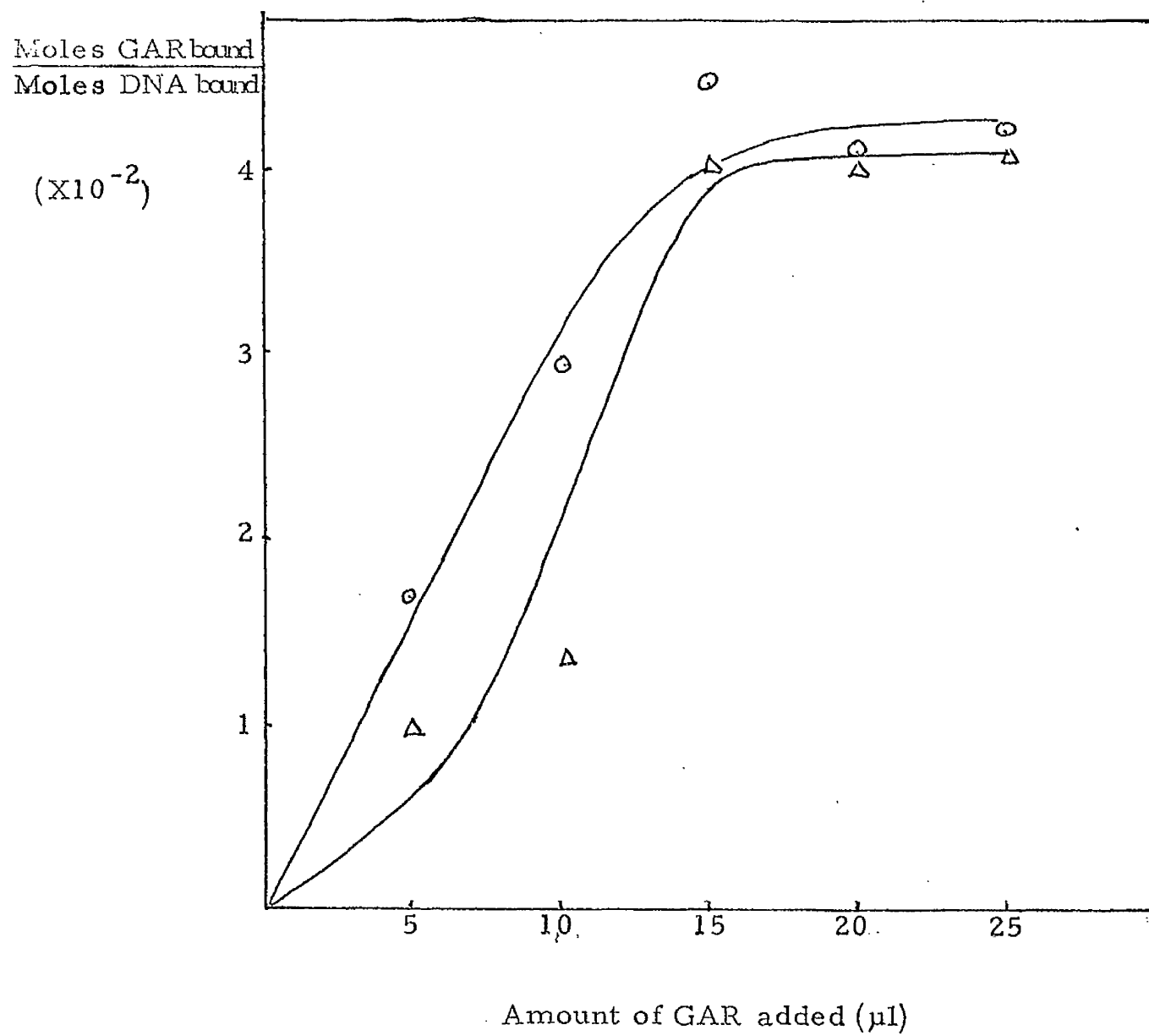


Fig. 29

may be attributed to co-operative binding of GAR molecules to the DNA, that is, the binding of one GAR molecule to a DNA molecule facilitates the subsequent binding of more GAR molecules to the same DNA molecule, in preference to other DNA molecules. If the binding of GAR to SV40 DNA was non-co-operative, that is, was a random process, then it might be expected that in conditions of excess DNA, as the amount of added histone is increased then the average number of histone molecules bound to each DNA molecule would correspondingly increase. The data of Figs. 28 and 29 at the higher concentrations of added GAR, clearly indicate the co-operativity of the binding process. Nevertheless, at very low concentrations of added GAR it can be seen that the number of molecules of bound GAR increases with the amount of GAR added. At low concentrations of added GAR, it is possible that the binding of histones to DNA is still co-operative but that saturation of each DNA molecule is impossible because of the limiting amounts of GAR present. The sedimenting boundary corresponding to the complex formed at very low concentrations of added GAR is too small to permit application of a  $g(s)$  analysis of distribution of sedimentation coefficient. Thus possible heterogeneity in the boundary corresponding to the complex formed in these conditions cannot be detected. At low concentrations of added GAR, the amount of complexed DNA is correspondingly small, thus making accurate determination of the concentration of the remaining 'supernatant' of unbound DNA difficult, since the boundary between free DNA and complex is very small. The presence of the effect for both forms of SV40 DNA each in both salt conditions seems to suggest, however, that the effect is real and not due to experimental error.

The estimated number of GAR molecules bound to each form of SV40 DNA in both salt conditions is shown in Table 16. Table 16 demonstrates that the number of GAR molecules bound to supercoiled SV40 DNA is slightly more than half the number bound to relaxed circular SV40 DNA. Table 16 also demonstrates that the number of histone

TABLE 16

ESTIMATIONS OF AMOUNT OF GAR HISTONE BOUND TO SV40 DNA

Preparations of GAR histone and of relaxed circular SV40 DNA and supercoiled SV40 DNA were dialyzed against buffers of 0.075 M NaCl, pH 5.0 or 0.15M NaCl, pH 5.0. Varying amounts of GAR histone of known concentration were added to known excess amounts of DNA and the mixtures sedimented in an AN-G rotor in a Beckman Model E ultracentrifuge equipped with UV optics. The amount of DNA bound to known amounts of GAR histone was calculated from the concentration of DNA remaining unbound. The molecular weight contribution of the histones to the complex was calculated from the number of histone molecules bound, using a value of 10600 for the molecular weight of each histone molecule. The molecular weight of the complex was obtained by adding the molecular weight of the DNA molecule ( $3.0 \times 10^6$  daltons) to the total molecular weight of the histones bound per DNA molecule.

TABLE 16

DNA	Salt Conc.	No. GAR molecules bound ( $\times w^{-2}$ )	mol. wt. contribution by GAR ( $\times 10^{-6}$ )	Total mol. wt. of Complex ( $\times 10^{-6}$ )
Super coiled SV40 DNA (I)	0.075	2.22	2.35	5.35
	0.15	2.320	2.46	5.46
Relaxed circular SV40 (II)	0.075	4.05	4.29	7.29
	0.15	4.19	4.44	7.44

molecules bound per DNA molecule is effectively independent of the salt concentration. It therefore appears that the state of aggregation of GAR may not affect significantly the binding to the DNA. In Table 16 are also shown the contributions of the protein moiety to the overall molecular weight of the nucleoprotein complex, calculated from the number of histone molecules bound, using a value of 10600 for the molecular weight of GAR.

Approximate sedimentation coefficients were calculated for the SV40 DNA-GAR histone complexes by measuring the rate of migration of the half-height point of the boundary corresponding to the complex. Results are shown in Table 17. It may be seen that in each case, the sedimentation coefficient for the complex formed by the addition of high concentrations of GAR histone to excess SV40 DNA is independent of the amount of GAR added. For both forms of DNA and in both salt conditions, the sedimentation coefficient of the complex decreases, however at low concentrations of added GAR histone. In this respect, the sedimentation data are broadly consistent with the data on the number of GAR molecules bound (Figs. 28 and 29). The experimental accuracy of the sedimentation coefficients of the complexes is however likely to be limited, since the method of using the rate of migration of the half-height point of the boundary is sensitive to errors of measurement, particularly when the sedimenting species is heterogeneous and the boundary height is small. In spite of the possible inaccuracies in the measurement of the sedimentation coefficients of the SV40-DNA-GAR histone complexes,  $S_{20,w}$  values were calculated and are shown in Fig. 30 as a function of molecular weight of the complex. The molecular weight of the complex was calculated by summing the molecular weights of the DNA and histone bound (Table 16). Included in Fig. 30 are data points corresponding to relaxed circular and supercoiled SV40 DNA which have a common molecular weight of  $3.0 \times 10^6$  but have  $S_{20,w}$  values of 16.0 and 21.0 Svedberg units respectively. It can be seen from Fig. 30 that in general,

## TABLE 17

### SEDIMENTATION COEFFICIENTS OF GAR HISTONE-SV40 DNA COMPLEXES

Small varying amounts of GAR histone (of concentration 0.41mg/ml for binding to relaxed circular DNA and 0.38mg/ml for binding to supercoiled DNA) were added with vigorous agitation to known excess amounts of SV40 DNA in 0.075M NaCl, pH 5.0 or 0.15M NaCl, pH 5.0 and the mixtures were centrifuged in a Beckman Model E analytical ultracentrifuge equipped with UV optics. The wavelength of the light used was generally 265nm but for higher concentrations of DNA, higher wavelengths were used. The sedimentation coefficients of the nucleoprotein complexes were estimated from the rates of migration of the points corresponding to the half-height of the boundary of the sedimenting nucleoprotein complex. Sedimentation coefficient were converted to  $S_{20,w}$  values using values of the density and viscosity of the solvent. Density and viscosity values were obtained from International Critical Tables.

TABLE 17

Types of DNA in Complex and salt concentr- ation	S <sub>20, w</sub> of complex (X10 <sup>13</sup> )	Amount of GAR added (μl)
SV40 I DNA 0.075M NaCl, pH 5.0	21.0	0
	24.1	10
	26.6	15
	26.6	20
	27.0	25
SV40 I DNA 0.15M NaCl pH 5.0	21.0	0
	26.5	10
	29.4	15
	29.2	20
	28.6	25
SV40 II DNA 0.075M NaCl, pH 5.0	16.0	0
	26.6	10
	30.8	15
	31.0	20
	31.0	25
SV40 II DNA 0.15M NaCl pH 5.0	16.0	0
	27.2	10
	33.6	15
	33.2	20
	33.0	25

FIG. 30

RELATIONSHIP OF THE SEDIMENTATION COEFFICIENTS OF GAR  
HISTONE - SV40 DNA COMPLEXES WITH MOLECULAR WEIGHT OF  
THE COMPLEX

The sedimentation coefficients of complexes of GAR histone with relaxed circular SV40 DNA and with closed circular SV40 DNA were estimated from the rate of migration of the half-height point of the sedimenting boundary corresponding to the nucleoprotein complex, formed by the addition of small amounts to excess amounts of DNA in 0.075M NaCl, pH 5.0 and 0.15M NaCl, pH 5.0.  $S_{20,w}$  values were calculated using values of the viscosity and density of the solvent obtained from International Critical Tables. The molecular weight of the complex was computed from the total molecular weight of the histones bound to each molecule of DNA. The molecular weight of GAR histone in all conditions was taken as 10,600 daltons.

○—○ Complex formed between relaxed circular SV40 DNA and GAR  
in 0.075M NaCl, pH 5.0

△—△ Complex formed between relaxed circular SV40 DNA and GAR  
in 0.15M NaCl, pH 5.0.

◻—◻ Complex formed between closed circular SV40 DNA and GAR  
in 0.075M NaCl, pH 5.0.

└— Complex formed between closed circular SV40 DNA and GAR  
in 0.15M NaCl, pH 5.0.



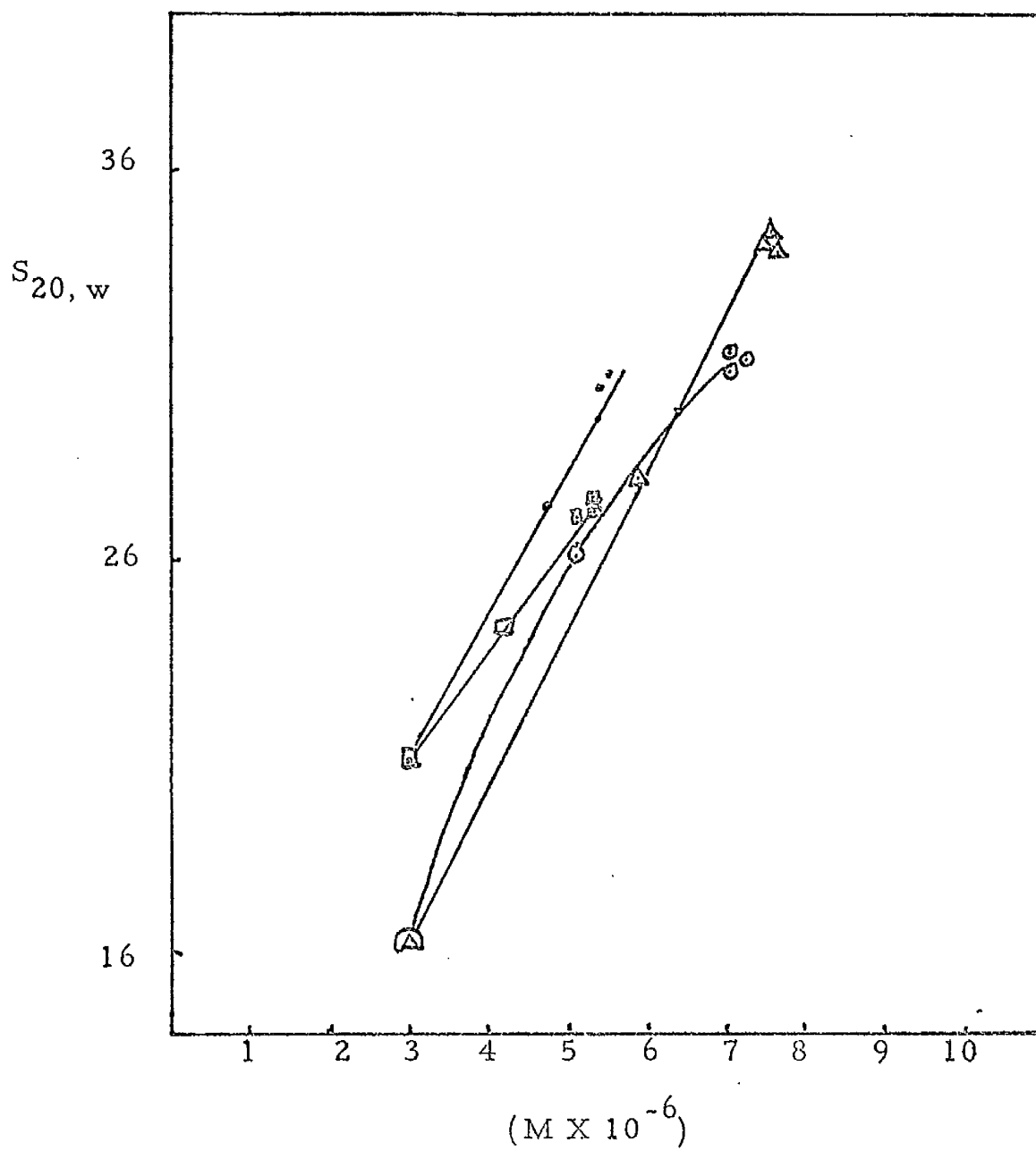


Fig. 30

for both forms of SV40 DNA and in both 0.15M NaCl, and in 0.075M NaCl, there is an approximately linear relationship between the  $S_{20,w}$  values and molecular weights of GAR histone-DNA complexes. These results must, however, be considered within the previously-stated limitations of the possible inaccuracies of measurement of the sedimentation coefficients.

Because of the difficulties in calculating accurate sedimentation coefficients for SV40 DNA-histone complexes, a  $g(s)$  analysis of the distribution of sedimentation coefficient was carried out for complexes of GAR with both forms of SV40 DNA each in both 0.075M NaCl, pH 5.0 and 0.15M NaCl, pH 5.0. The analysis of the distribution of sedimentation coefficients was carried out on complexes formed by the addition of relatively high concentrations of GAR histone to excess amounts of DNA. Earlier studies (Figs. 28 and 29) had indicated that the number of molecules of GAR histone bound in such complexes is independent of the amount of histones added presumably since all binding sites are occupied. Fig. 31(a) shows the distribution of sedimentation coefficients of the complex formed between GAR histone and supercoiled SV40 DNA and relaxed circular SV40 DNA in 0.075M NaCl, pH 5.0. It can be seen that two maxima occur. The faster components for supercoiled SV40 DNA-GAR complexes and relaxed circular SV40 DNA-GAR complexes have sedimentation coefficients of 26 s and 31 s respectively. The slower component may represent complexes of lower S value or alternatively may represent an artefact whose presence can be attributed to the overlapping distribution of free DNA and DNA histone complexes in the original boundary sedimentation traces. Fig. 31(b) shows the  $g(s)$  distribution obtained for complexes formed in 0.15M NaCl, pH 5.0. Patterns similar to those in 0.075M NaCl, pH 5.0 were obtained, the faster component for supercoiled SV40 DNA-GAR complexes and relaxed circular SV40 DNA-GAR complexes having sedimentation coefficients of 28 s and 34 s respectively.

DISTRIBUTION OF SEDIMENTATION COEFFICIENTS OF COMPLEXES  
OF GAR HISTONE WITH RELAXED CIRCULAR AND CLOSED CIRCULAR  
SV40 DNA

Preparations of GAR histone and both forms of SV40 DNA were dialyzed against 0.075M NaCl, pH 5.0 and 0.15M NaCl, pH 5.0. 25ul of a stock solution of GAR histone (concentration 0.41mg/ml) were added to excess relaxed circular SV40 DNA in a total volume of 1.0ml and 25ul of a stock solution of GAR histone (concentration 0.38mg/ml) were added to excess supercoiled SV40 DNA in a total volume of 1.0ml. The mixtures were centrifuged at 20000 rpm at 20°C in a Beckman Model E analytical ultracentrifuge equipped with absorption optics.  $g(s)$  distributions were calculated by the method of Schumaker and Schachman (1957).  $S_{20,w}$  values were calculated using the density and viscosity of the solvent as obtained from International Critical Tables.

Fig. 31(a)

- Complex of GAR with supercoiled SV40 DNA in 0.075M NaCl,  
pH 5.0
- Complex of GAR with relaxed circular SV40 DNA in 0.15M  
NaCl, pH 5.0.

Fig. 31(b)

- Complex of GAR with supercoiled SV40 DNA in 0.15M NaCl,  
pH 5.0
- Complex of GAR with relaxed circular SV40 DNA in 0.15M  
NaCl, pH 5.0.

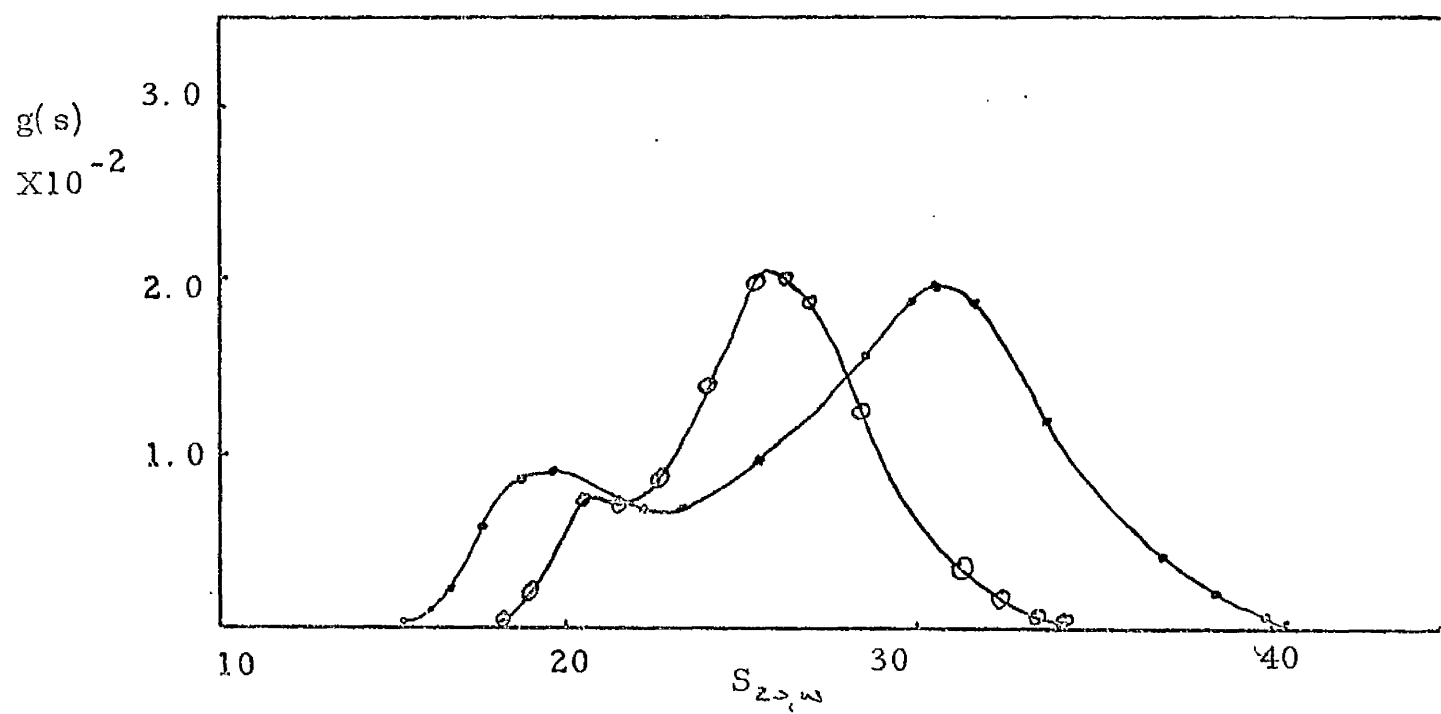


Fig. 31(a)

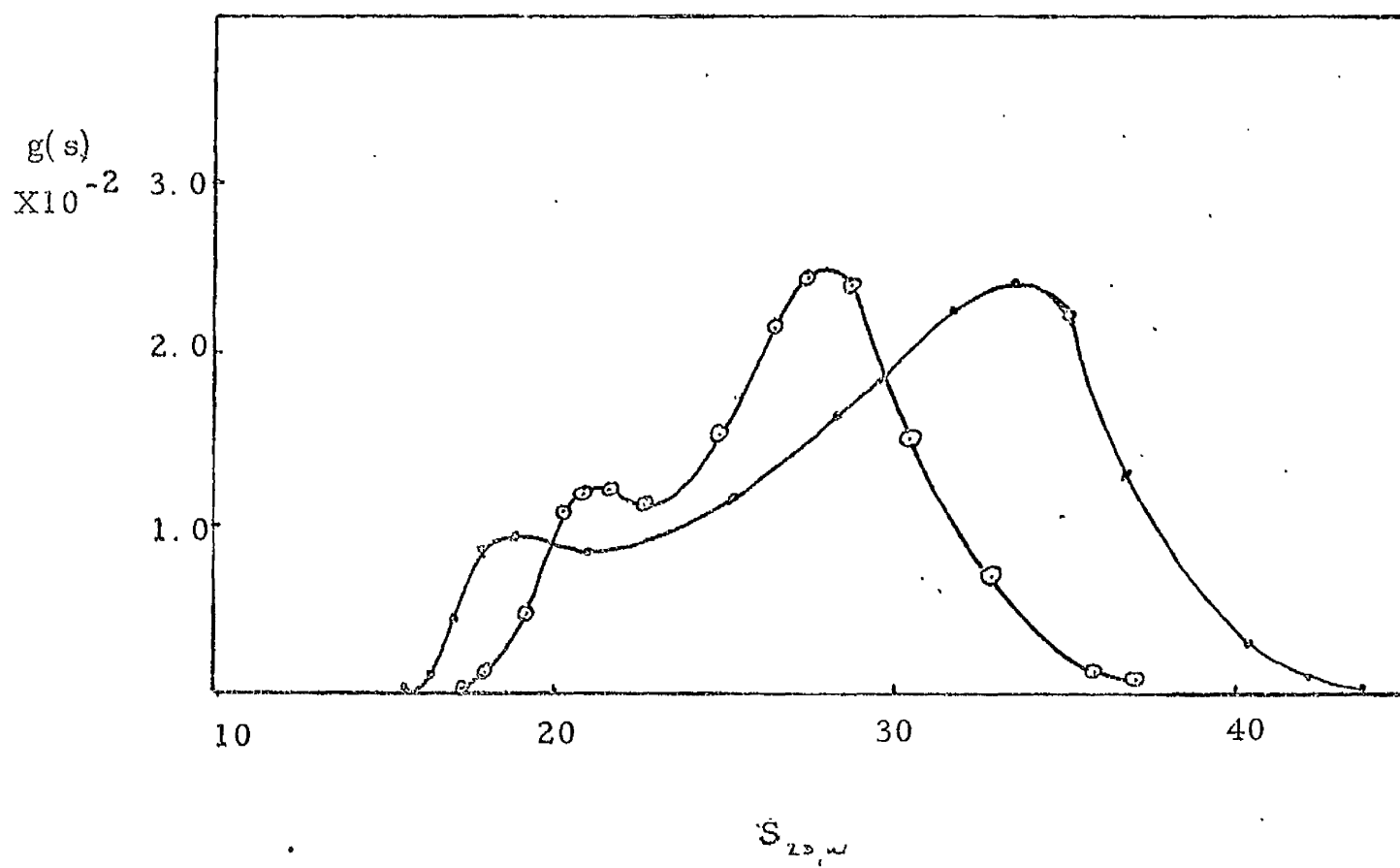


Fig. 31 (b)

From the number of GAR histone molecules bound to both forms of SV40 DNA (Table 16) and the relative molecular weights of both the protein and DNA moieties of the complexes, the partial specific volumes of the complexes were calculated, assuming that the partial specific volumes of each component were additive in the proportions in which the components of the complex combined. This assumption is generally made in the calculation of partial specific volumes of complexes, although there is little experimental evidence to justify it. Indeed, Bancroft and Freifelder (1970) have shown in the case of T5 bacteriophage, that the calculated value of  $\bar{v}$  differs from that obtained experimentally from density measurements. However, in most cases, experimental values of  $\bar{v}$  agree with those calculated assuming proportional additivity of the relative partial specific volumes of the components of a complex, and in the lack of any suitable alternative method, this method was used to calculate partial specific volumes of SV40 DNA-GAR histone complexes on the basis of their measured molecular composition. Calculated values are shown in Table 18.

No empirical equation, analogous to that of Crothers and Zimm (1965) relating the sedimentation coefficient of linear duplex DNA with its molecular weight, is available for the corresponding relation between molecular weight and sedimentation coefficient of DNA-histone complexes. Thus, information on the conformation of DNA-histone complexes cannot be attained simply by comparison of measured sedimentation coefficients with those calculated, by an empirical equation, from molecular weights. However,  $D$ , the diffusion coefficient and  $f$ , the frictional coefficient can be calculated for the nucleoprotein complexes from the experimental values of  $S_{20,w}$  and  $M$  and from these parameters preliminary information may be deduced concerning the shape of the nucleoprotein complexes. The sedimentation coefficients used in these calculations were not those at zero concentration. The errors introduced by failing to consider the

TABLE 18

HYDRODYNAMIC PROPERTIES OF GAR-SV40 DNA COMPLEXES

From the estimated molecular composition of SV40 DNA-GAR complexes (Table 16), values of  $v$  for the complexes were calculated using values of 0.556 and 0.729 for the partial specific volume of DNA and GAR histone respectively. Values of  $f$ , the frictional coefficient were calculated by the equation:

$$f = \frac{M(1 - \bar{v}\rho)}{Ns}, \quad \text{using the sedimentation}$$

coefficients of Table 17.  $\rho$  was taken as the density of the solvent and obtained from International Critical Tables. The diffusion coefficient  $D$  was calculated using  $D = \frac{KT}{f}$ .

Values of  $R_e$ , the radius of the equivalent hydrodynamic sphere of the complexes were evaluated using

$$f = 6 \pi \eta R_e$$

$\eta$  was taken as the viscosity of the solvent and was obtained from International Critical Tables. For SV40 virus, the molecular weight was calculated from the molecular composition published by Estes, Huang and Pagano, (1971). The sedimentation coefficient of SV40 virus <sup>used</sup> ~~had~~ was that reported by Black, Crawford and Crawford (1964).

TABLE 18

Salt Conc.	Complex	Calcd. $\bar{v}$ ml/mg	Calcd. D $\times 10^8$ $\text{cm}^2/\text{sec.}$	Calcd. f $\times 10^6$ $\text{sec} / \text{cm}^2$	$R_e$ $A^0$
0.075	SV40 I DNA - GAR	0.633	3.36	1.205	644
0.150	SV40 I DNA - GAR	0.638	3.48	1.160	616
0.075	SV40 II DNA - GAR	0.661	3.075	1.316	696
0.150	SV40 II DNA - GAR	0.662	3.26	1.248	654
-	SV40 I DNA	0.556	5.35	0.75	-
-	SV40 II DNA	0.556	2.92	1.38	-
-	SV40 Virus	0.681	16.9	23.90	-

concentration dependence of the sedimentation coefficient of the complex are, however, likely to be small since the experimental sedimentation coefficients were evaluated at low concentrations.  $f$ , the frictional coefficient was calculated using the equation:-

$$f = \frac{M(1 - \bar{v}\rho)}{NS}$$

where  $M$  is the molecular weight of the complex  
 $\bar{v}$  is the partial specific volume  
 $\rho$  is the density  
 $N$  is Avogadro's number  
and  $S$  is the sedimentation coefficient of the complex  
 $D$ , the diffusion coefficient of the complex, was calculated using the equation:-

$$D = \frac{KT}{f}$$

where  $K$  is Boltzmann's constant  
 $T$  is absolute temperature

For the calculation of  $D$  and  $f$ , the value of  $\bar{v}$  used was calculated from the molecular composition of the complex and the value of  $\rho$  was taken as the density of the solvent, which was obtained from International Critical Tables. The values of  $D$  and  $f$  calculated for GAR histone complexes with both forms of SV40 DNA in 0.075M NaCl/pH 5.0 and 0.15M NaCl, pH 5.0 are listed in Table 18. The values of  $D$  and  $f$  for the SV40 DNA-GAR complexes are of the same order of magnitude as those reported by Moller (1964) for spherical ribonucleoprotein particles. As pointed out by Tanford (1961), the frictional coefficient obtained from sedimentation measurements is that of the equivalent hydrodynamic sphere of the sedimenting species. Use of Stokes' law,  $f = 6\pi\eta R_e$ , where  $\eta$  is the solvent viscosity, permits the evaluation of  $R_e$ , the radius of the equivalent hydrodynamic sphere. Values of  $R_e$ , calculated from  $f$ , are shown in Table 18. For this calculation,  $\eta$  was obtained from



International Critical Tables. The diffusion coefficients of both forms of SV40 DNA are also shown in Table 18. These were calculated by the Svedberg equation using values of  $3.0 \times 10^6$  for molecular weight, 0.556 for partial specific volume,  $293^\circ\text{K}$  for temperature and values of 16 s and 21 s for the sedimentation coefficients of relaxed circular and supercoiled SV40 DNA, respectively. For molecules of the same molecular weight, the diffusion coefficients are different, illustrating the effect of conformation and confirming that supercoiled SV40 DNA is much more compact than the relaxed circular SV40 DNA.

Also shown in Table 18 are hydrodynamic parameters for a nucleoprotein complex involving SV40 DNA, namely SV40 virus itself. The sedimentation coefficient of the intact virus was taken from the studies of Black, Crawford and Crawford (1964) and Crawford and Black (1964). The molecular weight was calculated from the molecular weights of the components of SV40 as estimated by Estes, Huang and Pagano (1971).

With the elucidation of the molecular composition and of the experimental hydrodynamic parameters characterizing the complexes, information can be obtained on the shape of the complexes formed by the evaluation of corresponding hydrodynamic parameters for model structures of the complexes of varying geometrical shapes. Comparison of the experimental parameters with those of a particular model structure may indicate the most likely possibility of the shape of the complex.

#### 11. Model structures of SV40 DNA-GAR histone complexes

For construction of model complexes, it is desirable to know how many histone molecules are bound on average to a given length of DNA. Since the molecular dimensions of SV40 DNA are known accurately, and the number of histone molecules bound is also known, such a procedure seems possible in the case of SV40 DNA-GAR complexes.

The contour length of relaxed circular SV40 DNA is 1.7 micron (Rush, Eason and Vinograd, 1971). Assuming the diameter of the double helix structure to be  $27\text{\AA}$ , it can be shown by geometrical considerations, that the maximum number of histone molecules, taken as spheres of radius  $20.53\text{\AA}$ , (from the Sephadex studies in Section 2) which can be located around the double helix in any cross sectional area at any one point is 5. Again taking a histone molecule as a sphere of radius  $20.53\text{\AA}$ , the maximum number of histones which can be accommodated as a single row along a  $1700\text{\AA}$  stretch of DNA is 415. The total possible number of histone molecules, assuming a histone to be a sphere of  $20.53\text{\AA}$  radius, which can be bound along and around a relaxed circular molecule of SV40 DNA in the form of a hollow cylinder of histone molecules is therefore  $5 \times 415 = 2075$ . The experimental results reported in this work indicated that the actual number of histones bound per relaxed circular model of SV40 DNA was about 400. A likely model of relaxed circular SV40 DNA-GAR histone complexes is therefore as a length of DNA with spherical histone molecules attached linearly along the DNA. From the experimental number of histone molecules bound, it seems unlikely that the DNA is at the centre of a 'cylinder' of histone molecules. Olins (1969) has suggested that histones bind to the large groove of DNA. Accordingly, the total length of the large groove in a molecule of relaxed circular DNA was calculated from geometrical considerations and found to be approximately  $30000\text{\AA}$ . Assuming histone molecules to be spheres of radius  $20.53\text{\AA}$ , a maximum number of 730 histone molecules could be bound in the large groove. The discrepancy between this number and the number of histone molecules found experimentally to be bound to relaxed circular SV40 DNA, could be resolved by assuming that on association with the DNA, the histone molecule lost its spherical shape and adopted a more asymmetric shape. Nevertheless, for simplicity, it was assumed that a likely model for the relaxed circular SV40 DNA-GAR histone complex was a stretch of DNA with a linear array of spherical histone molecules attached.

The total length of a molecule of supercoiled SV40 DNA may be estimated from electron micrographs and is found to be approximately 0.81 microns (Rush, Eason and Vinograd, 1971). The thickness of the molecule may be assumed to be twice that of the double helix, namely approximately  $54\text{\AA}$ . On geometrical considerations, a maximum number of 7 GAR molecules, each assumed to be a sphere of radius  $20.53\text{\AA}$ , could be bound round the DNA at any one point. Along a total length of DNA of approximately  $8000\text{\AA}$ , the maximum possible number of histones bound is approximately 1400 which is much higher than the number found experimentally to be bound. Again, this discrepancy could be resolved by assuming that the histone molecules lose their spherical shape on association with DNA and become more asymmetric. For simplicity, however, it was assumed that at any one point on the DNA, only one histone molecule was attached. In this model, the number of histone molecules bound can be calculated by dividing the overall length of the DNA by the diameter of the spherical histone molecule. On this basis, the number of histone molecules bound is approximately 200, which is in good agreement with the number bound found experimentally. This agreement is subject to the same reservations as those put forward in the case of models of GAR histone complexes with relaxed circular SV40 DNA. Nevertheless, despite these reservations, the proposed models of complexes, provide a reasonable basis for comparison of the hydrodynamic properties of various conformations of the model complexes with the experimentally observed properties.

One approach to the problem of identifying tentatively the shape of the nucleoprotein complex is to calculate the radius of the equivalent hydrodynamic sphere for different shapes of models of the nucleoprotein complexes and compare these radii with the experimentally observed radius of equivalent hydrodynamic sphere. One extreme model of the shape of nucleoprotein complexes is a rod-shaped particle. For valid comparison of the dimensions of the experimentally measured

complexes with those of the model structures, the dimension of the model structures must be expressed in terms of the radius of the equivalent hydrodynamic sphere. A rod-shaped model is, however, best approximated by an oblate ellipsoid. Comparison of the radius of gyration of the rod with the radius of the equivalent hydrodynamic sphere obtained experimentally is likely to be more useful. The radius of gyration of a rod is given by the equation  $R_e^2 = \frac{L^2}{12}$ , where L is the length of the rod (Tanford, 1961). Assuming the complexes of GAR-histone with both forms of SV40 DNA to be rod-shaped, the radii of gyration were calculated to be approximately  $2300\text{\AA}^0$  for complexes with relaxed circular DNA and supercoiled DNA. Allowing for the fact that the radius of gyration of a rod is likely to be larger than the radius of the equivalent hydrodynamic sphere, comparison of these values with the values of the radii of the equivalent hydrodynamic spheres obtained experimentally (Table 18), shows little agreement between observed and predicted values. It therefore appears unlikely that the GAR-histone SV40 DNA complexes exist in rod-shaped structures. Assuming the basic model of the nucleoprotein complex to be a DNA molecule with a single row of histone molecules attached, the total hydrodynamic volume of the complex can be calculated from the length of the DNA molecule and the combined width of the DNA double helix and the histone molecule. Assuming the complex to have a spherical form, the radius of the sphere having the same hydrodynamic volume as the complex may then be calculated. For complexes of GAR histone with both forms of SV40 DNA, radius of such a sphere was calculated to be approximately  $130\text{\AA}^0$ . It can be seen from Table 18, that this value is considerably less than the radius of the equivalent hydrodynamic sphere found experimentally indicating that it appears unlikely that the nucleoprotein complexes are of a spherical, compact shape. Such a conclusion is supported by the fact that the experimentally observed diffusion coefficients of the complexes (Table 18) are very small,

possibly indicating molecular asymmetry. Small diffusion coefficients are, however, a property of molecules of large molecular weight and the relative contributions of asymmetry and molecular size to the smallness of the diffusion coefficient cannot adequately be distinguished. The diffusion coefficient of relaxed circular SV40 DNA at 20°C is  $2.92 \times 10^{-8} \text{ cm}^2/\text{sec.}$  and that of closed circular SV40 DNA is  $5.35 \times 10^{-8} \text{ cm}^2/\text{sec.}$  indicating that these molecules although of the same molecular weight have different conformations, with the supercoiled SV40 DNA having the more compact shape. It can be seen that on complexing of GAR histone to supercoiled SV40 DNA the diffusion coefficient becomes slightly smaller while on the formation of complexes of GAR histones to relaxed circular SV40 DNA, the diffusion coefficient increases slightly. In general, for molecules of the same shape an increase in molecular weight tends to cause a concomitant decrease in diffusion coefficient. Nevertheless, despite the increase in molecular weight by the addition of histones to relaxed circular SV40 DNA, the diffusion coefficient of the complex is greater than that of the DNA. This could be interpreted as arising from conformational changes induced by the binding of the histones, with a relatively more compact structure being formed. For supercoiled SV40 DNA, the diffusion coefficient decreases on the binding of GAR histone. Thus the effect of increasing molecular weight cannot be distinguished from any effects of conformational changes. It should be noted that diffusion coefficients are not absolute measures of molecular asymmetry, since, by definition, they express the ratio of sedimentation coefficient to molecular weight. Thus, the large diffusion coefficient of intact SV40 virus does not imply that the virus is smaller than SV40 DNA but simply that the ratio of the sedimentation coefficient to the molecular weight is larger than that for SV40 DNA. This is supported by the fact that the intact virus is relatively compact structure, namely a sphere of diameter approximately  $500\text{\AA}$ .

## DISCUSSION

## DISCUSSION

The aim of the present studies has been to study separately the physical properties of two of the components of chromatin, namely GAR histone and DNA, and to utilize this information to investigate the nature of GAR-DNA complexes. Such complexes of GAR histone and DNA represent simplified models of mammalian chromatin which is an extremely complex aggregate of DNA, several histone and non-histone protein species and chromosomal RNA.

The importance of the role played by histones in chromatin is illustrated by their ability to repress the DNA to which they are bound in vivo (Barr and Butler, 1963; Huang and Bonner, 1962). Consequently much effort has been directed towards the elucidation of the precise molecular structure and the chemical and physical properties of this class of proteins. Unfortunately the value of much of the early work was vitiated by the fact that the histone preparations used were heterogeneous. Recently, however, preparative methods have been developed which allow the isolation in large yield of effectively, pure, homogeneous discrete histone species (DeLange et al., 1968; Starbuck et al., 1968; Mauritzen et al., 1968). The amino acid sequences of several of the histone species prepared by these methods have been elucidated and details of their secondary and tertiary structure have been obtained using physical techniques such as ORD, CD, and proton magnetic resonance (Wagner, 1970; Wagner and Spelsberg, 1971; Li, Isenberg and Johnson, 1971; Boublik, Bradbury and Crane-Robinson, 1970; Boublik, Bradbury, Crane-Robinson and Johns, 1970). One aspect of the physical properties of purified histone species which has not been investigated on a detailed quantitative basis, however, is the ability of certain histone species, particularly the arginine-rich histones, to aggregate non-covalently.

### 1. Association of GAR histone

The recent development of extensive mathematical theories for the analysis of associating systems (e.g. Adams, 1965 a, b).

1967; Elias and Bareis, 1967; Roark and Yphantis, 1970; Haschemeyer and Bowers, 1970) enables the detailed investigation of the stoichiometry of the self-association process in histone molecules, using ultracentrifugal techniques. Of the currently available mathematical techniques for the analysis of associating protein systems, the most commonly used are those which involve the evaluation of molecular weight moments from  $M_{wapp}$  vs.  $c$  data. Adams' theory (Appendix 1), which was used in the present studies on GAR histone is one such molecular weight moments method. The precision of this method depends on the reliability of the original  $M_{wapp}$  data and on the accuracy of the mathematical manipulations required to generate the molecular weight moments. The use of the photoelectric scanning system, in conjunction with the absorption optical system of the ultracentrifuge enables the simple and accurate evaluation of  $M_{wapp}$  over a large concentration range. Unfortunately, in the particular case of GAR histone, the low extinction coefficient of the protein prevented accurate measurements of molecular weights at low concentration (Figs 3 and 4 Results Section), thus reducing the accuracy of the value of  $M_1$  obtained by extrapolation to zero concentration. The minimum molecular weights of several histone fractions have, however, been estimated by several groups of workers. Hnilica (1967) obtained a value of 13,000 for the minimum molecular weight of the  $F_2A$  group of histones using sedimentation equilibrium in 5.2M guanidine hydrochloride, while Edwards and Shooter (1969b), also using 5.2M guanidine hydrochloride found that  $M_1$  of the same group of histones was 8,300. These discrepancies are hard to rationalize but it is possible that the accuracy of the values of  $M_1$  reported by Hnilica (1967) and Edwards and Shooter (1969) may be affected by the fact that in their studies no correction was made for the binding of guanidine to the protein. High concentrations of guanidine hydrochloride cause denaturation of most proteins and alter significantly their partial specific volumes, thus affecting the molecular



weights obtained by sedimentation equilibrium. In addition, since heterogeneous preparations of histones were used in both the studies of Hnilica (1967) and Edwards and Shooter (1969b), differences in preparative techniques may have caused a difference in the relative amounts of each protein component in the histone fraction.

Using N-terminal analysis, Phillips (1963) estimated the molecular weight of histone fraction  $F_2(a)$  to be in the range 9,000 - 12,500. It is interesting to note that this range encompasses the monomer molecular weight of GAR histone determined by amino acid analysis (Starbuck et al. 1968). Large variations in the estimation of the minimum molecular weights of other histone fractions have been reported. Using sedimentation equilibrium in 5.2M guanidine hydrochloride, Hnilica (1967) estimated the molecular weight of the  $F_2^b$  histone fraction to be 12,000 while Phillips (1963) obtained a value in the range 10,000 - 11,000 and Edwards and Shooter (1969b) reported a range of molecular weights in guanidine hydrochloride from 8,000 to 12,600 for the same histone fraction. Published values of  $F_1$  histone range from 8,400 to 21,000 (Ui, 1957; Trautman and Crampton, 1959; Satake, Rasmussen and Luck, 1966; Teller, Kinkade and Cole, 1965). Sedimentation equilibrium studies on  $F_1$  histone by Haydon and Peacocke (1968) indicated significant non-ideality which was postulated as explaining the inconsistencies of the previous molecular weight estimations of this class of histone. The significance of the findings of Haydon and Peacocke (1968) must, however, be considered in the light of the heterogeneity of  $F_1$  histones (Kinkade and Cole, 1966). The lack of any published values of the minimum molecular weights of pure discrete histone species justifies to some extent the use of the molecular weight based on the amino acid analysis as  $M_1$  in studies of the association of the histones. Minimum molecular weights ( $M_1$ ) calculated from amino acid analyses have been used in several studies of associating protein systems (Deonier and Williams, 1971; Albright and Williams, 1968; Kelly and Reithel, 1971).

One basic requirement of methods for the analysis of associating protein systems is the determination of the mode of association prior to the evaluation of the equilibrium constants specifying the association. In this respect, the method using molecular weight moments suffers from the disadvantage that false solutions may be obtained where the predicted curves for different modes of association intersect (Adams and Filmer, 1966). The agreement at several different concentrations, between the experimental and the predicted data for monomer-dimer association in 0.075M NaCl and for monomer-dimer-tetramer in 0.15M NaCl in the present studies on GAR histone rules out the possibility that the mode of association has been falsely assigned. In addition, the agreement of the experimental  $M_1/M_{wapp}$  curve with those generated according to the type of association and the equilibrium constants and virial coefficient involved verifies the reliability of these parameters and permits meaningful interpretation of the monomer-dimer and monomer-dimer-tetramer association of GAR histone in terms of the biological significance of the associations.

One feature of the associations of GAR histone in 0.075M NaCl/0.01M HCl and 0.15M NaCl/0.01M HCl is the relatively low value of the second virial coefficient,  $BM_1$  (0.006ml/mg and 0.004ml/mg respectively). Non-ideal effects in solutions, which are quantitated by  $BM_1$ , generally arise from one or both of two effects. The first effect and probably the less significant in studies which encompass a wide range of concentrations, is due to the steric interactions of the excluded volumes of solute macromolecules. The ideal physical behaviour, more particularly the mobility of a solute macromolecule may also be affected by ionic interactions with neighbouring macromolecules or with buffer ions. The most important of these ionic interactions with respect to the non-ideality of the solution is that due to the Donnan effect in which small buffer ions are not distributed randomly in protein solutions but associate with the protein molecules. It has been shown by Tanford (1961) that the value of  $BM_1$

calculated for spherically shaped molecules on the basis of excluded volume contributions to non-ideality alone, may be given by  $BM_1 = 4 \bar{v}$  where  $\bar{v}$  is partial specific volume. For GAR histone,  $BM_1$  on the basis of excluded volume effects would equal 0.002956ml/mg which is slightly lower than the values of  $BM_1$  found experimentally for the associations of GAR. In solutions of 0.075M NaCl/0.01M HCl and 0.15M NaCl/0.01M HCl, however, GAR histone will undoubtedly be positively charged. From the amino acid composition it appears likely that the protein will have a net positive charge of 21 at the pH of 0.01M HCl. Tanford (1961) has described a relation between  $BM_1$  and the contribution to solution non-ideality imposed by the Donnan effect which predicts a value of  $BM_1$  approximately equal to 0.01ml/mg for a protein with a net charge of 21. An overall value of approximately 0.012ml/mg might therefore be expected for  $BM_1$  of GAR histone on the basis of both excluded volume effects and Donnan effects which contrasts with the experimentally determined values of 0.006ml/mg and 0.004ml/mg for the monomer-dimer association and monomer-dimer-tetramer associations of GAR respectively. The most likely explanation of the discrepancy between the experimentally obtained value of  $BM_1$  and the calculated value due to excluded volume and Donnan effects is that at low values of  $BM_1$  the precision of the experimental value of  $BM_1$  is poor. In Fig. 6(b) of Results Section,  $M_1/M_{wapp}$  values, predicted using a range of  $BM_1$  values of monomer-dimer association with  $K_2 = 2.203\text{ml/mg}$  and, for a monomer-dimer-tetramer association with  $K_2 = 0.169\text{ml/mg}$  and  $K_4 = 1.237\text{ml/mg}$  are compared with experimentally obtained values of  $M_1/M_{wapp}$ . It can be seen that over the range of  $BM_1$  values + 0.01ml/mg to -0.01ml/mg, there is approximate agreement between experimental and predicted values of  $BM_1$ . Since excluded volume and Donnan effects both tend to make  $BM_1$  positive, models of association requiring negative values of  $BM_1$  must be considered suspect. Nevertheless, the approximate agreement of experimental and theoretical data over the range of  $0 < BM_1 < 0.01\text{ml/mg}$ .

illustrates the relatively low precision of the experimentally obtained  $BM_1$ . It is possible that the low experimental values of  $BM_1$  for the self-association of GAR compared to the calculated value may be due to the fact that the theoretical equations relating  $BM_1$  to the Donnan effects are virtually ideal expressions ignoring all electrostatic interactions other than the Donnan effect. In GAR histone, the contribution to solution non-ideality due to the Donnan effect may be small compared to that due to other types of electrostatic interaction between the protein and the buffer ions. Deonier and Williams (1971) have reported a similar discrepancy between calculated and experimental values of  $BM_1$  for the dimerization of lysozyme and have pointed out that because of the limited knowledge about  $BM_1$  in associating systems, detailed interpretation of the discrepancies must be accepted with reservation.

The success of the ideal graphical procedure of Chun and Kim (1970) in correctly identifying the modes of association of GAR histone in 0.075M NaCl/0.01M HCl and 0.15M NaCl/0.01M HCl can be attributed to the low solution non-ideality; the minor discrepancies between the predicted and experimental curves almost certainly resulting from errors introduced in the mathematical processing of the data. Chun and Kim (1970) have applied their ideal graphical procedure to the re-analysis of published data on the association of glutamate dehydrogenase (Eisenberg and Tomkins, 1968), lysozyme (Adams and Filmer, 1966), chymotrypsin (Rao and Kegeles, 1958) and confirmed the modes of association previously assigned to these associating systems, despite the fact that the early studies had indicated some non-ideality. This raises the general question of the necessity of evaluating  $BM_1$  in the analysis of associating protein systems, which is of significance since several rigorous ideal analyses (for example, the thermodynamically ideal method of Haschemeyer and Bowers (1970) describing the molecular weight distribution of an associating protein system in terms of an exponential equation) have been neglected in favour of treatments which incorporate

quantitation of non-ideal effects. Solution non-ideality due to electrostatic interaction can be minimized by carrying out the analysis at the isoelectric pH of the protein and at high salt concentrations, thus allowing in some cases, accurate application of ideal treatments. However, it is frequently of biological significance to investigate the association of proteins in other conditions. In addition, large asymmetric molecules exhibit very large non-ideal effects because of excluded volume effects. In the cases of the dimerization of myosin at high ionic strength these effects are so large as to make the detection of the association difficult (Godfrey and Harrington, 1970 a, b). Such cases necessitate the application of non-ideal treatments thus illustrating the limitations of ideal analyses. A particularly effective application of ideal analyses is the determination of the mode of association, prior to the use of more detailed non-ideal analyses (Chun and Kim, 1970).

The values of the equilibrium constants for the monomer-dimer association of GAR histone in 0.075M NaCl/0.01M HCl ( $K_2 = 2.203$  ml/mg) and for the monomer-dimer-tetramer association of GAR in 0.15M NaCl/0.01M HCl ( $K_2 = 0.169$  ml/mg,  $K_4 = 1.237$  ml/mg) indicate that the equilibrium positions of the reversibly associating systems favour the formation of higher aggregates. Ultracentrifuge studies of  $F_2A_1$  class of histones (Edwards and Shooter, 1969 a) have also indicated progressive aggregation as the salt concentration is raised above 0.05M. Qualitative assessment of the association of histones in salt conditions was obtained by Edwards and Shooter (1969 a) by measurements of the increase in sedimentation coefficients with increasing salt concentration. This approach is satisfactory for obtaining qualitative information on the effect of salt in the association of this class of histones but suffers from the drawback that in certain cases the number of discrete sedimenting peaks does not correspond to the number of aggregates formed (Gilbert 1959; Gilbert and Jenkins, 1959). Edwards and Shooter (1969 a)

evaluated molecular weights from the sedimentation coefficients of the  $F_2A$  group of histones in increasing salt conditions using the diffusion coefficient and the Svedberg equation (Svedberg and Pedersen, 1940). Molecular weights calculated in this manner are smaller than the weight average molecular weight and corresponds to the mean molecular weight of the major component present (Pain, 1965). The heterogeneity of the  $F_2A_1$  group of histones, which is strikingly illustrated by chromatography on Sephadex G100 (Fig. 1(a)) of Results Section, is likely to detract from the value of this approach. Nevertheless, the results of Edwards and Shooter (1969 a) confirm the general effect of salt on the association of GAR histone detected in the present studies. Edwards and Shooter (1969b) have carried out similar analyses on the slightly lysine rich group of histones  $F_2b$ , using the Svedberg equation and the Archibald (1947) method for the determination of molecular weights. From their molecular weight data on histone fraction  $F_2b$ , Edwards and Shooter (1969b) postulated that the extent of aggregation of this histone fraction was greater than that of the  $F_2A$  histone fraction at similar salt concentrations. On the basis of their molecular weight measurements, Edwards and Shooter (1969b) suggested that histone fraction  $F_2b$  existed in an unaggregated state at 0.01M NaCl, as aggregates of, on average, 3 molecules in 0.10M NaCl and of about ten molecules in 1.0M NaCl. These estimates were obtained by considering the weight average molecular weight as a multiple of the monomer molecular weight and therefore suggest that the equilibrium position of the association lies far to the right. It is possible, however, that the measured  $M_{wapp}$  values correspond to intermolecular aggregates formed by inter-association of discrete protein species in the heterogeneous histone fraction.

Detailed analyses of associating protein systems not only permit identification of the mode of the association but also allow evaluation of thermodynamic parameters characterizing the association. Of these parameters probably the most useful is the free energy change of the reaction,  $\Delta G$ , which is a direct measure of the affinity of the

reactants (Moore, 1962). The negative values for  $\Delta G$  of -5.861K cal/mole for the dimerization of GAR in 0.075M NaCl/0.01M HCl and of -5.47K cal/mole and -5.52K cal/mole for the monomer-dimer and dimer-tetramer equilibria respectively of GAR in 0.15M NaCl/0.01M HCl, reflect the extent to which these equilibria lie in favour of the formation of complexes. The overall free energy change of any reaction can be considered as the sum of contributions from different physical and chemical features of the reaction. Tanford (1964) has pointed out that in the case of protein association, these contributions include the intrinsic free energy of dissociation (which is what  $\Delta G$  would be if there were no non-covalent interactions between the protein molecules or between the protein molecules and the solvent), and also the effect of non-covalent interactions such as hydrogen-bonding and hydrophobic bonding. Finally there is the electrostatic free energy term, which reflects interaction between charges. The electrostatic free energy term may be calculated on a theoretical basis using the Debye-Huckel theory (Tanford, 1961) or by using the theory of Verwey and Overbeek (1948) to calculate the surface potential of a charged sphere. Kelly and Reithel (1971) have used both approaches in their study of the dimerization of lactoglobulin and obtained similar results from both methods. In the present studies lack of knowledge of the dielectric constants of the particular solvents used prevented detailed calculations by any of the above theories of the electrostatic free energy of GAR and aggregates of GAR. However, the fact that under the experimental conditions used GAR histone almost certainly carries a large positive charge suggests that there will be a large electrostatic repulsion between GAR molecules, that is, the electrostatic free energy will be large and positive. To yield experimental values of  $\Delta G$  of approximately -6K cal/mole, it is apparent that there must exist some powerful compensatory attractive force ( $\Delta G$  of attraction large and negative). The amino acid sequence of GAR histone reveals that the hydrophobic residues in the protein occur in clusters, suggesting that the formation

of strong hydrophobic bonds from the 'salting out' of these clusters provides the significant attractive forces necessary to overcome electrostatic repulsion (Ogawa et al. 1968; DeLange et al. 1968). Since aggregation increases with salt concentration it appears unlikely that hydrogen bonding could carry out this function. The implication of hydrophobic bonding in the aggregation of GAR histone has been confirmed by the proton magnetic resonance studies of Boublik, Bradbury, and Crane-Robinson (1970). Using the amino acid sequence of GAR, Boublik et al. (1970) were able to identify parts of the proton magnetic resonance spectrum with the hydrophobic segments of the polypeptide chain and were thus able to detect the formation of hydrophobic bonds under conditions in which Edwards and Shooter (1969b) had demonstrated qualitatively the aggregation of the  $F_2A_1$  group of histones.

Gel-filtration analysis of the association of GAR in 0.15M NaCl/0.01M HCl by the method of Chun et al. (1969) indicated that the tetramer formed in such circumstances had a compact shape, similar to a tetrahedron. A possible source of error in the Chun et al. (1969) theory is the fact that it considers only ideal solutions. The small extent of non-ideality of these associations as indicated by the ultracentrifugal studies makes it unlikely, however, that this factor will affect seriously the validity of the analysis. It should be noted that in the present studies only two models of molecular shape were used in the gel-filtration analysis, namely compact and linear aggregation. The experimental data were found to fit best the theoretical data predicted for compact aggregation but it is possible that other models may provide closer fits with the experimental data. Alternative models of molecular shape intermediate between linear aggregation and compact aggregation, for example a linear trio of monomer units with a fourth monomer unit attached laterally to the other three, could be tested by the theory of Chun et al. (1969) if geometrical expressions were available to enable calculation of the molecular sieve coefficient ( $\sigma_i$ ) of aggregates. At



present, such expressions are available only for linear and compact aggregation. Calculation of the shape of a complex from the dimensions and juxta position of its constituent monomer species is a relatively simple problem of three-dimensional geometry but in practice it is unlikely that a protein complex will be accurately described by models of the complex which assume that the monomer units associate as discrete entities like a cluster of billiard balls. The formation of hydrophobic bonds between molecules of GAR histone, which are probably the most important forces maintaining the structure of the complex, would involve the aggregation of the hydrophobic segments of the molecules in a central compact core from which the rest of each molecule, that is the polar parts, would radiate outwards. The proton magnetic resonance studies of Boublik et al. (1970) implicate such a model in the association of GAR. Edwards and Shooter (1970) have used gel-filtration to study the shape of complexes of the  $F_2^b$  class of histones and found that the Stokes radius only increased slightly with increasing salt concentration, indicating that aggregation occurs with the formation of a compact complex. In their studies, they used small sample volumes which do not give rise to concentration-independent plateau regions in the elution profile. Such experiments are directly analogous to sedimentation velocity experiments and suffer from the drawback that each molecular aggregate will only be characterized by a unique peak if the association is irreversible, that is if the complex can exist independently. The heterogeneity of the histone fractions studied by Edwards and Shooter (1970) and Boublik et al. (1970) may also be potential sources of error in their studies. Nevertheless, it appears reasonable to conclude that these two histone fractions aggregate by the formation of a compact hydrophobic core with polar residues radiating outwards. This finding raises the possibility that such behaviour is common to all histone fractions, since all the histones whose amino-acid sequences have so far been studied possess irregularly-spaced clusters of hydrophobic residues. (Bustin et al. 1969; Iwai et al., 1970;

DeLange et al. 1968; Wilson et al., 1970). Indeed, it is possible that the strict evolutionary conservation of amino acid sequence in histones from different source materials is a consequence of the important biological significance of the irregularly-spaced clusters of hydrophobic residues, for example their role in the formation of aggregates. The studies of Haydon and Peacocke (1968) on the very lysine rich fraction of histone ( $F_1$ ) lessen this possibility. They showed that even at high salt concentrations this heterogeneous class of histones did not aggregate. Studies of the amino acid sequence of this class of histone have indicated the presence of clusters of hydrophobic and basic residues (Bustin et al. 1969). Apparently, hydrophobic bonding between these clusters to form aggregates of the histone does not occur in this histone fraction.

An increase in pH might be expected to affect the aggregation of GAR histone by decreasing the net charge on the molecule, thereby diminishing electrostatic repulsion between the molecules and so increasing the extent of aggregation. The present studies indicate that under the same salt conditions GAR histone undergoes the same mode of association at pH 5.0 and 7.0 as it does in 0.01M HCl. The equilibrium constants of the association at pH 5.0 and 7.0 were not measured but it is possible that they are significantly altered. A possible explanation for the lack of a pH effect on the association of GAR histone is that the repulsive ionic charge effects involved in the association process are of less significance than the attractive non-covalent forces. In view of the large magnitude of the positive charges on GAR histone at pH  $\leq$  7.0 this explanation seems unlikely. The lack of a pH effect has been confirmed by the sedimentation velocity studies of Edwards and Shooter (1969a) but Boublik et al. (1970) have interpreted their X-ray data on  $F_2A$  histones at pH 7.0 as indicating the existence of higher aggregates than at lower pH's. Both these studies are subject to the limitations imposed by the fact that heterogeneous fractions have been used.

The ORD studies confirm the previously reported low helicity of histones (Wagner, 1970). The association of GAR histone might be expected to be accompanied by changes in the secondary structure of the protein. Within the experimental accuracy, however, no significant change is observed in the helix content of GAR in 0.01M HCl as the salt concentration is increased from zero to 0.15M NaCl. In the light of the probable involvement of hydrophobic forces in the self-association of GAR histone it is significant that the  $A_{193}$  and  $A_{225}$  coefficients of the Schechter-Blout analysis are markedly different, suggesting the presence of structures other than  $\alpha$ -helix and random coil.

## 2. Analysis of C. T. DNA-GAR histone complexes

The thermal denaturation studies (Fig. 18, Results Section) of complexes formed between C. T. DNA and GAR in the monomer state and GAR in a monomer-dimer equilibrium reveal that the melting temperature corresponding to the complexes appears to be unaffected by the state of aggregation of the histone molecule, suggesting that the interaction of GAR histone with DNA may be independent of its aggregation state. The experimental data, however, are of limited precision, because of the high melting temperature of the nucleoprotein complex. Detailed study of the thermal denaturation of nucleoprotein complexes by Ansevin and Brown (1971) indicated that analysis of the first derivative curve can allow detection of small melting transitions which are difficult to identify in the absorbance melting profile. The experimental data of the present studies are not of high enough accuracy to warrant such a procedure. Smart and Bonner (1971) have pointed out that it may not be possible to relate in a simple manner the extent of stabilization by histones of the DNA double helix, as indicated by thermal denaturation studies, to the extent of transcription of DNA in the complex by RNA polymerase. It is possible that the histones prevent separation of the two polynucleotide chains of the DNA while the conformation of the nucleoprotein complex may be such that the

transcription of the genome by RNA polymerase is permitted. Accepting this reservation about the relevance of thermal denaturation studies to the biological function of nucleoprotein complexes, such studies can nevertheless provide useful information on the mechanisms of the binding of histone to DNA. In general, the biphasic nature of the absorbance melting profiles of nucleoprotein complexes has been taken as an indication that the binding of histones to DNA is co-operative, that is, the binding of one histone to a segment of the DNA facilitates the binding of a second histone at a site adjacent to the first histone molecule, in preference to another site on a different DNA molecule (Olins, 1969; Smart and Bonner, 1971). If the histone molecules were to bind to the DNA by a completely random process then it might be expected that the thermal denaturation profile of the nucleoprotein complex would be represented by a continuously rising monophasic curve. While the detailed analyses of Ansevin and Brown (1971) suggest that the biphasic melting profiles of nucleoprotein complexes may in fact be composed of several small transitions, most thermal denaturation studies have shown the melting profile of nucleoprotein complexes to be biphasic, the two transitions being taken to represent the melting of free DNA and of DNA completely complexed with histones, respectively. Accepting the biphasic nature of the melting curves of nucleoprotein complexes as indicating co-operativity of binding, the question is raised as to what chemical forces enable histones to bind to DNA at sites adjacent to other histone molecules in preference to other regions of free DNA. One explanation is that the initial binding of one histone molecule to a DNA strand alters the conformation of the DNA such that the chemical forces causing other histone molecules to bind are magnified. Circumstantial evidence for such a mechanism is provided by ORD and CD studies of nucleoprotein complexes which indicate that the normal B structure of DNA in solution is altered to the C structure when proteins are bound (Fasman et al., 1970; Simpson and Sober, 1970; Wagner, 1970; Shih and Fasman, 1970). However,

it is difficult to distinguish between the two possibilities that such conformational changes in the DNA cause the binding of histones or, as is more likely, such conformational changes result from the binding of histones. Analysis of the mechanism of the binding of histones to DNA is further complicated by the fact that currently much of the experimental data on nucleoprotein complexes is derived from studies in which heterogeneous DNA's of high molecular weight are used. The heterogeneity with respect to sedimentation coefficient and molecular weight of the C. T. DNA used in the present studies is demonstrated by the asymmetric  $g(s)$  distributions of Fig. 19(a) and (b) (Results Section). This heterogeneity in the C. T. DNA preparation can account for the biphasic melting profiles of C. T. DNA-histone complexes in that certain species of the heterogeneous DNA population may be completely bound with histone, while others are completely free. This concept of molecules of DNA being either completely free of histone or completely bound with histone seems reasonable since it is unlikely, but certainly not impossible, that an individual DNA molecule contains regions which are completely bound with histone with other regions of the same molecule devoid of histones. However, in the present studies it was observed that in the melting profile of nucleoprotein complexes, the first-step transition, attributed to the melting of unbound DNA, is in fact more diffuse and occurs at a higher temperature than the transition due to the melting of preparations of DNA alone. This observation, also reported by Ansevin and Brown (1971), Shih and Bonner (1970) and Olins (1969), could be a result of the slightly greater energy required to melt regions of unbound DNA which are adjacent to regions on the same molecule which are completely bound with histones.

Clark and Felsenfeld (1971) have recently reported studies in which chromatin was titrated with deoxyribonuclease, the rationale behind the experiments being that only regions of DNA uncomplexed with chromosomal proteins will be affected by the nuclease, while regions of DNA covered by proteins will be unaffected. From their studies,

it was deduced that as much as one half of the total DNA in their preparations of chromatin was not complexed with proteins. Studies of the binding of histone to DNA must therefore be considered in the light of the possibility that only parts of the DNA molecule are complexed with protein.

The problem of analyzing heterogeneous populations of DNA preparations also makes interpretation of the sedimentation studies of C. T. DNA-GAR histone complexes difficult (Figs. 22 and 23). The heterogeneity with respect to sedimentation coefficient of GAR histone-C. T. DNA complexes, encompassing the range of sedimentation coefficients of the DNA alone, makes it difficult to determine whether any species of DNA is completely devoid of histones. The observation that the  $g(s)$  distribution of sedimentation coefficients for the nucleoprotein complexes, encompasses the range of the  $g(s)$  distribution for DNA alone, allows the possibility of certain DNA species being completely devoid of histone. Comparison of the  $g(s)$  distribution of sedimentation coefficients of complexes prepared at different pH and also by both the salt gradient dialysis method and the method of direct addition suggests that no significant changes in the sedimentation properties of complexes results from such variations in the methods and conditions of preparation of the nucleoprotein complexes. This conclusion contrasts with the findings of Olins and Olins (1971) who showed that the structure, as visualized in the electron microscope, of complexes of the  $F_2A_1$  class of histones with T7 DNA prepared by the salt gradient dialysis method in the presence of urea differed from that of complexes prepared by the same method in the presence of guanidine hydrochloride. Complexes prepared by salt dialysis in the presence of urea sedimented as a single heterogeneous component and resembled rosette-like structure in the electron microscope; complexes from guanidine-salt dialysis revealed the presence of toroidal 'dough-nut' structures. On the basis of these electron microscope studies, it appears from the work of Olins and Olins (1971) that the conditions

of formation of the complexes affect the shape of the complexes formed. They concluded that the shape of nucleoprotein complexes was dependent on the extent to which the conformation of the protein was rendered more 'open' by the denaturing agent used in the preparation of the analyses, that is, to the extent of the denaturation of the tertiary structure of the protein.

One aim of the present studies has been to determine whether the state of aggregation of GAR histone from calf thymus affects its binding to calf thymus DNA. In 0.075M NaCl and 0.15M NaCl, pH 5.0, that is in conditions in which GAR histone probably exists in monomer-dimer and monomer-dimer-tetramer equilibria respectively, complexes of GAR histone with C. T. DNA exhibited the same distribution of sedimentation coefficients. Because of the heterogeneity of the complexes the conclusion cannot be drawn from these findings that the nature of the complex is unaffected by the state of aggregation of the histone, since similar overall sedimentation distribution patterns may be obtained for two populations of sedimenting macromolecules of different structure. For example, a particle sedimenting with a given sedimentation coefficient could consist of a relatively large molecule of DNA with only a small number of histones bound or could consist of a relatively small length of DNA with a large number of histone molecules bound. However, in 0.4M NaCl, pH 5.0, a  $g(s)$  distribution of sedimentation coefficients was obtained which showed a greater proportion of sedimenting species with higher sedimentation coefficients than in 0.15M NaCl or 0.075M NaCl. It is possible that this is due to the aggregation of GAR in 0.4M NaCl affecting the binding of the histone to the DNA in such a way as to produce complexes of relatively high sedimentation coefficients. Edwards and Shooter (1969a) have shown that in 0.4M NaCl the  $F_2A_1$  group of histones exists in a more aggregated state than at lower salt concentrations. Histones bind to DNA because of direct electrostatic interaction between the basic groups of the histone molecule and the negatively-charged phosphate backbone of DNA. The strength of this binding is indicated by the high salt concentrations needed to dissociate

histones from DNA (Murray et al. 1970). Because of the high strength of the DNA-histone ionic interactions, it might be expected that these attractive forces would 'overwhelm' the forces which cause histones to aggregate, so that histones are bound to DNA in a manner irrespective of their association state. The present studies have shown that tetramers of GAR histone probably exist in a compact form, and it has been postulated that such aggregation arises because of interactions between regions of hydrophobic residues in the histone forming an aggregate with a compact hydrophobic core from which polar residues of the histone molecules extend outwards. Although the experimental observations leading to this conclusion about the nature of the aggregation of GAR histone were not extended in the present studies to the higher salt concentration of 0.4M NaCl, it is likely that the same basic mechanism of aggregation applies at this salt concentration. With this form of aggregation of histones, it is likely that the external basically charged regions of the compact aggregate will bind to the phosphate residues of the DNA, so that the histone aggregate as a whole will attach itself to the DNA. With the form of histone aggregation described above, it appears less likely that the strong electrostatic forces binding the histone to the DNA will tend to dissociate an individual histone molecule from a compact aggregate and bind histones as single molecules. It is interesting to note that in an electron microscope study of the association of DNA polymerase with DNA, Griffith, Huberman and Kornberg (1971) observed that the enzyme was bound to the DNA in the dimer state rather than as individual monomer units, despite the fact that the bonds between the two monomer units of the enzyme were so flexible as to permit several configurations of the enzyme being bound to DNA. The experimental observation that complexes of GAR histone and C. T. DNA exhibited a different distribution of sedimentation coefficients in 0.4M NaCl than those in 0.15M NaCl and 0.075M NaCl, in which the GAR histone is in a less aggregated form, may be interpreted as confirmation of the above speculation regarding the binding of aggregates of histones to DNA. However, it is equally possible that the observed  $g(s)$



distribution for GAR histone-DNA complexes in 0.4M NaCl could result from the aggregation of the nucleoprotein complexes themselves. Little is known about the nature of nucleoprotein complexes which could justify valid predictions concerning their aggregation properties. Indeed it is possible that the experimentally observed heterogeneity of GAR histone-C. T. DNA complexes in 0.075M NaCl, 0.15M NaCl and 0.4M NaCl could result from random aggregation of nucleoprotein complexes which contain a constant number of histone molecules bound per unit length of DNA.

Since in the present studies, the heterogeneity of the complex formed by addition of small amounts of GAR histone to excess amounts of C. T. DNA prevented the measurement of the concentration of unbound DNA, evaluation of the stoichiometry of the complex could not be carried out. Instead, the less satisfactory system of small amounts of C. T. DNA added to excess amounts of histone was used for this purpose. The sedimentation experiments described in the Results Section using complexes of C. T. DNA with GAR histone and complexes of GAR with SV40 DNA are analogous to equilibrium dialysis methods for the evaluation of the stoichiometry of complexes of small molecules with macromolecules. One basic assumption in the theory of equilibrium dialysis methods is that the small molecule is univalent, that is, combines with only one molecule of the larger species, while the larger molecule can bind many of the smaller molecules. In conditions of excess histone, where precipitation of DNA occurs, it is possible that each histone molecule is in contact with and bound to several different DNA molecules. In addition, the physical formation of a precipitate may entrap otherwise unbound histone molecules leading on sedimentation, to erroneously high amounts of histones apparently bound to DNA in these conditions. The number of histone molecules bound to DNA must therefore be considered in the light of these possible sources of errors. A more serious obstacle to the meaningful interpretation of these results is, however, the heterogeneity of the complex. The stoichiometry of the formation of the complex in these studies was evaluated simply by measuring the amount of histone removed by

combination with a known amount of DNA. To express these amounts on a mole for mole basis the molecular weight of the DNA was taken as the weight average molecular weight of the heterogeneous population of DNA species, namely,  $8.2 \times 10^6$  daltons. The number of histone molecules bound must therefore be considered as relative to a molecule of DNA of this molecular weight. The heterogeneous nature of C. T. DNA makes it difficult to determine whether only certain sequences of C. T. DNA molecules are able to bind GAR histone, or whether some DNA molecules are capable of being entirely bound with histone molecules while other DNA molecules bind no histone at all. The weight average molecular weight of C. T. DNA was taken as representative of the population of DNA species of different lengths, and the concentration of DNA bound to the histone was expressed on a moles basis using this value of the molecular weight of the DNA. However, no one value of molecular weight adequately describes the heterogeneous population of DNA species. For this reason, it is possible that DNA molecules of molecular weight  $8.2 \times 10^6$  daltons do not bind any histone molecules, although the experimentally obtained numbers of histone molecules bound are expressed per DNA molecule of this molecular weight. Because of these problems of heterogeneity of the C. T. DNA, interpretation of the results of binding studies are limited to comparison of the relative number of GAR histone molecules bound in different conditions. Of these results, it is significant that in 0.4M NaCl the number of GAR histone molecules bound per DNA molecule of molecular weight  $8.2 \times 10^6$  is considerably less than those bound in 0.075M NaCl and 0.15M NaCl, although the g(s) distribution of sedimentation coefficients of complexes formed in 0.4M NaCl shows a greater preponderance of species of larger sedimentation coefficients. As salt concentration is increased, several effects influence the properties of nucleohistone complexes and their component molecular species. Arginine-rich histones aggregate in high salt conditions while proteins in general tend to be dissociated from nucleoprotein complexes as the salt concentration is increased. For GAR histone,

salt concentrations greater than 0.4M are required for dissociation from DNA complexes (Murray et al., 1970; Georgiev, Ananieva, Kozlov, (1966)). The relatively small number of histone molecules bound in 0.4M NaCl cannot therefore be totally attributed to dissociation from the nucleoprotein complex. The state of aggregation of GAR histone is unknown in 0.4M NaCl, but is likely to be considerable. This raises the question of whether it is valid to calculate the number of moles of histone molecules bound using a value of 10,600, the monomer molecular weight of GAR, when in 0.4M NaCl GAR histone probably exists in a more aggregated state. Since the use of a higher molecular weight would result in an apparently lower number of histone molecules bound, the relatively low number of histone molecules bound in 0.4M NaCl cannot be completely accounted for by the use of a molecular weight which was not representative of GAR histone. One possible explanation is that although GAR histone is not entirely dissociated from chromatin at 0.4M NaCl, nevertheless it is possible that some molecules may be.

The difficulties of interpretation of these results are the primary justification for using the biologically heterologous system of SV40 DNA and GAR histone from calf thymus. Prior to a discussion on the significance of the data obtained on the binding of GAR histone to the homogeneous forms of SV40 DNA, it may be considered relevant to discuss briefly the biological implications of the present studies of the aggregation of GAR histone and of its binding to C. T. DNA. The small number of discrete histone species isolated from mammalian chromatin makes it unlikely that individual histones specifically repress certain genes and it has been suggested that the multiplicity and specificity required of specific genetic repressors might be conferred on histones by self-aggregation (Stellwagen and Cole, 1969). At physico-chemical salt concentrations, the extent of association of GAR histone is limited to tetramer formation and it appears in the case of this histone at least that the multiplicity conferred on histones as a result of aggregation processes is so limited as to make it unlikely that the

histone acts as a specific repressor of genes. Proposed models of gene function suggest that the portion of the mammalian genome which is never transcribed in vivo is covered by a number of histone molecules which do not readily dissociate from the DNA of the genome, while the smaller portion of the genome which is selectively transcribed in vivo is bound with non-histone proteins which can bind to or dissociate from the DNA according to whether the specific genes which are masked by the non-histone molecules require to be expressed or repressed. Circumstantial evidence in support of this model is provided by the strength of the ionic interactions between histones and DNA. Histones require salt at higher than physiological concentration to dissociate them from the DNA (Murray et al., 1970; Georgiev, Ananieva, Kozlov, (1966)). In the light of this, it seems unlikely that histones bind reversibly to regions of the DNA, but rather that histones are passive, unselective repressors which are rarely if at all removed from the DNA. Lewin (1970) has, however, suggested that although histone molecules seem unlikely to attach to or dissociate from segments of DNA according to whether the DNA should be repressed or not, nevertheless repression or expression of the DNA could be achieved by modification of the structure of the attached histone molecules to prevent or allow the attachment of RNA polymerase molecules to the genome. In particular, Lewin (1970) implicated hydrogen bonds as the means whereby the conformation of histones may be altered to allow transcription of the genome, suggesting that the histone molecules while always attached to the DNA, could swivel outwards allowing the attachment of RNA polymerase to the DNA. No direct experimental evidence has been reported in support of such an hypothesis. In the light of the possibility that histones are relatively unspecific repressors, permanently attached to DNA it seems strange that histones isolated from widely varying sources have very similar sequences, suggesting that even minor modification of histone structure interferes with the normal biological function of the molecules. Also, in the light of the rather limited degree of self association of GAR histone, which makes

it improbable that the multiplicity and selectivity required of genetic repressors is conferred on histones by aggregation processes, the biological significance, if any, of the aggregation process remains unclear. Possible explanations of the exceptional evolutionary conservation of the sequence of histones and of the aggregation of certain histone species may be that these properties of histones are required for the maintenance of chromosomal structure or the formation in vivo of compact chromosomes from relatively diffuse interphase chromatin.

The work reported in these studies concerns only one species of histone. In vivo, however, mammalian DNA's are found complexes with several discrete species of histone. The respective roles of each discrete histone species in maintaining chromosomal structure or possibly in specifically repressing portions of the mammalian genome are therefore of interest biologically. In this respect, Wagner and Spelsberg (1971) have recently shown that when GAR histone is removed from chromatin, the conformation of DNA, as indicated by the C.D. spectrum, is significantly altered. They have correlated this change in conformation of DNA with the template activity of the chromatin and therefore deduce that the binding of GAR histone to DNA induces specific conformational changes in the DNA which result in specific template properties. In contrast, however, Li, Isenberg and Johnson (1971) have found that when GAR is complexed to DNA by salt-gradient dialysis the C.D. spectrum of the DNA remains almost identical to that of free DNA, suggesting that GAR histone does not play a major role in inducing specific conformations of the DNA. In another recent study of the complexing of GAR to C. T. DNA using C. D., Shih and Fasman (1971) reported that both the structures of DNA and GAR appeared to be altered on complex formation, with the structure of the histone in the complex dependent on its binding to DNA, and independent of the ionic strength in which the complex is formed.

### 3. Analysis of SV40 DNA-GAR complexes

The heterogeneity of C. T. DNA prevented detailed interpretation of the experimental data concerning GAR histone-C. T. DNA complexes. Both the nicked circular and supercoiled forms of SV40 DNA were therefore used as a source of homogeneous DNA

It was considered that the homogeneity of the SV40 DNA which permitted more detailed analysis of GAR-DNA complexes than in the case of the GAR histone-C. T. DNA system, justified the use of this biologically heterologous system. The interaction of histones with DNA is generally considered as one of low specificity and on this basis it seems unlikely that the properties of GAR histone-SV40 DNA complexes will be so unique as to prevent conclusions being drawn regarding the general nature of the binding of GAR histone to DNA molecules. However, SV40 DNA molecules are circular and this may impose special restrictions on the binding of histones to SV40 DNA.

As well as being a convenient system for the detailed analysis of histone-DNA interaction, the interaction of GAR histone with SV40 DNA may also serve as a model system for the study of the interaction of SV40 DNA with basic viral proteins. In this respect it is of interest to compare studies of the binding of SV40 virus core proteins to SV40 DNA with the present studies of the binding of histones to SV40 DNA. (Anderer, Koch and Schlumberger, 1968). In a recent study, Estes, Huang and Pagano, (1971) have estimated that a total number of 194 protein molecules of molecular weight equivalent to those of histone molecules are bound to super-coiled closed circular SV40 DNA. They also suggest, however, that an additional 80 protein molecules of molecular weight of approximately 23,000 daltons, may be bound to the DNA. The advantage of using both forms of SV40 DNA in the study of the binding of GAR histone is illustrated by the fact that on addition of GAR histone to excess DNA, the sedimenting boundary due to the excess unbound DNA could be distinguished from that due to the nucleohistone complex. Thus studies of GAR histone-SV40 DNA interaction were possible in conditions of low histone to DNA ratios, that is in conditions where precipitation of DNA by the histone molecules is unlikely. In addition very low concentrations of added GAR histone were possible since the

extremely high extinction coefficient of the DNA compared to the histone enabled quantitation of the amount of DNA bound to low concentrations of GAR histone. The fact that separate boundaries could be detected for complex and for unbound DNA suggested that the binding process was not a random one which might be expected to form a heterogeneous distribution of DNA molecules with varying amounts of histone molecules bound, ranging from effectively no histone molecules bound to a situation of complete saturation. This conclusion is confirmed by examination of the relative number of histone molecules bound per DNA molecule as a function of added histone concentration. In conditions of excess DNA, the constant number of histone molecules bound at higher concentrations of added GAR clearly suggests co-operativity, since a random process of binding would be expected to give rise to a heterogeneous population of nucleohistone molecules. It is interesting to note that both forms of SV40 DNA exhibited co-operativity in the binding of GAR histone, despite the fact that supercoiled closed circular SV40 DNA has a much more compact tightly wound structure. This raises the question of the nature of the chemical interactions which result in co-operativity, that is the question of what properties are endowed on a nucleoprotein complex by the attachment of the first GAR histone molecule which result in other histone molecules being subsequently bound to the same DNA molecule rather than to another completely unbound DNA molecule. One possible explanation to account for this co-operative effect is that the binding of the first molecule of GAR histone to DNA induces a conformational change in either or both of the histone or DNA molecule causing the exposure of powerful attractive forces which will preferentially bind subsequent GAR molecules. Such conformational changes in the DNA molecules must be possible in both supercoiled circular DNA and in relaxed circular DNA, since both molecules exhibit the co-operative binding effect. On the face of it, the limitations imposed by the tightly wound structure of closed

circular DNA seem to suggest that conformational changes of the type described above in this DNA molecule are unlikely. Changes in the conformation of the histone moiety of the nucleoprotein complex seem therefore more likely to produce the forces which cause co-operativity of binding. Evidence for conformational changes in histone molecules on binding to DNA has been reported by Wagner (1970) and Simpson and Sober (1970) using C. D. techniques. The changes of conformation of histone molecules on binding to DNA have generally been interpreted as being an increase in the helix content of the histone molecule. It is difficult to visualize exactly how an increase in helicity of histones bound to a DNA molecule could induce the preferential binding of subsequent histone molecules to the same DNA molecule but it is possible that hydrophobic forces of the same type as those implicated in the present studies in the aggregation of histones are involved. The above discussion of the changes in conformation of histone molecules causing co-operative binding of histones to DNA is purely speculative and it is possible that changes in the conformation of DNA, which are sterically possible in both supercoiled and relaxed circular SV40 DNA molecules, cause the co-operative effect. In view of the large differences in conformation of relaxed circular DNA and nicked circular DNA it is of interest that the former appears to bind approximately twice as many histone molecules as the latter type of DNA. These findings could result from a decrease in the negatively charged surface area in supercoiled SV40 DNA or from conformational restrictions imposed on the binding by the shape of the supercoiled SV40 DNA. Also of interest in the experimental data on the binding of GAR histone to SV40 DNA is the observation that at very low concentrations of added histone, the number of histones bound per DNA molecule is lower than the number bound at higher concentrations of added histone and that the sedimentation coefficient of nucleohistone complexes formed at low added histone concentrations is smaller than those of complexes formed at higher added GAR concentrations. In conditions of low



concentrations of added GAR, it therefore appears that each DNA molecule is not saturated with histone molecule. This can be rationalized with the earlier observation that the binding of histones was a co-operative effect by postulating that the addition of GAR histone to the DNA at low concentrations of added GAR still caused conformational changes which normally would result in more GAR histone molecules being bound to the same DNA molecule. In these conditions of low added histone concentrations, it is possible that no histone molecules were present in the local environment of the nucleoprotein complexes thus subsequent histone molecules could not be bound to the original DNA-histone complex so that DNA molecule remains less than completely saturated with histone molecules. In such conditions it would be interesting to study the distribution of sedimentation coefficients of the nucleoprotein complexes since it might be expected that the number of histone molecules bound per DNA molecule would vary randomly since the number bound would only be dependent on the number of histone molecules that happened to be in the local vicinity of the DNA molecule. The small size of the sedimenting boundary corresponding to the complex precluded the accurate application of a  $g(s)$  analysis. The above explanation of the binding of GAR histone to both forms of SV40 DNA at low concentrations of added GAR must, however, be considered with the fact that even at higher concentrations of added GAR, DNA is in excess and thus in the local environment of some DNA molecules there is effectively zero concentration of unbound GAR histone. It might then be expected that such DNA molecules, having already co-operatively bound some GAR histone molecules, would be unable to bind more. A heterogeneous population of nucleohistone complexes of varying histone content would therefore be formed. Thus the number of histone molecules quoted as bound per DNA molecule might only be an average value representing the mean number of histones bound per DNA molecule in a population which

comprises nucleohistone complexes with histone contents varying from effectively zero to a number greater than the mean value of histones bound. The approximate constancy of sedimentation coefficients of the nucleoprotein complex precludes this possibility and verifies that the number of histones bound per DNA molecule probably represents the number of histones required to saturate each form of DNA molecule. On the basis of the above discussion it seems difficult to rationalize the apparently inconsistent mode of binding of GAR histone to SV40 DNA at both low and high concentrations of added histone. In fact, the answer to the apparent paradox may be supplied by considering the concentration of added histone as an absolute amount and note as an amount relative to the amount of DNA, since in these experiments DNA is always in excess. Thus a DNA molecule with a histone molecule already bound will only be able to bind a second histone molecule if the concentration of histones in the solution is high enough to allow the forces causing co-operative binding to interact with a second molecule, irrespective of the presence or absence of other DNA molecules with or without histone molecules already bound. In such a process, the nucleation step, that is the binding of the first molecule of GAR to the DNA is obviously important. The mechanisms whereby a particular DNA molecule, among a population of many identical DNA molecules, can bind a histone molecule, thus subsequently binding several more histone molecules in a co-operative manner, remains unclear. One possibility is that the original binding of the first histone molecule is a relatively slow process while the subsequent binding of other histone molecules to a DNA molecule with the first histone already attached is relatively much faster. In this way histone molecules can completely bind to one DNA molecule with one histone already attached, before a second DNA molecule has bound its first histone molecule.

All of the above discussion concerning the binding of GAR histone must be considered in the light of the possibility that only part

of the DNA is complexed with protein as indicated in the studies on mammalian chromatin of Clark and Felsenfeld (1971). The conclusions regarding co-operativity of binding of histones to DNA remain valid, however, even if the DNA is only covered in part by histones. The present results do not allow estimation of the extent of the coverage of the DNA by histone.

Comparison of the  $g(s)$  distributions of the nucleoprotein complexes reveal that for complexes with both forms of SV40 DNA, the  $g(s)$  maxima occur at slightly greater sedimentation coefficients in 0.15M NaCl than in 0.075M NaCl. As in the case of C. T. DNA, this raises the question of whether the increase in sedimentation coefficient in higher salt concentrations is due to aggregation of the nucleoprotein complexes themselves or to the binding of histones in different aggregation states. Allied to this problem is the question of whether the number of histones bound should be calculated in both salt conditions using a histone molecular weight of 10,600, since the experimental studies on the association of GAR indicated that in 0.075M NaCl the protein was in a monomer-dimer equilibrium and in a monomer-dimer-tetramer equilibrium in 0.15M NaCl. Although these equilibria were found to lie to the right, it should be noted that the histone molecule does not exist solely as a dimer or tetramer respectively in these conditions. They are in an equilibrium state. If the histones existed as dimer or tetramer species which could be physically isolated, then  $M_{wapp}$  vs.  $c$  curves would be horizontal lines at around 20,000 daltons and 40,000 daltons, with perhaps some dissociation at lower concentrations. To some extent this justifies the use of 10,600 as the molecular weight of GAR histone in the calculation of histone bound. It should be noted that the observations on co-operative binding are not affected by the molecular weight of histone used to calculate the number of histones bound. The relative number of histones bound to supercoiled and relaxed circular SV40 DNA is also independent of the molecular weight of histone used. Indeed, even the models of nucleoprotein

complexes described in Results Section 11 are not seriously affected by the use of 10,000 for the molecular weight of GAR. If a higher molecular weight was used, the numbers of molecules bound to DNA would be correspondingly reduced, but each molecule bound would itself be of proportionally greater molecular weight. This last observation confirms the validity of using 10,600 as the molecular weight of GAR if the number of histones bound is expressed as corresponding to a molecular weight of 10,600.

The shape of the nucleoprotein complexes formed is also of importance. In this respect, it is possible that information can be obtained by considering several models of GAR-histone-SV40 DNA complexes (Results Section 11). Again, the validity of the models constructed is subject to the possible limitation that only portions of the DNA are covered by protein as indicated by the work of Clark and Felsenfeld (1971) on mammalian chromatin. No estimate is possible of the amount of DNA covered by protein in the present work, and for simplification it was considered that all the DNA was capable of binding histones. It should be pointed out that because of the simplifying assumption made to construct model structures of DNA-histone complexes, the agreement between the experimental number of histones bound and the number predicted for binding to DNA as a linear row of spheres attached to the DNA molecules may be fortuitous. Not the least of these assumptions is considering the histone molecule as a sphere. It has been postulated by Sung and Dixon (1971) that only the small regions of high positive charge of the histone molecule combine with the DNA. Although the Sephadex studies of GAR histone and its aggregates reported in this work indicated that the shape of the histone molecule was likely to be spherical, there is no evidence to indicate that the spherical shape is retained on association with DNA. Also, it is found that when the total length of the major groove of each SV40 DNA molecule is calculated, no agreement is observed between the experimental number of histones bound and the number of GAR

molecules calculated to be bound to the length of the major groove, assuming each histone molecule to be a sphere of radius  $20.53\text{\AA}$ . Evidence supporting the binding of  $F_1$  histones to the large groove of DNA has been cited by Olins (1969). The observation in the present studies that spermidine phosphate at low concentrations does not apparently affect the number of GAR molecules bound to C. T. DNA, also suggests that in this system GAR molecules may be bound to the large groove since Liquori et al. (1967) have demonstrated the binding of polyamines to the minor groove of DNA. These observations tend to invalidate models of nucleohistone which involve spherical GAR molecules. Nevertheless in the lack of any alternative information regarding shape the assumptions of spherical shape of GAR residues in nucleoprotein complexes are probably justified. It was found, (Results Section 11) that a spherical model of nucleohistone calculated by summing the hydrodynamic volumes of both the histone component and the SV40 DNA component of the complexes had a calculated radius much lower than that of the equivalent hydrodynamic sphere calculated experimentally from the sedimentation properties of the nucleohistone complexes. This implies that the nucleohistone complex is a more diffuse structure than a densely compact sphere. At the other extreme, rod-like models appeared to have greater equivalent radii than those calculated experimentally for the nucleohistone complexes. More rigorous identification of the shape of these complexes may be possible by the application of the theory of Kirkwood (1954) for the calculation of the hydrodynamic parameters of a molecule which could be represented as an association, in many different conformations, of bead-like spheres. Unique mathematical equations are necessary to describe the hydrodynamic behaviour of fixed conformations of the molecule. For this reason, only general shapes like rods, ellipses, tori, etc. can easily be considered by the Kirkwood theory and this approach was not pursued in the present studies. Nevertheless it is significant to note that Bloomfield, Van Holde and Dalton (1967), Gray (1967), Bloomfield

and Zimm (1966), Gray, Bloomfield and Hearst (1967) successfully applied the basic Kirkwood theory to theoretical calculations of the hydrodynamic behaviour of complicated structures like supercoiled closed circular DNA and replicating systems of circular DNA molecules. Another technique useful in determining the structure of the GAR histone-SV40 DNA complexes is likely to be light-scattering since the radius of gyration of the scattering molecules is obtainable experimentally and can thus be compared with the radii of gyration of differently shaped model compounds. By ultracentrifuge studies alone, only the radius of an equivalent hydrodynamic sphere or ellipse is obtainable, thus limiting the range of models that can be tested against this experimental parameter. It is interesting to note that the diffusion coefficient of complexes of GAR histone with the relaxed circular form of SV40 DNA is larger than that of relaxed circular DNA alone. Increases in molecular weight generally tend to decrease the diffusion coefficient and therefore it may be inferred that the structure of GAR complexes with this form of DNA is more compact than the free DNA. This may be a result of the formation of a coiled-coil or 'supercoil' structure of the type suggested by the X-ray diffraction studies of Pardon, Wilkins and Richards (1967) on mammalian chromatin. It is also of interest to note that the diffusion coefficient for the intact SV40 virus is considerably larger than those calculated for complexes of GAR with both forms of SV40 DNA. While the estimate of the molecular weight of the intact virus based on its composition as described by Estes, Huang and Pagano (1971), may not be completely rigorous, nevertheless it may be assumed that the large diffusion coefficient of the virus indicates a considerably more compact structure than the complexes of SV40 DNA with GAR histone. Electron microscope studies have indicated that the virus exists as a sphere of diameter  $450 - 550\text{\AA}$ . It may be that several core proteins are required to form a nucleoprotein complex of so compact a shape

while complexes of SV40 DNA with GAR histone alone adopt a more asymmetric conformation, with a correspondingly lower diffusion coefficient.

#### 4. Conclusions

The experimental observations reported in this work have allowed the quantitation of the self-association of GAR histone in salt conditions. Data on the interaction of GAR histone with DNA has allowed an evaluation of the problems involved in studies of the formation of nucleoprotein complexes. The model system of GAR histone bound to SV40 DNA may be useful in in vitro studies of virus assembly. In this work, some progress has been made in quantitation of the interaction of GAR histone with DNA species.

## SUMMARY



## SUMMARY

1. Several studies of chromatin have indicated that chromosomal proteins bound to the DNA of chromatin inhibit the extent of transcription of the DNA by RNA polymerase. Such an effect could possibly give rise to the phenomenon of cellular differentiation in eukaryotic organisms. The mechanisms whereby chromosomal proteins bind to DNA are therefore of biological importance. The approach adopted in the present studies has been to isolate two components of chromatin, namely GAR histone and DNA and characterize physico-chemical properties of each type of macromolecule thus providing a basis for the study of their interaction.
2. The Glycine-Arginine-Rich histone (GAR) has been isolated in a pure form from calf thymus tissue and gel filtration studies have indicated that the molecule may be described as a sphere of radius  $20.53\text{\AA}$  in  $0.01\text{M HCl}$ .
3. Studies of the self-association of GAR histone by ultracentrifugation have indicated that the histone probably exists in a monomer-dimer equilibrium in  $0.075\text{M NaCl}/0.01\text{M HCl}$  and in a monomer-dimer-tetramer equilibrium in  $0.15\text{M NaCl}/0.01\text{M HCl}$ . The possible biological significance of the aggregation of the histone molecule has been discussed.
4. The modes of association indicated by the ultracentrifuge studies of GAR histone in the above salt conditions were confirmed by studies using a combination of data from gel-filtration and ultracentrifugal techniques. These studies indicated that the tetramer formed is of a compact shape, similar to a tetrahedron.
5. Preliminary ultracentrifugal studies have indicated that the mode of association of GAR histone is independent of pH in the range  $2.5 - 7.0$ .

6. ORD studies of GAR histone in 0.01M HCl, 0.075M NaCl, 0.01M HCl; 0.15M NaCl, 0.01M HCl, suggested that the amount of  $\alpha$  helix present in the protein was low and approximately constant in all conditions.
7. Ultracentrifugal analysis of nucleoprotein complexes of GAR histone and C. T. DNA formed by salt gradient dialysis and by direct addition of GAR to C. T. DNA has indicated considerable heterogeneity with respect to sedimentation coefficient. Estimates were made of the number of histone molecules bound to the DNA in conditions of excess histone.
8. Thermal denaturation studies did not detect any significant differences in the absorbance melting profile of complexes formed by the direct addition of GAR to C. T. DNA in salt-free conditions at pH 5.0 and in 0.075M NaCl, pH 5.0 +  $2.5 \times 10^{-4}$  M EDTA.
9. The use of homogeneous preparations of relaxed circular SV40 DNA and supercoiled SV40 DNA permitted evaluation of the number of histone molecules bound per molecule of each form of DNA as a function of the concentration of histone added to the DNA preparations. The results were interpreted as indicating co-operative binding of histones to these forms of DNA. It was found that each molecule of supercoiled closed circular SV40 DNA bound a number of GAR molecules approximately half that bound by relaxed circular SV40 DNA. Sedimentation coefficient and sedimentation coefficient distributions are presented for complexes of GAR with each form of SV40 DNA in 0.075M NaCl, pH 5.0 and 0.15M NaCl, pH 5.0. Frictional ratios and diffusion coefficients were also evaluated and compared with those of free SV40 DNA and intact SV40 virus. The studies of the binding of GAR histone to SV40 DNA may be useful as a model system for studies of the binding of virus proteins to viral DNA.

10. Models of the complexes of SV40 DNA with GAR histone were constructed and comparison of some hydrodynamic properties of these complexes with those obtained experimentally suggested that the complexes were compact structures, slightly more asymmetric than a solid sphere.

## APPENDIX I

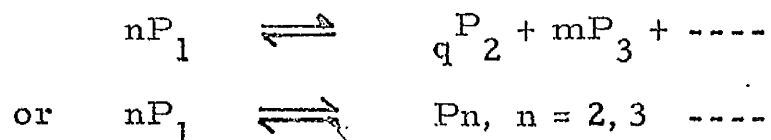
### ADAMS' THEORY FOR ANALYSIS OF ASSOCIATING PROTEIN SYSTEMS

(Adams and Fujita, 1963; Adams, 1964; Adams and Williams, 1964; Adams, 1965 a, b; Adams and Filmer, 1966; Adams, 1967 a, b, c; Adams and Lewis, 1968).

All symbols and nomenclature used in the following discussion are as defined by Adams (1967 c).

Adams and Fujita (1963) showed that methods used for obtaining  $M_w$  as a function of concentration in homogeneous systems also applied to the case of associating protein systems and that it was unnecessary to apply the sedimentation equilibrium equations separately to each solute species in an associating system.

For associations of the type:



the total concentration for ideal or non-ideal systems can be expressed as  $c = c_1 + K_2 c_1^2 + K_3 c_1^3$ , where the equilibrium constants,  $K_n$ , are defined by:

$$K_n = \frac{a_n}{a_1^n} = \frac{c_n}{c_1^n} \quad n = 2, 3, \dots$$

By definition:

$$M_n(c) = \frac{\sum n_i M_i}{\sum n_i} = \frac{c}{\sum (c_i / M_i)}$$

Rearrangement gives:

$$c / M_n(c) = \sum (c_i / M_i)$$

For a general monomer-n-mer equilibrium:

$$\frac{cM_1}{Mn(c)} = c_1 + \frac{K_n c_1^n}{n} = \int_0^c \frac{c}{c_1} dc_1$$

$$\text{Thus } \frac{cM_1}{Mn(c)} = \int_0^c \frac{1 + Knc_1^{n-1}}{1 + nKnc_1^{n-1}} dc = \int_0^c \frac{M_1}{M_w(c)} dc_1$$

For non-ideal systems  $M_w(c)$  is not measurable experimentally.

The experimentally obtained parameter,  $M_{wapp}$ , is related to  $M_w(c)$  by:-

$$\frac{M_1}{M_{wapp}} = \frac{M_1}{M_w(c)} + BM_1 c$$

Integration gives:

$$\begin{aligned} \int_0^c \frac{M_1}{M_{wapp}} dc &= \int_0^c \frac{M_1}{M_w(c)} dc + \int_0^c BM_1 c \\ &= \frac{cM_1}{M_n(c)} + \frac{BM_1 c^2}{2} = \frac{cM_1}{M_{napp}} \end{aligned}$$

Integration of  $M_1/M_{wapp}$  as a function of  $C$ , thus can give values of  $M_{napp}$  as a function of  $c$ .

The weight fraction of monomer,  $f_1$  is defined as:-

$$f_1 = \frac{c_1}{c}$$

In non-ideal cases, an apparent weight fraction of monomer,  $f_a$ , can be defined by:-

$$\ln f_a = \int_0^c \left( \frac{M_1}{M_{wapp}} - 1 \right) \frac{1}{c} dc = \ln f + BM_1 c$$

$$\text{i. e. } f_a = f e^{BM_1 c}$$

A quantity  $a$  may be defined as:

$$\begin{aligned} a &= c f_a \\ &= c f e^{BM_1 c} \\ &= c_1 e^{BM_1 c} \end{aligned}$$

From this, the concentration of monomer,  $c_1$ , is given by  $c_1 = a e^{-BM_1 c}$

and is obtained experimentally from integration of  $\left( \frac{M_1}{M_{wapp}} - 1 \right) \frac{1}{c}$

as a function of  $c$ .

The quantity  $\frac{\sum c_i M_i^2}{M_1^2}$  was found by Adams (1966) to be a useful parameter

in the analysis of interacting systems and is defined as follows:-

From definition  $M_{z(c)} = \frac{\sum c_i M_i^2}{c M_{w(c)}}$  for ideal systems

For non-ideal systems it can be shown that:

$$\begin{aligned} \frac{d}{dc} \left( \frac{M_1}{c M_{wapp}} \right) &= \frac{-M_1 M_{zapp}}{(c M_{wapp})^2} = \frac{-M_1 M_z(c)}{(1 + BM_{w(c)})^2} \frac{(1 + BM_{w(c)})^2}{(c M_{w(c)})^2} \\ &= \frac{-M_1 M_{z(c)}}{(c M_{w(c)})^2} = \frac{-\sum_i K_i c_1^i}{(\sum_i K_i c_1^i)^3} \end{aligned}$$

Rearrangement yields:

$$(\sum_i K_i c_1^i)^3 \frac{d(M_1/cM_{wapp})}{dc} = \sum_i^2 K_i c_1^i = \psi$$

The equation is rendered more useful by substitution for  $\sum_i K_i c_1^i$ ,

using the equation  $\frac{M_1}{M_{wapp}} = \frac{c}{\sum_i K_i c_1^i} + BM_1 c$

that is  $\frac{M_1}{c M_{wapp}} - BM_1 = \frac{1}{\sum_i K_i c_1^i}$

$$\frac{d}{dc} \left( \frac{M_1}{c M_{wapp}} \right) = - \sum i^2 K_i c_1^i = \psi$$

$$\left( \frac{M_1}{c M_{wapp}} - B M_1 \right)^3$$

Adams' theory makes two basic assumptions; that the partial specific volume of all associating species is the same, and that the logarithm of the activity coefficient of each associating species,  $i$ , can be represented by  $\ln y_i = i B M_1 c$ . The analysis allows full characterization of any self-association in terms of association constants and non-ideality coefficient from data consisting only of apparent weight average molecular weights,  $M_{wapp}$ , and concentration,  $c$ . The accuracy of the analysis is considerably increased by the use of data over a wide range of concentration. For this reason, as many sedimentation equilibrium runs as possible should be carried out, using varying starting concentrations. Pressure dependence of equilibrium may be compensated for by carrying out runs at the same starting concentrations, but at different speeds. The general theory may be demonstrated by the specific case of a non-ideal monomer-dimer-trimer (M-D-T) association as described by Adams (1965):-

By definition:  $Mn(c) = \frac{c}{\sum (c_i / M_i)}$

$$\begin{aligned} c / Mn(c) &= \sum \frac{c_i}{M_i} = \frac{c_1}{M_1} + \frac{c_2}{2M_1} + \frac{c_3}{3M_1} \\ &= \frac{1}{M_1} \left( c_1 + \frac{K_2 c_1^2}{2} + \frac{K_3 c_1^3}{3} \right) \end{aligned}$$

Non ideality can be accounted for by the introduction of  $B$ , using the previously derived equation:-

$$\frac{c M_1}{M_{napp}} = \frac{c M_1}{Mn(c)} = \frac{B M_1 c^2}{2}$$

By substitution:-

$$\frac{cM_1}{M_{napp}} = c_1 + \frac{K_2 c_1^2}{2} + \frac{K_3 c_1^3}{3} + \frac{BM_1 c^2}{2} \quad (A)$$

$$\psi = -\sum i^2 K_i c_1^i = \frac{d(M_1/M_{wapp})/dc}{(M_1/cM_{wapp}^{-BM_1})^3}$$

$$\text{For the specific case of M-D-T, } \psi = -c_1 - 4K_2 c_1^2 - 9K_3 c_1^3 \quad (B)$$

$$\text{Now } \frac{M_1}{cMw(c)} = \frac{M_1}{cM_{wapp}^{-BM_1 c}}$$

$$\text{But } Mw(c) = \frac{\sum c_i M_i}{\sum c_i} = \frac{1}{c} \sum c_i M_i$$

For the specific case of M-D-T,

$$\frac{M_1}{cM_{wapp}^{-BM_1 c}} = \frac{M_1}{c_1 M_1 + c_2 2M_1 + c_3 3M_1} = \frac{1}{c_1 + 2K_2 c_1^2 + 3K_3 c_1^3}$$

$$\therefore c_1 + 2K_2 c_1^2 + 3K_3 c_1^3 = \frac{1}{(M_1/cM_{wapp}^{-BM_1 c})} \quad (C)$$

$$(A) \quad \frac{cM_1}{M_{napp}} = c_1 + \frac{K_2 c_1^2}{2} + \frac{K_3 c_1^3}{3} + \frac{BM_1 c^2}{2}$$

$$(B) \quad \psi = -c_1 - 4K_2 c_1^2 - 9K_3 c_1^3$$

$$(C) \quad \frac{1}{M_1/cM_{wapp}^{-BM_1}} = c_1 + 2K_2 c_1^2 + 3K_3 c_1^3$$

$$(D) \quad C = C_1 + K_2 C_1^2 + 3K_3 c_1^3$$

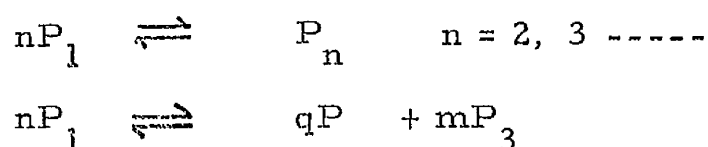
$$(E) \quad C_1 = a e^{-BM_1 c}$$

The only variables in the above equations which cannot be obtained from experimental data, are  $K_2$ ,  $K_3$  and  $B$ , but the equations can be combined to eliminate  $K_2$  and  $K_3$  by simple substitution, producing equations in only one unknown,  $B$ . Such an equation for the specific case of M-D-T is:-

$$\frac{12c M_1}{M_{napp}} - 4c = 6 a e^{-BM_1 c} + 6BM_1 c^2 + \psi + \frac{3}{(M_1/cM_{wapp}^{-BM_1})}$$



Successive approximation for different values of B may be used to find that value of B which satisfies the equation. Since  $\psi$  is a function of B,  $\psi$  must be calculated anew for each B used in the successive approximation process. When a value of B is found which satisfies the equations, values of  $K_3$  and  $K_2$  may be calculated by a reversal of the substitution process which led to the establishment of the general equation. Using directly analogous methods to those described above for an M-D-T association, characteristic equations for any particular systems of the form:



may be constructed. Equations for various associations of these general types are listed:-

Type of association	Equation	Equation No.
M-N	$(nC - (n-1) a e^{-BM_1 c}) ((M_1/M_{wapp})^{-BM_1 c}) = 0$	1.1
indefinite	$(2/(M_1/M_{napp}^{-BM_1 c/2}) - 1)(M_1/M_{wapp}^{-BM_1 c}) - 1 = 0$	1.2
M-D	$2cM_1/M_{napp}^{-c} = a \exp(-BM_1 c) + BM_1 c^2$	1.3
M-D	$2cM_1/M_{napp}^{-c} = \psi + 2/(M_1/cM_{wapp}^{-BM_1}) + BM_1 c^2$	1.4
M-T	$3cM_1/M_{napp}^{-c} = \psi + 3/(M_1/cM_{wapp}^{-BM_1}) + \frac{3}{2} BM_1 c^2$	1.5
M-D-Tr	$6cM_1/M_{napp}^{-5c} = 2a \exp(-BM_1 c) + 3BM_1 c^2 - 1/(M_1/cM_w^{-BM_1})$	1.6

Type of association	Equation	Equation No.
M-D-Tr	$30cM_1/M_{napp} - 19c = 12a \exp(-BM_1c) + \psi$ $+ 15 BM_1c^2$	1.7
M-D-Tet	$8cM_1/M_{napp} - 6c = 3a \exp(-BM_1c) +$ $4BM_1c^2 - 1/(M_1/cM_{wapp} - BM_1)$	1.8
M-D-Tet	$24cM_1/M_{napp} - 6c = 6a \exp(-BM_1c) + 12BM_1c^2$ $- \psi - 9.0/(M_1/cM_{wapp} - BM_1)$	1.9

## APPENDIX II (a)

### MOLECULAR SIEVE CHROMATOGRAPHY

#### (a) Calibration of column

It is assumed that the penetrable volumes which can accommodate a molecular species of radius,  $a$ , within the gel, are distributed randomly. It is also assumed that the fraction of the internal volume that is penetrable by a solute molecule of radius,  $a$ , can be represented by a gaussian probability curve.

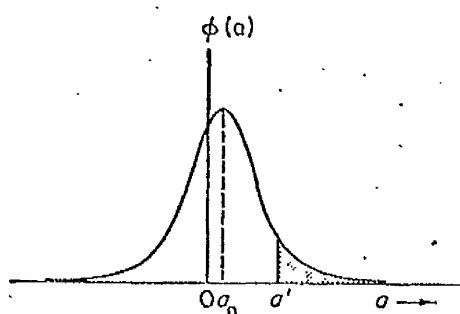


FIG. 6. Distribution of "internal volume" fractions,  $\phi$ , penetrable by a solute molecule of radius  $a$ . The shaded area represents the total fractional volume within the gel that can be occupied by a given molecular species of radius  $a'$ .

Diagram taken from Ackers and Steere (1967)

The total fractional volume  $\phi'$  of the internal volume occupied by a species of radius  $a'$  will be represented as the fraction  $\phi(a')$  that is just barely available to the molecule plus the sum of all similar fractions available to larger molecules. This volume is represented on the gaussian curve by the area extending outwards from  $a'$  and is given by the expression:

$$\text{erf c} \left( \frac{a' - a_0}{b_0} \right) = 1 - \frac{2}{\sqrt{\pi}} \int_0^{\left( \frac{a' - a_0}{b_0} \right)} e^{-a^2} da$$

$a_0$  and  $b_0$  are characteristics of the gaussian curve and the symbol erf c represents the error function complement.

For calibration of the column,  $a_0$  and  $b_0$  are required. Using two proteins of known Stokes radius  $a_1$  and  $a_2$ , the corresponding sieve coefficients  $\sigma_1$  and  $\sigma_2$  may be calculated. The respective values of  $(a-a_0/b_0)$  may be derived, using tables of the error function. (Applied mathematic series No. 41, National Bureau of Standards, United States Department of Commerce, 1954). The simultaneous equations may then be solved for  $a_0$  and  $b_0$ .

## APPENDIX II(b)

### (b) Analysis of associating systems using the method of Chun, Kim, Stanley and Ackers (1969) and Chun and Kim (1969)

The elution diagram for an associating system is represented below:-

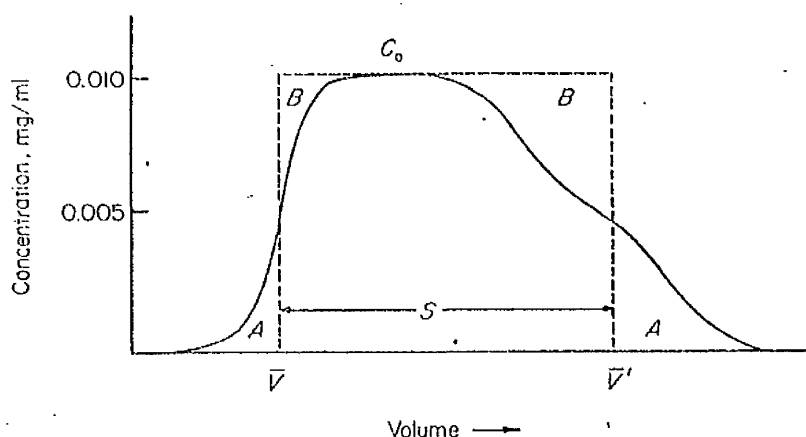


FIG. 9. Characteristic elution diagram for an associating system. The leading and trailing edges continually "feed" off the plateau,  $C_0$ , as they spread. The vertical dashed lines define the centroid positions for leading and trailing edges such that in each case the areas  $A$  below the elution curve (solid line) are equal to areas  $B$  above the curve.

Diagram taken from Ackers and Steere (1967).

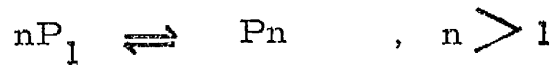
Weight average partition coefficients,  $\sigma_w$ , are defined by Ackers (1967 a, b) as:

$$\sigma_w = \sum \sigma_i f_i$$

where  $\sigma_i$  = molecular sieve coefficient of species i

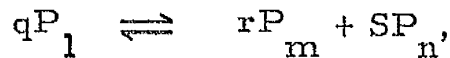
$f_i$  = weight fraction of species i

For a thermodynamically ideal monomer-n-mer association described by:



$$\text{then } \sigma_w = \sigma_n + f_1 (\sigma_i - \sigma_n) \quad (1)$$

In the case of a monomer-m-mer-n-mer association described by:



an approach analogous to that used in the monomer-n-mer case is applied, giving rise to the following equations:-

$$f_1^2 + 2a_1 f_1 + a = 0 \quad (2)$$

$$\begin{aligned} \text{where } a &= \frac{1}{\Delta} \left( \frac{(m-n)(\sigma_w^2 + \sigma_m \sigma_n) - 2\sigma_w(m\sigma_n - n\sigma_m)}{2(m+n)(\sigma_m - \sigma_n)} \cdot \frac{\eta}{c^2} \right) \\ 2a_1 &= \frac{1}{\Delta} \left( \frac{1}{(\sigma_m - \sigma_n)} \left( \frac{(\sigma_m + m\sigma_1)(\sigma_w - \sigma_n) - (\sigma_n + n\sigma_1)(\sigma_w - \sigma_m)}{(m+1)(n+1)} \right. \right. \\ &\quad + \frac{1}{(\sigma_m - \sigma_n)^2} \cdot X \left[ \left( \frac{m\sigma_n + n\sigma_m}{m+n} \right) (2\sigma_w \sigma_1 - \sigma_w \sigma_m - \sigma_1 \sigma_n \right. \\ &\quad \left. \left. - \sigma_w \sigma_n - \sigma_m \sigma_1 + 2\sigma_n \sigma_m) - \sigma_m (\sigma_w - \sigma_n)(\sigma_1 - \sigma_n) - \sigma_n \right. \right. \\ &\quad \left. \left. (\sigma_w - \sigma_m)(\sigma_1 - \sigma_m) \right] \right) \\ \Delta &= \frac{1}{(\sigma_m - \sigma_n)^2} \left( \frac{\sigma_m}{2} (\sigma_1 - \sigma_n)^2 + \frac{\sigma_n}{2} (\sigma_1 - \sigma_m)^2 - \right. \\ &\quad \left. \frac{m\sigma_n + n\sigma_m}{m+n} (\sigma_1 - \sigma_m)(\sigma_1 - \sigma_n) \right) - \frac{1}{\sigma_m - \sigma_n} \cdot X \\ &\quad \cdot \left( \frac{\sigma_m + m\sigma_1}{m+1} (\sigma_1 - \sigma_n) - \frac{\sigma_n + n\sigma_1}{n+1} (\sigma_1 - \sigma_m) \right) + \frac{\sigma_1}{2} \end{aligned}$$

For the case of indefinite association, the following equation was derived:-

$$\sigma_w = \sum i \sigma_i f_1 (1 - \sqrt{f_1})^{i-1} \quad (3)$$

Values of  $f_1$  as a function of  $c$  are obtained from molecular weight data by the method of Adams (See Appendix I) and are then substituted into equations (1) and (3) to produce theoretical plots of  $\sigma_w$  vs.  $c$ . Values of  $\sigma_n$  and  $\sigma_i$  used in these equations were computed according to two extreme models of molecular aggregation:-

a) Compact Aggregation

In this case all species were assumed to be spherical and  $a_i = a_1 c^{\frac{1}{3}}$  where  $a_i$  = Stokes radius of the complex of  $i$  species.

Molecular sieve coefficients may be calculated from the basic molecular sieve equation  $\sigma_i = \text{erfc}((a_i^{\frac{1}{3}} - a_0)/b_0)$ .

b) Linear Aggregation

In this case all species were assumed to be long rod-shaped molecules. Tanford (1961) has shown that molecules of length  $l$  and diameter  $d$  can be approximated by prolate ellipsoid whose semi-axes  $a$  and  $b$  are related to  $l$  and  $d$  by:-

$$\frac{a}{b} = \left(\frac{2}{3}\right)^{\frac{1}{2}} \frac{L}{D}$$

The fractional coefficients for a prolate ellipsoid have been shown by Perrin (1936) to be related by the following equation:-

$$\frac{f}{f_0} = \frac{(1 - \frac{b^2}{a^2})^{\frac{1}{2}}}{(\frac{b^2}{a^2})^{\frac{2}{3}} (\ln(1 + (1 - \frac{b^2}{a^2})^{\frac{1}{2}}) b/a)}$$

A combination of the above two equations was used by Chun et al. (1969) to predict the molecular sieve coefficients of complexes by substitution into:-

$$\sigma_i = \text{erf } c \left( \left( \frac{f}{f_0} a_1 i^{\frac{1}{3}} - a_0 \right) / b_0 \right)$$

A modification of the procedure outlined by Chun et al. (1969) was found to be necessary in the case of the monomer-m-mer-n-mer equilibrium, to permit ease of computation.

Experimental values of  $\sigma_w$  as a function of  $c$ , derived from molecular sieve data, were substituted into equation (2), using values of  $\sigma_m$  and  $\sigma_n$  computed according to the two extreme models of shape. Theoretical curves of  $f_1$  as a function of  $c$  were then obtained and compared with the experimental values of  $f_1$  obtained from molecular weight data.

In experimental studies, the value of  $\sigma_w$  was calculated from the centroid of the trailing boundary as described by Ackers and Steere (1967). The quadrature method of Simson's rule was the integration procedure used to locate that point, the centroid, on the trailing boundary where the area under the trailing boundary was equal to the area above the boundary up to an imaginary extension of the plateau region (Ackers and Steere, 1967).

## REFERENCES



## REFERENCES

- Ackers, G. K. (1964). Biochemistry, 3, 723
- Ackers, G. K. (1967a). J. biol. Chem., 242, 3026
- Ackers, G. K. (1967b). J. biol. Chem., 242, 3237
- Ackers, G. K. (1968). J. biol. Chem. 243, 2056
- Ackers, G. K. (1970). Adv. prot. Chem., 24, 343
- Ackers, G. K. & Steere, R. L. (1967). in 'Methods in Virology' ed. by Maramorosch, K. & Koprowski, H. p325, vol. 2. New York: Academic Press.
- Ackers, G. K. & Thompson, T. E. (1965). Proc. natl. Acad. Sci. U. S. A., 53, 342
- Adams, E. T. (1964). Proc. natl. Acad. Sci. U. S. A., 51, 509
- Adams, E. T. (1965a). Biochemistry., 4, 1646
- Adams, E. T. (1965b). Biochemistry, 4, 1655
- Adams, E. T. (1967a). Biochemistry, 6, 1865
- Adams, E. T. (1967b). Fedn. Proc. Fedn. Am. Soc. exp. Biol., 26, 778
- Adams, E. T. (1967c). in Fractions vol. 3. Palo Alto, Calif: Pub. by Spinco Division of Beckman Instruments Inc.
- Adams, E. T. & Filmer, D. L. (1966). Biochemistry, 5, 2971
- Adams, E. T. & Fujita, H. (1963). in 'Ultracentrifugal Analysis in Theory and Experiment' ed. by Williams, J. W., New York: Academic Press.
- Adams, E. T. & Lewis, M. S. (1968). Biochemistry, 7, 1044
- Adams, E. T., Pekar, A. M., Soucek, D. A., Tang, L. H., Barlow, G. & Armstrong, J. L. (1969). Biopolymers, 7, 5.
- Adams, E. T. & Williams, J. W. (1964). J. Amer. Chem. Soc. 86, 3454
- Adler, A. & Fasman, G. D. (1968). in 'Methods in Enzymology', ed. by Grossman, L. & Moldave, K. vol. XII, p268.
- Albright, D. A. & Williams, J. W. (1968). Biochemistry, 7, 67
- Ansevin, A. T. & Brown, B. W. (1971). Biochemistry, 10, 1133
- Anderer, F. A., Koch, M. A. & Schlumberger, M. D. (1968). Virology, 34, 452.
- Andrews, P. (1964). Biochem. J., 91, 222.

- Archibald, W. J. (1947). *J. phys. Colloid. Chem.* 51, 1204
- Bancroft, F. C. & Freifelder, D. (1970). *J. mol. Biol.* 54, 537
- Barr, G. C., & Butler, J. A. V. (1963). *Nature (Lond.)*, 199, 1170
- Black, P. H., Crawford, E. M. and Crawford, L. V. (1964). *Virology* 24, 381.
- Bekhor, I., Kung, G. M. & Bonner, J. (1969). *J. mol. Biol.*, 39, 351
- Bloomfield, V. A. (1968), *Science*, 161, 1212
- Bloomfield, V., Van Holde, K. E. & Dalton, W. O. (1967). *Biopolymers* 5, 149.
- Bloomfield, V. & Zimm, B. H. (1966). *J. chem. Phys.* 44, 315
- Bonner, J. & Huang, R. C. (1963). *J. mol. Biol.* 6, 169
- Bonner, J. & Huang, R. C. (1964). In 'Histones', Ed. by DeReuck, A. V. S. & Knight, J. London: Ciba Found. Study Gp. 24.
- Bonner, J. & Ts'o, P. O. P. (1964). *The Nucleohistones*. San Francisco: Holden-Day.
- Boublik, M., Bradbury, E. M. & Crane-Robinson, C. (1970). *Eur. J. Biochem.*, 14, 486.
- Boublik, M., Bradbury, E. M., Crane-Robinson, C. & Johns, E. W. (1970). *Eur. J. Biochem.* 17, 151.
- Boublik, M., Bradbury, E. M., Crane-Robinson, C. & Rattle, M. W. E. (1971). *Nature New Biol.* 229, 149
- Bowen, T. J. (1970). 'An Introduction to Ultracentrifugation', London: Wiley.
- Bram, S. & Ris, H. (1971). *J. mol. Biol.* 55, 325.
- Bauer, W. & Vinograd, J. (1965). *Biochim. biophys. Acta*, 108, 18.
- Brumbaugh, E. E. & Ackers, G. K. (1968). *J. biol. Chem.*, 243, 6315
- Bruner, R. & Vinograd, J. (1965). *Biochim. biophys. Acta*. 108, 18
- Burdon, R. H. (1971). *Biochim. biophys. Acta*, 232, 359
- Bustin, M., Rall, S. C., Stellwagen, R. H. & Cole, R. D. (1969). *Science*, 163, 391.
- Cassassa, E. F. & Eisenberg, H. (1964). *Advan. prot. Chem.*, 19, 287
- Caspar, P. L. O. & Klug, A. (1962). *Cold Spring Harb. Symp. Quant. Biol.* 27, 1

- Cassman, H. & Schachman, H. K. (1971). *Biochemistry* 10, 1015
- Chun, P. W. & Kim, S. J. (1969). *Biochemistry*, 8, 1633.
- Chun, P. W., Kim, S. J., Stanley, C. A. & Ackers, G. K. (1969)  
*Biochemistry*, 8, 1625.
- Chun, P. W. & Kim, S. J. (1970). *Biochemistry*, 9, 1957.
- Clark, R. J. & Felsenfeld, G. (1971). *Nature new Biol.* 229, 101
- Cohen, P. & Kidson, C. (1968). *J. mol. biol.*, 35, 241.
- Cohn, E. S. & Edsall, J. T. (1943) 'Proteins, Amino acids & Peptides'  
New York: Reinhold.
- Crampton, C. F., Stein, W. H. & Moore, S. (1957). *J. biol. Chem.*,  
225, 363.
- Crawford, L. V. & Black, P. H. (1964). *Virology* 24, 388.
- Creeth, J. M. & Pain, R. H. (1967). *Progr. biophys. mol. biol.* 17, 217.
- Crothers, D. M. & Zimm, B. H. (1965). *J. mol. biol.* 12, 525.
- Dahmus, M. E. & Bonner, J. (1970). *Fed. Proc: Fedn. Am. Soc. exp. Biol.*,  
29, 1255.
- Davidson, J. N. & Leslie, I. (1950a) *Nature (Lond.)*, 165, 49.
- Davidson, J. N. & Leslie, I. (1950b) *Cancer Res.* 10, 587.
- DeLange, R. J., Fanbrough, D. H., Smith, E. L., Bonner, J. (1968a)  
*Proc. natl. , Acad. Sci. U.S.A.*, 61, 1145.
- DeLange, R. J., Fanbrough, D. H., Smith, E. L., & Bonner, J.  
(1968b). *J. biol. Chem.* 243, 5906.
- Deonier, R. C. & Williams, J. W. (1970) *Biochemistry*, 9, 4260.
- Doty, P. & Myers, G. E. (1953). *Disc. Faraday Soc.* 13, 51.
- Dupraw, E. J. (1965). *Nature (Lond.)*, 206, 338.
- Dupraw, E. J. (1966a) *Nature (Lond.)*, 209, 577.
- Dupraw, E. J. (1966b). *J. Cell. biol.*, 31, 30A.
- Dupraw, E. J. & Bahr, G. F. (1968) *Abstr. Publ., 3rd. Intern. Congr.*,  
*Histochem. Cytochem*, New York.
- Edwards, P. A. & Shooter, K. V. (1969a). *Biochem. J.*, 114, 54P.
- Edwards, P. A. & Shooter, K. V. (1969b). *Biochem. J.*, 114, 227

- Edwards, P.A. & Shooter, K.V. (1970). *Biochem. J.*, 120, 61.
- Eisenberg, H. & Tomkins, G (1968), *J. mol. Biol.*, 31, 37.
- Elias, H.S. & Bareiss, R. (1967). *Chimia*, 21, 53.
- Elving, J., Markowitz, R.B. & Rosenthal, E. (1956) *Analyt. Chem.*, 28, 1179.
- Estes, M.K., Huang, E.S., & Pagano, J.S. (1971). *J. of Virology*, 7, 635.
- Fambrough, D.M. & Bonner, J. (1966). *Biochemistry*, 5, 2563.
- Fambrough, D.M. & Bonner, J. (1968). *J. biol. Chem.*, 243, 4434
- Fambrough, D.M. & Bonner, J. (1969). *Biochim. biophys. Acta*, 175, 113.
- Fambrough, D.M., Fujimura, F. & Bonner, J. (1968). *Biochemistry*, 7, 575.
- Fasman, G.O., Schaffhausen, G., Goldsmith, L. & Adler, A. (1970). *Biochemistry*, 9, 2814.
- Fujita, H. (1956). *J. Amer. Chem. Soc.*, 78, 3598.
- Georgiev, G.P., Ananieva, L.N. and Kozlov., J.V., (1966) *J. mol. Biol.* 22, 365.
- Gershey, E.L., Vidali, G. & Allfrey, V.G. (1968). *J. biol. Chem*, 243, 5018.
- Gilbert, G.A. (1955). *Disc. Faraday Soc.* 20, 68.
- Gilbert, G.S. (1959). *Proc. Roy. Soc. (Lond.)*. Ser.A. 250, 377.
- Gilbert, G.S. & Jenkins, R.C.L. (1956). *Nature (Lond.)*, 177, 853.
- Gilbert, G.S. & Jenkins, R.C.L. (1959). *Proc. Roy. Soc. (Lond.)* Ser.A. 253, 420.
- Gilmour, R.S. & Paul, J. (1969). *J. mol. Biol.* 40, 137.
- Godfrey, J.E. & Harrington, W.F. (1970a). *Biochemistry*, 9, 886.
- Godfrey, J.E. & Harrington, W.F. (1970b). *Biochemistry*, 9, 894.
- Goodrich, R., Swinehart, D.F., Kelly, H.J. & Reithel, F.S. (1969). *Anal. Biochem.* 28, 25.
- Goodrich, R. & Reithel, F.S. (1970). *Anal. Biochem.* 34, 538.
- Gray, H.B. (1967). *Biopolymers* 5, 109

Gray, H. B., Bloomfield, V. & Hearst, J. E. (1967). J. chem. Phys.

46, 1493.

Griffith, J., Huberman, J. A. & Kornberg, A. (1971). J. mol. Biol.

55, 209

Haschemeyer, R. H. & Bowers, W. F. (1970). Biochemistry, 9, 435.

Haydon, A. J. & Peacocke, A. R. (1968). Biochem. J. 110, 243.

Hearst, J. E. & Stockmayer, W. H. (1962). J. chem. Phys. 37, 1425.

Heyden, H. W. & Zachau, H. G. (1971). Biochim. biophys. Acta 232, 657.

Hnilica, L. S. (1966). Biochim. biophys. Acta. 117, 163.

Hnilica, L. S. (1967). In progr. Nucleic Acids Res. mol. biol. vol. 7 p25

Ed. by Davidson, J. W. & Cohn, W. E. New York: Academic Press.

Hnilica, L. S., Taylor, C. W. & Busch, H. (1963). Exptl. cell. res. suppl.

9, 367

Hoare, T. A. & Johns, E. W. (1970). Biochem. J. 119, 931

Huang, R. C. (1967). Fed. Proc: Fedn. Am. Soc. exp. biol. 26, 1933

Huang, R. C. & Bonner, J. (1962). Proc. natl. Acad. Sci. U. S. A., 49, 414

Huang, R. C. & Bonner, J. (1965). Proc. natl. Acad. Sci. U. S. A., 54, 960

Huang, R. C. & Bonner, J. & Murray, K. (1964). J. mol. biol. 8, 54.

Hudson, B., Clayton, D. A. & Vinograd, J. (1968). Cold Spring Harb.

symp. Quant. Biol. 33, 435

Inoue, S. & Ando, T. (1970a). Biochemistry, 9, 388

Inoue, S. & Ando, T. (1970b). Biochemistry, 9, 395

Iwai, K., Ishikawa, K. & Hayashi, H. (1970). Nature (Lond.), 226, 1056

Jacob, F. & Monod, J. (1961). J. mol. Biol. 3, 318

Jeffrey, P. D. & Coates, J. H. (1966). Biochemistry, 5, 489

Johns, E. W. (1964). Biochem. J., 92, 55

Johns, E. W. (1968). J. Chromatog. 33, 563

Johns, E. W. & Hoare, T. A. (1970). Nature (Lond.). 226, 650

Kelly, M. J. & Reithel, F. J. (1971). Biochemistry, 10, 2639

Kincade, J. M. & Cole, R. (1966). J. biol. Chem. 241, 5798

Kirkwood, J (1954). J. polymer Sci. 12, 1.

- Klaimmer, S. M. & Kegeles, G. (1956). Arch. biochem. biophys. 63, 247
- Kleinsmith, L. J., Allfrey, V. G. & Mirsky, A. E. (1966). Proc. natl. Acad. Sci. U.S.A. 55, 1182.
- Klotz, I. M. (1946). Arch. Biochem. 9, 109
- Klotz, I. M. (1953). The Protein, 1, 727
- Klotz, I. M., Walker, F. M. & Pivan, R. B. (1946), J. Amer. chem. Soc. 68, 1486
- Lamers, K., Putney, F., Steinberg, I. Z., Schachman, H. K. (1963). Arch. biochem. biophys. 103, 374
- Leng, H. & Felsenfeld, G. (1966). Proc. natl. Acad. Sci. U.S.A. 56, 1325
- Lewin, S. (1970). J. theoret. Biol. 29, 7.
- Li, H. J., Isenberg, I. & Johnson, W. C. (1971). Biochemistry, 10, 2587
- Liquori, A. M., Constantino, L., Crescenzi, V., Elia, V., Giglio, E., Puliti, R., DiSantis-Savino, M., & Vitagliano, V. (1967). J. mol. Biol. 24, 113
- Lowry, O. N., Rosenborough, N. J., Farr, A. C. & Randall, R. S. (1951). J. biol. Chem. 193, 265.
- Luck, J. H., Rasmussen, P. S., Satake, K. & Tsvetikov, A. W. (1958). J. biol. Chem. 243, 1403
- Marushige, K. & Bonner, J. (1966). J. mol. Biol. 15, 160
- Marushige, K. Brutlag, D. & Bonner, J. (1968). Biochemistry, 7, 3149
- Marushige, K. & Ozaki, M. (1967). Develop. Biol. 16, 474
- Mauritzen, C. M. Starbuck, W. C, Saroja, I. S., Taylor, C. W. & Busch, H. (1967). J. biol. Chem. 242, 2240.
- Mirsky, A. E. & Ris, H. (1951). J. Gen. Physiol. 34, 451
- Moffit, W. & Yang, J. T. (1956). Proc. natl. Acad. Sci. U.S.A., 42, 596
- Moller, W. (1964). Proc. natl. Acad. Sci. U.S.A. 51, 501
- Monod, J. Wyman, J. & Changeux, J. P. (1965). J. mol. biol. 12, 88
- Moore, W. J. (1962). 'Physical Chemistry', London: Longmans.
- Muller, W. & Crothers, D. M. (1968). J. mol. biol. 55, 251
- Murray, K. (1964). Biochemistry, 3, 10
- Murray, K., Bradbury, E. M., Crane-Robinson, C., Stephens, R. H., Haydon, A. J. & Peacocke, A. R. (1970). Biochem. J. 120, 859

- Neelin, J. M. (1968). Can. J. Biochem. 46, 241
- Nichol, L. W., Bethune, J. L., Kegeles, G. & Hess, E. I. (1964).  
'The Proteins'. vol. 2, p305, Ed. Neurath, H. New York:  
Academic Press.
- Ogawa, Y. Quagliarotti, C., Jordan, J., Taylor, C. W., Starbuck, W. C.,  
& Busch, H. (1969). J. biol. chem. 244, 4387
- Olins, D. E. (1969). J. mol. biol. 43, 439
- Olins, D. E., Olins, A. L. & Von Hippel, P. H. (1968). J. mol. biol. 33, 265
- Olins, D. E., Olins, A. L. (1971). J. mol. biol. 57, 437
- Pain, R. H. (1965). Biochim. biophys. Acta. 94, 183
- Pardon, J. F., Wilkins, H. H. F. & Richards, B. M. (1967). Nature (Lond.)  
215, 1967
- Paul, J. & Gilmour, R. S. (1966). Nature (Lond.). 210, 92
- Paul, J. & Gilmour, R. S. (1968). J. mol. biol. 34, 305
- Paul, J. Gilmour, R. S. & Thomou, H. (1970). FEBS. Symp., 21, 237
- Perrin, F. (1936). J. phys. Radium, 7, 1.
- Phillips, D. H. P. (1963). Biochem. J. 87, 258
- Porath, J. (1963). Pure Appl. Chem. 6, 233
- Radloff, R., Bauer, W. R. & Vinograd, J. (1967). Proc. natl. Acad. Sci.  
U. S. A. 57, 1514
- Rao, M. S. W. & Kegeles, G. (1958). J. Amer. Chem. Soc., 80, 5724
- Reisfeld, R. S., Lewis, M. J. & Williams, D. E. (1962). Nature (Lond.)  
195, 287
- Reisler, E. & Eisenberg, H. (1969). Biochemistry, 8, 4572
- DeReuck, A. V. S. & Knight, J. (1964). 'Histones' Ciba Found. Study Gp. 24.
- Richards, B. (1964). in 'The nucleohistones' ed. by Bonner, J. & Ts'o,  
P. O. P. San Francisco: Holden-Day
- Roark, D. E. & Yphantis, D. A. (1969). Ann. N. Y. Acad. Sci. 164, 245
- Rowe, H. J. & Rowe, A. J. (1970). FEBS Letters, 9, 124
- Rush, H. E. & Warner, R. C. (1970). J. biol. Chem. 245, 2704
- Rush, H. E., Eason, R., Vinograd, J. (1971). Biochim. biophys. Acta.  
228, 1585.

- Salser, J.R. & Balis, M.E. (1966). Proc.Amer.Assoc.Cancer Res. F, 61
- Satake, K., Rasmussen, P.A. & Luck, J.M. (1966). J.biol.Chem., 235,  
2801
- Schachman, H.K., (1963a). Biochemistry, 2, 887
- Schachman, H.K. (1963b), in 'Ultracentrifugal Analysis in Theory &  
Experiment' Ed. by Williams, J.W., New York: Academic Press,  
p. 171
- Schachman, H.K. & Edelstein, S.J. (1966). Biochemistry, 5, 2681.
- Schachman, H.K. Grappor, L. Hanlon, S. & Putney, F. (1962). Arch.  
biochem.Biophys. 99, 175
- Schechter, E. & Blout, E.R. (1964). Proc.natl.Acad.Sci.U.S.A. 51, 695
- Schechter, E., Carver, J.P. & Blout, E.R. (1964). Proc.natl.Acad. Sci.  
U.S.A. 51, 1029.
- Schmid, C.W. & Hearst, J.E. (1969). J.mol.Biol. 44, 143
- Scholte, T.G. (1968). J.Polymer Sci. 6, 111
- Schumaker, V.N., Richards, T. & Freer, N. (1967). J.mol.Biol. 29, 107
- Schumaker, V.N. & Schachman, H.K. (1957). Biochim.biophys.Acta, 33, 628
- Shih, T.Y. & Bonner, J. (1970). J. mol. Biol. 48, 469
- Shih, T.Y. & Fasman, G.D. (1970). J.mol.Biol. 52, 105
- Shih, T.Y. & Fasman, G.D. (1971). Biochemistry, 10, 1675
- Simpson, R.T. & Sober, M.A. (1970). Biochemistry, 9, 3103
- Sinsheimer, R.L. (1964). in 'The nucleohistones' eds. Bonner, J. & Ts'o,  
P.O.P. San Francisco: Holden-Day, p357
- Smart, R.E. & Bonner, J. (1971). J.mol.Biol., 55, 661
- Sophianopoulos, A.J. & Van Holde, K.E. (1964). J.biol.Chem. 239, 2516
- Spelsberg, T.C. & Hnilica, L.S. (1971). Biochim.biophys.Acta, 228, 202
- Starbuck, W.C., Mauritzen, C.M., Taylor, C.W., Saroja, R.S. & Busch,  
H. (1968). J.biol.Chem., 243, 2038.
- Stedman, E. & Stedman, E. (1950). Nature (Lond.). 166, 780.



- Steere, R. L. & Ackers, G. K. (1962). *Nature (Lond.)* 196, 475
- Steinberg, I. F. & Schachman, H. K. (1966). *Biochemistry* 5, 3728
- Steiner, R. F. (1952). *Arch. Biochem. Biophys.* 39, 333.
- Steiner, R. F. (1953). *Arch. Biochem. Biophys.* 44, 120.
- Steiner, R. F. (1954). *Arch. Biochem. Biophys.* 49, 400
- Stellwagen, R. H. & Cole, R. D. (1969). *Ann. rev. Biochem.* 32, 951.
- Stevely, W. S. & Stocken, L. A. (1966). *Biochem. J.* 100, 20p.
- Sung, J. T. & Dixon, G. H. (1970). *Proc. Natl. Acad. Sci. U. S. A.* 67, 1616.
- Svedberg, T. & Pedersen, K. O. (1940). *The Ultracentrifuge*, Oxford:  
Clarendon Press.
- Tanford, C. (1961) 'The Physical Chemistry of Macromolecules',  
New York: Wiley.
- Tanford, C. (1964). *Brookhaven Symp. Biol.* 17, 104.
- Teller, D. C. (1970) *Biochemistry*, 9, 4207
- Teller, D. C. Horbett, J. A., Richards, E. G. & Schachman, H. K. (1969).  
*Am. N. Y. Acad. Sci.*, 164, 66.
- Teller, D. C. Kinkade, J. H. & Cole, R. D. (1965). *Biochem. biophys.*  
*Res. Commun.* 20, 739.
- Thomas, J. O. & Edelstein, S. J. (1971). *Biochemistry* 16, 477.
- Tidwell, T. Allfrey, V. G. & Mirskey, A. E. (1968). *J. biol. chem.* 243,  
707.
- Tomimatsu, Y. & Gaffield, W. (1965). *Biopolymers* 3, 509.
- Trautman, R. & Crampton, C. F. (1959). *J. Amer. Chem. Soc.* 81, 4036.
- Tuan, D. Y. M. & Bonner, J. (1969). *J. mol. biol.* 45, 59.
- Ui, N. (1957). *Biochim. biophys. Acta* 25, 493.
- Urnes, P. & Doty, P. (1961). *Advan. Prot. Chem.* 16, 401.
- Van Holde, K. E., Rossetti, G. P. & Dyson, R. D. (1969). *Ann., N. Y.*  
*Acad. Sci.* 164, 279.
- Vendrely, R. Alfert, M., Matsudaira, H. & Knoblock, A. (1958). *Exptl.*  
*Cell. Res.* 14, 295.
- Verwey, E. J. W. & Overbeck, J. T. G. (1948). 'Theory of the Stability  
of Lyophobic Colloids' New York: Elsevier.

- Vinograd, J., Bruner, R., Kent, A. & Weigle, J. (1963). *Proc. natl. Acad. Sci. U.S.A.* 49, 102.
- Vinograd, J. & Lebowitz, J. (1966). in 'Macromolecular Metabolism' p.103. Boston: Little, Brown.
- Wagner, T.E. (1970). *Nature (Lond.)* 227, 65.
- Wagner, T.E. & Spelsberg, T.C. (1971) *Biochemistry*, 10, 2599.
- Walker, I.O. (1965). *J. mol. Biol.* 14, 381.
- Wang, T.Y. (1967). *J. biol. chem.* 242, 1220.
- Wang, T.Y. & Johns, E.W. (1968). *Arch. Biochem. biophys.* 124, 176
- Waring, M.J. (1965). *J. mol. Biol.* 13, 269.
- Watson, J.D. & Crick, F.H.C. (1953). *Nature (Lond.)* 171, 737.
- Wetlaufer, D.B. (1962). *Adv. Prot. Chem.* 17, 304.
- Wilkins, M.H.F., Stokes, A.R. & Wilson, H.R. (1953). *Nature (Lond.)*, 172, 759.
- Wilkins, M.H.F., Zubay, G. & Wilson, R. (1959). *J. mol. Biol.* 1, 179.
- Williams, J.W. (1963). (ed). 'Ultracentrifugal Analysis in Theory and Experiment'. New York: Academic Press.
- Williams, J.W., Van Holde, K.E., Baldwin, R.L. & Fujita, H. (1958). *Chem. Revs.* 58, 715.
- Wilson, R.K., Starbuck, W.C., Taylor, C.W., Jordan, J. & Busch, H. (1970). *Cancer Res.* 30, 2942.
- Winzor, D.J. & Nichol, L.W. (1965). *Biochim. biophys. Acta.* 104, 1.
- Winzor, D.J. & Scheraga, H.A. (1964). *J. Phys. Chem.* 68, 338.
- Winzor, D.J. & Scheraga, H.A. (1963). *Biochemistry*, 2, 1263.
- Yang, J.T. & Samejima, T. (1963). *J. biol. Chem.* 238, 3262.
- Yphantis, D.A. (1964). *Biochemistry*, 3, 297.
- Zimm, B.M. & Crothers, D.M. (1962). *Proc. natl. Acad. Sci. U.S.A.* 48, 905.
- Zimmerman, W.F., Cox, P. & Ackers, G.K. (1971). *J. biol. Chem.* 246, 1078.
- Zubay, G. (1964). in 'The Nucleohistones' ed. by Bonner, J. & Ts'o, P.O.P. San Francisco, Holden-Day.

Zubay, G. & Doty, P. (1959). J. mol. Biol. 1, 1.

## SUMMARY

As a first approach to the study of the interactions between the constituent macromolecules of mammalian chromatin, some physico-chemical properties of two components of chromatin, GAR histone and DNA, have been characterized. Studies of the self-association of GAR histone by ultracentrifugal techniques have indicated that the histone probably exists in a monomer-dimer equilibrium in 0.075M NaCl/0.01M HCl and in a monomer-dimer-tetramer equilibrium in 0.15M NaCl/0.01M HCl. Gel filtration studies confirmed these results, also indicating that the tetramer formed is of compact shape, similar to a tetrahedron. Preliminary ultracentrifugal studies indicated that the mode of association of GAR histone is independent of pH in the range 2.5 - 7.0. ORD studies of GAR histone in the above conditions suggested that the amount of helix present in the protein was low and was not altered by the self-association of the histone.

The heterogeneity of the C. T. DNA also used in these studies was quantitated using the  $g(s)$  distribution of sedimentation coefficients. Ultracentrifugal analysis of complexes of GAR histone-C. T. DNA prepared by salt-gradient dialysis and by direct addition of the two components, revealed considerable heterogeneity of the complex with respect to sedimentation coefficient.

Thermal denaturation studies did not detect any significant differences in the absorbance melting profile of complexes formed by the direct addition of GAR histone to DNA in conditions in which GAR existed as a monomer and in conditions where GAR probably existed as a monomer-dimer equilibrium.

To lessen the difficulties in interpretation of the properties of complexes of GAR histone with heterogeneous C. T. DNA, homogeneous preparations of relaxed circular SV40 DNA and supercoiled SV40 DNA were used. The number of histone molecules bound per molecule of

each form of DNA was calculated as a function of the amount of histone added to the DNA preparations and the results were interpreted as indicating co-operative binding. Sedimentation coefficients and sedimentation coefficient distributions of the complexes of GAR with each form of SV40 DNA in various salt conditions were measured. Comparison of the frictional coefficient and diffusion coefficients of the complexes with those of free SV40 DNA and SV40 virus suggested that the complexes were not as compact as the spherical virus particle.